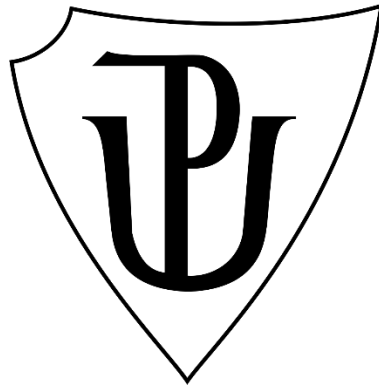


PALACKÝ UNIVERSITY IN OLMOUC

Faculty of Science

Department of Biochemistry



Initiation and development of crown roots in barley

(Hordeum vulgare L.)

DISSERTATION THESIS

Author:	Dieu Thu Nguyen, M.Sc.
Study Program:	P1416 Biochemistry
Form of Studies:	Full-time
Supervisor:	Véronique Hélène Bergounoux, Ph.D.
Consultant:	Prof. Pascal Gantet
Year:	2024

Bibliografická identifikace

Jméno a příjmení autora	Dieu Thu Nguyen
Název práce	Iniciace a vývoj nodálních kořenů u ječmene (<i>Hordeum vulgare</i> L.)
Typ práce	Disertační
Pracoviště	Český institut výzkumu a pokročilých technologií, Přírodovědecká fakulta, Univerzita Palackého v Olomouci
Vedoucí práce	Véronique Hélène Bergougnoux, Ph.D.
Rok obhajoby práce	2024

Abstraktní

Kořenový systém hraje klíčovou roli v růstu a vývoji rostlin, zajišťuje příjem vody a živin a reaguje na měnící se podmínky prostředí. Obiloviny se vyznačují svazčítým kořenovým systémem, který se skládá z primárního kořene a ze seminálních kořenů vyvíjejících se již během embryogeneze, a dále z post-embryonálních laterálních a nodálních kořenů (NK), které se vyvíjí z kořene nebo ze stonku. Porozumění mechanismům regulace zakládání a vývoje kořenů představuje první krok k selekci plodin s vylepšenými vlastnostmi kořenové architektury, a to prostřednictvím buď markerem asistované selekce nebo přímé genetické modifikace. Ječmen (*Hordeum vulgare* L.) je významnou plodinou, která se umísťuje na čtvrtém místě na světě jak z hlediska množství, tak pěstební plochy a stal se modelovou rostlinou pro malozrnné obiloviny z rodiny *Triticaceae* pěstované v mírném pásu. V první části výzkumu jsme provedli kompletní transkriptomickou studii báze stonku semenáčků ječmene 1 den po vyklíčení a 10 dní po vyklíčení, kdy se tvoří NK, abychom pochopili molekulární mechanismus řídící tvorbu NK. RNA-seq analýza ukázala, že vývoj NK zahrnuje geny kódující proteiny s úlohami v určení identity buněk, aktivaci buněčného cyklu, kontrole hormonálního stavu, buněčné smrti a modifikaci buněčné stěny. Tyto geny jsou pravděpodobně zapojeny do různých kroků tvorby NK, od založení a diferenciacie primordia až po jeho průnik skrze epidermis, a odhalily aktivaci různých hormonálních drah během tohoto procesu. Ve druhé části studie jsme se podrobně

zaměřili na identifikaci a funkční charakterizaci genů kódujících rostlinné LATERAL ORGAN BOUNDARIES (LOB) DOMAIN (LBD) transkripční faktory (LBD TF), které mají úlohu během zakládání NK v ječmeni. U rýže je CROWNROOTLESS1 (CRL1) LBD TF hlavním regulátorem zakládání NK, ten je pod přímou kontrolou auxinem řízené signalizační dráhy zprostředkované přes auxin response factor (ARF) TF. Ve studii byly v ječmeni identifikovány dva fylogeneticky úzce příbuzné geny CRL1 (nazvané HvCRL1 a Hv-CRL1-L1). V indukovatelném systému NK jsou oba kandidátní geny exprimovány v reakci na auxin během raných stádií tvorby NK v bázi stonku, přičemž HvCRL1-L1 vykazuje časové zpoždění ve srovnání s HvCRL1. Transientní aktivační eseje v protoplastech rýže ukázaly, že HvCRL1 může vázat známou DNA sekvenci rozpoznávanou LBD TF, zatímco HvCRL1-L1 ne. Oba geny mohou částečně komplementovat mutanta *crl1* u rýže. Mutace vedoucí ke ztrátě funkce v každém genu dramaticky narušuje tvorbu NK v ječmeni. Výsledky dokazují, že oba TF jsou zapojeny do regulace tvorby NK v ječmeni, ale pravděpodobně v tomto vývojovém procesu působí prostřednictvím odlišných a vzájemně se doplňujících drah.

Klíčová slova	Ječmen, <i>Hordeum vulgare</i> L., nodální kořeny, doména laterálních hranic orgánů, transkripční faktor, funkce genu, architektura kořenového systému.
Počet stran	209
Počet příloh	8
Jazyk	Anglický

Bibliographical identification

Author's first name and surname	Dieu Thu Nguyen
Title	Initiation and development of crown roots in barley (<i>Hordeum vulgare</i> L.)
Type of thesis	Ph.D.
Workplace	Czech Advanced Technology and Research Institute – crops engineering and biotechnology, Centre of the Haná Region for Biotechnological and Agricultural Research, Palacký University Olomouc
Supervisor	Véronique Hélène Bergougnoux, Ph.D.
Year of presentation	2024

Abstract

Root systems have critical roles in plant growth, development, ensuring water and nutrient uptake, and response to changing environmental conditions. In cereals, the fibrous root system comprises primary and seminal roots that develop during embryogenesis, and lateral- and crown roots (CRs) that develop post-embryonically from root or stem, respectively. Understanding the mechanisms regulating root initiation and development represents the first step towards the selection of crops with enhanced root architectural traits via either marker-assisted-selection or direct genetic modification. Barley (*Hordeum vulgare* L.) is an important crop, ranking at the fourth place worldwide both in terms of quantity and cultivation area, and has become a plant model for the small-grain temperate cereals of the Triticaceae family. In the first part of the research, we investigated a whole transcriptomic study in the barley stem base of 1 day-after-germination (DAG) and 10DAG seedlings, when CRs are formed to understand the molecular mechanism controlling CR formation. The RNA-seq analysis indicated that CR development involved genes encoding proteins with roles in cell identity priming, cell cycle activation, hormonal status control, cell death and cell wall modification. These gene are likely involved in the different steps of CR formation from initiation to primordia differentiation and emergence and revealed the activation of different hormonal pathways during this process. In the second part of the study, we deeply focus on identification and functional characterization of genes encoding the plant-specific LATERAL ORGAN BOUNDARIES (LOB) DOMAIN

(LBD) Transcription factors (LBD TFs) with roles during CR initiation in barley. In rice, the CROWNROOTLESS1 (CRL1) LBD TF is the core regulator of CR initiation and a direct target of the auxin response factor (ARF)-mediated auxin signaling pathway. In our study, two CRL1 phylogenetically closely related genes (named HvCRL1 and Hv-CRL1-L1) were identified in barley. In a CR inducible system, both candidate genes are expressed in response to auxin during the early stages of CR formation in stem base, with a time delay for HvCRL1-L1 in comparison with HvCRL1. Transient activation assays in rice protoplast showed that HvCRL1 could bind a known consensus DNA sequence recognized by LBD transcription factors, whereas HvCRL1-L1 did not. Both genes can partially complement the *cr11* rice mutant. Loss-of-function mutation in each gene dramatically impairs CR formation in barley. The results prove that two TFs are both involved in the regulation of CR formation barley but likely act through distinct and complementary pathways in this developmental process.

Keywords	Barley, <i>Hordeum vulgare</i> L., crown roots, Lateral organ boundaries domain, transcription factor, root system architecture.
Number of pages	209
Number of appendices	8
Language	English

I hereby declare that this Ph.D. thesis has been written solely by me. All the sources used in this thesis are cited and listed in the “References” section. All published results included in this work are approved by co-authors.

Olomouc,.....

.....

M.sc NGUYEN, Dieu Thu

Acknowledgments

First, I would like to express my greatest gratitude to my doctoral supervisor, Dr. Véronique H elene Bergougnoux-Fojt ık, and my doctoral consultant, Prof. Dr. Pascal Gantet. I want to express my deep gratitude to Dr. Bergougnoux for accepting my doctoral work, her expert guidance, and important constructive suggestions as well as kind support and great correction during my PhD studies. Thank you very much for your patience, kindness and help to navigate the completion of my PhD. I want to express my sincere gratitude to Prof. Dr. Pascal Gantet for his kindness, encouragement, and great patience in dedicating his valuable time to discussing and supporting me in my scientific career. He taught me how to be passionate in science and become a good scientist.

I am grateful to him and Dr, Hoang Thi Giang for introducing me to this PhD program and helping me get this study opportunity.

I want to thank Prof. Mgr. Marek Petřivalsk y, Dr. – Head of Biochemistry Department for his willingness to support me to finish my long Ph.D study.

I also would like to thank all my colleagues at the Palack y University Olomouc, especially at the barley research group, who supported and encouraged me in my research. I would particularly thank to Cintia and Yuliya. They are not only my excellent senior colleagues in science, but also my good friends for the life in Czech Republic. I also would like to especially thank all PhD students in the group: Nikola, Betka, junior David, Alexi, Carlos for accompanying me through the journey with a lot of discussions and help, both in the lab and outside the lab. They are my great scientific teachers. My special thanks go to V era Chytilov a for her kind help in plant growing in greenhouse, to all kind and nice technicians in the group for the barley transformation work and their nice company. I am also really appreciated to Ass. Prof. Petr Galuszka for his open mind and help in the beginning of my PhD study in Olomouc. I would like to thank Prof. Ivo Fr ebort for giving me the opportunity to work in the University in the beginning.

I would like to thank to Dr. Goetz Hensel and his transforation group in IPK, Germany for signifiant help in preparation of barley transgenic CRISPR/Cas⁹ lines.

I would like to thank Dr. Mathieu Gonin and Myriam Colin for their open and guidance in transactivation assay and histology in IRD, Montpellier and their great friendship. I would like to express my gratitude to my master supervisor, Dr. St ephane

Jouannic, all my dear senior colleagues in Agricultural Genetic Institute, Hanoi for their kindness, encouragement, open mind, and availabilities for all my questions and emails during my scientific career. I also thank all my friends/colleagues (Jérémy Lavarenne, Luong Ai, My Nguyen Trang Hieu, Phan Thi Ngan) in IRD, Montpellier for helping me during the time I made the internship there.

I would like to express my feelings of gratitude to all the friends who support me last seven years of my life in Czech Republic. They are my second family in Czech Republic. Please let me give my heartfelt thanks to: Kristina and her family, both Katka J., Claudia, Alba, Honza and Venca, Auguste and Justinas, Denisa and whole family, Pepa, Domcha and all my best friends in Vietnam

Finally, my special appreciation and gratitude would like to go to my great family, beloved parents, brother and his little family in Vietnam, my love and his family in Czech, my best friend – Hanh. This PhD would not be possible without their love, endless support, and encouragement.

Contents

Index of tables and figures	1
Tables.....	1
Figures.....	2
FREQUENTLY USED ABBREVIATIONS	10
CHAPTER I: General introduction.....	13
I.1 Barley	14
I.1.1 Botanical description.....	14
I.1.2 The origin and domestication of barley.....	19
I.1.3 Adaptability of barley (<i>Hordeum vulgare</i> L.) to environments	20
I.1.4 Genomics of barley and its genetic modification.....	21
I.1.5 The production and nutritional data of barley	25
I.2 The root system of cereals.....	26
I.2.1 The necessity to study root systems in cereals	26
I.2.2 Overview of phenotyping methods to study root system.....	29
I.2.3 The root types, organization, and their function in cereals	36
I.2.4 Description of cereal roots' origin	43
I.2.5 Regulation of root architecture.....	48
I.3 Molecular mechanism controls root formation and development.....	55
I.4 How to study and discover the genetic mechanism, genes and gene network involved in RSA	58
I.5 Background and study significance	60
I.6 Study aims and experimental approaches:	61
CHAPTER II: Identification and characterization of genes involved in crown root initiation and development in barley (<i>Hordeum vulgare</i> L.)	62
II.1 Introduction.....	63
II.2 Materials and methods	65
II.2.1 Plant materials and cultivation conditions	65
II.2.2 Imaging of CR primordia by light and confocal microscopy.....	66
II.2.3 Evans blue staining.....	67
II.2.4 Library preparation and transcriptomic analysis	68
II.2.5 Analysis of gene expression by quantitative real-time PCR (qRT - PCR)	69

II.2.6	Prediction of putative <i>cis</i> -regulating elements related to ethylene and cell death.....	71
II.2.7	Statistical analysis	71
II.3	Results and Discussion.....	74
II.3.1	Crown-root primordia development in the stem base of the spring barley cv. Golden Promise	74
II.3.2	Transcriptomic changes in the stem base of 1DAG and 10DAG seedlings of spring barley cv. Golden Promise and functional annotation of differential expressed genes (DEGs).....	76
II.3.3	Cell identity priming and cell cycle activation during CR development in barley	83
II.3.4	Hormonal status during crown-root development in barley.....	83
II.3.5	Emergence of CR induces cell death and cell wall modification.....	85
II.4	Conclusions	89
CHAPTER III: Two lateral organ boundary domain transcription factors HvCRL1 and HvCRL1-L1 regulate shoot-borne root formation in barley (<i>Hordeum vulgare</i> L.)		90
III.1	Introduction.....	91
III.1.1	Structure of lateral organ boundaries domain proteins	92
III.1.2	Function of LBD proteins in root initiation and development	94
III.1.3	Aims of this study	97
III.2	Materials and methods:	98
III.2.1	Plant materials.	98
III.2.2	Identification of barley LBD proteins and construction of the phylogenetic tree	99
III.2.3	Primer design for gene expression analyses, cloning and plant genotyping.....	100
III.2.4	Crown-Root Inducible System (CRIS)	106
III.2.5	Histology analysis	107
III.2.6	Gene expression of barley LBD family.....	107
III.2.7	Genes' expression analysis of the putative <i>HvLBD</i> genes under CRIS	109
III.2.8	Bacterial transformation and culture	113
III.2.9	Transactivation assay in rice protoplasts.....	114
III.2.10	Knock-out barley <i>crl1</i> mutant generated by CRISPR-Cas ⁹	118

III.2.11	Nuclear DNA ploidy assessment of transgenic plants:	128
III.2.12	Complementation of two putative genes in rice <i>crl1</i> mutant	130
III.3	Results and discussions	131
III.4	Conclusions	154
ANNEXES – Supplementary data		156
REFERENCES		164
SUPPLEMENT 1		194
SUPPLEMENT 2		195
SUPPLEMENT 3		196
SUPPLEMENT 4		197
SUPPLEMENT 5		198

Index of tables and figures

Tables

Table I.1: Non-exhaustive list of barley databases:	24
Table I.2: Different approaches for root phenotyping in the field, laboratory and greenhouse, and their advantages and disadvantages. Field: overview of an alfalfa field trial. Shovelomics approaches wheat roots. Washed roots from field-grown alfalfa plants. Tractor for acquiring core samples. Outline of root area for harvest. Greenhouse: EnviroKing® (Harrington Industrial Plastics, Albuquerque, NM, USA) UV clear PVC piping at a slanted angle. Black deepots. Semi-cylindrical mesocosm fronted with clear plexiglass; mesocosms with plastic liners. Individual EnviroKing® UV clear PVC piping for real-time observation of RSA including root depth. Laboratory: alfalfa (<i>Medicago sativa</i> L.) roots in clear vials and growth media. Wheat seedlings growing on germination paper in plastic trays. Alfalfa seeding imaged using flatbed scanner. <i>Arabidopsis thaliana</i> roots stained with propidium iodide to observe cell wall and green fluorescent protein (GFP) labeling the actin cytoskeleton. <i>A. thaliana</i> root showing lateral root initiation. Alfalfa seedlings growing in glass cylinders with growth media. <i>Brachypodium distachyon</i> (model grass) seedlings growing in growth media in plates (Adapted from Paez-Garcia et al. 2015).	31
Table I.3: Relationships between root architecture and environmental factors.	53
Table II.1: Sequences of forward and reverse primers used for qRT-PCR for 10 genes with a putative role in CR initiation and development and 3 genes ^(a) used as reference genes for normalization.	72
Table II.2: Quality statistics of RNA-seq data:	76
Table II.3: BIN enrichment for genes up- and down-regulated in the stem base of 10DAG seedlings.	77
Table II.4: Functional annotation enrichment of genes differentially regulated in the crown of 10 DAG-old seedling of barley cv. Golden Promise. The automated annotation was performed using the Mercator resource (Lohse et al. 2014). Only the most enriched category ($\geq 10\%$) are represented; complete information is provided in supplemental table S.II.3). Values represent the percentage of genes in the specific category which were down- or up-regulated in DO10DAG and UP10DAG, respectively.	78
Table III.1: List of primers using in this study:	101
Table III.2: List of samples and their code for HvLBD family's expression profile	109
Table III.3: Sequences of selected gRNAs	118
Table III.4: <i>HvLBD</i> family genes in barley	133

Figures

Figure I.1: Structure of barley plant. From left to right, structures of root system, whole barley plant, spike, triplet, new germinated grain (with acrospire growing up and rootlets growing out from grain) and barley floret are illustrated in detail (Adapted from image courtesy of Patricia J. Wynne: <https://www.americanscientist.org/article/why-brewers-choose-barley>; and Campaign 2011, with own root structure photo). 16

Figure I.2: Structure of barley spike. (a) two-row barley spike (left), in which kernels tend to be symmetrical and of even size; six-row barley spike (right), in which the two lateral rows of kernels are a little shorter, thinner, and slightly twisted; (b) enlarged view on spike with grains attached to the rachis at their base; some organs (lemma with long awns) change from green to yellow during grain maturation. (c) naked grain (no hull) on the left; embryo region is arrowed; hulled grain on the right; hull (palea) is slightly wrinkled (Borisjuk, Rolletschek, and Radchuk 2020). 16

Figure I.3: Schematic diagram of the major development phases of barley. (A) Vegetative development, reproductive development and mature plant including illustration of two row and six row spikes. (B) Germination, seedling, tillering, stem elongation, booting, ear emergence, flowering, milk development, dough development and ripening. The scale was modified for cereals after Zadoks *et al.* 1974 (Ahmad M. Alqudah. 2015)..... 18

Figure I.4: Visualization of the Anatomics pipeline from sample collection through identifications of genetic markers. From left to right of the figure: samples are first collected from field-grown plants and preserved in 75% (vol/vol) ethanol, then imaged directly from storage in ethanol with laser ablation tomography (LAT), after that images are phenotyped using image analysis software, and finally genetic markers are identified. The LAT is composed of a pulsed UV laser (1), which is modified through beam-shaping optics (2) to create a ‘cutting sheet’ (3) and directed onto a sample of plant tissue (4). The sample is advanced into the ablation plane by a motorized stage (5) while a high-resolution camera (6) images the anatomy that is exposed as the tissue is ablated (Strock, Schneider, and Lynch 2022). 36

Figure I.5: Illustration of root structure of a barley mature plant (left) and a healthy soil-removed root system of a barley (right) (adapted from Macleod *et al.* 2008). ... 37

Figure I.6: Organization of cereal root systems. (a) Embryonic primary (PR) and seminal (SR) roots of 5-day-old rice, maize and barley seedlings (from left to right). (b) detail of a 10-day-old maize, seedling with two new shoot-borne crown roots (CR). (c) Aboverground brace roots (BR) of adult rice plants (Caroline Marcon , Anja Paschold and Frank Hochholdinger 2013)..... 39

Figure I.7: Longitudinal view of root tip. The zones of maturation, elongation, and cell division (the apical meristem) were illustrated. Root hairs begin to develop in the mature zone. Different cell layers were also distinguished (adapted from Sheldon and Munns 2023). 41

Figure I.8: Development and anatomical differences between embryonic/seminal roots (SR) and crown root/nodal root (NR) in barley. (A) Emergence of the primary root from the seed 4 day after sowing (DAS). (B) SRs at 7 DAS. (C) Apical root zone of one SR at 25 DAS. (D) Cross-section of SR from mature zone at 25 DAS. (E) First emerged NR at 20 DAS. (F) NR development at 39 DAS. (G) Apical root zone of an NR at 39 DAS. (H) Cross-section of NR from mature zone at 39 DAS. (I) Root diameter in the mature root zones of SR and NR. (J) Area of epidermal, cortical or xylem cells calculated from cross-sections of SR and NR. (K) number of central metaxylem vessels in SR and NR (Zhaojun Liu et al. 2021)..... 42

Figure I.9: Illustration of barley primary and seminal root primordia. (A) Longitudinal median section through a mature barley embryo. (B) Cross section through a mature barley grain shows the primary root primordium and five secondary seminal root primordia. Note: prp: primary root primordium, sc: scutellum, srp 1,2: secondary seminal root primordia, e: embryo (Luxovx 1986)..... 43

Figure I.10: Lateral root development in barley. (A) illustration of a longitudinal section showing the typical tissue organization of cereal roots. (B) Succession of morphological stages during lateral root development and emergence. (C) Original toluidine blue stained sections used for illustrations in (B). (D) Periclinal and (E) anticlinal longitudinal sections of the growing lateral roots. The sections show an extensive cortical region around the primordium where divisions are taking place. (F) Radial tissue organization of cereal roots (toluidine blue staining). (G) illustration of the section in (F) to highlight the deformation of the cortex that occurs during lateral root penetration. (Scale bars = 50 μ m). Figure and footnotes are cited from Orman-Ligeza et al. 2013. 46

Figure I.11: A fine anatomical view of crown root development in rice. (A) Establishment of initial cells. (B) Establishment of epidermis, endodermis and root cap initials. (C) Differentiation of epidermis-endodermis initial into epidermis and endodermis. (D) Cortex differentiation. (E) Establishment of fundamental organization of root primordium. (F) Onset of cell vacuolation (arrowhead) in cortex and elongation (arrow) in stele. (G) Crown-root emergence (from Itoh et al., 2005). (H) The rice stem transversal section showing the crown root initiation area. Staining: periodic acid-Schiff and naphthol-blue-black (Gonin et al. 2019). IC: initial cells; PV: peripheral cylinder of vascular bundle; C: root cap or its initials; EE: epidermis-endodermis initials; S: stele; EP: epidermis; EN: endodermis; CO cortex, COL columella, MXII late meta-xylem vessel; CRP: crown root primordium; GM: ground meristem; L: leaf; S: stele; VB: vascular bundle. The black dotted lines indicate the separation of the ground meristem. Scale bar, 50 μ m..... 47

Figure I.12: Example of the impact of soil conditions on roots. (A) Gravity: soil-grown seedlings of hybrid wheat with acute gravity angle (left) and rye with wider seminal root angle (right). (B) Hardness: wheat. Janz seminal roots grow through pores (left) and in hard soil (right). (C) Water: the nodal roots of a well-watered wheat (left) and in dry soil (insert). (D) Oxygen: maize grown in drained soil (left) or soil

waterlogged for 21 days (right). **(E)** Nutrients: wheat with a uniform phosphate supply (left) compared to a phosphate pad applied at 8 μM between blue beads (right). **(F)** Temperature: MRI of maize roots grown with a root zone temperature of 14 $^{\circ}\text{C}$ (left) or 24 $^{\circ}\text{C}$ (right). 48

Figure I.13: Description of nutrient distribution in the soil and different structures of barley root system architecture can adapt to different soil environmental conditions (created in BioRender.com). 52

Figure I.14: The molecular regulatory mechanisms of root development in rice. Arrows represent positive regulatory actions. Lines ending in a flat head indicate a negative regulatory action. Dashed lines represent interactions that have not been experimentally confirmed. Double-headed arrows indicate that two proteins interact. Text color code: genes or protein, black; hormones, yellow; signals, red; biological processes, green (from Meng et al. 2019). 57

Figure II.1: Mini-hydropony system. **(A)** A deep-plastic and untransparent 1ml-pipet-tip boxe for the system. 25 seedlings were grown in 1 box, filled with 350 mL of $\frac{1}{2}$ Hoagland solution. **(B)** Putting one barley seedling into one bottom-cut-1ml pipet tip and put in Mini hydropony system. **(C)** 1 day after germination (DAG) barley seedling cv. GP. **(D)**10-DAG barley seedling cv. GP. In (C) and (D), grain tegument and the rest of the endosperm were removed to keep only the young seedling. Bar: 1 cm..... 66

Figure II.2: Crown-root primordia development in young barley seedlings. In 3DAG-old seedling, one primordium is formed at the outermost side of the pericycle **(A)**; PAS-NBB staining). The pericycle is surrounded by cells rich in starch as shown by the presence of purple-black dots after staining with lugol solution **(B)** (Figure A and B were conducted by my supervisor, Dr. Bergougnoux V.). **(C)** Result of a block reconstruction in the 3D transparency mode of the whole stem base of a 10 DAG-old barley seedling. CR primordia are identified by different colors: blue, green and yellow **(D)** z-axis cross section; the colored traits indicate the angle between each CR primordia (Figure C and D were conducted by Dr. Lavarenne J., IRD, Montpellier, France). Bars in A and B represent 100 μm 75

Figure II.3: Functional annotation of genes differentially regulated in the stem base of 10 DAG-old seedling of barley. The functional annotation was done with Mercator4; the number of genes in one category is expressed as a percentage of the total number of genes that were annotated. 78

Figure II.4: **(A)** Comparison of expression as determined by RNA-seq and real-time PCR. All expression data were normalized to the log₂ scale. The coefficient of Pearson correlation was determined to be $r=0.94$. **(B)** Validation of differential expression by qRT-PCR of 6 genes with a potential role in CR initiation and development. qRT-PCR was run on the same samples as those used for RNAseq analysis. Normalization was done using the 3 most stable reference genes: Actin, Hv5439 and EIF152. The graph shows means \pm SEM (n=3). The statistical significance was assessed by a two-way

ANOVA followed by a Bonferroni multiple comparisons test (GraphPad Prism 9.2.0). ****: adjusted P-value < 0.0001; *: adjusted P-value < 0.005..... 80

Figure II.5: Gene expression analysis by qRT-PCR of PIN (A), SCR-like1 (B), ARGO (C), AuxIAA20 (D) and RRB9 (E) in the roots, crowns and shoots of cv. Golden Promise seedlings grown for 10 days in hydroponic conditions. Normalization was done using 3 reference genes: Actin, Hv5439 and EIF152. The graph shows means ± SEM (n=3). The statistical significance was assessed by a two-way ANOVA followed by a Bonferroni multiple comparisons test (GraphPad Prism 9.2.0). ****: adjusted P-value < 0.0001; ***: adjusted P-value < 0.001; **: adjusted P-value < 0.001; *: adjusted P-value < 0.005..... 82

Figure II.6: Involvement of ethylene in cell death during crown-root emergence in barley cv. Golden Promise. (A) Ethylene biosynthetic and signaling pathway in the context of cell death. Genes identified in the RNAseq data as differentially expressed are indicated (MLOC); colored scars indicate whether they were up-regulated (red) or down-regulated (blue) in the stem base of 10 days-old seedlings. (B) Evans blue staining indicates the cell death of the epidermal cell at the site of crown-root emergence. (C) Prediction of the presence of ethylene-related cis-regulating elements (AP2/ERF and EIN3 motifs). Prediction was done with PlantPAN3.0, using rice database..... 88

Figure III.1: Structure of LBD proteins..... 94

Figure III.2: a summary of molecular pathways and interaction of LBD-mediated processes during root initiation and development. The LBD proteins are presented in red, the plants are presented in green. Positive and negative regulatory actions are indicated by arrows and lines with bars, respectively. Physical protein interactions are indicated by '+'. Abbreviations: ARF, AUXIN RESPONSE FACTOR; CRL1, CROWN ROOTLESS 1; IAA, Indole-3-acetic acid; LBD, LATERAL ORGAN BOUNDARY DOMAIN; RTCL, RTCS-LIKE; RTCS, ROOTLESS CONCERNING CROWN AND SEMINAL ROOTS; MOR: MORE ROOT; SBRL/SILBD: SHOOTBORNE ROOTLESS; BSBRL/SILBD16: BROTHER OF SHOOTBORNE ROOTLESS (modified from C. Xu, Luo, and Hochholdinger 2016)..... 95

Figure III.3: schema of principle of crown-root inducible system in out study 106

Figure III.4: The plasmid pRT104 map. The vector carries the quantitative 35S promoter and the polyadenylation signal of CaMV strain Cabb B-D and was constructed in modified polylinkers of pUC18/19..... 115

Figure III.5: *Trans*-activation assay in rice protoplast. (A) Reporter constructs consisted of the GUS gene under the control of a minimal promoter (-47 to 0) and driven by enrichment of native or mutated (m) cis-regulatory motif sequences (-138 to -92). Bold nucleotides indicate point mutation in *LBD* and *CRL1*-boxes. Numbers indicate positions relative to the start site of transcription of the GUS gene (Gonin et al. 2022). (B) A scheme of transcriptional ability of candidate HvLBD transcription factors (TFs) to induce the expression of GUS reporter gene in rice protoplast. Rice protoplasts were co-transformed with reporter plasmids carrying the GUS reporter

gene placed under the control of a minimal promoter and tetramers of cis-regulatory motif (i.e., LBD-box, CRL1-box and their mutated form) fused to GUS and overexpression vectors with the candidate HvLBD genes driven by the CaMV 35S promoter and the p2rL7 normalization plasmid (De Sutter et al. 2005) carrying the *Renilla reniformis* luciferase (LUC) gene driven by CaMV 35S promoter. The expression of the gene can be followed by enzymatic activity or fluorescence activity is detected. If the protein is not a TF (empty vector), no change in fluorescence or activity is detected. If the cis-regulatory motif was mutated, no significant change in fluorescence activity is detected. *Cis*-RM or *mCis*-RM: *Cis*-regulatory motif or mutated *cis*-regulatory motif; Pro: promoter. CRISPR/Cas⁹-mediated gene knock-out.

..... 117

Figure III.6: Whole cassette of oligonucleotide duplex structure for CRISPR-Cas⁹ sub-cloning. Protospacer sequence is presented in red color; specific overhang at 5'-end of single oligonucleotide is presented in blue color. Oligonucleotides containing protospacer and complemented sequence are illustrated as forward (F) and reverse (R), respectively. 120

Figure III.7: SnapGene-constructed genetic map of the pSH91 plasmid for CRISPR-Cas⁹ system establishment. The size of DNA circular plasmid is 12198 bp. KanK, Kanamycin resistance gene. SpecR, Spectinomycin/Streptomycin (Strep/Spec) resistance gene for bacterial selection. OsU3p/t: U3 snRNA promoter/terminator from rice. ZmUbi1p/int, Ubiquitin 1 promoter/first intron from maize. zCas⁹, *Zea mays*-codon-optimized Cas9. NOST: Nopaline synthase gene terminator; 35St, 35S terminator. NLS, a nuclear localization signal, which helps Cas⁹ complex can localize to the nucleus immediately upon entering the cell. 3xFLAG, small tags sequence, used for protein affinity purification with less likely to affect protein function (Geny et al. 2021). Cas9-ORF, Open reading frame of Cas9 protein. Restriction enzymes are listed outside of circular plasmid. 120

Figure III.8: Molecular feature circle map of binary vector 271p6i-2x35s-TE9 (DNA-Cloning-Service, Hamburg, Germany) (Holubová et al. 2018). The size of DNA circular plasmid is 10052 bp. The vector was established by ligation of P2x35s-Xba-Xho into 269p6i-TE9. Hpt: Hygromycine resistant gene for transgenic plant selection. STLS1: Intron (upstream region) of the nuclear photosynthetic gene ST-LS1 from potato. E9: terminator of the ribulose-1,5-isphosphate carboxylase small subunit (*rbcS*) E9 gene from *Pisum sativum* L. RB: right border. LB: left border. ColE1: ColE1 Origin region for high-copy-number of replications. pVS1: origin of replication for the *Pseudomonas* plasmid pVS1. Sm/Sp: Strep/Spec resistance gene for *Agrobacterium* bacteria. 2Px35S: cauliflower mosaic virus (CaMV) 35S promoter with a duplicated enhancer region. Restriction enzymes are listed outside of circular plasmid. 122

Figure III.9: The map of the final CRISPR-Cas9-sgRNA cassette. A CRISPR-Cas9 cassette was inserted in the 271p6i-2x35s-TE9 vector. 123

Figure III.10: Strategy to select T-DNA-free stable mutant from CRISPR/Cas9 method. PCR to check T-DNA present was done using primers on the gRNA, Cas9

and HPT region. To detect mutations, a series of PCR and CAPS assays were done based on each specific sequence of mutation. The mutation was finally sequenced by the Sanger method..... 126

Figure III.11: CAPS/DCAPS markers can distinguish alleles. **(A)** Diagram of CAPS technique. An amplicon centered on a restriction site (blue bar) disrupted by a SNP or indel (red bar) is differentially cleaved by a restriction enzyme (RE) in the wild-type vs mutant. **(B)** Diagram of the dCAPS technique. A restriction site can be introduced into either the wild-type or mutant target sequences using mismatched oligonucleotide primers to discriminate two sequences. The mutation (green bar) disrupts the introduced restriction site such that it is not cleaved by the restriction enzyme (RE). Gel electrophoresis can be used to identify the size difference between the wild-type and mutant fragments in both the CAPS and dCAPS methods (Hodgens, Nimchuk, and Kieber 2017)..... 128

Figure III.12: In silico characterization of barley LBD proteins. **(A)** Localization of the putative LBD proteins on the 7 chromosomes of barley. The chart has been built with MG2C (Chao et al. 2021). **(B)** Phylogenetic analysis of the 31 barley LBD proteins. The analysis has been ran with learnMSA (Becker and Stanke 2022) and default parameters. Sequences of rice (Os), maize (Zm) and Arabidopsis (At) genes encoding known key initiators of crown (Os and Zm) and adventitious (At) roots have been included in the analysis. The protein-coding sequences were aligned using learnMSA (Becker and Stanke 2022) under default options. The phylogenetic tree was analysed with IQtree 1.6.2. (Nguyen et al. 2015). The best protein model was identified using -m MFP option, and the branch supports were tested by UFBoot2 (Hoang et al. 2018) with 10000 replicates. **(C)** Phylogenetic relationship among the thirty-one HvLBD proteins. The gene structure of the 31 HvLBD genes was drawn with CFVisual tool. The tree was generated in the form of an Inferred ancestral state, using the Maximum Likelihood method and Jones et al. w/freq. model. Evolutionary analyses were conducted in MEGA 11(Tamura, Stecher, and Kumar 2021). The tree shows a set of possible amino acids (states) at each ancestral node based on their inferred likelihood at site 1. Initial tree(s) for the heuristic search were obtained automatically by applying Neighbor-Join and BioNJ algorithms to a matrix of pairwise distances estimated using the JTT model, and then selecting the topology with superior log likelihood value. The rates among sites were treated as a Gamma distribution using 5 Gamma Categories (Gamma Distribution option). All positions containing gaps and missing data were eliminated (complete deletion option). There were a total of 71 positions in the final dataset. Bootstrap analysis was conducted with 500 iterations 138

Figure III.13: Heat map of the expression profiling of HvLBD genes in different tissues. The heat map was created with ClustVis web tool (<https://biit.cs.ut.ee/clustvis/>)(Metsalu and Vilo 2015), using the barley reference transcript dataset (BART) in EoRNA barley expression database with transcripts per million (TPM) (<https://ics.hutton.ac.uk/eorna/index.html>). Original values are $\ln(x)$ -

transformed; Columns are centered; Unit variance scaling was applied to columns; Both rows and columns are clustered using correlation distance and average linkage including 26 rows corresponding to 26 genes with available expression profile and 16 columns corresponding to different tissues. The color scale bar represents the expression values of the genes. Three bio replicates were selected for each sample. Current EoRNA contains both BART transcripts and the predicted transcripts from the Barley Pseudomolecules (HORVU 2017). Senescing leaf (2 months): (SEN). Epidermis (4 weeks): (EPI). Developing tillers at six leaf stage, 3rd internode: (NOD). 4-day embryos dissected from germinating grains: (EMB). Root (4 weeks): (ROO2). Roots from the seedlings (10 cm shoot stage): (ROO). Developing grain, bracts removed (15 days post anthesis (DPA): (CAR15). Developing grain, bracts removed (5DPA): (CAR5). Palea (6 weeks PA): (PAL). Lemma (6 weeks PA): (LEM). Rachis (5 weeks PA): (RAC). Lodicule (6 weeks PA): (LOD). Etiolated (10-day old seedling): (ETI). Shoots from the seedlings (10 cm shoot stage): (LEA). Young developing inflorescences (5mm): (INF1). Developing inflorescences (1-1.5cm): (INF2). 141

Figure III.14: Crown-root inducible system (CRIS). **A)** Schematic representation of the system and the sample collection. The picture was prepared with Biorender. **B)** and **C)** Hand-made transversal section across the stem base of 5 days-old seedlings grown for 3 days in 50 μ M NPA (B) or in 50 μ M 1-NAA (C). Sections were stained in 0.1% toluidine blue. Pictures were acquired with a Zeiss microscope with a 5x objective. The full section was reconstructed using the Free Online Image Combiner (Adobe Express). ti: new tiller; st: stele; *: root apical meristem. **D)** Determination of the number of crown root in barley 10 days after auxin-induction. Student's *t* test was performed to determined the statically significance; n = 10. 142

Figure III.15: PCR products of housekeeping genes showed a single band. L (0321): Ladder GeneRuler 100 bp Plus DNA Ladder - Thermo Fisher Scientific 144

Figure III.16: Expression levels of candidate reference genes across all samples. The line across the box depicts median. 144

Figure III.17: Gene expression stability and ranking of 6 candidate reference genes as calculated by geNorm (Vandesompele et al., 2002). 145

Figure III.18: Gene expression analysis by qRT-PCR of two *LBD* genes (*HvCRL1* and *HvCRL1-L1*) of Class IB expressed in the stem base of young barley seedlings grown in the Crown Root Inducible System (CRIS) based on auxin-induced root initiation (Crombez et al. 2016). Normalization was done using 3 reference genes: *Actin*, *Hv5439* and *EIF152*. The graph shows means \pm SEM (n=6). The statistical significance was assessed by a non-parametric Kruskal-Wallis followed by a multiple comparisons test (GraphPad Prism 10). a: statistically significantly different from the control "0h-NPA" (*p*-value < 0.001). 146

Figure III.19: Identification of AuxRE (TGTCNN) and LBD-box (GCGGCG)/CRL1-box (CAC[A/C]C) in the 5000 bp-promoter sequence of **A)** *HvCRL1-L1* and **B)** *HvCRL1* genes. 147

Figure III.20: The another phylogenetic tree of the LBD proteins including known rice sequences (Os) was built by MEGA11 (Tamura, Stecher, and Kumar 2021). . 148

Figure III.21: Transactivation assay in rice protoplast with HvCRL1 and HvCRL1-L1. Rice protoplasts were co-transformed with an effector plasmid carrying either HvCRL1 or HvCRL1-L1 gene under the control of the 35S promoter and reporter plasmids carrying LBD box motif (LBD-box) or its mutated version (LBD-box mutated) fused to GUS. A reference plasmid carrying the Renilla luciferase gene under the control of the 35S promoter was co-transformed to correct for transformation and protein extraction efficiencies. The control represents protoplasts that were transfected with an empty effector plasmid. The data were expressed as a percentage of the highest activity observed for HvCRL1. The graph represents the average +/- SEM of 5 independent experiments. The statistics were assessed with GraphPad Prism 10 (One-way ANOVA non-parametric Kruskal-Wallis followed by a Dunn's multiple comparisons test)..... 149

Figure III.22: Schematic representation of the position of the sgRNA on the *HvCRL1* and *HvCRL1-L1* genes, and the sequence (nucleotide and protein) of the different mutant lines. The typical LOB domain is indicated in light blue, inside the coding region of the gene (purple). The presence of the single intron in *HvCRL1-L1* gene is represented by a dark line. 152

Figure III.23: Role of HvCRL1 and HvCRL1-L1 in the formation of crown roots. (A) Number of crown roots of different *hvcrl1* and *hvcrl1-l1* knocked-out lines of barley obtained by CRISPR-Cas⁹. (B) Fresh weight of the total root system of different *hvcrl1* and *hvcrl1-l1* knocked-out lines of barley obtained by CRISPR-Cas⁹. (C) Complementation of the crown-root less phenotype of the rice *crl1* mutant by overexpression of *HvCRL1* or *HvCRL1-L1* genes. *HvCRL1* or *HvCRL1-L1* were overexpressed in the rice *crl1* mutant in the cv. TC65 genetic background. An empty vector was used as a control (ϕ). The graphs represent average +/- SEM; Statistical significance was assessed by a Brown-Forsythe and Welch ANOVA test followed by Dunn's multiple comparisons (GraphPad Prism 10.2.2). Bars with identical letters are not significantly different ($p < 0.05$). 153

FREQUENTLY USED ABBREVIATIONS

AA	Amino acid
AP2	ethylene-responsive element-binding protein
ARF	AUXIN RESPONSE FACTOR
AS	ASYMMETRIC LEAVES
ASL	ASYMMETRIC LEAVES-LIKE
AUX/IAA	AUXIN/INDOLE-3-ACETIC ACID
AUX1	Auxin permease 1
BGFD	barley gene family database
BGFD	The barley gene family database
bp	Base pair
CAPS	Cleaved amplified polymorphic sequences
cDNA	complementary deoxyribonucleic acid
CDS	Coding sequence
CR	Crown root
CRIS	Crown Root Inducible System
CRL1	CROWN ROOTLESS1
DAG	Days after germination
DNA	Deoxyribonucleic acid
DPA	Days Post Anthesis
EXP	expansin
FAO	Food and Agriculture Organization
FL-cDNA	Full-length complementary deoxyribonucleic acid
Gbp	gigabases

GFP	green fluorescent protein
GP	Golden Promise
GS	Growth stages
IAA	Indole-3-acetic acid
IBSC	The International Barley Genome Sequencing Consortium
indels	Insertions/deletions
IPK	Institute of Plant Genetics and Crop Plant Research
LAX	Like-AUX1
LBD	Lateral organ boundaries domain
LOB	Lateral organ boundaries
LR	Lateral root
LRIS	Lateral root inducible system
LRP	Lateral root primodium
mRNA	Messenger RNA
MYB	myeloblastosis
NAA	Naphthalene-1-acetic acid
NMR	nuclear magnetic resonance
NPA	1-naphthylphthalamic acid
nt	nucleotide
ORFs	Open reading frames
PCR	Polymerase chain reaction
qRT-PCR	Quantitative Real-time polymerase chain reaction
QTL	Quantitative trait locus
RE	Restriction enzyme

RGA	Shallower root growth angle
RNA	Ribonucleic acid
RNA-Seq	RNA sequencing
ROX	6-Carboxy-X-Rhodamine
RS	Root system
RS2	ROUGH SHEATH2
RSA	Root system architecture
SAM	shoot apical meristem
SNPs	Single nucleotide polymorphisms
SOR	soil-surface roots
TF	Transcription factor
WT	Wild type

CHAPTER I: General introduction

I.1 Barley

I.1.1 Botanical description

Cultivated barley (*Hordeum vulgare* ssp. *vulgare*) is a major annual cereal, member of the monocotyledonous grass family Poaceae, growing in temperate and subtropical climates (Taner, Muzaffer, and Fazil 2004). It belongs to the tribe Triticeae, together with two other small-grain cereal species: wheat (*Triticum aestivum* L.) and rye (*Secale cereale* L.) (Bothmer, Sato, Komatsuda, et al. 2003). It is considered monophyletic and represents a good example of a plant group with a high degree of biological diversity including diploids, self-pollinating, versatility in life forms, reproductive and dispersal patterns (Bothmer, Sato, Knüpffer, et al. 2003; Bothmer, Sato, Komatsuda, et al. 2003). Thus, it is known as a model crop for plant breeding methodology, genetics, cytogenetics, pathology, virology, physiological and biotechnology studies. The genus *Hordeum* is unusual among the Triticeae as it contains both annual species such as *H. vulgare* and *H. marinum* and perennial species such as *H. bulbosum* (Blattner 2018). Barley is an early-maturing, short-season grain, which is found in a variety of environments globally with a high-yield potential (T. Li et al. 2022)(Gozukirmizi and Karlik 2017).

The cultivated barley plant is made up of (i) the roots, both embryonic roots (primary and seminal roots) and post-embryonic roots (i.e., adventitious/or nodal/ or crown/or shoot-born roots and lateral roots) (Fig.I.1.A). Barley has a strong, fibrous root system that can attain a depth of as much as 1.8 - 2.1 m on deep soils (Valenzuela et al. 2002; Akman and Topal 2014) The deepest roots are seminal origin, whereas crown roots usually explore the upper soil. The barley root system becomes highly branched and remains active through the growth; (ii) the crown or the first phytomers in which internodes do not elongate, from the basal region (Shaaf et al. 2019). The phytomers are stem units of the shoot architecture and originated from shoot apical meristem (SAM). The phytomer consists of the internode, and a node with a leaf and an axillary bud); (iii) the erect stem (culm), cylindrical with hollow internodes and five to seven solid nodes (joints). The barley plant has two kinds of stems, namely a main stem and lateral branches or tillers. The main stem develops first and is considered as

the parent shoot and called primary tiller. Through the process of tillering, lateral stems or branches also develop from the main shoot or basal phytomers of the stem, corresponding to the crown region of non-elongated internodes and produce their adventitious roots and spikes during their development (Campaign 2011; RIAZ et al. 2023). Barley plants freely tiller and typically produce one to six stems; (iv) leaf blades, born alternately and sheathed at 180° to each other (Shaaf et al. 2019). Each leaf of barley attaches to the stem at a node, with an associated dormant axillary bud. As long as the apical meristem remains intact, it can produce new alternating and sheathed leaves. Later in the development of the tiller, the apical vegetative meristem undergoes a transition: the tiller stops producing leaves and its upper internode begin to elongate and eventually raise the inflorescence; (v) the spike (inflorescence, head, ear), ultimately emerging from the “boot” (the flag leaf), at the top of the tiller. The spike contains flowers arranged in single flowered spikelet (each bearing two glumes and the floret). Three spikelets, which later contain the individual grains, are attached together at each rachis node of a flat, called a triplet, on a zigzag rachis. In some barley varieties, there are awns emerging upward from lemma (Fig.I.1). The two lateral florets are pedunculate, or sessile and can be sterile (as in two-row cultivar) or fertile (as in six-row barley) (Fig.I.2 and I.3.A), the glumes are placed on the adaxial side of the spikelet (not surrounding) (Komatsuda et al. 2007). The floret consists of the lemma and the palea, which enclose the male and female flower parts (Fig.I.1); and (v) the kernels, including the caryopsis with embryo in the bottom, and endosperm covered by an aleurone layer (in naked barleys) but including the lemma, the grain palea, and the rachilla, which adhere to the caryopsis (in hulled barley) (Fig.I.1 and I.2). Barley plant can range in height from 60 to 120 cm depending on the variety and growing conditions (Samarah et al. 2009; Alqudah et al. 2016; He, Angessa, and Li 2023).

The development of barley can be described using several scales that have been defined over the years. There are three typical scales: the BBCH-scale (Campaign 2011), the Feekes scale (Large 1954) and the Zadoks scale (Zadoks, J.C., Chang, T.T. and Konzak, C.F. 1974). Zadoks scale has become the most widely used to help in many management decisions of plant growth (LANDES and PORTER 1989).

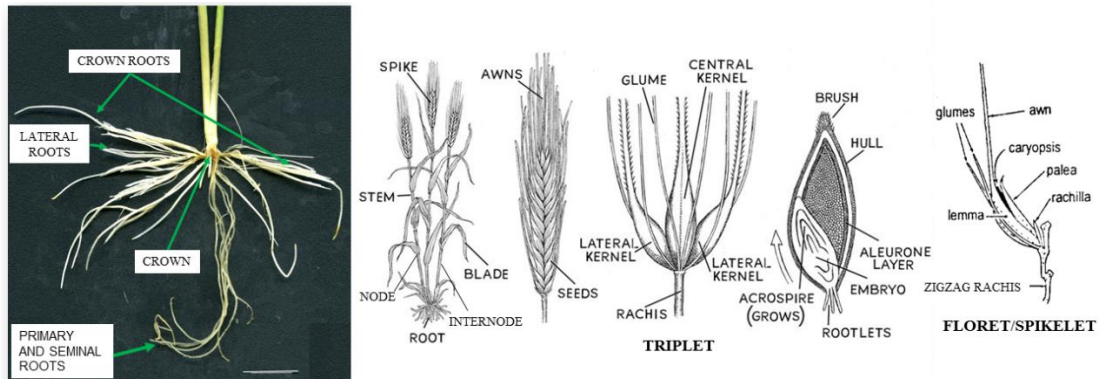


Figure I.1: Structure of barley plant. From left to right, structures of root system, whole barley plant, spike, triplet, new germinated grain (with acrospire growing up and rootlets growing out from grain) and barley floret are illustrated in detail (Adapted from image courtesy of Patricia J. Wynne: <https://www.americanscientist.org/article/why-brewers-choose-barley>; and Campaign 2011, with own root structure photo).

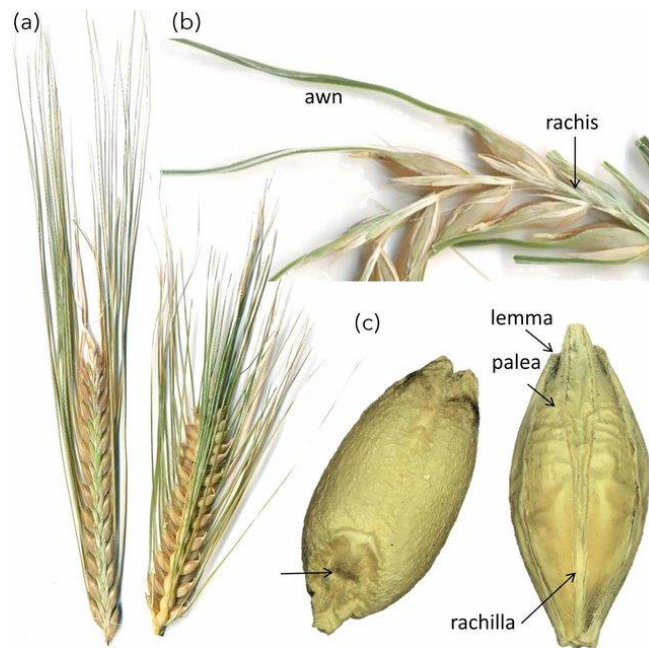


Figure I.2: Structure of barley spike. (a) two-row barley spike (left), in which kernels tend to be symmetrical and of even size; six-row barley spike (right), in which the two lateral rows of kernels are a little shorter, thinner, and slightly twisted; (b) enlarged view on spike with grains attached to the rachis at their base; some organs (lemma with long awns) change from green to yellow during grain maturation. (c) naked grain (no hull) on the left; embryo region is arrowed; hulled grain on the right; hull (palea) is slightly wrinkled (Borisjuk, Rolletschek, and Radchuk 2020).

Barley development can be divided into three main development phases (Campaign 2011; Alqudah and Schnurbusch 2017) including vegetative, reproductive, and finally grain filling (Fig I.3.A). The vegetative phase starts by germination of grain and continues with the flag leaf initiation (booting); the reproductive phase starts afterwards and lasts until the flowering stage (anthesis stage). The grain-filling phase starts with the onset of grains dry-matter accumulation to the end of ripening stage. The two first phases (vegetative and reproductive phases) are also referred to as the pre-anthesis phase. Furthermore, barley development can be divided into 10 majors' development stages, which extend the scale from 00 to 99 (Fig I.3.B) (Zadoks et al., 1974), as described below:

- (0) Germination stage is counted from dry seed to first green leaf just at tip of coleoptile, where correspond to growth stages (GS) 00 - 09. Seedlings have germinated and begin breaking through the soil crust.
- (1) The seedling stage starts from the first leaf through coleoptile to nine or more leaves emerged, corresponding to GS 10 – 19 in scale.
- (2) The tillering stage starts from the time the first auxiliary stem formed from main stem (GS 20) until plant has nine or more tillers (GS 29).
- (3) The stem elongation stage is from the time the pseudostem (the youngest leaf sheath erection) appears (GS 30) until the flag leaf ligule is just visible (GS 39). Generally, it could be counted with swollen nodes which can be felt on the main stem.
- (4) booting stage starts when the flag leaf sheath extends (GS 41) until the first awns are visible (GS 49).
- (5) Awn emergence stage is from when the tip of ear is just visible (GS 51) until the ear emergence completes (GS 59).
- (6) Flowering (anthesis) stage is from the beginning of anthesis (few anthers at middle of ear) to completed anthesis (GS 69).
- (7) Milk development starts from the kernel without starch (GS 71) to the late milk stage (GS 79).

(8) Dough development is from the early dough (GS 83) to hard dough (GS 87). In this stage, the lernel is no longer watery, but still soft and dough-like.

(9) Ripening is from the grain hard, difficult to divide (GS 91) to the secondary dormancy lost stage (GS 99).

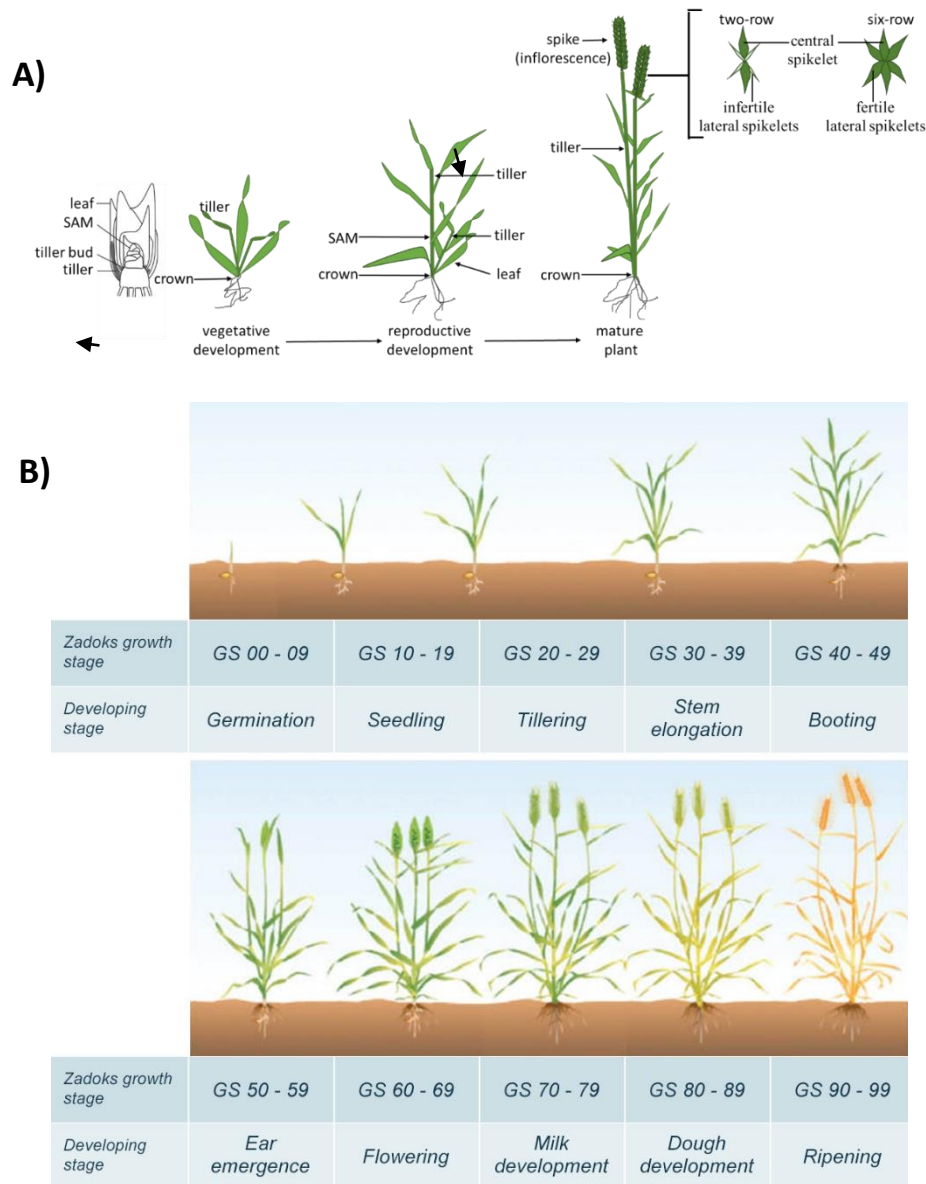


Figure I.3: Schematic diagram of the major development phases of barley. **(A)** Vegetative development, reproductive development and mature plant including illustration of two row and six row spikes. **(B)** Germination, seedling, tillering, stem elongation, booting, ear emergence, flowering, milk development, dough development and ripening. The scale was modified for cereals after Zadoks *et al.* 1974 (Ahmad M. Alqudah. 2015).

Barley is classified as spring or winter, two-row, or six-row, with or without husk depending on whether the husk is firmly attached to the grain. Spring barley can grow in the areas with moderate temperatures and sufficient rainfall and usually be sown in the beginning of spring (March). In contrast, Winter barley is mainly grown in the drought and semi-drought regions and sown in the early winter (October) (Pržulj et al. 1998). Winter barley varieties frequently require a period of exposure to cold temperatures (vernalization) (J.G.Kling, P.M. Hayes 2004). They are usually photoperiod-sensitive, that prevents them from flowering in the winter. Those traits reduce chances for cold damage. Winter barley is potentially higher yielding than spring barley, in the areas where it is adapted. In two-row barley, only the central spikelet is fertile, while the other two are reduced (Fig.I.2 and I.3.A). In six-rowed barley cultivars, all three spikelets of spikes develop completely fertile and then likely to be full grains. Furthermore, based on grain composition, barley is further classified as normal, waxy, or high amylose starch types, high lysine, high β -glucan and proanthocyanin-free (Suman 2019).

I.1.2 The origin and domestication of barley

Wild barley (*H. vulgare* ssp. *spontaneum*) is the progenitor of cultivated barley (*H. vulgare* L. ssp. *vulgare*), that is considered as the most ancient domesticated cereal crops worldwide (since approximately 8000 B.C. in the Fertile Crescent of the Middle Eastern Mediterranean) (Taner, Muzaffer, and Fazil 2004). The earliest type of cultivated barley appeared was a two-rowed barley, which was a direct derivation of ssp. *spontaneum* ancestor. Then six-rowed types occurred later circa 9500 years ago, and from approximately 6000 BC, naked forms prevailed (Bothmer, Sato, Komatsuda, et al. 2003). In the early research, due to the obvious morphological differences between two- and six-rowed barley (i.e., the lateral spikelets of *H. vulgare* ssp. *spontaneum* were too small to evolve into forms with large lateral spikelets of the six-row barley), it was firmly believed that these two forms would entirely represent separate, divergent evolutionary events. The discovery of a six-rowed form with brittle rachis in western China in the early 1930s seemed to prove that *H. agriocrithon* is the ancestor of the six-rowed barley (Murphy et al. 1978). Nevertheless, the present

opinions and studies have proved that six-rowed barley are not wild forms, but rather a result of mutational events, hybrids of diverse origins and segregation (Murphy et al. 1982; Komatsuda et al. 2007; Koppolu et al. 2013; Guo et al. 2022). The recent genetic studies have revealed that a mutation in one gene, *vrs1* (*six-rowed spike 1*), is responsible for the transition from two-row (carrying WT allele form of *Vrs1* or *HvHox1* encoding VRS1 protein, which suppresses development of the lateral rows) to six-row spike in barley (carrying mutated allele form of *vrs1*) (Komatsuda et al. 2007; Gauley and Boden 2019). This natural feature of the two-rowed progenitor barley is an evolutionary adaptation, which facilitates seed dispersal after rupture, whereas spontaneous six-rowed mutants are eliminated quickly from wild barley populations and only occurs mainly as cultivars or weeds (Komatsuda et al. 2007). Thus, there is only one evolutionary line leading to the two-rowed barley with ssp. *spontaneum* as the only progenitor from the Fertile Crescent. Then, the cultivation of barley reached Greece and Iran, and move eastwards to India very early on, approximately 8000 years ago. The first barley remains found in Spain from 5000 BC and barley reached Northern Germany and Southern Scandinavia approximately 6000 years ago. In addition, the expansion included the North African coastal region of the Mediterranean area and moving upwards along the Nile and Ethiopia ca 8000 years ago. The cultivated barley had reached China about 3000 years ago, possibly by seed exchange. Later, six-rowed hulled and naked barley became essential crops for feed and food supply in Japan.

1.1.3 Adaptability of barley (*Hordeum vulgare* L.) to environments

The sustainability and adaptation of crop populations are decided by their genetic background. Plant perception and responses to the external environment are regulated by physiological signaling pathways, underpinned by genetic networks regulating plant development, structure, and phenology. In the wild and cultivated barley, natural evolution, and human activities, respectively, resulted in the selection of beneficial pathways, genes and alleles that have allowed barley to adapt to a wide range of environmental conditions. Barley shows spring and winter growth habits, as demonstrated by its natural occurrence in extreme environments such as the north

Scandinavia, the Himalayan mountains (polar circle) or the Arabic desert, where other cereals (i.e., wheat) fail to grow (Nevo et al. 1992). Thus, barley has been cultivated in contrasting climates and various locations worldwide for centuries due to its versatility and ability to widely adapt to unfavorable climatic (cold or drought) and soil (alkalinity or salinity) conditions (Suman 2019; Taner, Muzaffer, and Fazil 2004). In this regard, barley became a model for comprehending responses of crops to climate changes (Dawson et al. 2015). Modern barley varieties have a narrow genetic basis compared to their wild ancestors because of genetic drift and high levels of inbreeding that occurred during domestication (Caldwell et al. 2006). Nevertheless, barley seed banks found all over the world represent a collection of cultivars and hybrids, and wild barley ancestors, and hence a genetic resource to discover genes that govern the adaptative mechanisms towards abiotic and biotic stresses but have been lost during domestication (Newton et al. 2011). For instance, under winter cultivating conditions, growth habit lifestyle of wild barley was optimized during the strong selection of domestication, with better adaptability such as day-length insensitivity and loss of the vernalization requirements. Comadran et al. (2012) identified natural alleles in a chromosome of barley corresponding to the EARLINESS PER SE locus EPS2, responsible for not only regulating the time of the flowering but also the yield and thousand-kernel weight. Furthermore, EPS2 seems to be not only an important factor in enabling geographical range extension but also in the gradual differentiation between winter and spring-sown barley gene pools.

I.1.4 Genomics of barley and its genetic modification

Barley genome consists of a small chromosome number ($2n = 2x = 14$) for cultivated barley (*Hordeum vulgare* L. ssp. *vulgare*) and its wild ancestor (*H. vulgare* L. ssp. *spontaneum*), but a large haploid genome size of 5.1 gigabases (Gbp) with approximately 84% of mobile or repetitive elements (larger than other cereal crop genomes including rice, but only approximately 30% of wheat genome size) (Bothmer, Sato, Knüpfner, et al. 2003; International Barley Genome Sequencing Consortium 2012; Mayer et al. 2012; Sato 2020). Within the Triticeae family, in terms of genomic size, gene content, and repetitive elements, barley has been well studied genetically

and became a prominent genomic model plant for cereal genetic research due to its similar and simpler genetic components, predominantly self-pollinating and diploid genome (Middleton et al. 2013). For example, knowledge from the diploid barley genome is especially relevant to other members of the Triticeae, particularly to the hexaploidy bread wheat, which has a more complex and larger genome. Since the beginning of the 21st century, the genome of barley has been sequenced and assembled at the chromosome-scale through multiple available genetic and genomic resources (Sato 2020). To generate a high-quality barley genome sequence, the International Barley Genome Sequencing Consortium (IBSC) was established in 2006 (Schulte et al. 2009). The cultivar (cv.) Morex, a spring six-row malting barley, has been used as a reference genome. In the 5.10 Gbp of the barley genome, the IBSC developed a physical map of 4.98 Gbp, with more than 3.90 Gbp anchored to a high-resolution genetic map (International, Genome, and Consortium 2012). Middleton et al. (2013) identified that the sequences of chloroplast from cultivated and wild barley were closely related up to 99.98% (Middleton et al. 2013). In 2016, Hisano and his colleagues assembled the complete nucleotide sequences of the mitochondrial genomes from wild and cultivated barley (Hisano et al. 2016). Two independent circular maps of the 525,599-bp barley mitochondrial genome were constructed by *de novo* assembly of high-throughput sequencing reads from the wild accession H602 and from the cv. Haruna Nijo. There were only three SNPs between the two haplotypes. Both mitochondrial genomes contained 33 protein-coding genes, 3 ribosomal ribonucleic acids (RNAs), 16 transfer RNAs, 188 new open reading frames (ORFs), 6 major repeat sequences and several types of transposable elements. The deep sequencing of the transcriptome (RNA sequencing or RNA-seq) of the cv. Morex and the full-length complementary deoxyribonucleic acid (FL-cDNA) of the cv. Haruna Nijo helped to annotate the reference genome of the cv. Morex (International, Genome, and Consortium 2012; Schreiber et al. 2020).

In 2020, Schreiber and the colleagues have developed the genome assembly for cv. Golden Promise (Schreiber et al. 2020). The cv. Golden Promise is a two-row salt-tolerant spring malting barley that was identified as a semi-dwarf mutant after a γ -ray treatment of the cv. Maythorpe, that was extensively used for malting, whisky

production and distilleries (Walia et al. 2007). The mutation at the *Arie-e* locus on chromosome 5 confers a dwarf phenotype, making cv. Golden Promise more resistant to lodging, as well as higher tolerance to a large panel of abiotic stresses (Walia et al. 2007). Even though it is no longer widely grown commercially, the cv. Golden Promise is the most efficient genotype for genetic transformation. For stable transformation of barley, PEG-mediated DND uptake into barley protoplast, particle bombardment and *Agrobacterium*-mediated DNA delivery are the main methods used (Lazzeri 1995; Travella et al. 2005; Hensel et al. 2009). For the classical stable *Agrobacterium*-mediated transformation, gene transfer target explants used are crucial for successful genetic transformation of plants. The immature embryo (Cornelia Marthe, Jochen Kumlehn 2015), androgenetic pollen cultures (Kumlehn et al. 2006), and isolated ovules (Holme et al. 2006) have been used in the barley transformation by *Agrobacterium*. Even though transformation techniques have been developed for a variety of barley cultivars (Vyroubalová et al. 2011), its transformation efficiency of barley embryos significantly depends on genotype. Hence, with the high regeneration rate, the spring cv. Golden Promise, and the winter cv. Igri, have been widely used for genetic manipulation and transformation (Dahleen and Manoharan 2007).

Several databases of barley and their respective information type are listed (Table I.1). For genomic information and available databases, EnsemblPlants provides convenient access to the most updated barley genome assembly and annotation, namely chromosome sequences, genes, transcripts, and predicted proteins. Furthermore, this website supports Basic Local Alignment Search Tool (BLAST) searches based on the barley genome. Similarly, IPK allows the user to conduct BLAST searches against all sequence resources published by the worldwide barley community, including activities related to the International Barley Sequencing Consortium. Furthermore, IPK produces not only genomic databases of the Morex cultivar, but also the barley transformation cultivar Golden Promise, to help user to blast and search for the sequences (Schreiber et al. 2020). PLEXdb hosts microarray data sets and a public resource for gene expression analysis in barley and wheat. HarVEST is essentially an EST database viewing platform emphasizing gene function. barleyGenes provides access to predicted genes from an assembly of whole-genome

shotgun sequences from barley in both cultivar Morex and Golden Promise. The expression of these genes was calculated from their RNA-seq data, which was mapped to the genome assembly. bex-db also provides FL-cDNA clones and their expression data. GrainGenes provides information including genetic maps, genes, alleles, etc. Barley DB contains information on the barley germplasm and the expression data of FL-cDNAs from Okayama University. Barley gene family databses (BGFD) includes gene information, gene structure and conserved motif analysis, synthetic analysis, phylogenetic relationships, expression patterns and genetic variation of barley genes (T. Li et al. 2022).

Table I.1: Non-exhaustive list of barley databases:

Databases	Links	Information
For barley cvs. Morex		
EnsemblPlants	http://plants.ensembl.org/Hordeum_vulgare/Info/Index	Browser, BLAST
IPK (IBSC) barley BLAST server	https://galaxy-web.ipk-gatersleben.de/	BLAST
PLEXdb	http://www.plantgdb.org/prj/PLEXdb/	Gene expression analysis
HarvEST	https://harvest.ucr.edu/	cDNA sequence
barleyGenes	https://ics.hutton.ac.uk/barleyGenes/	RNA-seq data
bex-db	https://barleyflc.dna.affrc.go.jp/bexdb	cDNA, gene expression
GrainGenes	http://www.graingenes.org	Markers, maps, mutants, etc.
Barley DB	http://www.shigen.nig.ac.jp/barley/	Seed collection, cDNA sequence
Barley gene family databses (BGFD)	http://barleygfdb.com/index.html	cDNA, structure of genes
For the barley ‘transformation reference’ cvs. Golden Promise		
IPK (IBSC) barley BLAST server	https://galaxy-web.ipk-gatersleben.de/static/galaxyweb/tables.html	BLAST
barleyGenes	https://ics.hutton.ac.uk/gmapper/	RNA-seq data

I.1.5 The production and nutritional data of barley

Barley cultivars represent the fourth most abundant cereal in both area and tonnage harvested in the World ranking next to maize (*Zea mays* L.), rice (*Oryza sativa* L.), and wheat (Faostat). According to FAOSTAT (2022), 61.7%, 15%, 13.6%, 5.9% and 3.9% of global barley production came from Europe, Asia, Americas, Oceania, and Africa, respectively (FAO 2022). Like total production, the distribution of harvested area across the continents indicated that Europe covered the most with more than 50% of barley harvested area over last 62 years. It plays essential roles including human food, animal feed and alcohol production from brewing malts (Schmid, Kilian, and Russell 2018). Whereas six-rowed barley has a higher protein content and is more suited for animal feed, two-rowed barley has a higher sugar content and is thus more commonly used for malt production. Hulled barley grains are preferred for malting and brewing due to the impact on beer flavor (Baik and Ullrich 2008). Barley is a soft straw, used mostly as bedding for livestock and as a feed providing bulk roughage. Thanks to its high carbohydrate and protein contents in kernel as well as comparatively cheaper production than the other cereals such as wheat, barley is used broadly for animal feeding (grains and straws). In addition, barley silage is fed to beef cattle and dairy cows because of its high digestibility and nutritive value for meat and milk production (Wallsten and Martinsson 2009). More importantly, there is an increased interest in barley and barley foods as healthy alternative to refined grains and as a functional food ingredient because of its capacity to reduce the risk of coronary heart disease and the rise of blood glucose after a meal (Sullivan, Arendt, and Gallagher 2013).

Barley cultivars can vary widely in their nutrient composition due to differences in genotype, growing environment, and the interaction between these factors (Aldughpassi, Wolever, and Abdel-Aal 2015). Due to the high nutritional value, some reports highlighted the importance of barley as human food sources. In general, normal barley consists of approximately 60 – 70% starch, which is mostly found in endosperm. The next abundant compound are fibers ranging from 11% to 34%, of which 3-20% are soluble dietary fibers with 5-10% β -glucan (depending on the cultivar), proteins (10 -20%), free lipids (2-3%) and minerals (1.5-2.5%) mostly

calcium and phosphorus (Newton et al. 2011) (<https://www.britannica.com/plant/barley-cereal>). Barley has a small percentage of simple sugars like glucose, fructose, sucrose, and maltose (range of 0.03-0.83%). Fibers in barley are found almost throughout the kernel. The recent focus and renewed interest in barley as a human food are largely due to the health benefits attributed to β -glucan. The β -glucan content of barley is generally higher than oats and wheat (Aldughpassi, Wolever, and Abdel-Aal 2015). The health benefits associated with consuming β -glucan rich foods include lowering blood glucose, insulin, and blood lipids, particularly the serum total LDL (low-density lipoprotein) cholesterol (referred to as bad cholesterol). Rich source of fibers in barley makes it become a comfortable diet crop for heart patients and colorectal cancer (Collins et al. 2010). Barley also contains a myriad of other components including several phenolic acids, flavonoids, lignans, phytosterols, tocols (both tocopherols and tocotrienols) and folate, and all these compounds have strong antioxidant, bioactive, antiproliferative and cholesterol lowering abilities and scavenging free radicals. Thus, barley is potentially useful in lowering the risk of certain diseases (Suman 2019). Barley is also a rich source of essential B vitamins. The short-chain fatty acid production, especially butyrate and propionate give benefit in improvement in bowel function.

I.2 The root system of cereals

I.2.1 The necessity to study root systems in cereals

Roots are crucial for plant anchorage, absorption of water and nutrients from the soil, and response to different environments and stresses. As plants cannot relocate, they require effective and dynamic root systems for water and nutrient uptake. Optimized root systems allow crops to withstand stresses of environments and efficiently utilize nutrients, which ultimately drives plant growth and yield. Root development plasticity enables plants to adapt to different environmental conditions. For instance, soil-surface roots, another unique root system, are likely to enhance plants to adapt to waterlogging, by allowing them to obtain oxygen from the air (Lone et al. 2016; Mano and Nakazono 2021). The root system architecture is determined by the interaction between genetically driven endogenous growth processes and

environmentally determined exogenous constraints such as the water content in the soil, the temperature, the nutrients and pH, and the enclosed microbial communities (Barthélémy and Caraglio 2007; Paez-Garcia et al. 2015; Rogers and Benfey 2015). Thus, understanding the root system architecture plasticity significantly helps humans improve crops with higher adaptability to different environmental conditions, especially under climate change. In cereals, a complete comprehension of root system architecture is promising to improve not only the plants adaptation to different environments but also the crop productivity (Uga et al. 2015; Lynch 2019) Typically, a deep root system is beneficial for enhancing drought avoidance, whereas a shallow root system facilitates the acquisition of essential nutrients such as nitrogen (N), phosphorus (P) and potassium (K). A deep and extensive root system permits plants to uptake soil nutrients and water from a large soil volume. Thus, the crop root system affects production, particularly under abiotic stresses including drought, waterlogging, and salinity (Kitomi et al. 2020). In 2020, Kitomi and the colleagues demonstrated that a shallower root growth angle, genetically controlled by the *quantitative trait locus for SOIL SURFACE ROOTING 1* (*qSOR1*), enhances rice yields in saline environment (Kitomi et al. 2020). *qSOR1* is negatively regulated by auxin, predominantly expressed in root columella cells, and involved in the gravitropic responses of roots. *qSOR1* was found to be a homolog of *DROI* (*DEEPER ROOTING 1*), which is known to control root growth angle and cell elongation in the root tip (Uga et al. 2013). Introducing *DROI* into a shallow-rooting rice cultivar by backcrosses enabled the resulting line to avoid drought by increasing deep rooting, and consequently to maintain high yield performance under drought conditions. The introgression lines combining the gain-of-function and loss-of-function alleles in *qSOR1* and *DROI*, respectively demonstrated four different root system architectures (ultra-shallow, shallow, intermediate, and deep rooting), suggesting that natural alleles of the *DROI* homologs could be utilized to control root system architecture variations in rice. In saline fields, the near-isogenic lines carrying the *qsor1* loss-of-function allele had soil-surface roots that enabled rice to avoid the reducing stresses of saline soils, resulting in increased yields compared to the parental cultivars.

Furthermore, the roots are the foundation of the soil health, which refers to the ability of the soil to act as a living ecosystem sustaining plants, animals, and ultimately humans. In agroecosystems, the interaction between root system, microbe, soil complex and the biochemical mechanisms is responsible for soil health (Yang, Siddique, and Liu 2020). Especially, crops can produce a variety of residues, organic matter and root exudates to enhance soil microbial diversity and activity, increase soil microbial biomass, and nutrient cycling (Gurr et al. 2016; Xiaogang Li et al. 2019; Yang, Siddique, and Liu 2020). Cong et al., (2015) found that intercropping systems, including corn, wheat, and faba beans, had about 23%, 4%, and 11%, respectively, higher root biomass and organic carbon (C)/N contents in the top 20 cm soil layer than those species in rotation (Cong et al. 2015). Root exudates released by plants are important carbon and energy sources for soil microorganisms, helping to cycle nutrients and kill pathogens (L. Chen and Liu 2024).

Importantly, after extracting the root data, it is necessary to identify the traits that are meaningful and pertinent for a specific agronomical condition. For instance, the “Steep, cheap, and deep” model has been proposed as an ideotype for the cereal root system cultivated with limitation of nitrogen and water input (Lynch 2013). Under nitrate-deficient conditions, less lateral root branching and low crown root numbers (“steep”) are (Saengwilai, Tian, and Lynch 2014; Zhan and Lynch 2015). A deep root system (“deep”) is required because water percolates and soluble nitrates leach into deeper soil layers. This ideotype represents an optimized root system for nitrogen and water in depth together with a low cost in terms of carbohydrates allocated to roots. However, when the relative immobile phosphorus, potassium, calcium, and ammonium are limited to short and shallow root systems with numerous lateral roots and long root hairs is more effective to utilize these resources. Root traits are becoming a key target for a second green revolution and crucial for high-yield crop production (Lynch 2007)(Herder et al. 2010). Therefore, comprehension of the factors and mechanisms affecting the root system architecture will significantly help to design root ideotypes, that integrate the root number, diameter, growth angle, and branching pattern, for the healthy agronomical system. Additionally, engineered plant root systems provide a means to react to rapidly altering environmental conditions and

changes in soil characteristics of different habitats and global climates changes, thereby ensuring the security of food Worldwide (Shekhar et al. 2019).

I.2.2 Overview of phenotyping methods to study root system.

I.2.2.1 Methods for root phenotyping the root system Architecture (RSA)

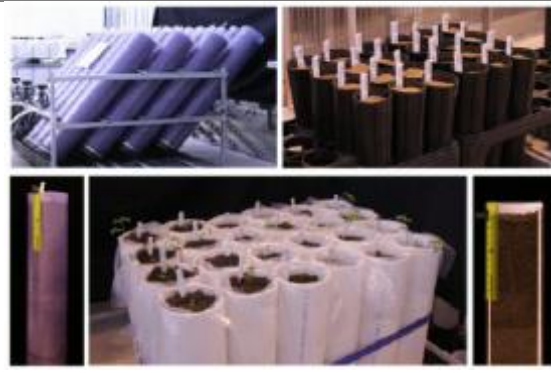
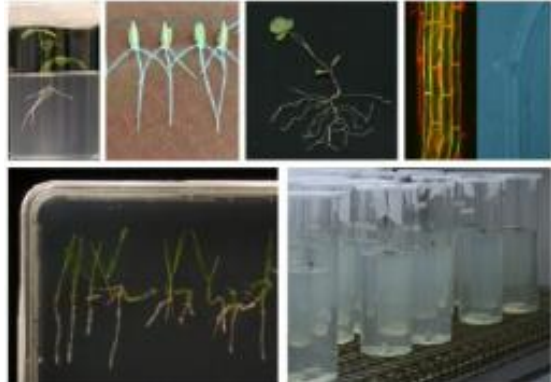
To comprehensively understand the structure of root systems in cereal crops and improve crop performance, the development of phenotypic analysis technologies is a critical aspect for the characterization of root growth patterns and functional analysis of genes involved in root development. Root system architecture (RSA) refers to the shape and spatial arrangement of root systems within the soil (de Dorlodot et al. 2007). Roots are challenging to access into the soil, making them difficult to measure or phenotyping. This “phenotyping gap” hinders research aimed at understanding how roots forage and influence crop productivity. To phenotype RSA, accessible tools are available to allow researchers to study the shape and arrangement of roots within the soil. The phenotyping methods can be carried out at different scales and in different scopes of experiments. There are two main components concerning root phenotyping including methods for culturing the plants and root image tools (Maqbool et al. 2022). In general, the methods for plant growing can be divided into different practical areas including field methods, greenhouse methods and laboratory methods, and they have their own advantages and disadvantages (Figure I.4) (Paez-Garcia et al. 2015). Furthermore, root phenotyping methods can be divided into destructive methods and non-destructive methods. The traditional root phenotyping methods including soil core (Kücke, Schmid, and Spiess 1995), trenches (Weaver, J.E. 1922; Sekiya et al. 2013), mesh bag, shovelomics, and monolith are all destructive and mostly applied for field experiments. They involve extraction of the root system from the soil for phenotyping analysis. However, root phenotyping under field conditions is a major obstacle to tracking these below-ground traits due to cost, time and labor intensity, and partial destruction at specific times. For instance, soil core provide only partial root system data due to the limited sample collection (Hirokazu Takahashi and Pradal 2021). The trenches method is time-consuming and labor-intensive. The mesh bag method is

limited to studying the roots only in the upper soil. In addition, the soil structure and composition in the field are not homogeneous, which could impact the RSA by other confounding factors at different sites of plant growing within a field due to the genetic, the plasticity of roots and the environment interactions (Bao et al. 2014; Correa et al. 2019; Takahashi and Pradal 2021). Thus, it is crucial to achieve appreciate sampling and field design, uniform field management and environmental recording. These require a growth system, imaging device and software tools. A variety of manual (e.g. DART), semi-automatic (e.g. SmartRoot and RootNav) and automated (e.g. DIRT, REST, GiAroots and RhizoVision Explorer) software programs have been established for characterizing RSA traits (Lobet et al. 2015). Phenotyping pipelines have been adapted to artificial growth conditions in order to strategically calculate easily measurable root traits. On the other hand, powerful non-destructive three-dimensional (3D) imaging technologies like X-ray computed tomography (X-ray CT; Mooney et al., 2012, magnetic resonance imaging (MRI; van Dusschoten et al., 2016), position emission tomography (PET; Harbout et al., 2020) offer new opportunities for *in situ* visualization of roots at a higher resolution. In greenhouse, root box-pinboards, soil filled grass rhizotrons and polyvinyl chlorides (PVC) tubes have been used (Shashidhar 2012).

In the field condition, from simple measurements of root intersection densities (number of roots intersecting a vertical plane per unit of surface; RID) on trench profiles, Faye and colleagues (2019) developed a model to predict and map root length density (total length of roots per unit of soil volume; RLD) of pearl millet (*Pennisetum glaucum* (L.) R. Br.) and predict the RSA *in silico* (Faye et al. 2019). They showed that root orientation – an essential parameter to improve the relationship between RID and RLD, depends on soil depth and differ between thick root (i.e., seminal and crown roots; more anisotropic with soil depth) and fine roots (i.e., different types of lateral roots; isotropic at all with soil depth). In addition, the model uses the RLD as a key factor to estimate the soil volume and profile (i.e., amount of available water and nutrients) explored by a root system of the plant, hence to screen drought-tolerant varieties and measure the effect of water stress on RSA in the field conditions.

Table I.2: Different approaches for root phenotyping in the field, laboratory and greenhouse, and their advantages and disadvantages. Field: overview of an alfalfa field trial. Shovelomics approaches wheat roots. Washed roots from field-grown alfalfa plants. Tractor for acquiring core samples. Outline of root area for harvest. Greenhouse: EnviroKing® (Harrington Industrial Plastics, Albuquerque, NM, USA) UV clear PVC piping at a slanted angle. Black deepots. Semi-cylindrical mesocosm fronted with clear plexiglass; mesocosms with plastic liners. Individual EnviroKing® UV clear PVC piping for real-time observation of RSA including root depth. Laboratory: alfalfa (*Medicago sativa* L.) roots in clear vials and growth media. Wheat seedlings growing on germination paper in plastic trays. Alfalfa seeding imaged using flatbed scanner. *Arabidopsis thaliana* roots stained with propidium iodide to observe cell wall and green fluorescent protein (GFP) labeling the actin cytoskeleton. *A. thaliana* root showing lateral root initiation. Alfalfa seedlings growing in glass cylinders with growth media. *Brachypodium distachyon* (model grass) seedlings growing in growth media in plates (Adapted from Paez-Garcia et al. 2015).

Approaches	Advantages	Disadvantages	
Field methods	Physiological and practical relevance.	Labor and time intensive. Challenges due to variability in the field, particularly for soil conditions. Intensive root clean-up. Destructive assays. Permits are required for evaluation of transgenic plants. Very difficult, costly, time-consuming.	

<p>Greenhouse methods</p>	<p>Intermediate system between lab and field. Enables control of certain conditions including soil type and moisture, light intensity, temperature, pot sizes and water and nutrient inputs. Evaluate genetic potential of plant RSA without intraspecific competition. Easy to measure strategical target components of the root system.</p>	<p>Labor and time intensive Challenges due to variability in the field, particularly for soil conditions Intensive root clean-up Destructive assays No competition evaluation</p>	
<p>Laboratory methods</p>	<p>Control and evaluate root growth in real time. Non-destructive. Many controlled growth conditions can be tested. Repeatable conditions. Large space for plant growth is not required. Easy to handle and clean roots. Reduce environmental noise by allowing a higher throughput and more standardized micro-environment.</p>	<p>RSA may be affected by the growth container. Sterile conditions for evaluation exclude the effect of possible interaction with beneficial microbes. Plants are not exposed to environmental conditions and therefore no physiological relevance.</p>	

Several alternative methods for culturing the plants are developed for the different requirements of RSA data selection (Kujken et al. 2015). For different purposes, the plant culture methods include artificial gel-based media or soil-filled containers and rhizotrons, hydroponic and aeroponic (Paez-Garcia et al. 2015). Naturally, root growth is easily influenced by short-term environmental stimuli. For instance, microscale soil water content pattern and soil compaction may affect the RSA and influence root growth and extension, which cause the differences in RSA between plants grown in soils and those raised hydroponically (Takahashi and Pradal 2021). Various approaches have been used for phenotyping RSs including destructive, non-destructive. High throughput phenotyping is important to bridge genotype and phenotype. Individual parameters include root length, branching and diameter, which can be described in both static and dynamic observation (Fang, Yan, and Liao 2009; Clark et al. 2013; Topp et al. 2013). Root system architecture incorporates root surface area, root density and root volume. *Ex situ* platforms can capture a static assessment of root architecture metrics. *In situ* platforms enable direct imaging roots within the growth medium to characterize dynamic metrics. Various phenotypic technologies have been implied for the identification of diverse root traits in the field as well as laboratory conditions, such as root-box pinboards, rhizotrons, shovelomics, ground-penetrating radar, etc. These phenotypic analyses also help in identifying the genetic regulation of root-related traits in different crops.

The downstream analysis of RSA images is also a crucial component for root phenotyping strategies. Hence, the methods used to evaluate the RSA should provide an accurate representation of root growth. Several software packages have been developed for imaging roots and extracting quantitative data from captured root images. A few examples of those software tools are RootScan, RootNav, DART, GiARoots, IJ Rhizo, RootSystemAnalyzer, RootReader, RootReader3D, and RootTRack (Paez-Garcia et al. 2015). The growing number of image analysis techniques for RSA phenotyping led to the development of Root System Markup Language (RSML) format, to share RSA data between different software packages as well as establish centralized repositories of RSA traits data (Lobet et al. 2015). Each method has its advantages and disadvantages. There are both traditional and current

root structure phenotyping including advanced digital photography, X-ray computed tomography, transparent soils, automated rhizotron and aeroponic installations, high-throughput 3D reconstructions, fluorescence-based and luminescence-based imaging systems and so on (Motte, Vanneste, and Beeckman 2019) to better understand RSA. Advances in high-throughput root phenotyping, computer vision applications and genomic approaches now allow direct selection of desirable root traits (Maqbool, Hassan, et al. 2022).

In conclusion, the methods chosen for culturing plants for root imaging will depend on a suite of factors including the specific root trait of interest (Primary and seminal roots, crown roots, lateral roots and so on), the desired timescale for sampling (hours, days, months and so on), infrastructure capacity and costs. For example, of one complex research of RSA phenotyping is a semi-hydroponic phenotyping system that was developed for barley (J. Wang et al. 2021). describe it and give its advantages Root images then is analyzed in WinRHIZO Pro. Say what kind of parameters you can measure and why it is well adapted to barley The high-throughput phenotyping system using clear pots (Richard et al. 2015). It requires less time, space, and labor compared to the growth pouch method. It is suitable for large-scale and high-throughput screening of seedling root characteristics in crop improvement programs, to characterize root angle and root number.

I.2.2.2 Methods for root phenotyping the root anatomy and physiology

The root anatomy and physiology represent new frontiers for high throughput phenotyping of crop roots, in that researchers can visualize, quantify, and conceptualize root architecture and its relationship to crop adaptation and productivity. Exploring the basis of root anatomy can dramatically enhance the future of plant improvement because a fundamental feature of plant form and function is the structure and organization of cells and tissues. Root anatomical traits play crucial roles in understanding root functions and root form-function linkages in their genetic and physiological analysis (Lynch et al. 2021a). For the purpose of anatomical phenotyping, anatomics has become a novel phenotyping strategy, which deeply used the advantage of high-throughput imaging and quantification of plant anatomy (Strock,

Schneider, and Lynch 2022). Imaging is the first crucial step. Light microscopy is well suited for imaging superficial structures (i.e., root hairs). In the field experiment, an inexpensive and compact portable microscope using a smartphone allows rapid in imaging and is highly practical (Y. Liu et al. 2021). Then, high-throughput, field-based imaging from portable microscopes will be analyzed by multiple disciplines such as ecology, physiology, and crop breeding (Strock, Schneider, and Lynch 2022). For imaging internal structures, the advent of laser ablation tomography (LAT) addresses gap in sample throughput and spatial scale (Hall and Lanba 2019; Strock et al. 2019) (Fig.I.5). A fundamental objective is a 2D structure image and possibly a 3D imaging by combining with advanced techniques such as confocal microscopy, nuclear magnetic resonance (NMR), micro-computed tomography (micro-CT), and LAT. Moreover, all these advanced techniques have unique capabilities and limitations in their capacity to capture anatomy in 3D. NMR is limited by imaging resolution, the exclusion of ferromagnetic instruments for simultaneous physiological measurements, and the size constraints of current generation NMR magnets (i.e., 1m length and 10cm narrow diameter) (Brodersen and Roddy 2016). Although NMR and micro-CT are nondestructive, the limited throughput in image resolution of these methods diminishes their utility. Confocal microscopy is well suited for 3D imaging but is low throughput and is constrained by tissue opacity. Perhaps, the most advantages of these new visualization techniques are not the ability to grasp static anatomical and morphological features, but rather their ability to observe the physiological processes *in vivo*. Anatomic requires accurate and precise measurement to determine the relationships between plant structures and the genetic control of anatomical phenotypes. Nowadays, all resources of software for imaging analysis are available.

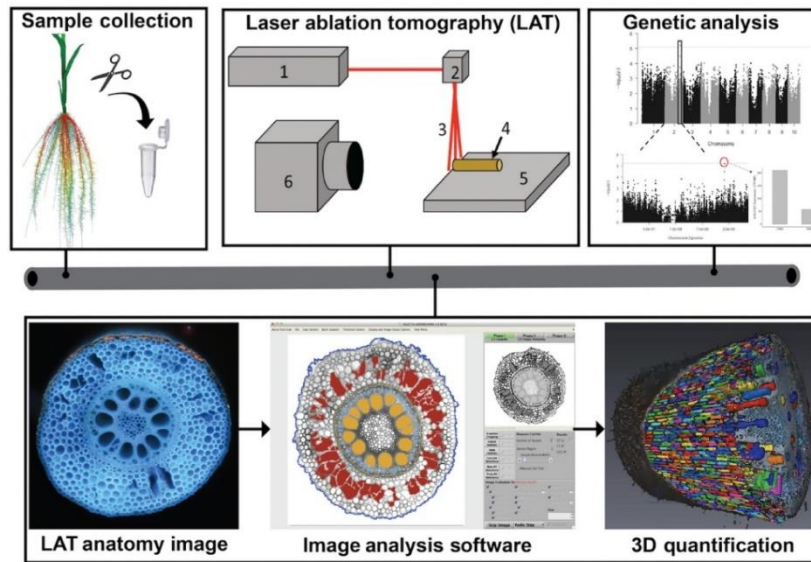


Figure I.4: Visualization of the Anatomic pipeline from sample collection through identifications of genetic markers. From left to right of the figure: samples are first collected from field-grown plants and preserved in 75% (vol/vol) ethanol, then imaged directly from storage in ethanol with laser ablation tomography (LAT), after that images are phenotyped using image analysis software, and finally genetic markers are identified. The LAT is composed of a pulsed UV laser (1), which is modified through beam-shaping optics (2) to create a ‘cutting sheet’ (3) and directed onto a sample of plant tissue (4). The sample is advanced into the ablation plane by a motorized stage (5) while a high-resolution camera (6) images the anatomy that is exposed as the tissue is ablated (Strock, Schneider, and Lynch 2022).

I.2.3 The root types, organization, and their function in cereals

I.2.3.1 Types of roots in cereals

The root system of cereals, and other monocotyledonous plants, comprises of embryonic roots (primary and seminal roots) and post-embryonic roots (crown roots/nodal roots/shoot-born roots/adventitious roots and lateral roots/root-born roots) (Fig.I.6) (Orman-Ligeza et al. 2013; Atkinson et al. 2014). Primary, seminal and crown roots can produce new branched roots - called lateral roots, which can develop in turn successively higher order branched roots, up to the third order. Whereas the dicots have only one primary root that branches continuously to create several orders of lateral roots (tap root system), monocots or cereals have a fibrous root system mainly made up by post-embryonic shoot-born crown roots and root-born lateral roots. The root system architecture includes two important concepts: (1) the geometric dispersion

or spatial configuration (the shape) of roots within the soil space and (2) its structure consisting of the number and length of post-embryonic roots, and the total surface of whole root system (de Dorlodot et al. 2007; Kuijken et al. 2015; Lynch 2019). Up to date, cereals root systems have been studied in different species of cereals including rice (Zhang and Wing 2013; Mai et al. 2014; Meng et al. 2019), maize (Hochholdinger 2009), Pearl millet (Passot et al. 2016), barley (Stein and Muehlbauer 2017; Robinson et al. 2016), *Brachypodium* (Ogden et al. 2020), wheat (Pflugfelder et al. 2022; Maqbool, Ahmad, et al. 2022) and Sorghum (*Sorghum bicolor* (L.) (Rostamza, Richards, and Watt 2013).

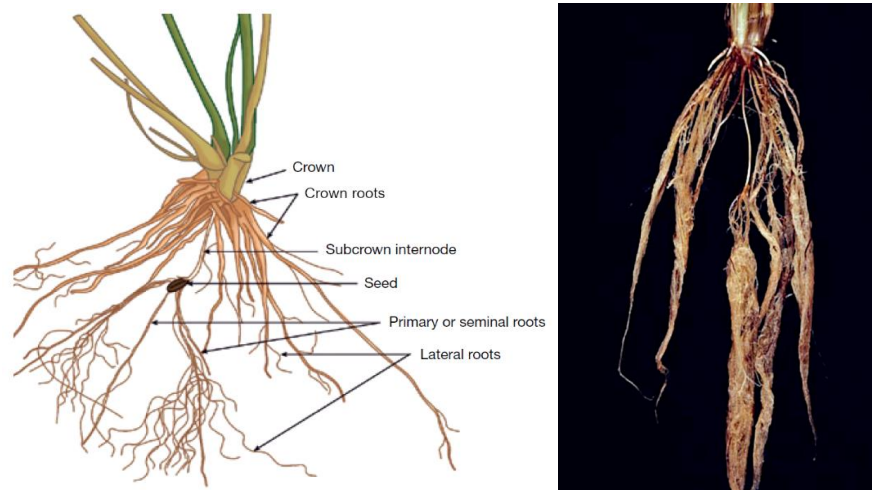


Figure I.5: Illustration of root structure of a barley mature plant (left) and a healthy soil-removed root system of a barley (right) (adapted from Macleod et al. 2008).

I.2.3.2 The organization and functions of cereals root systems

The embryonic roots (Fig.I.7-A), whose primordia are laid down during embryogenesis, grow after germination and functions to ensure seedlings' water and nutrients uptake. They are important for plant establishment at early developmental stages and sometimes persist functional over the whole life cycle (Caroline Marcon , Anja Paschold and Frank Hochholdinger 2013). In rice, pearl millet, sorghum and *Brachypodium distachyon*, only a single embryonic primary (or radicle) root is formed from the seedling basal pole. However, maize, barley, and wheat form a primary root and a variable number of seminal roots/ or basal root roots arising from a scutellar node, in the embryonic hypocotyl region (Luxovx 1986; Hochholdinger et al. 2004). In some cereals like barley, it is not possible to visually distinguish between primary

root and seminal roots because of their simultaneous emergence and similar diameter. Moreover, in some other cereals like maize, the seminal roots appear after few days of the primary root's emergence, and it is able to clarify between them (Fig.I.7-A) (B. Orman-Ligeza et al., 2013; Caroline Marcon, Anja Paschold and Hochholdinger 2013).

After germination, the root system is made up by the development of the postembryonic roots, which allow plants to exploit soil resources and respond to changing environmental conditions such as lack of nutrients, flooding or drought. Postembryonic roots include a class of shoot-borne roots called nodal roots, developing from a node of the main stem and tillers. It exists two types of nodal roots: crown roots developing from the underground nodes, and brace roots formed from aboveground nodes (Fig.I.7-B and C) (Caroline Marcon , Anja Paschold and Frank Hochholdinger 2013) (Atkinson et al. 2014). Crown roots are essential for plants at later stages when they dominate the root system of adult cereals (Hochholdinger et al. 2004 and 2018). Crown roots are produced both during normal development and in response to stress conditions (Stein and Muehlbauer 2017; Gonin et al. 2019). Brace root not only solely ensures anchorage of the plants like in maize (Hochholdinger, Yu, and Marcon 2018) but also have function in the uptake of water and nutrients (Hostetler et al. 2021; Sparks 2023). In cereals, the post-embryonic shoot-borne root system keeps the major backbone of the root stock (Hochholdinger et al. 2004). The elongation of crown roots predominantly increases the volume of soil explored.

Embryonic roots and crown roots differ in their anatomy and physiology. A very early study with hydroponically cultured wheat, barley and rye plants has indicated that embryonic roots only absorb 25% of the water between flowering and maturity, while the other 75% of water was absorbed via nodal roots (Krassovsky, I. 1926). Whereas the primary roots are very slender and branched throughout their length, having a thin-walled cortex with no exodermis, the crown roots are centrally thicker, and possess a wider central stele and larger metaxylem areas (in maize and pearl millet), than seminal roots (Yu et al. 2015; Passot et al. 2016). When exposed to hypoxia, wheat can form a 30% larger aerenchyma area in the crown roots than in the embryonic roots, suggesting that the crown roots have higher anatomical plasticity and

can transport O₂ more efficiently under hypoxic conditions (Thomson et al. 1990). At the physiological level, crown roots can have higher hydraulic conductivity (Tai et al. 2016) and water uptake capacity (Ahmed et al. 2018) than the primary and seminal roots. Furthermore, maize brace roots have been shown to respond more strongly than seminal root to locally supplied nitrate (Yu et al., 2016). This suggests that the postembryonic root type has a superior morphological plasticity allowing for more efficient adaptation to external nitrogen availability (Zhaojun Liu et al. 2021). In barley, the crown roots have a larger metaxylem area that is associated with a higher capacity for nitrate uptake and translocation (Z. Liu et al. 2021). Thus, the number and area of metaxylem vessels in the crown roots could represent interesting targets when selecting genotypes for higher nitrogen uptake and translocation efficiencies.



Figure I.6: Organization of cereal root systems. (a) Embryonic primary (PR) and seminal (SR) roots of 5-day-old rice, maize and barley seedlings (from left to right). (b) detail of a 10-day-old maize, seedling with two new shoot-borne crown roots (CR). (c) Aboverground brace roots (BR) of adult rice plants (Caroline Marcon , Anja Paschold and Frank Hochholdinger 2013).

Lateral roots, another class of post-embryonic roots, are root-borne roots branched from primary, seminal and crown roots; they produce additional branching levels. The aboveground brace roots branch lateral roots only after penetrating the soil (Hochholdinger et al. 2004). Most lateral roots are small and thin, elongate laterally, exhibit agravitropic and determinate growth, and never bear lateral roots, whereas

there are also a few large, long and thick lateral roots, which are thinner in diameter than primary and crown roots and display indeterminate growth. These large lateral roots elongate downward in response to gravity and can also bear higher-order lateral roots including both small lateral roots and large lateral roots. The bigger type of lateral roots plays an important role in expanding the root network in the soil. The small lateral roots largely contribute to the hydraulic conductivity of the whole root system, representing the water uptake ability (Q. Zhang and Wing 2013). For example, in rice, the plastic development of lateral roots plays an essential role in adapting to soil water fluctuation (Lucob-Agustin et al. 2021). In maize, three to four lateral root types have been reported (Varney et al., 1991), while three in rice (Gowda et al., 2011; Henry et al., 2016), three in pearl millet (Passot et al. 2016) and five in wheat, barley, and triticale (*Triticale hexaploide*) (Watt et al., 2008). The formation of mostly lateral roots enlarge the absorptive surface of the root system (Hochholdinger et al., 2004 and 2017).

The anatomical point of view shows different specific cell layers of a root including root epidermis, cortex cell layer (8 to 15 layers in cereals), endodermis, pericycle and a central cylinder (Fig.I.8). Along the longitudinal view, a root consists of three zones: a zone of cell division, a zone of elongation, and a zone of maturation and differentiation (Fig.I.8). Root growth is scoped to a region of the root tip that includes the cell division zone and elongation zone (Fig.I.8). All root cells originate from the apex stem cell core (quiescent center), where the cell cycle is tightly controlled. From the quiescent center, cells migrate to its boundary and differentiate to root cell files. The meristematic zone extends to about 1 mm from the tip and the zone extends another 2 mm from the tip (Shelden and Munns 2023). The tip of root is protected by a root cap – an exclusive structure to the root.

Root hairs, which are unicellular functional units of the root system, are also an important component of the root system architecture as they increase the surface for water and nutrients uptake and represent the interface for plant-microbe interaction (Fig.I.8) (Cai and Ahmed 2022). They contribute to almost 50% of water absorption by the plant (Paez-Garcia et al. 2015). Root hairs initiate in the maturation zone of the root tip (Fig.I.8), and are formed from all of primary, seminal, crown and lateral roots.

Root hairs, which are long tubular-shaped, develop due to the asymmetric cell division of trichoblastic cells on the outer surface of the root epidermis (Marzec, Melzer, and Szarejko 2013). Their development is significantly impacted by environmental signals, ensuring optimal acquisition of nutrients.

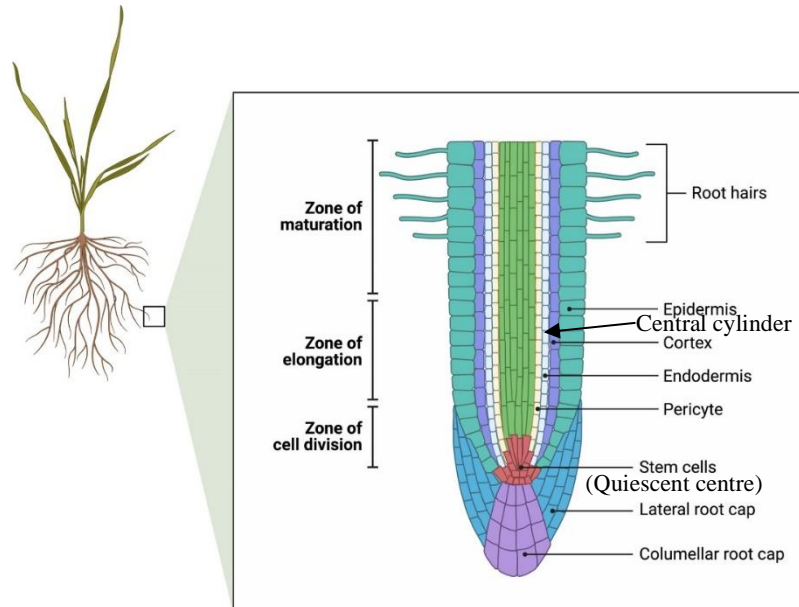


Figure I.7: Longitudinal view of root tip. The zones of maturation, elongation, and cell division (the apical meristem) were illustrated. Root hairs begin to develop in the mature zone. Different cell layers were also distinguished (adapted from Sheldon and Munns 2023).

I.2.3.3 Barley root system

Barley, like other cereals, has a typical fibrous root system. Distinct embryonic and postembryonic root types that are formed during different phases of development determine barley root system architecture. While embryonically preformed roots dominate the early seedling root system, an extensive shoot borne rootstock determines the adult rootstock of barley (Robinson et al. 2016). The embryonic root system of barley is not only essential during plant establishment but also usually remains functional over the whole life cycle.

In barley, primary and seminal roots may differ to crown root in function during plant development. Crown roots have the greatest in thickness, larger diameter, larger metaxylem area and a larger number of metaxylem vessels than primary and seminal root (Fig.I.9-C,D,G,H,I to K) (Zhaojun Liu et al. 2021). This larger metaxylem

volume of crown roots, which are regulated by some cell wall and cytoskeleton organizing proteins as well as with higher level of auxin content, is able to enhance predominantly the low-affinity uptake and translocation capacities of nutrients that are transported with the bulk and higher flow of water, like nitrate.

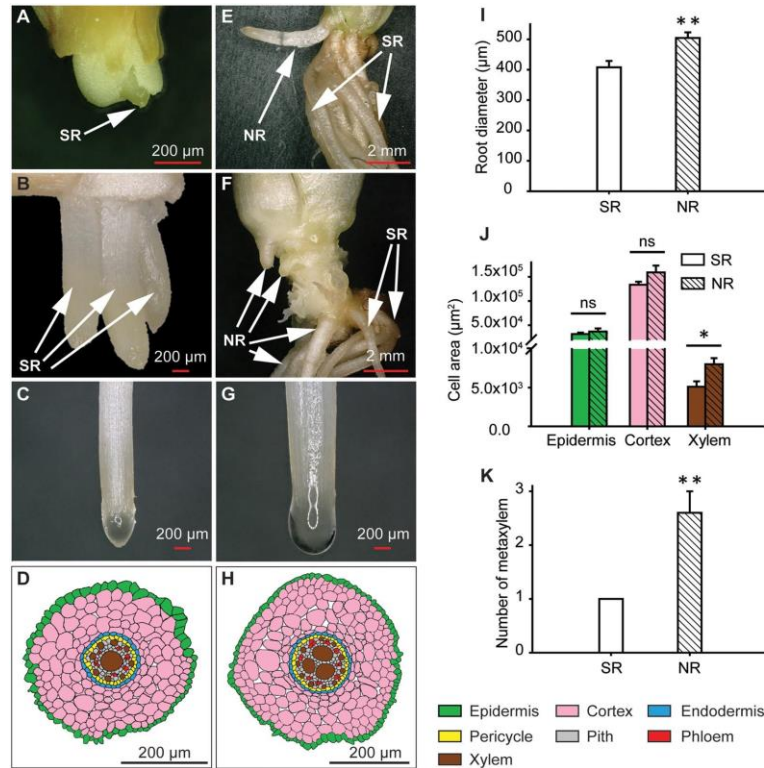


Figure I.8: Development and anatomical differences between embryonic/seminal roots (SR) and crown root/nodal root (NR) in barley. (A) Emergence of the primary root from the seed 4 day after sowing (DAS). (B) SRs at 7 DAS. (C) Apical root zone of one SR at 25 DAS. (D) Cross-section of SR from mature zone at 25 DAS. (E) First emerged NR at 20 DAS. (F) NR development at 39 DAS. (G) Apical root zone of an NR at 39 DAS. (H) Cross-section of NR from mature zone at 39 DAS. (I) Root diameter in the mature root zones of SR and NR. (J) Area of epidermal, cortical or xylem cells calculated from cross-sections of SR and NR. (K) number of central metaxylem vessels in SR and NR (Zhaojun Liu et al. 2021).

There are two types of crown root in barley. The type one, two short crown roots (Fig.I.9-E and F), come off from the grain at the early stage of barley seedlings, however they do not arise from the same point as primary and seminal roots (Fig.I.9-A,B,E,F). The type two – the majority of the crown roots in barley form from nodes above the grain. However, the study of anatomy and functions of crown root in barley is not still fully explored. There is undoubtedly a connection between the tillering of a

plant and its formation of crown roots. In the soil, crown roots are nearer the surface of the soil than are the primary and seminal roots.

I.2.4 Description of cereal roots' origin

I.2.4.1 Primary and seminal root initiation and development

In the embryo, the primary root primordium (i.e., in rice, there is one primary root) and the primordia of seminal roots (i.e., in maize and barley, there are several seminal roots) are initiated. In barley, the primary root is initiated below the scutellar node (embryonic root-shoot junction) at the basal pole of the embryo, while the seminal roots are formed later at the scutellar node from the mesocotyl (Fig.I.10). The number of seminal roots depends on genotypes.

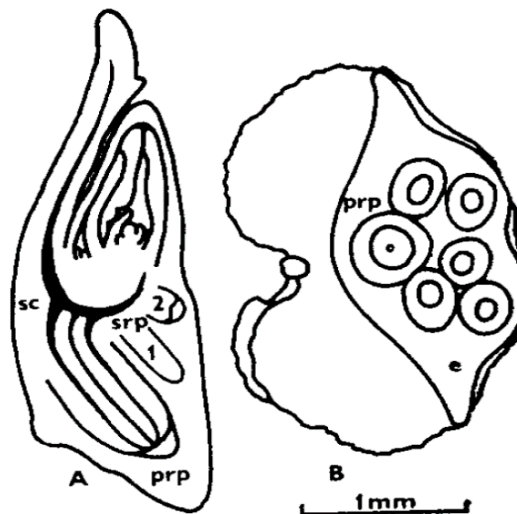


Figure I.9: Illustration of barley primary and seminal root primordia. (A) Longitudinal median section through a mature barley embryo. (B) Cross section through a mature barley grain shows the primary root primordium and five secondary seminal root primordia. Note: prp: primary root primordium, sc: scutellum, srp 1,2: secondary seminal root primordia, e: embryo (Luxovx 1986).

In maize, the primary root is formed endogenously deep inside the embryo and becomes visible in the embryo region about 10-15 days after pollination (DAP) (Abbe and Stein 1954). In rice, the primary root/radicle can be recognized at the ventral side of the embryo from around 5 DAP (Zhang and Wing 2013). In maize, primary root emerges at the coleorhiza of the seed (Hochholdinger, Woll, et al. 2004).

I.2.4.2 Lateral roots initiation and development

In most angiosperms, the initiation of lateral roots occurs frequently away from the root meristem, in the mature zone of the root. In cereals, lateral root primordia commonly originate from a subset of cells in this mature zone, which are referred to as founder cells, at the periphery of the parent root's stele. In some cereals such as maize, rice, barley and wheat, founder cells arise from pericycle and endodermis cells, that are located opposite to the phloem poles (Casero, Casimiro, and Lloret 1995; Demchenko and Demchenko 2001; Hochholdinger, Park, et al. 2004; P. Yu, Gutjahr, et al. 2016), contrasting with eudicots, in which primordia initiate from pericycle cells opposite to the protoxylem poles (Casimiro et al. 2001). This arrangement leads to protophloem-based longitudinal files of lateral cells (also termed ranks or poles) at the end of which lateral root primordia (LRP) are initiated during parent root growth, in a strict acropetal sequences, with the youngest primordia appearing closest to the root tip (Draye 2002; Orman-Ligeza et al. 2013; P. Yu, Gutjahr, et al. 2016). In the most of cereal roots, which contain the polyarchy stellar organization including several phloem poles alternating with the same number of xylem poles, lateral roots appear in several longitudinal files, the number of which is roughly proportional to the stele diameter (Orman-Ligeza et al. 2013). Within each file, LRP formation follows an acropetal sequence, often at a predictable distance and conserved among genotype (Mallory et al. 2013; Orman-Ligeza et al. 2013). However, the stability of acropetal sequence in cereals can easily be affected when the development of LRP is disturbed before emergence (Lavigne et al. 2012). The first morphological events of lateral root initiation are observed on the proximal side of the elongation zone of the parent root (Demchenko and Demchenko 2001; Orman-Ligeza et al. 2013).

Lateral root formation in cereals has been classified into three developmental stages: organ initiation, growth through the cortex, and emergence through the epidermis (Orman-Ligeza et al. 2013). Figure I.10 describes the different steps of lateral root formation in barley. Initially, the lateral root initiation starts with asymmetric anticlinal cell divisions of two longitudinally adjacent pericycle cells, opposite to a protophloem pole (Fig.I.10-B-I and I.10-C) (P. Yu, Gutjahr, et al. 2016). Subsequently, the two daughter short cells expand radially and then start asymmetric

periclinal divisions, forming two inner and two outer cells (Fig.I.10-B-II and I.10.C). Following, pericycle cells continue their periclinal divisions and endodermal cells start dividing anticlinally (Fig.I.10-B-III and I.10-C). In subsequent stages, a multistep process of anticlinal and periclinal divisions of outer daughter cells give rise to new LRP (Fig.I.10-B-IV-V, I.10-C and I.10-D-E). Later, a few cells in front of the primordium divide synchronously and periclinally to generate an inner layer of root cap initials and an outer layer of root cap cells (Fig.I.10-B-VI and I.10.C). When the primordium has progressed halfway through the cortex, a morphologically distinguishable meristematic zone and root cap are possibly observed (Fig.1.10-B- VI, I.10-C and I.10-F-G). The region where the stele develop can be distinguished easily from cortical area in which the cells are larger and slightly elongated suggesting that pro-vascular tissue is differentiating but no true vascular tissue forms until the primordium has reached the outside (Fig.I.10-B- VII and I.10-C). After emergence, the apical meristem of lateral root is activated, and the lateral root continues growing.

The reprogramming of the cells in the pericycle layers supports the LRP growing and emerging through the overlying cortical and epidermal layers of the parent root. For example, in the initial stages of lateral growth in maize, the loosening of the walls of the cortical cells was observed all around the primordium; that process involves the action of cell wall enzyme such as a subtilisin-like protease (AIR3), pectate lyase (PLA2), polygalacturonase (PG), a xyloglucan: xyloglucosyl transferase (XTR6), expansin (EXP17) and a glycosyl hydrolase (GLH17) (Swarup et al. 2008). The division of cortical cells directly covering the lateral root primordia initiates this loosening.

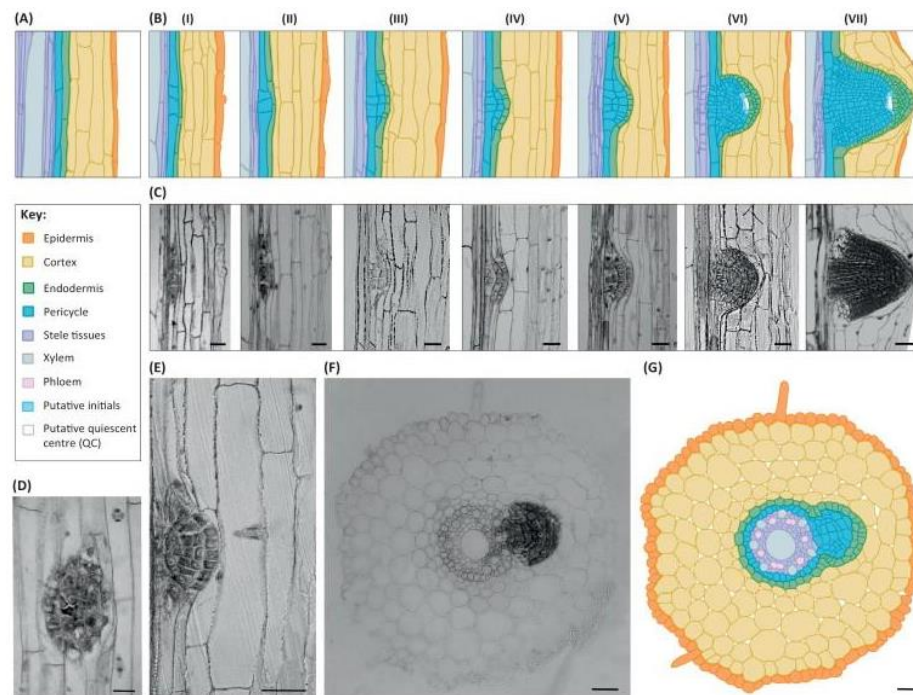


Figure I.10: Lateral root development in barley. (A) illustration of a longitudinal section showing the typical tissue organization of cereal roots. (B) Succession of morphological stages during lateral root development and emergence. (C) Original toluidine blue stained sections used for illustrations in (B). (D) Periclinal and (E) anticlinal longitudinal sections of the growing lateral roots. The sections show an extensive cortical region around the primordium where divisions are taking place. (F) Radial tissue organization of cereal roots (toluidine blue staining). (G) illustration of the section in (F) to highlight the deformation of the cortex that occurs during lateral root penetration. (Scale bars = 50 μm). Figure and footnotes are cited from Orman-Ligeza et al. 2013.

I.2.4.3 Crown roots initiation and development

Crown roots initiate in cereals from different specific cell types compared to the lateral roots. Whereas lateral roots initiate from the pericycle and endodermal cells of the parents' roots (Yu et al. 2016), crown roots develop from a region, called ground meristem (similar to the pericycle of lateral root initiation area), adjacent to the peripheral cylinder of the vascular bundles in the stem nodes, located between stele and the starch granule rich cell layers that constitute the shoot endodermis (Fig.I.12-H) (Itoh et al. 2005; Morita et al. 2007; Orman-Ligeza et al. 2013). The initiation of both lateral and crown roots entails the specification of founder cells, their coordinated division and differentiation to produce an organ primordium, characterized as a small

group of cells with enlarged nuclei. Anticlinal and periclinal divisions allow the development of the root primordium (Fig.I.12-A and B).

Up to date, the fine description of crown root development at the anatomy level has been studied in rice. The developmental process of rice crown root was divided into seven stages (Fig.I.11-A to G) (Itoh et al. 2005). At the first stage, the initial primordial cells form in a few layers by one or two periclinal divisions of the ground meristem that is adjacent to the peripheral cylinder of vascular bundles in the stem (Fig.I.12-A). After that, the initial cells divide anticlinally and periclinaly to form the epidermal-endodermal initial, central cylinder initial and root cap initial cells (Fig.I.12-B). The epidermal-endodermal initials differentiate into the epidermis, and endodermal cells begin to form cortical cells during the third and fourth stages (Fig.I.12-C-D). During stage 5 and 6 the fundamental organization of the root is formed with the establishment of columella from the root cap initial cells, and cells in the basal region commence of cell elongation vacuolation (Fig.I.12-E-F). Finally, the cells of all tissues elongate concurrently with emergence of the crown roots (Fig.I.12-G). Crown root development begins with the appearance of tillers (Webb 1936)(Coudert et al. 2010).

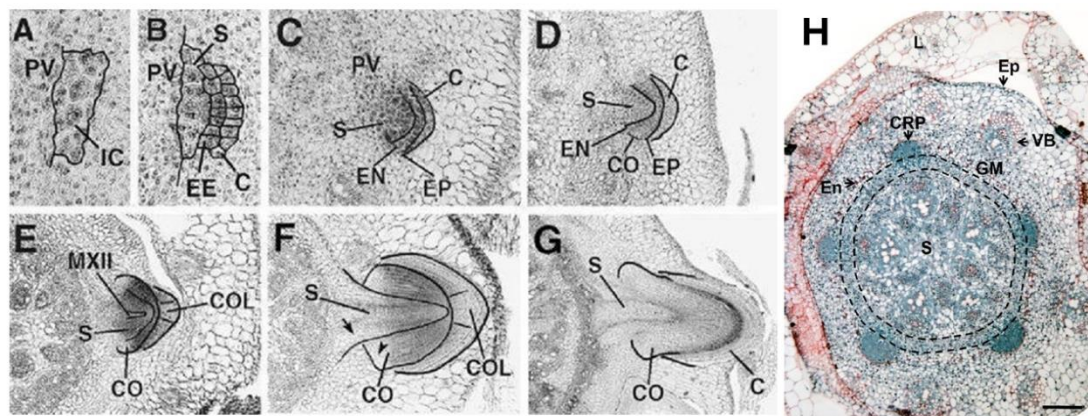


Figure I.11: A fine anatomical view of crown root development in rice. (A) Establishment of initial cells. (B) Establishment of epidermis, endodermis and root cap initials. (C) Differentiation of epidermis-endodermis initial into epidermis and endodermis. (D) Cortex differentiation. (E) Establishment of fundamental organization of root primordium. (F) Onset of cell vacuolation (arrowhead) in cortex and elongation (arrow) in stele. (G) Crown-root emergence (from Itoh et al., 2005). (H) The rice stem transversal section showing the crown root initiation area. Staining: periodic acid-Schiff and naphtol-blue-black (Gonin et al. 2019). IC: initial cells; PV: peripheral cylinder of vascular bundle; C: root cap or its initials; EE: epidermis-

endodermis initials; S: stele; EP: epidermis; EN: endodermis; CO cortex, COL columella, MXII late meta-xylem vessel; CRP: crown root primordium; GM: ground meristem; L: leaf; S: stele; VB: vascular bundle. The black dotted lines indicate the separation of the ground meristem. Scale bar, 50 μm .

I.2.5 Regulation of root architecture

RSAs of cereals, which grow in the field and have to face multiple stimuli. The root system tends to have the structure due to its genetic background, however, as soon as they emerge, the soil conditions will take influence, and the soil conditions are much more complex than aerial conditions experienced by shoots. During the growing and development of plant, roots are continuously subjected to gravity (Fig.I.13-A), soil characteristics (Fig.I.13-B), water content (Fig.I.13-C), oxygen availability (Fig.I.13-D), nutrient patches (Fig.I.13.E) and temperature changes (Fig.I.13-F)(Rich and Watt 2013). . Gravity remains constantly throughout the plant's life cycle, but other stimuli are heterogeneous in both space and time and can be locally attenuated or supplemented, hence consequently lead to changes to the root architecture. The relationship between root system architecture and environmental factor was summarized in table I.2.

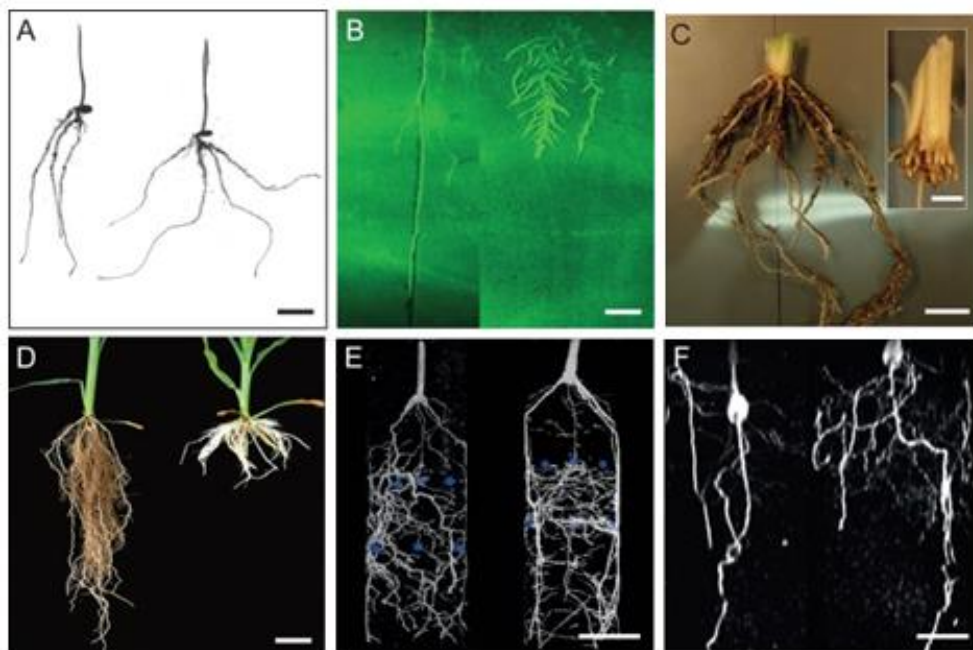


Figure I.12: Example of the impact of soil conditions on roots. (A) Gravity: soil-grown seedlings of hybrid wheat with acute gravity angle (left) and rye with wider seminal root angle (right). (B) Hardness: wheat. Janz seminal roots grow through pores

(left) and in hard soil (right). **(C)** Water: the nodal roots of a well-watered wheat (left) and in dry soil (insert). **(D)** Oxygen: maize grown in drained soil (left) or soil waterlogged for 21 days (right). **(E)** Nutrients: wheat with a uniform phosphate supply (left) compared to a phosphate pad applied at 8 μM between blue beads (right). **(F)** Temperature: MRI of maize roots grown with a root zone temperature of 14 °C (left) or 24 °C (right).

Gravitropism of root is regulated by redistribution of auxin acrossing the elongation zone of root. Auxin accumulates at the bottom, leading to differential growth inhibition, resulting to downward curvature. The angle where roots emerge is presented as the “gravitropic set-point angle”, controlled by a genetic component, has been used as an early screen for root traits in breeding (Uga et al. 2015). The gravitropic set point angle has been linked to the depth of the mature root system in the field. This association between deeper rooting and root angle triggers to the quantitative trait loci (QTL) of a narrower and deeper root idea phenotype (Lynch 2013). Although gravity is evenly distributed throughout the roots in the soil, the actual growth direction of the roots in the soil is different and depends on the type of root, soil conditions and genotype. For example, the primary roots and crown root of cereals have plagio gravitropic behavior as they do not grow directly downward, but after appearing, they may elongate horizontally for some time before bending vertically downward in optimal soil conditions. In addition, root angle can be affected by temperature and water availability (Ali et al. 2015).

Soil structure: Because soil has three phase structures, consisting of solid particles, liquid water and air, and rarely uniform, the soil characterization strongly influences on root architecture such as root elongation through the soil and root diameter of seminal and crown roots in cereals. Primary wheat roots in dense soil have reduced elongation but faster branch root formation rate than wheat roots in loose soil (Rich and Watt 2013). The lateral root branching density is also strongly impacted by soil texture. Shorter total root length in hard soils reduces the effective soil exploration and consequently causes lower water and nutrient retention, thereby reducing the supply to the shoot, which can lead to a decrease in the growth and yield on compacted soil. Hard soils may reduce rooting depth, although this does not necessarily correlate with lower overall root mass as plants may respond to increased lateral root exploration

above hard soil layers. The root systems favor areas with lower soil compaction, and this is especially evident in soils with cracks or pores or low impediment pathway (Figure I.13-B). Probing soil cracks and pores can allow plant roots to penetrate hard soil areas or explore deeper areas of soil, thereby accessing larger pools of water and nutrients (Correa et al. 2019). Root expansion is carried out when pressure pulls inside the cells of the elongation zone become strong enough to overcome the limitations imposed by cell wall resistance and the resistance of the surrounding environment. The mechanical impedance increases ethylene biosynthesis and is controlled by genotypes. Root penetration is a complex trait. The differences in root thickness in different genotypes possibly allow roots to resist buckling or less, may be the main factor contributing to root penetration (Lynch et al. 2021).

Soil water content: Lack of water is the most common limitation to plant growth. Drought stress results in dehydration and loss of cell turgor, often leading to severe limitations in root length (Figure I .13-C). However, tolerant plants tend to develop deeper root systems under water-limited conditions, to allow root to expand into wet deeper zones (Uga et al. 2013). Under limited water condition, tolerant plants reduce the shoot growth, to prior support root elongation. However, roots develop and elongate during water stress condition are frequently thinner, and the rates of elongation and branching are usually lower than those in the well-watered conditions. Moreover, in some cases, elongation rates in water-stressed roots exceeded those in well-watered soil. In maize, root system is hydrotropism and its hydrosensory site is located within the root cap (Hideyuki Takahashi and Scott 1991). It has been reported that cell wall loosening proteins such as expansin are involved in maintaining root apical elongation of water-stressed roots as well as the roles of abscisic acid (ABA) and ethylene in the drought tolerant process.

Anoxia and hypoxia: hypoxia (low oxygen) or anoxia (no oxygen) is usually caused by waterlogging. Although the response of root systems to excess water widely varies, the combination of reduced primary root growth and the root to shoot ratio in low or no oxygen conditions. Excess hypoxic conditions inhibit the elongation of primary and crown roots, and the formation of lateral root. However, it has been indicated that the growth of new nodal roots are promoted by waterlogging (Figure

2D) (Lone et al. 2016). These new nodal roots may be thicker (due to aerenchyma formation) and shorter than pre-existing roots and branching patterns may also differ. The ability of these nodal roots to survive waterlogging varies between species, but if maintained, can influence future root system structure. In cereals, Phytohormones signalling (auxin, abscisic acid, gibberellin and ethylene) have been demonstrated as involved in initiation of new adventitious roots after soil waterlogging (Tong et al. 2021).

Nutrients: Root structure determines access to nutrients in the soil, hence all of the basic processes of root including curving, elongation, and branching are affected by internal and external nutrient availability. Limited plant phosphorus availability is associated with a more horizontal root angle, that keeps the roots close to the soil surface where immobile phosphorus mainly accumulate. The nutrient abundance promotes the root elongation and branching. The model computed tomography allowing non-destructive demonstration of root growth in nutrient patches showed the higher root growth (more branching and higher elongation) in more concentrated nutrient available (Fig.I.13-E). The angle at which side root branches appear will influence the area over which the root spreads, hence a narrower branching angle will produce a denser patch, especially if the root also changes its branching pattern (Fig.I.14, left). Shallow root growth can occur in soils with high nutrient content such as Phosphate, Potassium, Calcium, Ammonium (Figure I.14, left); however, for some nutrients such as nitrate, low concentrations may increase root length in some genotypes (Fig.I.14, right) (Wang et al. 2018). Excessive nutrient deficiencies hinder root system development, but if nutrient deficiencies are less severe, carbon will be distributed away from the shoot and toward the roots, leading to root elongation and branching (Steingrobe, Schmid, and Claassen 2001). Nutrient uptake, especially fixed nutrients such as phosphorus and nitrogen, is limited by the root surface area available for uptake, and elongation increases soil exploration.

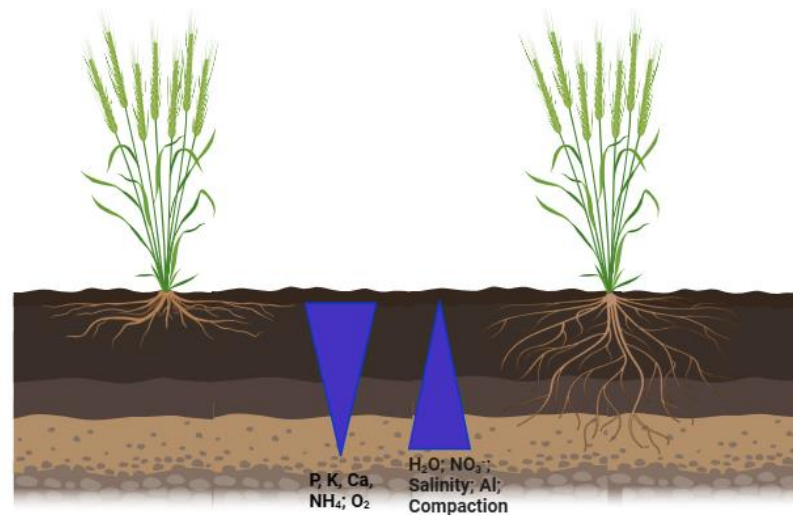


Figure I.13: Description of nutrient distribution in the soil and different structures of barley root system architecture can adapt to different soil environmental conditions (created in BioRender.com).

Temperature: Soil temperature directly affects root elongation, metabolism and transporters and indirectly affects the shoot process. Especially, roots elongate more rapidly in warm condition (Figure I.13-F), reaching a peak after that the rate gradually declines (Gregory 2007). However, the association between root elongation and temperature range depends on genotypes and root age (Rich and Watt 2013). Moreover, while the elongation rate of individual roots increased with temperature, the overall length of the root decreased. In addition, the soil temperature might sometimes impact on root diameter. The cold tolerance in cereal controlled by cell membrane stability and phytohormones auxin, and could promote root elongation (Zhou, Sommer, and Hochholdinger 2021).

Table I.3: Relationships between root architecture and environmental factors.

Root traits/Phenes	Description	References
Root depth		
Primary root length	Inhibited by P-limitation	(López-Bucio, Cruz-Ramírez, and Herrera-Estrella 2003)
	Inhibited by moderately high rate of nitrate supplies	(Forde 2014)
	Deeper roots provide plants with better access to stored water in the deeper layers of the soil substratum.	(A. P. Wasson et al. 2012)
Root tip diameter	In hard and drying soils, root tips with large diameters help to improve root penetration.	(Haling et al. 2013)
Gravitropism	Plants, which are more tolerant to drought, have steeper root angles and more gravitropic responses.	(Uga et al. 2013)
Root hairs		
Root hairs	Proliferation of root hairs is stimulated in P-limited conditions, root hairs contribute up to more than 70% of the total root surface area and be responsible for up to 90% of P acquired.	(Haling et al. 2013)

Root branching		
Length and number of lateral roots (LRs)	LP initiation and emergence is stimulated during P limitation/ or densely spaced, short laterals are optimal for phosphorus acquisition	(Postma, Dathe, and Lynch 2014)
	Sparsely spaced, long laterals are optimal for nitrate acquisition. External nitrate stimulates LR initiation and elongation, whereas a high plant internal nitrate/N status inhibits LR growth. Early LR development can also be systemically inhibited by N deficiency. Reduced frequency of LR branching and longer LR improve N capture from low-N soils in maize.	(Postma, Dathe, and Lynch 2014; Forde 2014)
	Increase for water resources store	(Rewald, Ephrath, and Rachmilevitch 2011)
Shallow/adventitious roots	A reduced gravitropic trajectory of basal roots, adventitious rooting and altered dispersion of lateral roots enable topsoil foraging in response to low P availability. Recombinant inbred lines of common bean with shallow basal roots have better P acquisition in the field. Maize plants with brace and crown roots growing at a shallower angle are more efficient in N use.	(Miguel, Postma, and Lynch 2015; Herder et al. 2010)

I.3 Molecular mechanism controls root formation and development

It is well known that the plant hormone auxin positively regulates root formation. Auxin has a special transport mechanism and its signaling promotes the degradation of the AUXIN/INDOLE ACETIC ACID (AUX/IAA) transcriptional repressors through the ubiquitin protein ligase SCR^{TIR1} complex (Dharmasiri, Dharmasiri, and Estelle 2005; Tan et al. 2007). Aux/IAA proteins are repressors of AUXIN-RESPONSIVE FACTOR (ARF) transcription, and the degradation of AUX/IAA proteins allow transcriptional factor ARF to alter their downstream auxin-responsive genes' expression in order to induce developmental responses (Dharmasiri and Estelle 2004). In the model plant *Arabidopsis thaliana*, the LATERAL ORGAN BOUNDARIES-DOMAIN/ASYMMETRIC LEAVES 2-LIKE (LBD/ASL) transcription factor (TF) family member LBD29, which is regulated downstream by auxin and ARF7 (Porco et al. 2016), directly and positively regulate the *LAX3* (encodes an auxin-inducible auxin influx carrier) auxin-dependent expression in the lateral root (LR) emergence regulatory network. ARF7 is important to regulate and induce *LAX3* indirectly during LR emergence. In the case of rice, gain-of-function mutants *Osiaa11*, *Osiaa13*, and *Osiaa23* also result from a stabilizing mutation in their domain II, and the number of lateral roots in these mutants are dramatically decreased (Ni et al. 2011; Kitomi et al. 2012; Zhu et al. 2012). On the other hand, *arf7 arf19* double knockout mutants in *Arabidopsis thaliana* also show a remarkable reduction in lateral root formation (Kitomi et al. 2011). This study also indicates that ARF7 and ARF19 directly regulate the auxin-mediated transcription of *LATERAL ORGAN BOUNDARIES-DOMAIN16/ASYMMETRIC LEAVES2-LIKE18* (*LBD16/ASL180*) and/or *LBD29/ASL16* in lateral roots.

In grains, reactive oxygen species (ROS) play roles in endosperm weakening, mobilization of seed reserves, protection against pathogens and programmed cell death (Li et al. 2017) which are involved in monocot seed germination including embryonic root emergence. In *Arabidopsis*, lateral root formation commences when the founders divide and create a dome-shaped lateral root primordium (LRP), which has to cross three overlying tissues to emerge at the surface of the parent root: the adjacent

endodermis, the cortex and the outer-most layer, the epidermis. The rigid cell wall linking plant cells to each other prevents any sliding or migration. To preserve the structural and functional integrity of the primary root, it is necessary to coordinate growth and proliferation within the LRP and the responses of the overlying tissues. Auxin plays a pivotal role in coordinating these responses. Auxin prominently involves in the modification of cell wall properties and then resulting in the changes of biomechanics, to support intercellular communication. LRP development correlates with the establishment of an auxin response maximum at the primordium tip, a process dependent on auxin transport mediated by PIN auxin efflux transporters. At the transcriptional level, auxin modulates the expression of different sets of genes by triggering the degradation of the repressors AUX/IAA, which interact with the auxin response factors (ARFs) transcription factors. As the ARFs and the AUX/IAA are members of multi-genes families, the transcriptional effects of auxin depend on its concentration and the combinatorial of expression of AUX/IAA and ARFs. In addition, PICKLE (PKL) encodes a ATP-dependent CHD3-chromatin remodeling factor. The mutation of *PKL* results in phenotypes including pickle roots and substantial changes in root secondary metabolism (Dean et al. 2004). gain-of-function *slr-1* mutant, stabilized mutant SOLITARY-ROOT (SLR)/IAA14 (mIAA14) protein inactivates ARF7/19 functions, thereby completely blocking lateral root (LR) initiation. The *ssl2* (suppressor of *slr2*)/*pkl* mutant specifically restores LR formation in the *slr-1* mutant. These mutants suggest that PKL/SSL2-mediated chromatin remodeling negatively regulates the auxin-induced pericycle cell divisions required for LR initiation (Fukaki et al., 2006).

Crown root formation is a special case of adventitious root formation which is highly dependent on auxin signaling pathway (Lakehal et al. 2019). Rice nodal crown root primordia formation requires many genes including the auxin regulated. Crown Rootless *CRL1* (also referred as Adventitious rootless1 – *ARL1*), which encodes a LOB domain transcription factor conserved across monocots and dicots (H. Liu et al. 2005; Y. Inukai 2005). Additionally, another transcription factor, crown rootless5 (*CRL5*), belongs to the *APETALA2/ETHYLENE RESPONSE FACTOR (ERF)* gene family, involves in crown root development. Both *CRL5* and *CRL1* are direct targets of

Text color code: genes or protein, black; hormones, yellow; signals, red; biological processes, green (from Meng et al. 2019).

In corn (*Zea mays*), a responsive LOB domain transcription factor Rootless concerning Crown and Seminal root (*RTCS*) and its downstream target Auxin Response Factor (*ARF34*) control nodal root formation (Majer et al. 2012). In addition, an Aux/IAA response regulator encoded by the *RUMI* locus modulates seminal and lateral root initiation in maize (Von Behrens et al. 2011).

I.4 How to study and discover the genetic mechanism, genes and gene network involved in RSA

The primary role of roots as part of plant development has aroused renewed interest in understanding the molecular mechanisms controlling RSA in crops (Meister et al. 2014). Strategies to understand root development and RSA comprise forward and reverse genetics using mutants of the model plant or quantitative trait locus (QTL) identification underlying natural phenotypic variation in root traits between populations (Paez-Garcia et al. 2015). Integrating knowledge from the genetic mechanisms underlying RSA to identify ideal root phenotypes for plants growing in a particular environment could allow breeders to select root traits target for existing or reclaimed land to improve agricultural production.

In recent years, several genome-wide large-scale studies have been performed to uncover the molecular mechanism that regulates rice root development (Takehisa et al. 2012). For instance, Jiao et al. used laser microdissection and microarray profiling from 40 different cell types, comparing transcriptome atlas (Yuling Jiao et al. 2009). In this method, the previously undiscovered properties including cell-specific promoter motifs, interaction partner candidates, co-expressed cognate binding factor candidates and hormone response centers, were uncovered. Takehisa et al. also adopted the same technique to perform an even more comprehensive analysis, by combining 38 microarray data that cover eight developmental stages along the radial axis of the crown root (Takehisa et al. 2012). They focused on root development, function of the root cap, lateral root formation and water and nutrient absorption, to identify genes and gene networks associated specifically with the function and formation of the root system.

Other commonly used techniques make use of a combination of forward and reverse genetics methods, including quantitative trait loci (QTLs) analysis, ethyl methane sulfonate (EMS) mutagenesis and T-DNA insertional mutagenesis screens, gene knockdown, and overexpression experiments. Forward genetics seeks to find the genetic basis of a phenotype or trait, reverse genetics seeks to find what phenotypes arise because of genetic sequences.

Quantitative trait locus (QTL) analysis is a statistical method that links two types of information consist of phenotypic data (trait measurements) and genotypic data (usually molecular markers), to explain the genetic basis of variation in complex traits. QTL mapping has provided valuable information on genomic regions controlling the genetic variation of root traits in barley (Chloupek, Forster, and Thomas 2006; Naz et al. 2012; 2014; Arifuzzaman et al. 2014; Robinson et al. 2016; 2018), and the flowering regulator *VRNI* has been demonstrated in regulating root system architecture in wheat (Voss-Fels et al. 2018).

Genome-wide association studies (GWAS), also known as linkage disequilibrium (LD) mapping, provide an alternative way to identify associations between quantitative values of phenotypic traits and molecular markers. In principle, GWAS takes advantage of the large number of historically and evolutionarily occurred recombination events and links these events with phenotype, allowing mapping at a more refined scale.

CRISPR (Clustered Regularly Interspaced Short Palindromic Repeats) genome editing, which is a revolutionary method derived from a native adaptive immune system in eubacteria and archaea for protection from invading viruses (bacteriophage), allows the alteration of DNA sequence in numerous organisms to achieve precise genome modifications (Jaganathan et al. 2018). In that system, the CRISPR-associated endonuclease (Cas) requires the 20-bp spacer sequence of a guide RNA (gRNA) to recognize a complementary target DNA site upstream of a protospacer adjacent motif (PAM) and generates a double-stranded break (DSB) near the target region (Kořínková et al. 2022). The PAM is a short DNA sequence (usually 2-6 base pairs in length) that follows the DNA region targeted for cleavage by the Cas. The PAM is required for a Cas nuclease to cut and is generally found 3-4 nucleotides downstream from the cut

site. DSBs are repaired through either non-homologous end joining (NHEJ) or homology-directed recombination (HDR) resulting in small insertions/deletions (indels) or substitutions at the target region, respectively (Jinek et al. 2012). For instance, the most widely used Cas9 recognises a 5'-NGG-3' PAM, where "N" can be any nucleotide base, in *Streptococcus pyogenes*, whose spacers in CRISPR array are coded differently and Cas 9 cannot cut the bacteria's own genome. Compared to other genome editing tools such as zinc finger nucleases (ZFNs) and transcription activator-like effector nucleases (TALENs), CRISPR/Cas is more robust in that the Cas protein can theoretically bind to any genomic region preceding a PAM site and, importantly, target multiple sites simultaneously. However, the possibility of off-target mutations caused by CRISPR/cas is a potential concern in both basic and applied research in plants, although it has been reported that off-target effects of CRISPR/Cas occur at a much lower frequency in plants.

I.5 Background and study significance

Climate change challenges food security for the world's growing population, while agricultural areas are shrinking. Changing climatic conditions and the need to reduce fertilizer inputs for the sake of improving environmental quality place increasing constraints on agricultural crop production (Jia et al. 2019). Therefore, global agriculture urgently needs eco-friendly crops with reduced fertilizer and water needs, providing optimal natural resource usage mechanisms to adapt to harsher conditions (Lynch 2019). In addition, further improvement of fertilization and crop management practices, exploitation of endogenous plant mechanisms and adaptation strategies gain importance in the development of resource-efficient crop cultivars. Therefore, current breeding approaches need to consider plant traits, which allow the cultivars to overcome challenging growth conditions, including transient periods of drought or suboptimal nutrient supplies. In this regard, root development plays a key role, as roots express a large range of highly variable physiological and morphological traits that favor water and nutrient uptake. More recently, root system architecture has received a particular increased attention, as it determines the three-dimensional shape of the root system and thus the soil volume that can be explored for water and nutrients

as well as yield formation (Giehl and von Wirén 2014; Voss-Fels, Snowdon, and Hickey 2018). Crown-roots (CRs) are shoot-borne roots that represent the major constituent of the mature root system in cereals, playing fundamental roles in plant growth, development, and response to different environmental stresses. Understanding the mechanisms that regulate important agronomic traits such as roots has become crucial to improve plant production (Paez-Garcia et al. 2015). In addition, there is a need for faster genetic improvement of crop varieties to better adapted to future climate and agricultural management conditions (Ray et al. 2013). Crop-optimized RSA can facilitate higher crop yields (A. Wasson et al. 2016).

I.6 Study aims and experimental approaches:

The aim of the PhD study is to investigate the molecular mechanism and the anatomic origin of the crown-root (CR) initiation and development in barley (*Hordeum vulgare* L.). To achieve this goal, the study has been divided into two following specific objectives:

- 1) Identification and characterization of genes involved in crown root initiation and development in barley (*Hordeum vulgare* L.). For these strategies, a whole transcriptomic study of stem base of barley seedling at the development stages of 1 day after germination (DAG) and 10 DAG, as well as an anatomical overview of crown root initiation in young barley seedlings were revealed.
- 2) Identification and functional characterization of genes encoding LATERAL ORGAN BOUNDARIES (LOB) DOMAIN (LBD) transcription factors in barley. For this purpose, methods such as phylogenetic tree analysis, transcriptomic analysis, histology, gene expression analysis by real-time quantitative reverse transcription polymerase chain reaction (qRT-PCR), transactivation assay in mesophyll protoplast, CRISPR-Cas9 genome editing, and complementation in the rice knock-out mutation were used.

**CHAPTER II: Identification and characterization of genes involved
in crown root initiation and development in barley
(*Hordeum vulgare* L.).**

Thu Dieu Nguyen, Filip Zavadil Kokáš, Mathieu Gonin, Jérémy Lavarenne, Myriam Colin, Pascal Gantet and Véronique Bergounoux (2023). Transcriptional changes during crown-root development and emergence in barley (*Hordeum vulgare* L.). *BMC plant biology*

II.1 Introduction

Despite their hidden nature, roots play fundamental roles in the growth and development of plants, ensuring not only anchorage in the soil, but also water and nutrient up-take, and interaction with soil microorganisms which contribute to the regulation of crop productivity (Gonin et al., 2019). Plants can dramatically modify their root system in response to environmental and nutrient conditions (López-Bucio, Cruz-Ramírez, and Herrera-Estrella 2003; Gao and Lynch 2016; Xinxin Li, Zeng, and Liao 2016). Even though studying root systems in natural environment is laborious, *in situ* root phenotyping methods have evolved from invasive, destructive methods, such as shovelomics, to non-destructive, non-invasive 2-D and 3-D methods (A. Li et al. 2022). Those methods allowed us to visualize the foraging activity of roots and understand the molecular mechanisms regulating root growth and development. Ultimately, it offers the opportunity to manipulate root systems with the aim of improving crop productivity while modifying agricultural practices and optimizing land use.

Cereals represent the most important source of proteins in human diet, with wheat, rice, maize representing in 2020 more than 35% of proteins consumed per capita each day, far before poultry and pig meat (11.8%; FAO stat). However, the mentioned species have a limited natural geographical repartition and already nowadays suffer from drastic climatic changes (Ciais et al. 2005). Climatic changes are characterized by increasing number and severity of episodes of drought and heat that are responsible for drops in yield. As roots are the first interface between plant and environment, sensing changes in soil moisture and nutrient availability, they represent a good target for new breeding programs.

The typical root system of cereals is composed of the embryonically formed primary and seminal roots, and of the post-embryonically formed adventitious roots that are shoot-borne roots, called crown roots (CR) appearing quickly after germination at the junction between the stem and the root. Primary and seminal roots, and CR have the ability to form lateral roots of different orders. All together, they form the characteristic fibrous root system of monocots (Bellini, Pacurar, and Perrone 2014). In some monocots, embryonic primary and seminal roots are not persisting, and

the mature root system is constituted exclusively from the CR (Smith and De Smet 2012; Atkinson et al. 2014).

Maize (*Zea mays* L.), wheat (*Triticum aestivum* L.), rice (*Oryza sativa* L.) and barley (*Hordeum vulgare* L.) represent 39% of the crops cultivated worldwide. Due to its significance for human feeding, rice has been chosen since 1985 as the model plant for monocots. This was justified by the fact that the cultivated rice has been adapted to many culture conditions, its genome has been sequenced, several mutant collections are available, as well as a wide range of genetically and phenotypically diverse varieties are available (Coudert et al., 2013). The development of rice functional genomics, QTL analysis and genome-wide association studies allowed to decipher the molecular mechanisms controlling the initiation and differentiation of CR (Mai et al., 2014; Meng et al., 2019). However, the tropical growth habit of rice is different from that of cereals grown under the European temperate climate, and one could address whether molecular mechanisms controlling root development in rice are conserved among European-type cereals.

Barley is the fourth most cultivated cereal worldwide (<http://faostat.fao.org/>). Except for human food supply, barley is used in breweries, distilling industry and animal feeding. Its area of production is very large, covering a range of extreme environments, suggesting the ability to adapt to different environment (Pasam et al. 2014), suggesting an under-exploited genetic diversity with high potential for new breeding programs (Milner et al. 2019). The development of high-throughput sequencing in the last decade resulted in the availability of barley genome sequence and annotation (Mayer et al. 2011; Mascher et al. 2017; Monat et al. 2019; Mascher et al. 2021). Finally, the genetic modification of barley for bioengineering is possible since *Agrobacterium*-mediated transformation can be successfully achieved both from immature embryo (Cornelia Marthe , Jochen Kumlehn 2015) or embryogenic pollen culture (Kumlehn et al., 2006). All these criteria, together with its diploid genome, make barley serve as a complementary model in addition to rice to study the root system development in Triticaceae. For instance, in 2018, Ramireddy and colleagues generated a novel enlarger root system, nutrient enrichment, biofortification, and drought tolerance transgenic barley line, by overexpressing cytokine degradation in

roots (Ramireddy et al. 2018). In this chapter, we present data from the whole transcriptome analysis of barley seedlings stem base developing CRs and discuss the possible mechanism underlying CR development and emergence in barley and revealed the activation of different hormonal pathways during this process. RNA-seq analysis was investigated to determine the changes in gene expression in the barley stem base of 1 day-after-germination (DAG) and 10DAG seedlings when CRs are formed. This whole transcriptomic study is the first study aiming at understanding the molecular mechanisms controlling CR development in barley.

II.2 Materials and methods

II.2.1 Plant materials and cultivation conditions

The spring barley cultivar Golden Promise (cv. GP) was used in this study. For the requirement of sterilization growing conditions, wild-type (WT) GP grains were surface sterilized for 30 sec in 70% ethanol, then washed 3 times in autoclaved water, continuing with immersing in 3% sodium hypochlorite for 5 min and followed by extensively rinsed in water. Finally, grains were placed on wet paper in Petri dishes and placed in the dark for 2 days at 4°C. Germination was induced by transferring Petri dishes to a culture chamber with a long-photoperiod (16h-day/8h-night) and a temperature regime of 21°C-day/18°C-night. The day of appearance of the primary roots and coleoptile through the seed husk was considered as the germination day. One DAG (Fig.II.1-C), half of the germinations were sampled, separating roots, stem bases (1 mm fragment from the root – shoot junction/crown) and shoots. The rest of the seedlings were kept for 3 more days on wet filter paper in petri dishes, then transferred into a mini-hydropony system (Fig.II.1-A and B) in a modified half-strength Hoagland solution (supplementary table S1) (Vlams and Williams 1962). At 10 DAG (Fig.II.1-D), the rest of the seedlings were harvested, separating roots, stem bases (1.5-2 mm fragment from the root – shoot junction/crown) and shoots as in 1 DAG. Each kind of sample (roots, stem bases, and shoots) was represented a pool of 5 seedlings; samples were immediately frozen in liquid nitrogen and stored at -80°C freezer until use. The experiment was conducted on three independent biological replicates.

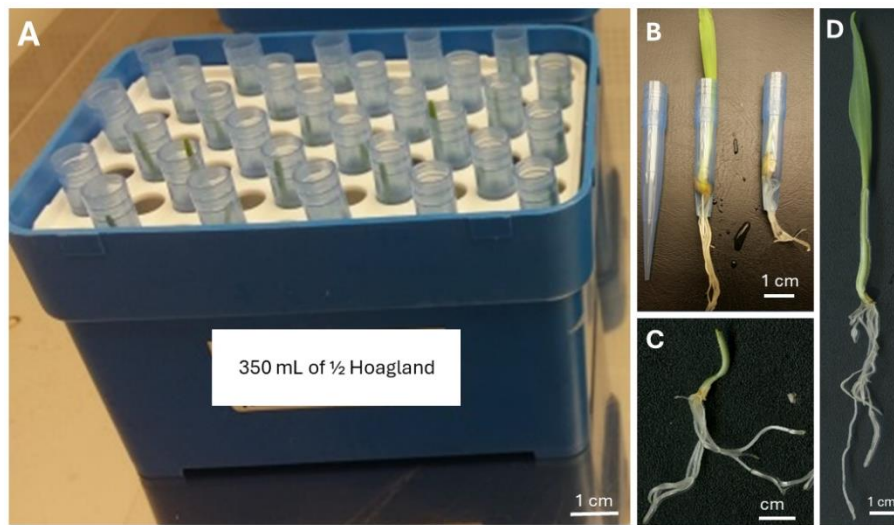


Figure II.1: Mini-hydropony system. (A) A deep-plastic and untransparent 1ml-pipet-tip boxe for the system. 25 seedlings were grown in 1 box, filled with 350 mL of $\frac{1}{2}$ Hoagland solution. (B) Putting one barley seedling into one bottom-cut-1ml pipet tip and put in Mini hydropony system. (C) 1 day after germination (DAG) barley seedling cv. GP. (D)10-DAG barley seedling cv. GP. In (C) and (D), grain tegument and the rest of the endosperm were removed to keep only the young seedling. Bar: 1 cm

II.2.2 Imaging of CR primordia by light and confocal microscopy

Plantlets were grown as previously described in I.2.1, for the light microscopy experiment. The developing young seedlings was separated from the rest of the grain; primary roots were removed from the rest part of plantlet with a blade, and a 2 mm-long section from the stem base was excised with a scalpel and immediately immersed in fixative solution (4% paraformaldehyde in 1X of phosphate-buffered saline (PBS), pH 7.4). After that, vacuum was applied twice for 1 min 30 sec. Then, the fixative was changed, and samples were placed overnight at 4°C in the dark. The next day, samples were washed 4 times in 1X PBS for 15 min. Samples were dehydrated in an ethanol series from 50 to 100 % into a sonication condition. Samples were embedded in resin (Technovit® 7100; Electron Microscopy Sciences) according to the instructions (The polymerization solution was prepared by adding 0.5 ml of Technovit 7100 hardener 2 into 7.5 ml of unused infiltration medium). Sections of 4.5 μm were obtained with a HYRAX M40 microtome (Zeiss), stained with either periodic acid Schiff-naphthol blue black (PAS-NBB) or lugol, and mounted in Clearium® Mounting Media (Electron Microscopy Sciences). Sections were observed with an Imager M2 microscope

equipped with an Axio Cam MrC5 camera (Zeiss). Pictures were acquired and analyzed with the ZEN software (Zeiss).

The imaging of the stem base by confocal microscopy was performed as previously (Lavarenne et al. 2019). Briefly, the 1 mm-long and 2 mm-long crown of barley seedlings, which should contain whole stem bases, were harvested at 1DAG and 10DAG, respectively, and immediately immersed in ½ Hoagland medium at 4°C overnight. The harvested stem bases were embedded in 5% agarose (ref. A1203; Duchefa Biochemie) in sterile distilled water (w/v). Agarose blocks were mounted into an Automate 880 (Phiv platform, MRI imaging facility, Montpellier, France, <https://www.mri.cnrs.fr/>), which includes a custom machine combining an LSM NLO 880 multiphoton microscope (Zeiss, <https://www.zeiss.com>)-incorporated custom machine and is equipped with a Chameleon Ultra II tunable pulsed laser (690-1080 nm range excitation; Coherent, <https://www.coherent.com>) and an HM 650V vibratome (Microm Microtech, <http://www.mm-france.fr>) for automation of sample cutting (60 µm) and instant imaging. The images were obtained with an A20x/1.0NA (2.4 mm WD) objective. ZEN and a custom package ZEN EXTENSION NECE (Zeiss) was used for the instrument. Images were acquired and proceed along the whole stem base. An application of ImageJ – Fiji was applied to align the imaged sections (Schindelin et al. 2012). All aligned sections in one stem base were reconstructed in 3 spatial dimensional (3D) structure by using in IMARIS 9.1 (Imaris, <https://imaris.oxinst.com>).

II.2.3 Evans blue staining

Evans blue staining was applied to detect the cell death at the site of root emergence (Mergemann and Sauter 2000). Briefly, 10 DAG seedlings of cv. GP grown in hydroponic conditions, which were described in I.2.1, were carefully removed the remaining grains tegument and the rest of the endosperm without any damage, then immersed in 2% (w/v) Evans blue, prepared in water, for 3 min and subsequently washed in water. Evans blue penetrates only dead cells. Samples were observed with a Zeiss Axio Zoom. V16 Stereo Microscope system (Carl Zeiss, Germany) equipped with a camera, set up in the bright field illumination (objective lenses PlanApo Z 1.5x,

FWD = 30 mm). Serial pictures were taken and analyzed with Zen Blue 2012 Carl Zeiss software, image processing: extended depth of focus. We thank the kind instruction of Dr. Yuliya Krasylenko, Department of Cell Biology, Faculty of Science, Palacký University Olomouc for the microscope.

II.2.4 Library preparation and transcriptomic analysis

For both 1DAG and 10DAG, seedlings were grown as previously described in I.2.1. Grain tegument and the rest of the endosperm were removed to keep only the young seedling (Fig.II.1-C and D) composed of the small primary and seminal roots and the stem enclosed in the coleoptile. The stem base (1 to 2mm-long), corresponding to the zone of emergence of CRs in barley, was excised, flash frozen in liquid nitrogen and stored in deep freezer at -80°C until used for RNA extraction and transcriptomic analyses.

Total RNA was extracted according to the instructions of the ZymoResearch Plant RNA extraction kit and treated by TURBOTM DNase (Invitrogen). Libraries were prepared from 2.5 µg of total RNA according to instructions of the Illumina TruSeq1 Stranded mRNA Sample Preparation Kit (Illumina). Library concentration was assessed with the Kapa Library Quantification Kit (Kapa Biosystem) and all libraries were pooled to the final 8 pM concentration for cluster generation and sequencing. The clusters were generated using an Illumina TruSeq1 PE Cluster Kit v3cBot HS and sequenced on HiSeq PE Flow Cell v3 with a HiSeq 2500 Sequencing System. Three independent biological replicates were sequenced for each sample.

The reads with 50bp-long, generated by sequencing were quality checked and trimmed prior mapping to the reference genome of barley cv. Morex IBSC_v1 (International, Genome, and Consortium 2012) using the Tophat2 splice-read mapper with default parameters (D. Kim et al. 2013). The mapped reads were quantified using HTSeq with respect to the stranded library (Anders, Pyl, and Huber 2015). The differentially expressed gene expression was calculated with the DESeq2 package (Love, Huber, and Anders 2014). Only genes harboring a significant induction or inhibition were considered for further analyses (p -adjusted value ≤ 0.05 , $|\log_2\text{foldchange}| \geq 1$).

The functional annotation and enrichment of the differentially expressed genes was performed using the automated MapMan BIN ontology in Mercator4 (Lohse et al. 2014; Schwacke et al. 2019). Barley sequences were searched against Arabidopsis TAIR release 10, PPAP, ORYZA TIGR5 rice proteins, KOG, CDD. The blast-cutoff was set up to 80 and no multiple bin assignment was accepted. Using the whole barley genome functional annotation, the over-representation of a specific functional group among the differentially expressed genes was performed (Muthreich et al. 2013). In brief, the expected number of genes for each category was calculated based on the distribution of functional categories in the whole barley transcriptome. Indeed, the widely used Gene Ontology (GO) comprises more than 34000 terms organized in 3 categories: “Biological process”, “Molecular Function” and “Cellular component”. This rich annotation can lead to a strong redundancy and problem to visualize data from RNAseq. In opposite, Mapman/Mercator was specifically developed for plants with the goal to visualize omics data, such as transcriptome, on plant pathways (Thimm et al. 2004). Currently, MapMan ontology covers 27 functional top-categories, referred to as BIN Transcriptomic of barley crown-root development (Schwacke et al. 2019; Klie and Nikoloski 2012). In parallel, the GO enrichment analysis limited to “Biological process” was performed with Shiny GO: the 40 most enriched GO terms were sorted based on their fold enrichment. All data are available at the NCBI archive database under the GEO accession number GSE87737 (<https://www.ncbi.nlm.nih.gov/geo/query/acc.cgi?acc=GSE87737>).

II.2.5 Analysis of gene expression by quantitative real-time PCR (qRT - PCR)

To confirm the differential expression of several interesting genes, qRT-PCR analysis was performed with i) samples used for RNA-seq focused on the crown (1-2mm of stem base) region of seedlings at 1DAG or 10DAG, and ii) with samples obtained from various tissues (roots, crowns, and shoots) of cv. GP seedlings at 1DAG and 10DAG.

For the analysis of gene expression in different tissues, total RNA was extracted from roots, crowns and shoots. Each sample was prepared in 3 independent

biological replicates, with each replicate being composed of tissues of 5 seedlings. For this purpose, seedlings were grown and harvested as described for the preparation of the RNAseq libraries. Total RNA was extracted with the Quick-RNA Plant Kit (Zymo Research) following manufacturer's instructions. Any potential trace of genomic DNA was removed with an additional treatment with 2U of TURBO™ DNase (Invitrogen) for 30 min at 37°C, and subsequent precipitation with lithium chloride. Total RNA was finally dissolved in RNase-free water. The quantity was determined with a NanoDrop™ One/OneC Microvolume UV-Vis Spectrophotometer (ThermoFisher scientific).

For both experiments, the oligo(dT)₁₈-based cDNA synthesis was performed from 2 µg of the total RNA according to the instructions of the RevertAid First Strand cDNA synthesis kit (Thermo Fisher Scientific). For real-time PCR, cDNA samples were diluted 10 times and used in a reaction containing 1X gbSG PCR master mix (Generi biotech), 200 nM of each primer and 500 nM of ROX as a passive reference. Three technical replicates were run for each sample on a StepONE Plus thermocycler (Applied Biosystems) in a two-step amplification program. The initial denaturation at 94 °C for 2 min was followed by 45 cycles of 94 °C for 5 s and 60 °C for 20 s. A dissociation curve was obtained for each sample. To determine the best reference gene(s), we both use the information from the available literature, our previous research work, but also the advance of the RefGenes tool under Genevestigator (Hruz et al. 2008). The expression profile across the different samples was analyzed for 6 potential reference genes (HvACT: AK248432.1; HvEF2α: AK361008.1; Hv5439: AK360511.1; Hv20934: AY972629.1; HvTIP41: AK373706.1; HvEIF5A2: AK357300.1) (Hua et al. 2015). Their stability was determined using RefFinder (Xie et al. 2012) that integrates the currently available major computational programs (geNorm, Normfinder, BestKeeper, and the comparative ΔCt method) to compare and rank the tested candidate reference genes. Based on our data, HvACT (AK248432), Hv5439 (AK360511, HORVU5Hr1G073510) and EIF5A2 (AK357300) genes were found to be the most stable across the samples under investigation and were consequently used as normalizer. Cycle threshold values for the gene of interest were normalized in respect to the three reference genes and the geometric mean of

expression was calculated. The relative expression was determined using the $\Delta\Delta C_t$ mathematical model corrected for the PCR efficiency (E) (Michael W. Pfaffl 2001). The relative quantification was estimated in comparison with either “crown-1DAGRNASeq” or “roots-1DAG” sample. Primers were designed using Primer3Plus (<https://primer3plus.com/cgi-bin/dev/primer3plus.cgi>). Their specificity was firstly checked by blast restricted to barley genome and validated by the dissociation curve and sequencing of the amplified product. Sequences of primers are given in table II.1.

II.2.6 Prediction of putative *cis*-regulating elements related to ethylene and cell death

The presence of putative *cis*-regulating elements related to ethylene was predicted with PlantPAN3.0 (Chow et al. 2019) for 3 genes with a potential involvement in cell death during crown-root emergence. For this purpose, the 1kb-long sequence upstream of the ATG was retrieved from barley genome. The sequences were scanned with the “Promoter analysis” tools using the transcription factor binding motifs database from rice.

II.2.7 Statistical analysis

GraphPad Prism version 9.2.0. was used to prepare all figures and evaluate the statistical analysis. In all cases, the statistical significance was assessed by a two-way ANOVA followed by a Bonferroni multiple comparisons test.

Table II.1: Sequences of forward and reverse primers used for qRT-PCR for 10 genes with a putative role in CR initiation and development and 3 genes^(a) used as reference genes for normalization.

Gene	Accession	Description		Primer sequence
CRL1.1	MLOC_10784	LBD protein, orthologue to CRL1/RTCS	q10784-Fw q10784-Rv	GGAGACAACAACGATCAGGTC ACTTGCGACGCAGAACTTG
IRL1	MLOC_70768	IAA-amino acid hydrolase	qIRL1-Fw qIRL1-Rv	CATGACGGATGAAGGGTTGT TCGTTTCTCCATGAAGTCC
PIN	MLOC_24846	Auxin Efflux carrier protein	q24846_Fw q24846_Rv	CGACGGAGTACAATGGAAGG CATACTGACACTCTCCAAGCC
SCARECROW-like1	MLOC_6971	GRAS family transcription factor	q6971_Fw q6971_Rv	GTGAACATCTTGGCTTGTGAAG TCATTCTCGCCCTCCATTTTC
Argonaute	MLOC_4898	(Argonaute/Dicer protein, PAZ	q4898_Fw q4898_Rv	TTATAAAGCCCCTTCCCCTTG GTACTIONTCTGCTTAGTCTTCCGG
AUX/IAA20	MLOC_73144	Auxin response factor 20	q73144_Fw q73144_Rv	TTGACATTGGTAGGTTCTCTGG TGCCCCTCTATACCAAACATG
ARRB	MLOC_61880	Response regulator B-type	q61880_Fw q61880_Rv	TCGGAGTTTCTGCCAATCTG CATCAAGTTTTGTACGCCG
CRY1b	MLOC_64083	cryptochrome 1b	q64083_Fw q64083_Rv	CGTGTGGAGCAATGAGGG AATCTGAGGTGTGCAAGGAG
CRY2	MLOC_8289	cryptochrome 2	q8289_Fw q8289_Rv	AAAGATGGAAGACACAGGCTC ACTGAAGACGAACAAGATGGG
HADC	MLOC_71091	histone deacetylase	q71091_Fw q71091_Rv	CCTAGCGTCCAGTTTCAAGAG TGCTGAGTCTTCCAAAGGTG
EIF5A2 ^(a)	AK357300	Mitochondrial substrate carrier family protein	qEIF5A2_fw qEIF5A2_rev	GGGTGTATGCGGATGTGA AATAGCATTCTCGGCTTCCA

ACT ^(a)	AK248432	actin	qHvACTrt_fw w qHvACTrt_r ev	TTGACCTCCAAAGGAAGCTATTCT GGTGCAAGACCTGCTGTTGA
Hv5439 ^(a)	AK360511	unknown protein	qHv5439_fw qHv5439_re v	GATTGAGGTGGAGAGGGTATTG CTCCTGGTCTGTTAGCAGTTT

II.3 Results and Discussion

II.3.1 Crown-root primordia development in the stem base of the spring barley cv. Golden Promise

In rice, the plant model for monocots since 1985, CRs originate from periclinal and anticlinal divisions of a part of a layer of meristem called ground meristem (GM) cells which adjacent to the peripheral cylinder of vascular bundles in the stem (Itoh et al. 2005; Coudert et al. 2010). This meristematic cell layer can be assimilated to a shoot pericycle-like tissue by analogy with the root pericycle in terms of position that is surrounded by a starch-rich endodermis and outer to vascular tissues of the stem (Itoh et al. 2005; Coudert, Le Thi, and Gantet 2013). Using classical histology and biphoton confocal microscopy, we evidenced that in barley the first CR primodium is already formed at 3DAG (Fig. II.2-A and II.2-B) at the outermost side of the pericycle, that is characterized by cells rich in starch. We designed this region as a ground meristem in comparison to rice. The earliness of CR primordia during seedling establishment has already been described in other monocots. Indeed, in rice, CRs emerge from the coleoptilar node already 2 to 3DAG (J. Xu and Hong 2013), and in maize, CR already emerge 10 DAG (Hochholdinger et al., 2004). The study of 10 DAG-old seedlings by biphoton confocal microscopy suggested that CR primordia are formed sequentially, i.e., one after each other, with a seemingly averaged distance of 76 μm and 140° angle between two CR primordia (Fig. II.2-C and II.2-D). This disagrees with the observation done in rice or maize, where several CR are produced in whorls (Lavarenne et al., 2019). Therefore, further anatomical study will be required to describe in detail the formation of CR in barley. In the crown of 1DAG-old seedlings neither CR initium could be observed by biphoton confocal microscopy, nor by classical histology (data not shown).

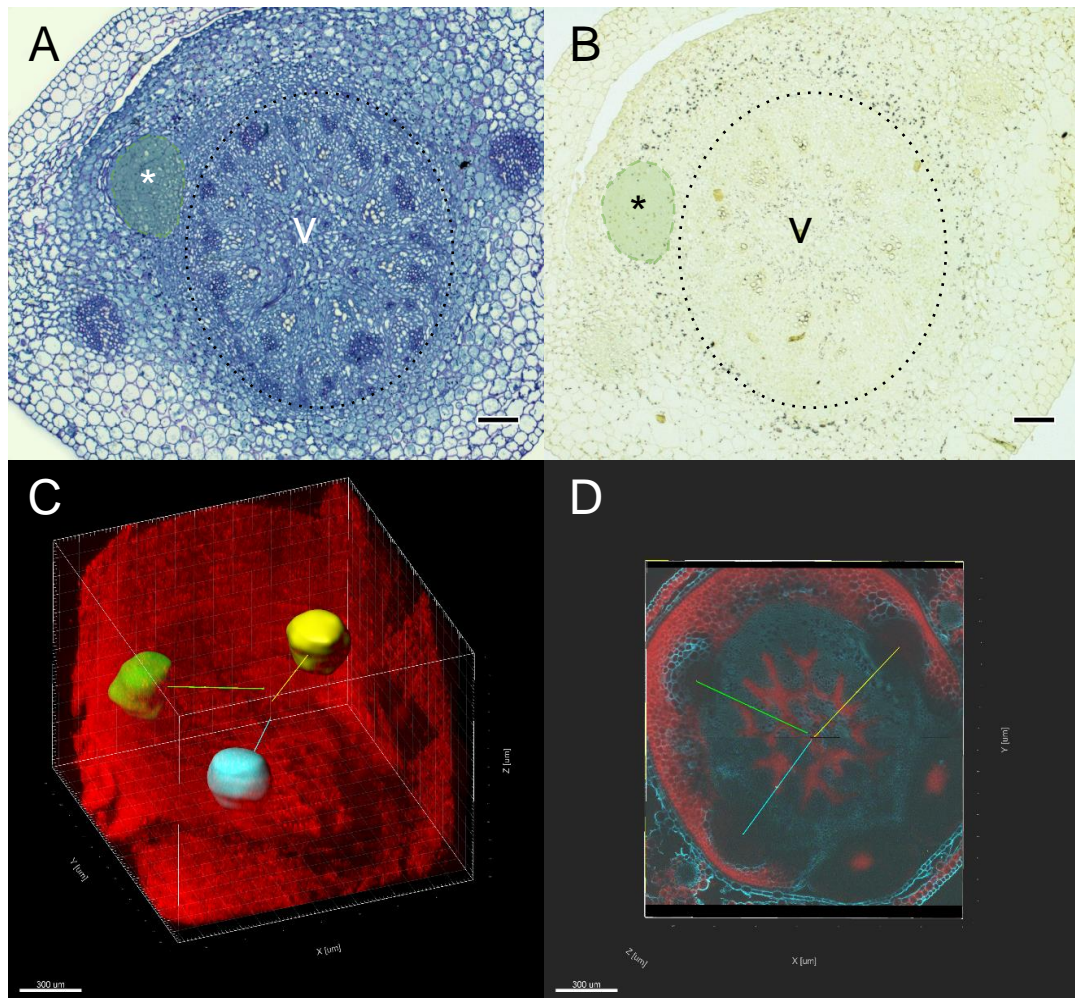


Figure II.2: Crown-root primordia development in young barley seedlings. In 3DAG-old seedling, one primordium is formed at the outermost side of the pericycle (**A**); PAS-NBB staining). The pericycle is surrounded by cells rich in starch as shown by the presence of purple-black dots after staining with lugol solution (**B**) (Figure A and B were conducted by my supervisor, Dr. Bergougnoux V.). (**C**) Result of a block reconstruction in the 3D transparency mode of the whole stem base of a 10 DAG-old barley seedling. CR primordia are identified by different colors: blue, green and yellow (**D**) z-axis cross section; the colored traits indicate the angle between each CR primordia (Figure C and D were conducted by Dr. Lavarenne J., IRD, Montpellier, France). Bars in A and B represent 100 μm .

For the study, we compared the transcriptome of the crown of 1DAG-old seedlings when no CR primordia could be seen to that of 10 DAG-old seedlings when 1 to 2 CRs already emerged, forming a “bud” at the surface of the stem and CR primordia are formed.

II.3.2 Transcriptomic changes in the stem base of 1DAG and 10DAG seedlings of spring barley cv. Golden Promise and functional annotation of differential expressed genes (DEGs)

Gene profiling of the CR development in barley was investigated by RNA-seq whole transcriptome analysis, comparing the transcriptome of crown of 10 DAG-old seedlings to that of 1 DAG-old seedlings of the spring barley cv. Golden Promise. For this purpose, 6 libraries (GP-1DAG-rep1, GP-1DAG-rep2, GP-1DAG-rep3, GP-10DAG-rep1, GP-10DAG-rep2 and GP-10DAG-rep3) were constructed from the basal portion of barley seedling's stem. These libraries were sequenced using an Illumina HiSeq2000 system. After adaptor trimming and masking low-complexity or low-quality sequence, we obtained 54-77 million raw single-end reads. The 45 bp-reads were mapped to the reference genome of barley cv. Morex IBSC_v1 (International, Genome, and Consortium 2012) using TopHat with default parameters. The averaged total single mapping rates of all samples was around 92.3 % (**Table II.2**). Differentially expressed genes were determined with DESeq2. Taking the limits of p-adjusted value < 0.05 and a log2foldchange excluding values from -1 to 1, there were 5264 DEGS between GP-10DAG and GP-1DAG, of which 2931 were up-regulated (UP10DAG, **Supplemental table II.1**) and 2333 were down-regulated (DO10DAG, **Supplemental table S.II.2**) in the crown of 10DAG-seedlings compared to the crown of 1DAG-seedlings.

Table II.2: Quality statistics of RNA-seq data:

Sample	Total raw read	Uniquely mapped reads	Multiple mapped reads	Single mapping ratio
GP-10DAG-rep1	77,896,964	72,832,121	2,254,880	93.50%
GP-10DAG-rep2	54,220,130	50,523,987	1,603,667	93.18%
GP-10DAG-rep3	61,531,385	57,026,131	1,827,334	92.68%
GP-1DAG-rep1	76,177,362	68,259,699	2,443,519	89.61%
GP-1DAG-rep2	63,227,909	58,405,829	2,338,714	92.73%
GP-1DAG-rep3	60,991,125	56,452,330	2,374,448	92.56%

The gene functional annotation was done using the MapMan BIN ontology in Mercator4 (Lohse et al., 2014; Schwacke et al., 2019). Indeed, the widely used gene

ontology (GO) comprises more than 34000 terms organized in 3 categories: “Biological process”, “Molecular Function” and “Cellular component”. This rich annotation can lead to a strong redundancy and problem to visualize data from RNAseq. In contrast, Mapman, specifically developed for plants, aims in assigning genes to as few functional categories as possible without losing information. Currently, MapMan ontology covers 27 functional top-categories (Klie and Nikoloski 2012; Schwacke et al. 2019). Among the 24,210 predicted genes, only 11,289 genes were annotated and categorized into different BINS. The BIN enrichment for genes up- and down-regulated in the stem base of 10DAG seedlings was indicated in table II.3. The functional annotation of the DEG revealed different that different pathways are represented in the stem bases of 1DAG and 10DAG seedlings (Fig.II.3).

Table II.3: BIN enrichment for genes up- and down-regulated in the stem base of 10DAG seedlings.

BIN_code	BIN_description	UP	DOWN
1.	Photosynthesis	5%	50%
2.	Cellular respiration	2%	8%
3.	Carbohydrate metabolism	10%	18%
4.	Amino acid metabolism	15%	9%
5.	Lipid metabolism	16%	7%
6.	Nucleotide metabolism	10%	15%
7.	Coenzyme metabolism	4%	15%
8.	Polyamine metabolism	14%	10%
9.	Secondary metabolism	16%	10%
10.	Redox homeostasis	20%	9%
11.	Phytohormone action	22%	7%
12.	Chromatin organisation	1%	19%
13.	Cell cycle organisation	1%	35%
14.	DNA damage response	1%	21%
15.	RNA biosynthesis	14%	8%
16.	RNA processing	1%	13%
17.	Protein biosynthesis	3%	21%
18.	Protein modification	17%	5%
19.	Protein homeostasis	13%	7%
20.	Cytoskeleton organisation	4%	16%
21.	Cell wall organisation	10%	7%
22.	Vesicle trafficking	6%	2%
23.	Protein translocation	2%	15%
24.	Solute transport	23%	4%
25.	Nutrient uptake	12%	0%

26.	External stimuli response	14%	5%
27.	Multi-process regulation	9%	5%

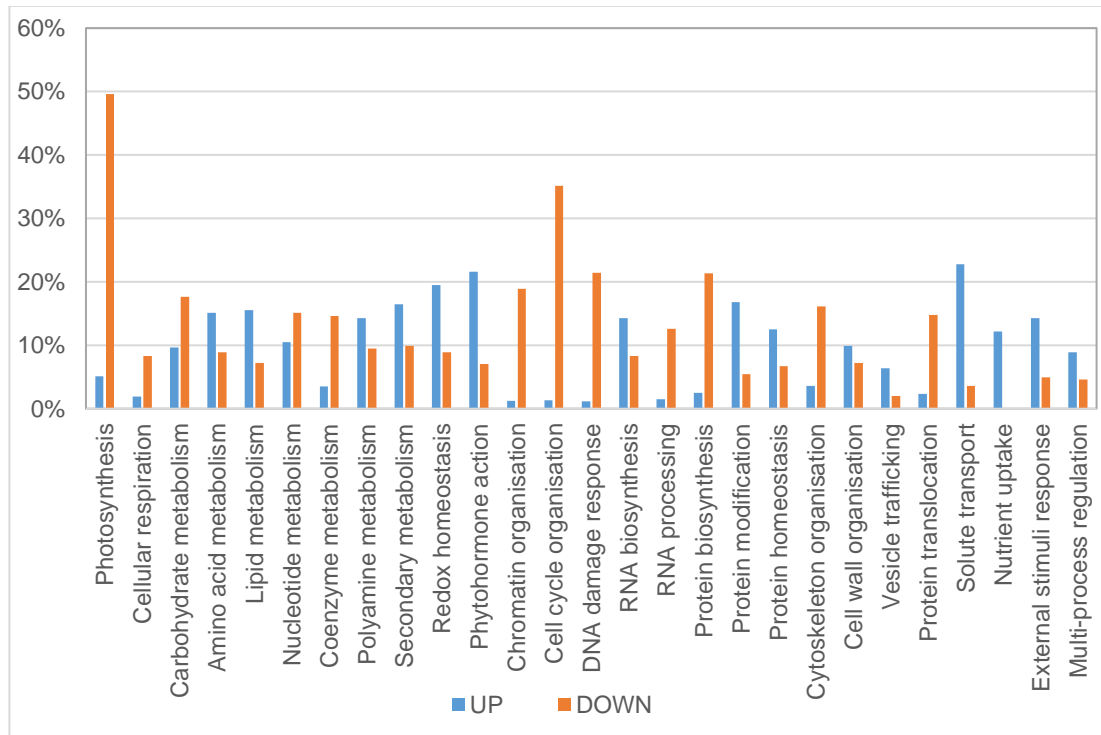


Figure II.3: Functional annotation of genes differentially regulated in the stem base of 10 DAG-old seedling of barley. The functional annotation was done with Mercator4; the number of genes in one category is expressed as a percentage of the total number of genes that were annotated.

Over-represented functional categories are summarized in table II.4 and figure II.2. Sequences with unknown functions represented up to 50% of the total sequences. Among genes down-regulated in the crown of 10 DAG-old seedlings, “DNA”, “cell”, “nucleotide metabolism” and “RNA” represented 19% of the DEGs. This suggested that profound molecular modifications occurred in the crown of seedlings that will enter the program of CR initiation and development. In opposite, genes up-regulated in the crown of 10 DAG-old seedlings belonged to categories “hormone metabolism”, “signaling”, “development”, “stress” and “cell wall”, suggesting a cellular/tissular organization.

Table II.4: Functional annotation enrichment of genes differentially regulated in the crown of 10 DAG-old seedling of barley cv. Golden Promise. The automated annotation was performed using the Mercator resource (Lohse et al. 2014). Only the most enriched category ($\geq 10\%$) are represented. Values represent the percentage of

genes in the specific category which were down- or up-regulated in DO10DAG and UP10DAG, respectively.

DO10DAG		UP10DAG	
Photosynthesis	50%	Solute transport	23%
Cell cycle organization	35%	Phytohormone action	22%
DNA damage response	21%	Redox homeostasis	20%
Protein biosynthesis	21%	Protein modification	17%
Chromatin organization	19%	Secondary metabolism	16%
Carbohydrate metabolism	18%	Lipid metabolism	16%
Cytoskeleton organization	16%	Amino acid metabolism	15%
Nucleotide metabolism	15%	Polyamine metabolism	14%
Protein translocation	15%	External stimuli response	14%
Coenzyme metabolism	15%	RNA biosynthesis	14%
RNA processing	13%	Protein homeostasis	13%
Secondary metabolism	10%	Nutrient uptake	12%
Polyamine metabolism	10%	Nucleotide metabolism	10%
		Cell wall organization	10%
		Carbohydrate metabolism	10%

Changes in gene expression determined by RNAseq were validated by qRT-PCR analysis. For this purpose, the change in expression of 9 genes was investigated (Fig.II.4-A) and the correlation between RNA-seq data analysis q PCR was confirmed (coefficient of Pearson correlation, $r=0.94$; Fig.4-A). Six genes with a potential role in CR development (*Plant intracellular Ras-group-related LRR protein 1/IRL1*; *PIN-FORMED-LIKES/PILS*, *SCARECROW-LIKE1 /SCR-like1*, *ARGONAUTE/ARGO*, *AuxIAA20* and *RESPONSE REGULATOR9/RRB9*) were confirmed by qRT-PCR to be up-regulated in the crown of 10DAG seedlings (Fig.II.4-B).

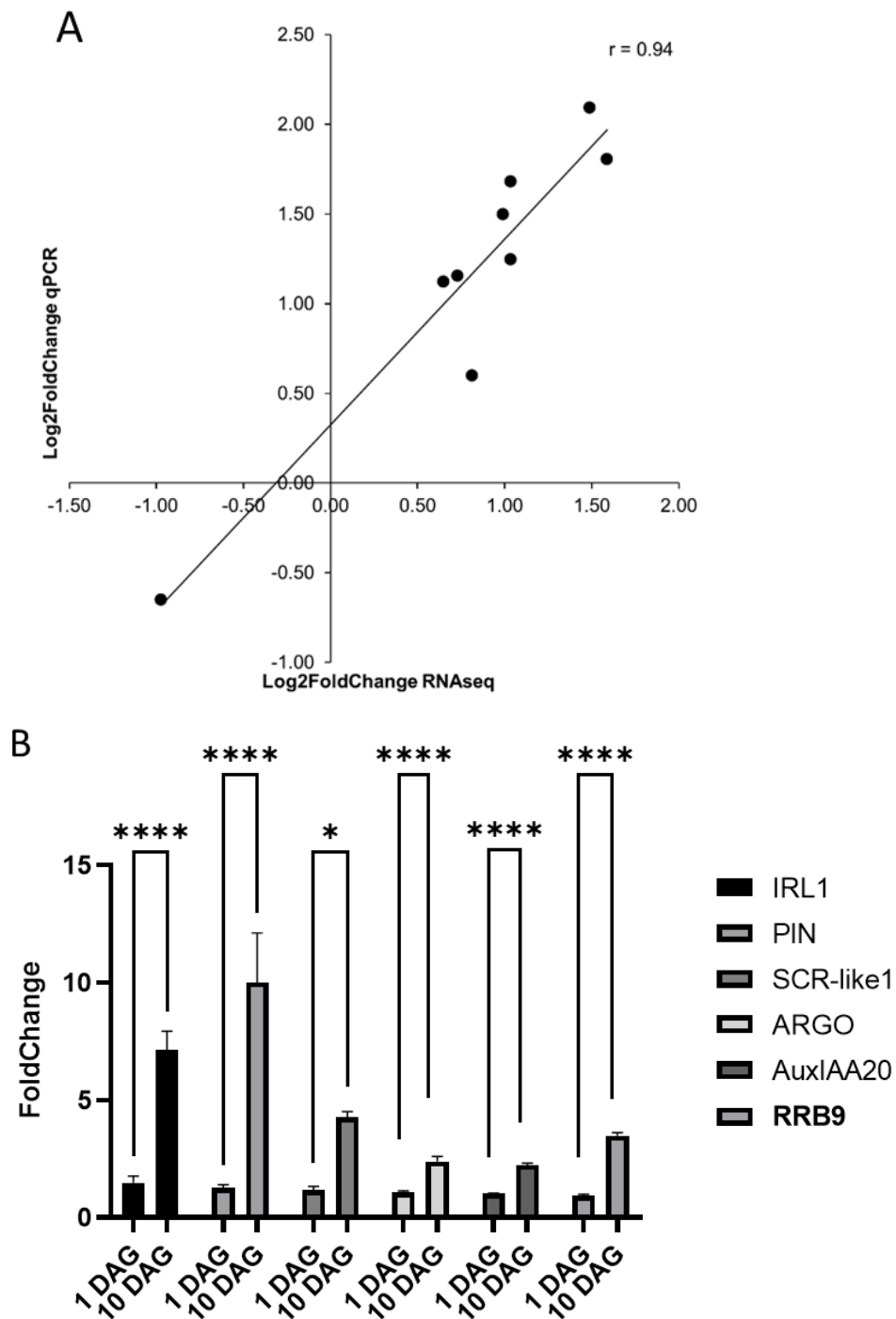


Figure II.4: (A) Comparison of expression as determined by RNA-seq and real-time PCR. All expression data were normalized to the log₂ scale. The coefficient of Pearson correlation was determined to be $r=0.94$. (B) Validation of differential expression by qRT-PCR of 6 genes with a potential role in CR initiation and development. qRT-PCR was run on the same samples as those used for RNAseq analysis. Normalization was done using the 3 most stable reference genes: Actin, Hv5439 and EIF152. The graph shows means \pm SEM ($n=3$). The statistical significance was assessed by a two-way

ANOVA followed by a Bonferroni multiple comparisons test (GraphPad Prism 9.2.0). ****: adjusted P-value < 0.0001; *: adjusted P-value < 0.005.

Moreover, we showed that their expression was significantly increased not only in the stem base, but also in the primary and seminal roots of the 10DAG seedlings (Fig.II.5). Even though our study did not focus on the lateral root development, these genes could be also involved in the initiation and development of lateral roots. Indeed, it has been demonstrated that development of lateral roots and CR shared common molecular regulators (Bellini, Pacurar, and Perrone 2014; Meng et al. 2019).

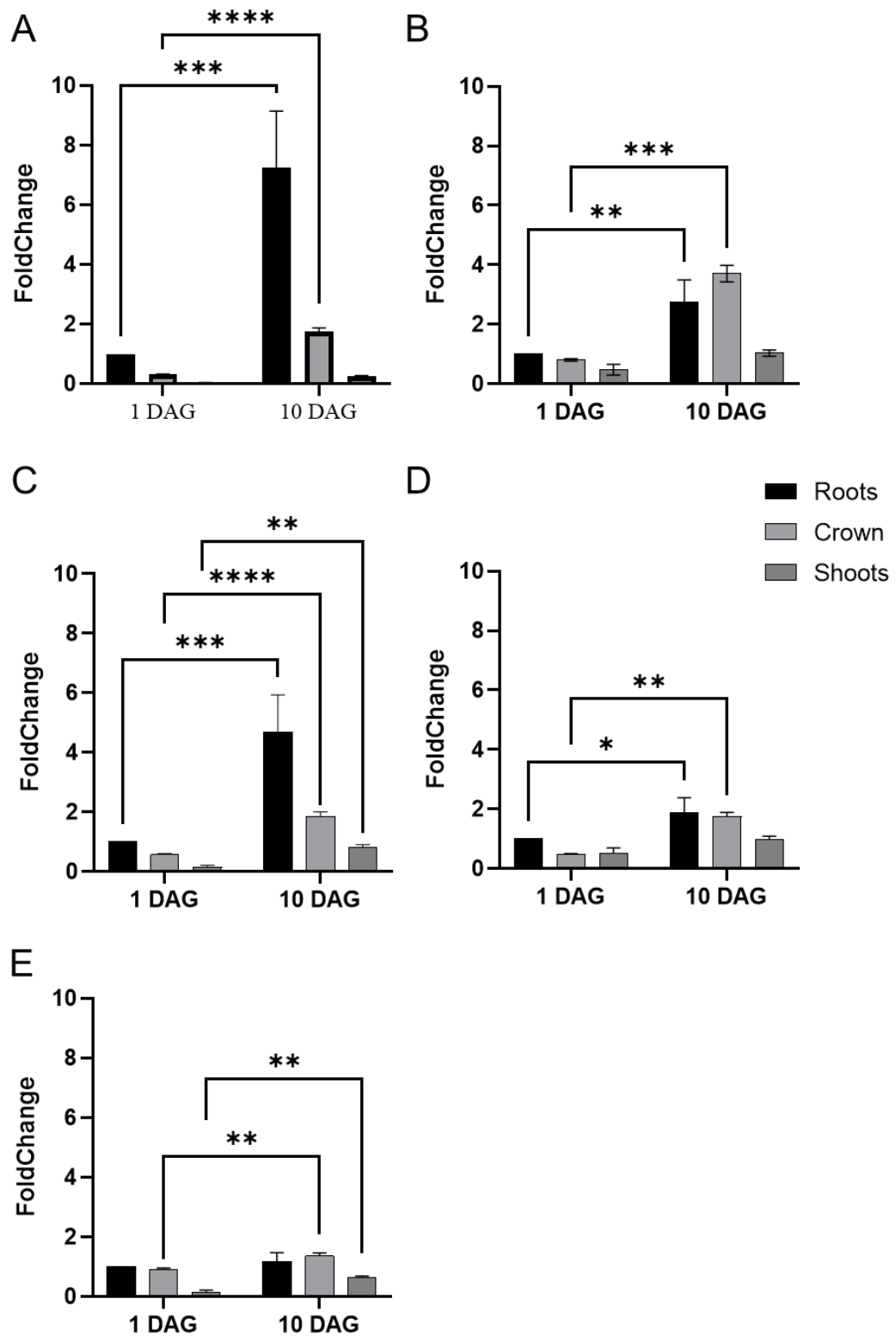


Figure II.5: Gene expression analysis by qRT-PCR of PIN (A), SCR-like1 (B), ARGO (C), AuxIAA20 (D) and RRB9 (E) in the roots, crowns and shoots of cv.

Golden Promise seedlings grown for 10 days in hydroponic conditions. Normalization was done using 3 reference genes: Actin, Hv5439 and EIF152. The graph shows means \pm SEM (n=3). The statistical significance was assessed by a two-way ANOVA followed by a Bonferroni multiple comparisons test (GraphPad Prism 9.2.0). ****: adjusted P-value < 0.0001; ***: adjusted P-value < 0.001; **: adjusted P-value < 0.001; *: adjusted P-value < 0.005.

II.3.3 Cell identity priming and cell cycle activation during CR development in barley

In the crown of 1DAG-seedlings, 12 genes encoding cyclin, cyclin-dependent kinases were up-regulated, suggesting an important activation of the cell cycle. In addition, cdc proteins and anaphase promoting proteins suggested that active cell division occurs. We also found that 32 kinesin and kinesin-related proteins were up-regulated in the crown of 1DAG seedling initiating CRs. Kinesins form a superfamily of microtubule motor proteins and trigger the unidirectional transport of vesicles and organelles, affect microtubule organization and cellulose microfibril order. They were also described to be involved in cell division and growth (J. Li, Xu, and Chong 2012).

In Arabidopsis, LR initiation is characterized by founder cell identity priming, cell cycle activation and asymmetric division of the founder cells. Auxin maxima are responsible for the up-regulation of cyclins and cyclin-dependent kinases (CDKs) and the concomitant repression of CDK repressors such as KRP1 and KRP2 which inhibits the G1/S transition (Perrot-Rechenmann 2010; Himanen et al. 2002; Fukaki, Okushima, and Tasaka 2007). Interestingly, in Arabidopsis, auxin alone is not sufficient for LR initiation. Moreno-Risueno and coworkers demonstrated the existence of a so-called “oscillation zone” which is primordial for the spatial and temporal definition of LR initiation sites. Transcription factors of the ARF, NAC, myeloblastosis (MYB) and SOMBRERO families are important for the determination of LR initiation sites (Moreno-Risueno MA, Van Norman JM, Moreno A, Zhang J, Ahnert SE 2010).

II.3.4 Hormonal status during crown-root development in barley

Genes belonging to the category “hormone metabolism” account for a large proportion of sequences over-represented in the crown of 10 DAG-old seedlings

(enrichment: 22%), suggesting an important modification in hormonal status during the development and emergence of CR in barley.

Auxin is probably the most important hormone that regulates initiation of CRs. Among the genes abundant in the crown of 10DAG-old seedlings, we found 27 genes related to auxin (IAA) metabolism, signal transduction or induced by auxin. IAA maxima are fundamental for root primordia formation and emergence (Kitomi et al. 2008; Jansen et al. 2012; Péret et al. 2009). In Arabidopsis, a local auxin maximum, generated by the auxin efflux carrier PIN1 (PINFORMED1), is required to properly trigger the asymmetric division of the two pericycle cells to generate an LR primordium (Péret et al. 2009). In rice, OsPIN1 plays a role during CR development rather than during the CR primordia initiation. Other PINs (OsPIN2, OsPIN5b and OsPIN9) are likely to be involved in this process (S. Liu et al. 2009). In our data, two auxin transporter-like proteins and one auxin efflux carrier were identified as up-regulated in the crown of 10DAG-seedlings. These 3 auxin transporters might participate in establishing auxin gradient required for CR development in barley. The release of free auxin from conjugates is often neglected. In the present study, we identified a gene annotated as IAA-amino acid hydrolase (ILR1). IAA-amino acid conjugates function in both the permanent inactivation and temporary storage of auxin, participating thus in auxin homeostasis regulation. ILRs allow releasing free IAA from the amino acid conjugates (LeClere et al. 2002). The Arabidopsis triple hydrolase mutant, *ilr1 iar3 ill2*, had fewer lateral roots than the wild-type, demonstrating the importance of IAA release from conjugate in the initiation of lateral roots (Rampey et al. 2004). Whether IAA is released from IAA-conjugates via ILR1 to support CR primordia formation and development in barley represents an interesting challenge to solve.

Our study revealed that at least 18 genes related to ethylene metabolism and signaling pathway were up-regulated in the crown of 10DAG-seedling, when CRs are already initiated and are emerging from the stem. In rice, ethylene induces the death of epidermal cells at the site of CRs emergence. Thus, through the crack of the epidermis the newly formed root can emerge without damages (Mergemann and Sauter 2000). Our data suggest that in barley, the emergence of CRs is possibly correlated

with death of cortex and epidermal cell in an ethylene-mediated response. This is supported by the fact that a gene associated with development and cell death was also up-regulated in the crown of 10DAG-seedling.

Abscisic acid (ABA) is another important hormone. Its role as inhibitor or stimulator of plant growth and development is a constant question of debate (Humplík, Bergougnoux, and Van Volkenburgh 2017). ABA has a dual role in root development: whereas it stimulates the initiation and primordia formation in different species, it often inhibits the emergence from the stem and the subsequent elongation of the root (Harris 2015). Fifteen genes related to ABA synthesis and signaling pathway were found to be up-regulated in 10DAG-seedlings developing CRs. Among these genes belong two transcripts, annotated as 9-cis-epoxycarotenoid dioxygenase/ NCED, which catalyzes the first committed step of ABA synthesis. This suggested that ABA synthesis takes place in the crown of seedlings developing CRs and that ABA is also important for the development of CRs in barley. Nevertheless, deeper studies would be necessary to precisely determine the role of ABA in the different steps of CR development, i.e., primordium initiation, emergence, and root elongation.

We also found that a gene encoding a gibberellin 2-oxidase, highly abundant in the crown of barley seedling, was up-regulated in 10DAG-seedlings. GAox2 are responsible for the degradation of active gibberellins (GAs). In poplar, GAs negatively regulates lateral root, specifically inhibiting root primordium initiation. The role of GA2ox in regulating GAs homeostasis was also proved in the same study (Gou et al. 2010). In rice, overexpressing GA2ox led to the decrease of endogenous GAs and enhanced CRs root growth (Lo et al. 2008). Similarly, the silencing of SLR1, a negative regulator of the GA signaling pathway, resulted in lower number of CRs in rice (Ikeda et al. 2001). It is thus tempting to postulate that GAs are inhibitors of CR initiation and development in barley and a precise regulation of its homeostasis via GA2ox is required.

II.3.5 Emergence of CR induces cell death and cell wall modification

The molecular events of LR and CR emergence are still unclear. Nevertheless, two different modes of root emergence have been assumed: i) “active removal” of the

cortical cells most probably induced by root primordia, implying death of cells covering the root primordia, and ii) “mechanical breakage” of epidermal cells by the tension resulting from the growth of the root (Charlton 1996).

In rice, the emergence of CRs happens concomitantly to death of nodal epidermal cells above CR primordia (Mergemann and Sauter 2000). In maize, Park and coworker reported the formation of a cavity in the cortex of primary root around the LR primordia, resulting probably from the death of the cells (Park, Hochholdinger, and Gierl 2004). Apoptosis of epidermal cells is controlled by ethylene and is mediated by reactive oxygen species (ROS), which are also involved in CR primordia growth (Steffens et al. 2012), allowing coordinating CR growth with local weakening of the epidermal cell barrier (Steffens and Sauter 2009). In the present study, we demonstrated that genes involved in the ethylene pathway were up-regulated in the crown of 10 DAG-old seedlings (Fig.II.5-A). The use of the Blue Evan’s staining showed that cell death occurred at the site of emergence of CRs (Fig.II.5-B). It was shown that epidermal cells covering CR primordia might be targeted to die, as they contain lower amount of the METALLOTHIONEIN2b (MT2b), a scavenger of ROS (Steffens and Sauter 2009). Interestingly, a gene encoding a metallothionein was strongly down-regulated in the crown of 10 DAG-old seedlings, suggesting a reduction in ROS scavenging. Our transcriptomic data suggest that emergence of CRs in barley is correlated with cell death, mediated by ethylene and ROS. Thirteen genes annotated as (endo)-chitinases were up-regulated in the crown of 10 DAG-old seedlings. Chitinases are glycosyl hydrolases that catalyze the degradation of chitin, a major constituent of fungi cell wall and exoskeleton of insects. Commonly induced upon pathogen attack, they were for long associated with plant defense. However, growing evidence determined that (endo)-chitinases have different functions during plant growth and development. The analysis of Arabidopsis chitinases revealed 5 classes, some of them having functions in “cell wall synthesis” or in “cell rescue, defense, cell death and aging” (Passarinho and de Vries 2002). The role of class IV chitinase in cell death was recently reported in pepper (D. S. Kim, Kim, and Hwang 2015). Genes of the functional category “Cell wall” were overrepresented among genes up-regulated in the crown of 10 DAG-old seedling (13%), indicating that profound modifications

occur when CR primordia form and develop. These genes are mainly related to pectin lyases, expansins and xyloglucan endotransglucosylases/hydrolases (XEGs). In Arabidopsis, the newly formed LR has to pass through 3 cell layers: endodermis, cortex and epidermis (Péret et al. 2009). Cells are particularly well attached to each other, especially epidermal cells. Genes encoding proteins affecting cell wall-property integrity (expansins, pectin lyases or XEGs) are expressed in tissues covering the emerging LR primordia. The activity of these enzymes most probably promotes cell separation in advance of developing lateral root primordia to avoid damages of the root meristem (Swarup et al. 2008). Moreover, the cell-wall properties could contribute to the number of LR produced (Roycewicz and Malamy 2014). Indeed, the high-affinity auxin importer Like Aux1 (LAX3) is an important regulator of LR emergence. Its expression in cells situated over the LR primordia regulates the activity of cell wall remodeling enzymes, which are likely to promote cell separation in advance of developing lateral root primordia (Roycewicz and Malamy 2014). In the present study, a gene encoding LAX3, was up-regulated in the crown of 10 DAG-old seedlings where CR are formed and emerging.

The analysis of the 1.5 kb promoter sequence of three genes encoding a metallothionein, a chitinase and an expansin revealed the presence of numerous AP2/ERF and EIN3 motifs, reinforcing the hypothesis that those gene could be regulated by ethylene during CRs emergence (Fig.II.5-C).

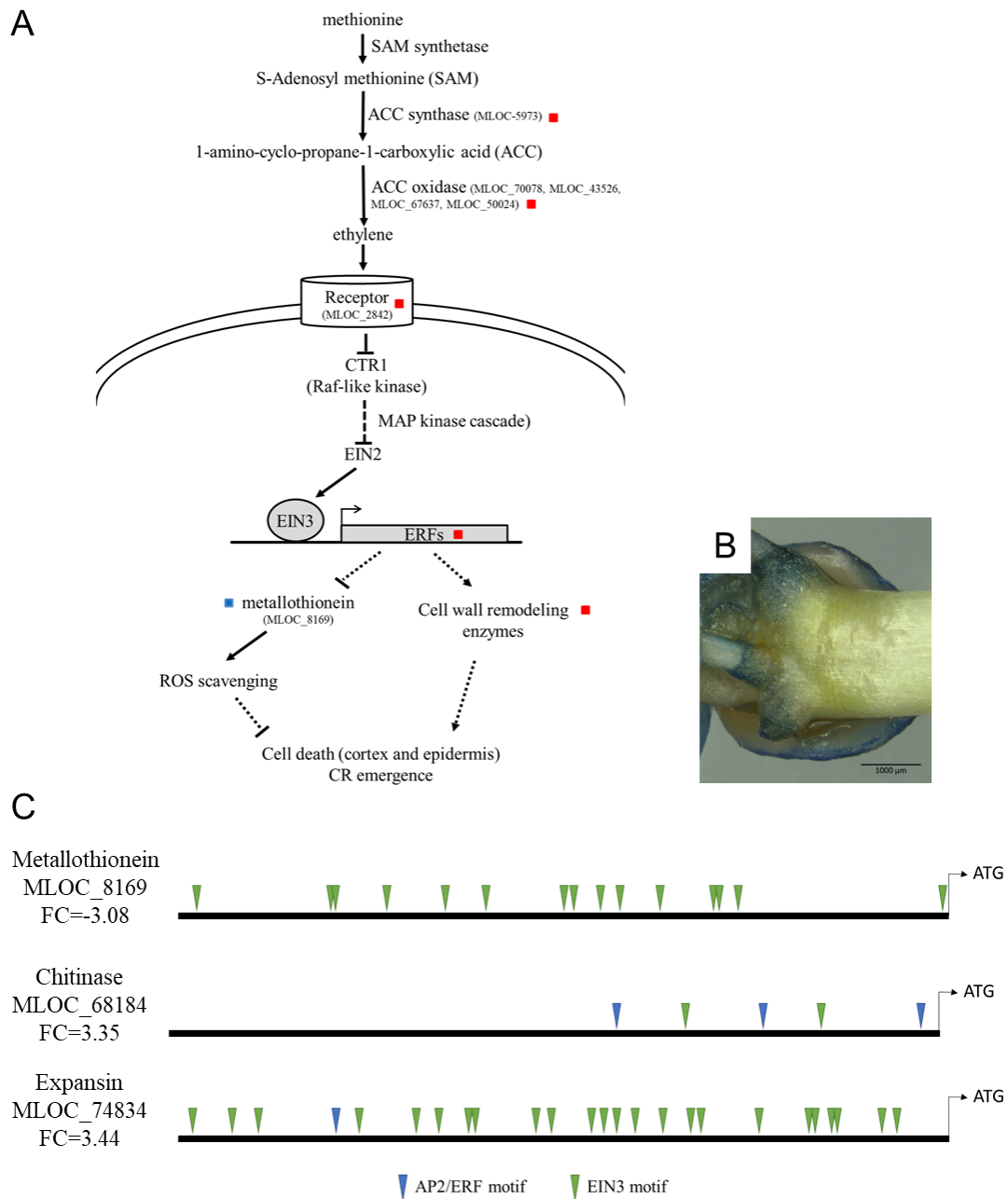


Figure II.6: Involvement of ethylene in cell death during crown-root emergence in barley cv. Golden Promise. **(A)** Ethylene biosynthetic and signaling pathway in the context of cell death. Genes identified in the RNAseq data as differentially expressed are indicated (MLOC); colored scales indicate whether they were up-regulated (red) or down-regulated (blue) in the stem base of 10 days-old seedlings. **(B)** Evans blue staining indicates the cell death of the epidermal cell at the site of crown-root emergence. **(C)** Prediction of the presence of ethylene-related cis-regulating elements (AP2/ERF and EIN3 motifs). Prediction was done with PlantPAN3.0, using rice database.

It was supposed that the site of epidermis breakage in relation to root emergence may represent a site of infection by pathogens (Charlton 1996). Benzoxazinoids are plant secondary metabolites involved in resistance against pathogens. They are present in grasses and in some dicots. Maize was the most important source of studies concerning these compounds. Their biosynthesis branches off from tryptophan at the indole-3-glycerol phosphate, which is converted into indole by indole-3-glycerol phosphate lyase (BX1). Four cytochrome P450 monooxygenase (BX2-BX5) are responsible for the subsequent production of DIBOA, the most effective benzoxazinoid (Makowska, Bakera, and Rakoczy-Trojanowska 2015). In maize, benzoxazinoids defense molecules were found to accumulate at the site of crown-root emergence, preventing pathogenic infections, which could occur during the crack of the epidermis. It is interesting to observe that in the crown of barley 10 DAG-old seedling, genes encoding enzymes of the benzoxazinoid biosynthesis were up regulated. Two genes were orthologues to the maize indole-3-glycerol phosphate lyase (BX1) and others were related to BX2 and BX4, suggesting that this synthetic pathway was stimulated during CR development and emergence.

II.4 Conclusions

We analyzed the transcript profiles of barley young seedlings to increase our understanding of the mechanisms underlying the mechanisms regulating crown-root development and emergence. Our study constitutes the first step toward understanding the molecular and physiological mechanisms involved in development and emergence of CR in barley. Whereas we identified a similar role of auxin, CK and other hormones in the process as described in other species, our study brings novelty concerning the last stage of CR development, i.e. emergence. Further functional studies of identified key genes will be necessary to precise their involvement in CR formation.

CHAPTER III: Two lateral organ boundary domain transcription factors HvCRL1 and HvCRL1-L1 regulate shoot-borne root formation in barley (*Hordeum vulgare* L.)

Thu Dieu Nguyen, Mathieu Gonin, Michal Motyka, Antony Champion, Goetz Hensel, Pascal Gantet, Véronique Bergougnoux (2024). *Journal of Plant Growth Regulation*.

III.1 Introduction

Roots play fundamental roles in plant growth and development, allowing not only anchorage but also water and nutrient uptake. In cereals, the major structure of the root system is formed by specific shoot-borne roots called crown-roots (CR). The cereals' crown root system dominates and ensures resource acquisition during vegetative growth as well as during reproductive and grain-filling phases (SHA et al. 2023). Different grass species adapt to water shortages by inhibiting the growth of newly formed crown roots and promoting the growth of established soil roots to go deeper (Sebastian et al. 2016). In contrast, multiple crown roots help plants anchor themselves to the soil and create a multiaxial and redundant system, allowing for greater soil exploration volumes, rapid water capture, and security to minimize damage caused by biotic stresses (Hochholdinger, Woll, et al. 2004). Genetics of CR initiation and development have been investigated in the rice plant model (Mai et al. 2014; Meng et al. 2019). Less information is available for European cereals such as wheat or barley. Barley (*Hordeum vulgare* L.) is the fourth most economical important crop used both for human and animal feeding, and brewery (FAO 2022). Due to its relative genome for cereals, diploid barley has become a genetic model for generating induced mutants and identifying potential agronomical genes as well as genetic markers for the small-grain temperate cereals of the Triticaceae family (i.e., allohexaploid bread wheat), since the early 20th century (Nadolska-Orczyk et al. 2017). In barley, like other cereals, the root system mainly consists of postembryonic shoot roots, named crown roots (Orman-Ligeza et al. 2013; Gonin et al. 2019; Jia et al. 2019). One of the critical pathways in CR initiation is controlled by transcription factors (TFs) encoded by the *LATERAL ORGAN BOUNDARIES (LOB) Domain (LBD)* genes (Coudert et al. 2015; C. Xu, Luo, and Hochholdinger 2016). The genome-wide analysis of *LBD* gene family is available for barley since 2016 (B.-J. Guo et al. 2016). Moreover, the particular functions of LBD TFs in various developmental processes have not been determined, yet, especially during crown root formation.

III.1.1 Structure of lateral organ boundaries domain proteins

One of the most prominent patterning decisions in plants is to define boundaries between organs or between organs and meristems. Typically expressing at the adaxial base of initiating lateral organs and regulating plant pattern formation that precisely coordinates temporal and spatial developmental programs, the LBD proteins play a fundamental role in the determination of the boundaries of the plant lateral organ. Thus, they are key factors involved in almost all aspects of plant development such as in meristem programming, cell proliferation and differentiation during growth and development in many plant species, pollen and embryo development, root formation, leaf morphology mold, vascular differentiation, plant regeneration and inflorescence (Aida and Tasaka 2006; Majer and Hochholdinger 2011). Furthermore, this protein family plays essential roles and function in the regulation of metabolism and physiology, namely anthocyanin, nitrogen metabolism photosynthesis and disease susceptibility (B.-J. Guo et al. 2016). It is frequently observed that orthologue *LBD* genes exhibit similar or partially conserved biological functions and regulation in different angiosperm species (Okushima et al. 2007). In 2009, Matsumura and colleagues showed that the function of LBD cannot be replaced by other members of the LBD family, proving that dissimilar amino acid (AA) residues in the LOB domains are also crucial for characteristic functions of the family members (Matsumura et al. 2009).

The LBD proteins, also referred to as ASYMMETRIC LEAVES2-LIKE (AS2-like) domain (ASL) (hereafter referred to as LBD) proteins, which are originated from green charophyte algae and moss to angiosperms (Y. Zhang et al. 2020; Gonin et al. 2022), constitute a class of the plant-specific DNA-binding transcription factors because of their nuclear localization and DNA-binding ability (Husbands et al. 2007; Gonin et al. 2022). The LBD proteins are defined by containing a relatively conserved characteristics N-terminal LOB domain and a variable C-terminal region (Y. Zhang et al. 2020). The LOB domain is approximately 100 AAs in length and is usually composed of three main motifs, including: (1) four conserved cysteine residues (CX₂CX₆CX₃C/ or C-motif) in a zinc finger-like motif where X residues are variable and followed by; (2) an invariant Gly–Ala–Ser (termed the GAS motif) block, and (3)

a conserved C-terminal leucine-zipper-like coiled-coil motif (LX₆LX₃LX₆L) (Shuai, Reynaga-pen, and Springer 2002; Majer and Hochholdinger 2011). The structure of LBD TFs is illustrated in **Fig.III.1**. The zinc finger C-motif functions in binding to a DNA sequence (W. F. Chen et al. 2019). Several consensus DNA binding sequences of LBD TFs were previously identified and described *in vitro* and *in vivo* such as 6-bp GCGGCG (*LBD-box*) (with the conserved 4-nt core sequence CGGC and G being the most common nucleotide at both the 5' and 3' flanking positions), 6-bp CATTAT and 6-bp CACA[A/C]C (*CRL1-box*) sequences, which are present in promoters of several target genes of LBD nuclear proteins (Husbands et al. 2007; Ohashi-Ito, Iwamoto, and Fukuda 2018; Gonin et al. 2022). The leucine-zipper-like coiled-coil motif is responsible for protein homo-dimerization based on its five repetitions of the hydrophobic amino acids (valine, isoleucine, leucine) separated by other six variable amino acid residues (Shuai, Reynaga-pen, and Springer 2002; Kong et al. 2017; Majer and Hochholdinger 2011). The C-terminus of the LBD TFs were reported to have functions in stabilization or enhancement protein-protein interactions (Husbands et al. 2007). Some LBD proteins have been illustrated that they do not have homodimerize but might interact with their conserved partners (Majer and Hochholdinger 2011). For instance, Lin Xu et al, (2003) indicated that the MYB (**myeloblastosis**)-domain protein AtAS1 in *Arabidopsis* and the LBD domain protein AtAS2 (LBD6) bind to each other to form a complex (L. Xu et al. 2003). Furthermore Matthew M.S. Evans (2007) reported in maize that the LBD protein ZmIG1 (ZmLBD19) heterodimerizes with the AtAS1 ortholog ROUGH SHEATH2 (ZmRS2) (Evans 2007). In addition, the conserved LOB domain can interact with other proteins, including the helix-loop-helix (bHLH) TF bHLH048, and the interaction consequently changes the affinity of the LBD protein for the consensus DNA motif (Husbands et al. 2007).

The LBD protein family has been divided into two major classes (**Fig.III.1**), that are normally characterized by the presence (class I) or absence (class II) of the functional leucine-zipper-like motif (Y. Zhang et al. 2020). The majority of LBD proteins belong to class I that normally has a zinc finger-like motif, GAS block and a leucine zipper-like coiled-coil motif, while class II contains only a zinc finger-like domain (Shuai, Reynaga-pen, and Springer 2002; Husbands et al. 2007). Class II LBD

proteins have no or incomplete GAS and leucine zipper domains, which consequently has no coiled-coil structure and therefore they were speculated to have different function or no function (Majer and Hochholdinger 2011; C. Xu, Luo, and Hochholdinger 2016). One reason could explain why LBD TFs are involved in a lot of distinct development and regulation in plants is they have a slacken DNA binding specificity (Gonin et al. 2022). Up to now, numbers of LBD proteins have been reported in the model eudicot *Arabidopsis thaliana* (43 members) and important cereals including *Oryza sativa* (37 members), *Zea mays* (49 members) and *Triticum aestivum* (86 members) (Y. Zhang et al. 2020), which were based on the published genome and protein sequence similarity.

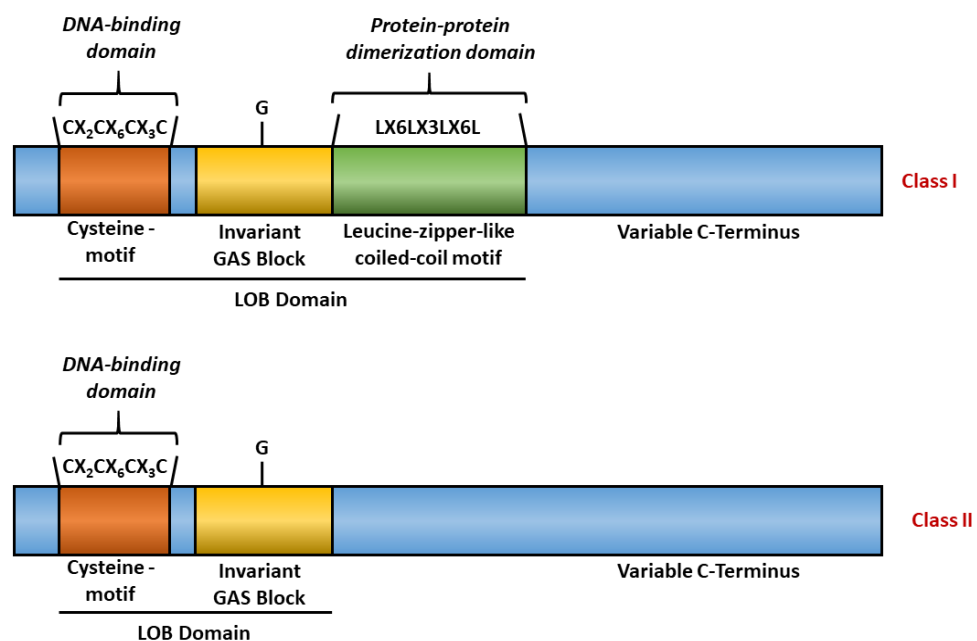


Figure III.1: Structure of LBD proteins.

III.1.2 Function of LBD proteins in root initiation and development

LBD genes, especially belonging to class IB clade, have been reported to be essential regulators of post-embryonic root formation in monocotyledonous and dicotyledonous species (C. Xu, Luo, and Hochholdinger 2016; Y. Zhang et al. 2020; Kidwai, Mishra, and Bellini 2023). A summary of the molecular frameworks and

interaction of LBD-mediated processes during root initiation and development is illustrated in figure III.2.

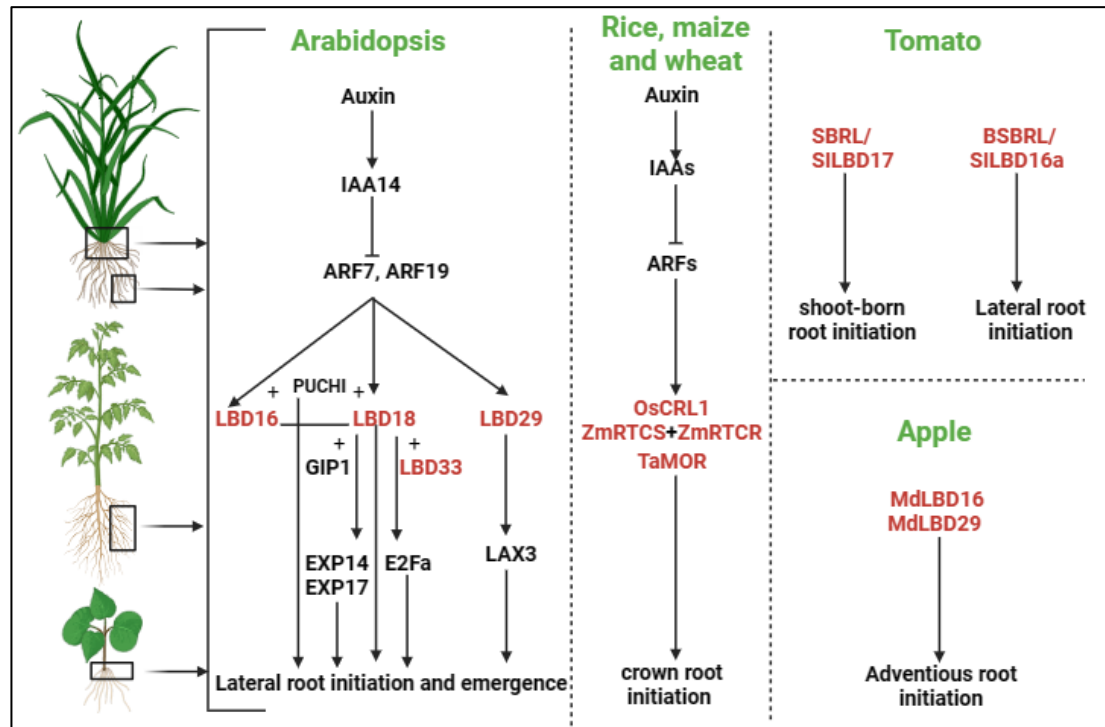


Figure III.2: a summary of molecular pathways and interaction of LBD-mediated processes during root initiation and development. The LBD proteins are presented in red, the plants are presented in green. Positive and negative regulatory actions are indicated by arrows and lines with bars, respectively. Physical protein interactions are indicated by '+'. Abbreviations: ARF, AUXIN RESPONSE FACTOR; CRL1, CROWN ROOTLESS 1; IAA, Indole-3-acetic acid; LBD, LATERAL ORGAN BOUNDARY DOMAIN; RTCL, RTCS-LIKE; RTCS, ROOTLESS CONCERNING CROWN AND SEMINAL ROOTS; MOR: MORE ROOT; SBRL/SILBD: SHOOTBORNE ROOTLESS; BSBRL/SILBD16: BROTHER OF SHOOTBORNE ROOTLESS (modified from C. Xu, Luo, and Hochholdinger 2016)

In *Arabidopsis thaliana*, the *AtLBD16*, *AtLBD18*, *AtLBD29*, and *AtLBD33* genes, which are induced by auxin through the activation by their Auxin Response Factor (ARF) transcriptional activators *AtARF7* and *AtARF19*, promote lateral root initiation (Okushima et al. 2007; Berckmans et al. 2011; Bargmann, Birnbaum, and Brenner 2014; Lee et al. 2019). Whereas *AtARF7* and *AtARF19* directly regulate *AtLBD16*, *AtLBD18* and *AtLBD29*, they do not directly regulate *AtLBD33*. Both *AtLBD16* and *AtLBD29* are expressed in the root stele and lateral root primordia (LRP), whereas *AtLBD33* activity is localized in only LRP (Okushima et al. 2007; Lee

et al. 2009). A later research of Porco S. et al (2016) proved that AtLBD29 is not only expressed in LRP, but also in the cells directly overlying the new root organ and acts as TF binding to promoter of the auxin influx carrier *like-auxin permease 1 (AUX1)-3 (LAX3)* gene during lateral root (LR) emergence (Porco et al. 2016). Furthermore, AtLBD18 in conjunction with AtLBD16 functions in the initiation and emergence of adventitious roots (Lee et al. 2019). LBD18 and LBD33 cooperate as a dimer and transcriptionally activate the *E2Fa* gene, which regulates the asymmetric cell division in lateral root initiation (Berckmans et al. 2011). AtLBD18 regulates the expression of *EXPANSIN14 (EXP14)* and *EXP17* encoding a cell-wall loosening factor, which facilitates lateral root emergence (Lee et al. 2013)(Lee and Kim 2013). Auxin inducible PUCHI, an AP2/EREBP (ethylene-responsive element-binding protein) transcription factor, synergistically act with LBD16 and LBD18 downstream of the Aux/IAA-ARF7 and 19 module during lateral root development (Kang, Lee, and Kim 2013).

In rice (*Oryza sativa* L.), a homolog of *AtLBD16* and *AtLBD29*, the *CROWN ROOTLESS1/ADVENTITIOUS ROOTLESS1 (OsCRL1/OsARL1)* gene encodes an LBD transcription factor which is also promoted through auxin and acts as a positive regulator for crown root and lateral initiation (Y. Inukai 2005; H. Liu et al. 2005). *CRL1* is an auxin-responsive gene regulated by ARF1 (Inukai 2005). As an auxin-responsive factor involved in auxin-mediated cell de-differentiation, OsCRL1 can promote the initial cell division in the ground meristem, which is adjacent to the ground meristem vascular cylinder of the rice stem base (Coudert et al. 2015). OsIAA31 promotes the induction of CRL1 expression by auxin, which is involved in CR initiation (Coudert et al. 2011). *CRL1* gene is expressed not only in ground meristem of coleoptilar node of the stem, which is the initiation site of crown roots, but also in pericycle cells, where lateral roots initiate. Interestingly, although there are various morphological and anatomical difference, an auxin-AUX/IAA/ARF-LBD molecular module is conserved in regulation of postembryonic root formation in both dicotyledons and monocotyledons (Coudert et al. 2013; Orman-Ligeza et al. 2013).

In maize, the *rootless concerning crown, and seminal roots (rtcs, Zmlbd2)* mutant is impaired in the initiation of embryonic seminal and post-embryonic shoot-

borne roots (Taramino et al. 2007; C. Xu et al. 2015; Hochholdinger, Yu, and Marcon 2018). The *RTCS* is orthologous to *AtLBD16*, *AtLBD29* and *OsCRL1* in Arabidopsis and rice, respectively. The *RTCS*-like (*RTCL*, *ZmLBD43*), a paralog of *RTCS*, is also preferably expresses in roots. Both *RTCS* and *RTCL* genes are auxin inducible and contain auxin response elements in their promoters. Both proteins are involved in the early events that lead to the initiation and maintenance of seminal and shoot-borne root primordium formation. Both act as transcription factors and bind to promoters of genes downstream of *LBD* genes (Taramino et al. 2007).

In wheat, the LBD protein MORE ROOT (TaMOR) interacting with ARF5 also controls the formation of crown root (C. Li et al. 2022). In tomato (*solanum lycopersicum*), the LBD transcription factor SHOOTBORNE ROOTLESS (SBRL/SILBD17) determines shoot-born root formation, whereas BROTHER OF SHOOTBORNE ROOTLESS (BSBRL/SILBD16a) determines lateral root initiation (Omary et al. 2022). In apple (*Malus domestica* Borkh), MdLBD16 and MdLBD29 proteins stimulate the formation of adventitious root primordia initiation and promote the number of adventitious root in the cut stems (Bai et al. 2020). Therefore, these LBD genes perform remarkably similar biological functions in different plant species and constitute useful regulators of root system structure.

III.1.3 Aims of this study

The present study aims to understand the role of LBD transcription factors during initiation and development of crown roots in barley. Based on the new annotation, the barley reference genome contains 31 *LBD* genes. The phylogenetic analysis of barley LBD proteins identified two closest orthologous namely *HvCRL1* and *HcCRL1-L1* to the rice *CRL1* gene and the maize *RTCS* and *RTCL* genes, which were characterized as being involved in CR initiation and development (H. Liu et al. 2005; Inukai 2005; Majer et al. 2012; C. Xu et al. 2015). Through real-time PCR analysis, the expression of both genes is accumulated in the stem base of barley seedlings in response to auxin induction, with *HvCRL1* transcripts being accumulated earlier than *HvCRL1-L1* transcripts. The *in-silico* analysis of the *HvCRL1-L1* promoter indicated that this gene could be a downstream target of *HvCRL1*. In addition, using

the knock-out barley lines in each of the two genes, as well as the complementation of the *crown rootless1* (*crl1*) rice mutant, we investigated the involvement of these two genes during CR initiation and development in barley.

III.2 Materials and methods:

III.2.1 Plant materials.

The two-rowed spring homozygous diploid 1-6 (DH 1-6) barley (*Hordeum vulgare* L.) cultivar Golden Promise was used for all barley experiments in this study. Plants were sown and grown in 2 L pots containing a 3:1:2 mixture of garden soil/sand/white and black peat (Klasmann Substrate 2). At the tillering stage (BBCH code 29/30), plants were fertilized with 15g of Osmocote (N, P, K: 19%, 6%, 12%; Scotts, The Netherlands). Cultivation was carried out in a greenhouse in Olomouc (Czech Republic) maintained at 18°C day/16°C night, under varying natural light. When necessary, a 14 h photoperiod was maintained with artificial lighting provided by sodium vapor lamps combined with mercury vapor lamps (500 mmol.m⁻².s⁻¹ at the top of the plant).

Seeds of the *O. sativa* L. cv. Taichung 65 (TC65), *crl1* mutant in the genetic background Taichung 65 and cv. Kitaake were originally provided by UMR DIADE-Montpellier (France). TC65 and *crl1* seeds were previously obtained from Professor Y. Inukai, Japan (Inukai et al. 2005). For the purpose of seed multiplication and selection of transgenic rice, plants are grown in greenhouses. Seeds were sown in 2 L pots containing ProfiSubstrate (Gramoflor) and placed in pot plates filled with water to maintain wet-soil growing conditions. Plants were fertilized twice a month with 0.3g of AGRO NPK 11/7/7 during vegetative growth and with Kristalon Plod a květ fertilizer (NPK: 5/15/30; AGRO CS a.s., Czechia) from flowering until the seed maturity. The temperature was maintained at 25°C. During winter, a 14 h photoperiod was ensured by a sodium vapor lamp combined with a mercury vapor lamp (500 mmol.m⁻².s⁻¹ at the top of the plant); In Summer, no additional lighting was provided.

III.2.2 Identification of barley LBD proteins and construction of the phylogenetic tree

Initially, all 31 barley LBD proteins were searched and retrieved from the Barley Gene Family Database (2022) (BGFD: <http://barleygfdb.com>), compared to the Plant Transcription Factor Database (2017) (PlantTFDB: <https://planttfdb.gao-lab.org/>) and the Plant Transcription factor & Protein Kinase Identifier and Classifier (2016) (iTAK: <http://bioinfo.bti.cornell.edu/tool/itak>) (Zheng et al. 2016; Jin et al. 2017; T. Li et al. 2022). Furthermore, the BLAST programs (TBLASTN and BLASTN) available on the Institute of Plant Genetics and Crop Plant Research (IPK) barley genome database and Ensemble Plants databases (http://plants.ensembl.org/Hordeum_vulgare/Tools/Blast) were used to search new potential LBD proteins against sequence homology between annotated barley LBD proteins and LBDs known from rice, maize and *Arabidopsis* as query, which play roles in crown root and lateral initiation.

The phylogenetic tree of HvLBD protein was constructed based on the alignment using MUSCLE algorithm and the maximum likelihood (ML) tree construct in the Molecular Evolutionary Genetics Analysis cross computing Platforms (MEGA-11) (Tamura, Stecher, and Kumar 2021), with the following parameters: Bootstrap method with 500 replicates, a non-uniformity of evolutionary rates among sites modeled by using a discrete Gamma distribution (+G), General Time Reversible (JTT) with frequency (+F) model, complete deletion. Barley sequence data, including exon/intron structures were sourced from the available Morex assembly (International Barley Genome Sequencing Consortium (IBSC) et al., 2012), Ensemble Plants database (<https://plants.ensembl.org/index.html>). The zinc finger-like motif, the GAS block, and the leucine-zipper-like coiled-coil motif were determined manually (Y. Zhang et al. 2020). The visualization of gene structures was performed using CFVisual tool (<https://github.com/ChenHuilong1223/CFVisual>) (H. Chen et al. 2022).

To predict the barley close orthologs of LBD proteins, which were identified in rice and maize with functions in crown root initiation, and in *Arabidopsis* with functions in lateral root initiation, 31 barley LBD protein sequences were aligned to the sequences from rice OsCRL1/Os03t0149100-01 and OsCRL1-like (OsCRL1-

L1)/Os03t0149000-01, maize RTCS/GRMZM2G092542_P01 and RTCL/AC149818.2FG009 and Arabidopsis AtLBD16/AT2G42430, AtLBD18/AT2G45420. The analysis involved 37 amino acid sequences and was performed with the same parameters described above.

III.2.3 Primer design for gene expression analyses, cloning and plant genotyping

The genomic DNA sequences and coding sequence (CDS) of *HvLBD* genes were retrieved from the newest genome assembly of the barley ‘transformation reference’ cv. Golden Promise (<https://ics.hutton.ac.uk/gmapper/>). According to the corresponding sequences, primers were designed for real-time PCR analyses, DNA cloning for transient and stable transformations, CRISPR-Cas⁹ and complementation assay genotyping, using Primer3plus software (<https://www.primer3plus.com/index.html>). Concerning cloning and real-time PCR, each primer was blasted on the barley genome databases on the BLAST server (https://plants.ensembl.org/Hordeum_vulgare/Tools/Blast; https://ics.hutton.ac.uk/gmapper/blast_page.html and <http://webblast.ipk-gatersleben.de/barley/>) for their specificities on the barley genome. Furthermore, each primer was checked for self-complementarity, self-dimerization, and no hairpin loop formation, using <http://biotools.nubic.northwestern.edu/OligoCalc.html>. The primer list used in the study is presented in table III.1. The primers were ordered from Sigma-Aldrich in dry form and desalt purification and dissolved in Tris-EDTA (TE: 10mm Tris; 0.1mM EDTA; pH 8.0) buffer as a 100µM stock solution and stored at -20°C to -80°C for long-term storage.

Table III.1: List of primers using in this study:

Gene	Accession ^(a)	Primer/Probe ^(b)	Sequence from 5' to 3'	Primer efficiency/Purpose
Gene expression analysis by qRT-PCR				
LBD	MLOC_52276 HORVU.MOREX.r3.4HG033 1440	qMLOC-52276_F qMLOC-52276_R	AGGCTGCAGTCACCATCTCT CGTGCAGGTCAGAGCAAATA	96%
LBD	MLOC_61947 HORVU.MOREX.r3.6HG063 0410	qMLOC-61947_F qMLOC-61947_R	CCTCCAGTACCTTGCTCAGG GATCGGTCGATGAGGTTGAT	78%
LBD	MLOC_55239 HORVU.MOREX.r3.4HG039 1970	qMLOC_55239_F qMLOC_55239_R	TCGTCACCATCTGCTACGAG CTGGAGATTCACCACCTGCT	undetermined
LBD	MLOC_10783 HORVU.MOREX.r3.4HG040 8270	qMLOC10783_F qMLOC10783_R	ACGACCACCACTCCATCAC TAGCCGCATGCGTACATC	undetermined
LBD	MLOC_10784 HORVU.MOREX.r3.4HG040 8280	qMLOC10784_F qMLOC10784_R	ACCGGAGACAACAACGATCAG ACTTGCGACGCAGAACTTG	94%
HK_5439 ^(RG)	AK360511.1 HORVU.MOREX.r3.5HG049 0950	qHv5439_F qHv5439_R	GATTGAGGTGGAGAGGGTATTG CTCCTGGTCTGTTAGCAGTTT	93%
(Actin-related protein 9) HvACT ^(RG)	AK248432.1 HORVU.MOREX.r3.2HG009 9270	HvACTrt_F HvACTrt_R	TTGACCTCCAAAGGAAGCTATT CT GGTGCAAGACCTGCTGTTGA	99%
(barley elongation factor2)	AK361008.1 HORVU.MOREX.r3.5HG052 9120	HvEF2rt_F HvEF2rt_R	CCGCACTGTCATGAGCAAGT GGGCGAGCTTCCATGTAAAG	98%

HvEF2 α ^(RG)				
cyclic nucleotide-gated ion channel 1 (CNGC1) gene	AY972629.1 HORVU.MOREX.r3.6HG058 3650	qHv20934_fw qHv20934_rev	AGTCACAACCCAAGTGGTAAA CAGGACAAGCGGTCTATCTATG	
Hv20934 ^(RG)				
HvTIP41 ^(RG)	AK373706.1/ MLOC_59064.1 HORVU.MOREX.r3.5HG051 2360	qTIP41_fw qTIP41_rev	TGGTTGGTTTCTGCTCTTGC CGGCTTTGCTTCCTCCTTAC	PCR to control gDNA contamination in RNA samples
HvEIF5A2 ^(RG)				
	AK357300.1 HORVU.MOREX.r3.4HG038 3910	qEIF5A2_fw qEIF5A2_rev	AGGGTGTATGCGGATGTGA AATAGCATTCTCGGCTTCCA	
Trans-activation assay in protoplast				
HvCRL1	HORVU.MOREX.r3.4HG040 8280	MLOC10784_NcoI_F MLOC10784_BamHI_R	CATGCCATGGCGCTCGGCCGGC CAT CGGGATCCCGTTACGAGCGATT AAGGTAAGCAT	amplification of full-length ORF and cloning into pRT104
HvCRL1-L1	HORVU.MOREX.r3.6HG063 0410	Hv61947_NcoI_F Hv61947_BamHI_R	CATGCCATGGCTGCGGCTCCTG GC CGGGATCCCGCTACAGGGAGT AGTTGGAGCT	amplification of full-length ORF and cloning into pRT104
pRT104 vector		pRT104_fw pRT104_rv	CAACCACGTCTTCAAAGCAA AACACATGAGCGAAACCCTA	screening and sequencing of vector screening and sequencing of vector
rice <i>crI</i> mutant complementation				
	HORVU.MOREX.r3.4HG040 8280	10784_attB_F	ggggacaagttgtacaaaaagcaggctATG GCGCTCGGCCGGCCATTGCA	amplification of HvCRL1 (MLOC_10784)

HvCRL1		10784_attB_R	ggggaccactttgtacaagaaagctgggtTTAC GAGCGATTAAGGTAAGCAT	amplification of HvCRL1 (MLOC_10784)
HvCRL1-L1	HORVU.MOREX.r3.6HG063 0410	61947_attB_F	ggggacaagttgtacaaaaagcaggctATG GCTGCGGCTCCTGG	amplification of HvCRL-L1 (MLOC_61947)
		61947_attB_R	ggggaccactttgtacaagaaagctgggtCTAC AGGGAGTAGTTGGAGCT	amplification of HvCRL-L1 (MLOC_61947)
OsCRL1	Os03t0149100	OsCRL1_fw_attB	ggggacaagttgtacaaaaagcaggctATG ACGGGATTTGGATCGCC	amplification of OsCRL1 (Os03t0149100)
		OsCRL1_rv_attB	ggggaccactttgtacaagaaagctgggtTTAC GAGCGGTTAAGGTAAGCG	amplification of OsCRL1 (Os03t0149100)
		PUBIF	GGATGATGGCATATGCAGCAG	validation by sequencing of the final vector
		a3NOS-rev	TAACATAGATGACACCGCGC	validation by sequencing of the final vector
		MLOC10784_Fw	ACCGGAGACAACAACGATCAG	validation by PCR of transgenic plants
		10784_seq1_rv	GAAGATGTGGGCGACGCA	validation by sequencing of transgenic plants
		61947_seq1_fw	CGTCACCATCACCTACGAGG	validation by sequencing of transgenic plants
		61947_seq1_rv	CTCATCAGCTCCGGCAGAAG	validation by sequencing of transgenic plants
		OsCRL1_fw_attB	ggggacaagttgtacaaaaagcaggctATG ACGGGATTTGGATCGCC	validation by PCR of transgenic plants and sequencing for final vector
		OsCRL1_rv_attB	ggggaccactttgtacaagaaagctgggtTTAC GAGCGGTTAAGGTAAGCG	validation by PCR of transgenic plants and sequencing for final vector
		Hyg-F	AAACTGTGATGGACGACACC	validation by PCR of transgenic plants/present of T-DNA
		Hyg-R	CTTCTGCGGGCGATTTGT	validation by PCR of transgenic plants/present of T-DNA
		UBI-F	AAATAGACACCCCCTCCACA	validation by PCR of transgenic plants/present of T-DNA
		UBI-R	ATGACCCGACAAACAAGTCC	validation by PCR of transgenic plants/present of T-DNA

Generation of <i>HvLBD</i> knock-out mutants by CRISPR-Cas ⁹				
HvCRL1	HORVU.MOREX.r3.4HG040 8280	10784-gRNA1_fw 10784-gRNA1_rv	GGCGATGACCGCTGGATCGCTC GG AAACCCGAGCGATCCAGCGGT CAT	preparation of the HvCRL1-gRNA1 containing <i>Bsa</i> I restriction site for Gateway TM cloning into pSH91 vector
HvCRL1	HORVU.MOREX.r3.4HG040 8280	10784-gRNA2_fw 10784-gRNA2_rv	GGCGAGACAACAACGATCAGG T AAACACCTGATCGTTGTTGTCT	preparation of the HvCRL1-gRNA2 containing <i>Bsa</i> I restriction site for Gateway TM cloning into pSH91 vector
HvCRL1-L1	HORVU.MOREX.r3.6HG063 0410	61947-gRNA1_fw 61947-gRNA1_rv	GGCGAGACAACAACGATCAGG T AAACACCTGATCGTTGTTGTCT	preparation of the HvCRL-L1-gRNA1 containing <i>Bsa</i> I restriction site for Gateway TM cloning into pSH91 vector
HvCRL1-L1	HORVU.MOREX.r3.6HG063 0410	61947-gRNA2_fw 61947-gRNA2_rv	GGCGAGACAACAACGATCAGG T AAACACCTGATCGTTGTTGTCT	preparation of the HvCRL-L1-gRNA2 containing <i>Bsa</i> I restriction site for Gateway TM cloning into pSH91 vector
HvCRL-L1-L1	HORVU.MOREX.r3.6HG063 0410	61947-gRNA3_fw 61947-gRNA3_rv	GGCGAGACAACAACGATCAGG T AAACACCTGATCGTTGTTGTCT	preparation of the HvCRL-L1-gRNA3 containing <i>Bsa</i> I restriction site for Gateway TM cloning into pSH91 vector
pSH91		pSH91_rev	AATGTGGCGCCGTAATAAG	validation by Sanger sequencing of the pSH91 containing the gRNA
gRNA-coding gene		OsU3P_F1	CAGGGACCATAGCACAAGAC	validation by PCR of T-DNA integration into the barley genome
Cas9 gene		OsU3T_R1	TCAGCGGGTCACCAGTGTTG	
		GH_UBI-F4	TGGTTAGGGCCCCGGTAGTTC	
		GH_zCas9-R1	TTAATCATGTGGGCCAGAGC	
Hygromycin		Hygro-Fw Hygro- Rev	GAATTCAGCGAGAGCCTGAC ACATTGTTGGAGCCGAAATC	
HvCRL1	HORVU.MOREX.r3.4HG040 8280	10784_CRISPR_fw 10784_CRISPR_Rv	TGGTGCCTCTTTTCAAACG TTGTACCATTGGTAGGCGCC	screening of the mutation by PCR coupled to dCAPS assay

		dCAPs_T4_10784_fw	GCAGCAGCGATCACCGCAGCA CCGGAGACAACAACGAGC	
		HvCRL1_CRISPR_Fw	CAACCATCCTCAGCAGCAG	
		HvCRL1_CRISPR_Rv	CTGCTCGTGGCAGAAGTAGG	Sanger sequencing of the CRISPR-Cas ⁹ targeted region
HvCRL1-L1	HORVU.MOREX.r3.6HG063 0410	TN_61947_CRISPR_Fw	TTGCTCCCCTCAAACCAGAC	screening of the mutation by PCR coupled to dCAPS assay
		TN_61947_CRISPR_Rv	CCCTCCTGCGTTCTTCTAGC	
		Cis-cas9_61947_2_rv	CTCTGAGCTGAAGTAGGGCG	
		TN_61947_CRISPR_Fw	TTGCTCCCCTCAAACCAGAC	Sanger sequencing of the CRISPR-Cas ⁹ targeted region

(a) MLOC: correspondence of IDs in the 2012 annotation of the barley cv. Morex reference genome (Mascher M. et al. 2013) – HORVU.MOREX.r3: correspondence of IDs in the last available annotation of the barley cv. Morex reference genome (Mascher M et al. 2021).

(b) "F" denotes forward and "R" reverse primer orientation. (RG)- reference gene

III.2.4 Crown-Root Inducible System (CRIS)

Because the location and timing of initiation of crown root is unpredictable and occurs only in a few cells in the ground meristem of the stem base, determining its molecular regulation is challenging. To circumvent this problem, a crown-root inducible system (CRIS), that synchronizes the initiation of several crown-roots, was developed. This system is based on the role of the phytohormone auxin and has been adapted from the lateral root inducible system (LRIS), which was developed in the dicot plant model *Arabidopsis* and maize (Kristiina Himanen et al. 2002; Jansen et al. 2012; Crombez H. et al. 2016). The principle of CRIS was illustrated in fig.III.3.

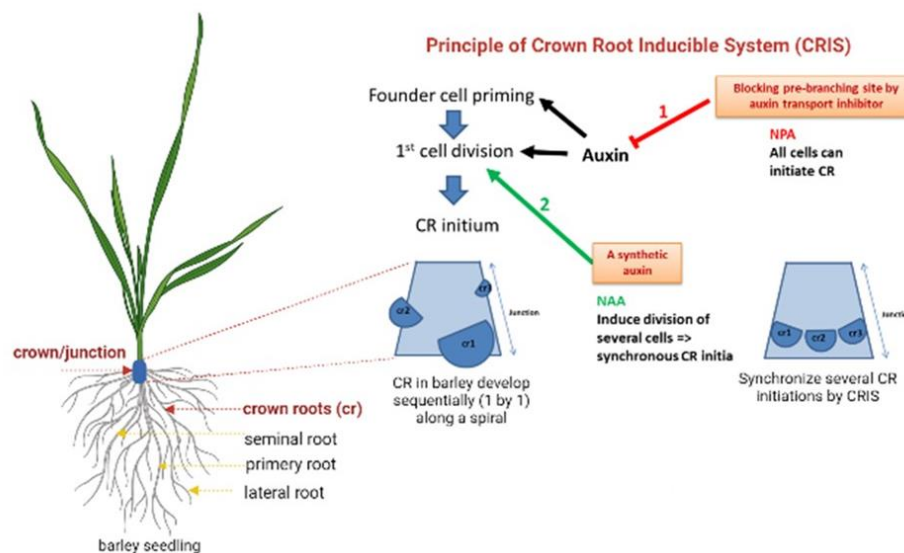


Figure III.3: schema of principle of crown-root inducible system in out study

Initially, the barley cv. Golden Promise grains were sterilized by immersion in 70% ethanol (v/v) for 3 min, rinsed once in sterilized deionized water, prior to immersion in 3% hypochlorite for 5 min, followed by extensively rinsing in sterilized deionized water. After sterilization, the grains were placed in petri dishes on 3 layers of sterilized wet filter papers containing 50 μM N-1-naphthylphthalamic acid (NPA; Sigma Aldrich), an inhibitor of auxin polar transport and put at 4°C for 3 days to mimic vernalization and ensure a homogeneous germination. Then, the grains were transferred for germination in phytotron with a photoperiod of 16°C/12 hours light and 13°C/12 hours darkness, light intensity at 170 $\mu\text{mol photons}\cdot\text{m}^{-2}\cdot\text{s}^{-1}$ and 60% relative humidity. Three days after germination (DAG), young seedlings with approximately

3 cm of shoot length were transferred to hydroponical culture in ½ strength Hoagland solution (supplementary Note S1) (Vlamis and Williams 1962) containing 50 µM NPA and grown for three more days. Then, the hydroponic solution was replaced by ½ fresh strength Hoagland solution containing 50 µM 1-Naphthaleneacetic acid (1-NAA; Sigma Aldrich) as a source of active auxin. Seedlings were grown in this condition for 24 hours. After that, the NAA-containing solution was replaced by ½ Hoagland solution. Parallely, seedlings grown in only NPA solution were used as negative control. One mm crowns of stem bases, where locates the junction between stem and root, were harvested at different time-points just before applying NAA (0 hour (h)), and after NAA induction at 3h, 6h, 12h and 24h for gene expression analysis and anatomical observation experiments. For each time point, each pool sample was collected from 10 stem bases and flash frozen in liquid nitrogen, or immediately used for histological experiment. Each sample was prepared in 6 independent biological replicates.

III.2.5 Histology analysis

Barley stem bases were fixed overnight at 4°C in a formaldehyde: acetic acid solution (FAA: 2% (v/v) formaldehyde, 5% (v/v) acetic acid and 63% (v/v) ethanol). Samples were washed three times for 10 min in an ethanol: glacial acetic acid (63%:5%; v/v) solution. Then, samples were washed in PBS three times for 3 min before agarose-embedding in 5% agarose. Blocks were sectioned at 25 - 35 µm thickness using a Leica VT1000 S vibrating blade Vibratome. The slides were stained with Toluidine Blue O (198161, Sigma-Aldrich) solution (0.1%; w/v) that stains nucleic acids in blue and polysaccharides in purple. Stained sections were observed under AXIO Scope.A1 (Zeiss) microscope and photographs were acquired using Axiocam 305 color camera and saved as a 600 dpi tiff images.

III.2.6 Gene expression of barley LBD family

To investigate and predict the potential functions of the HvLBDs during the development of barley, the expression profiles of public available RNA-seq samples of HvLBD proteins from different tissues (epidermis, embryos, anthers, internodes, leaves, root, grains, palea, lemma, rachis, lodicule, etiolated, inflorescences and

shoots) (Table III.2) in different development stages were retrieved from the current public available barley reference transcript dataset (BaRTv1.0) with transcripts per million (TPM) of the cultivar “Morex” in EoRNA (<https://ics.hutton.ac.uk/eorna/index.html>) (Mascher et al. 2017; Milne et al. 2021). Heat map of HvLBDs’ expression profile was visualized by ClustVis web tool (<https://biit.cs.ut.ee/clustvis/>) (Metsalu and Vilo 2015), using the following parameters: Original values are $\ln(x)$ -transformed; Columns are centered; Unit variance scaling was applied to columns; Both rows and columns are clustered using correlation distance and average linkage including 26 rows corresponding to 26 genes with available expression profiles and 16 columns corresponding to different tissues. Three bio replicates were selected for each sample.

Table III.2: List of samples and their code for HvLBD family's expression profile

Tissue description	Tissue code
Developing grain, bracts removed (15 DPA) ⁽¹⁾	CAR15
Developing grain, bracts removed (5 DPA)	CAR5
4-day embryos dissected from germinating grains	EMB
Epidermis (4 weeks)	EPI
Etiolated (10 day old seedling)	ETI
Young developing inflorescences (5mm)	INF1
Developing inflorescences (1-1.5 cm)	INF2
Shoots from the seedlings (10 cm shoot stage)	LEA
Lemma (6 weeks PA) ⁽²⁾	LEM
Lodicule (6 weeks PA)	LOD
Developing tillers at six leaf stage, 3rd internode	NOD
Palea (6 weeks PA)	PAL
Rachis (5 weeks PA)	RAC
Root (4 weeks)	ROO2
Roots from the seedlings (10 cm shoot stage)	ROO
Senescing leaf (2months)	SEN

(1) DPA: Days Post Anthesis; (2) PA: Post Anthesis

III.2.7 Genes' expression analysis of the putative *HvLBD* genes under CRIS

III.2.7.1 RNA extraction and DNase treatment

Total RNAs from the samples prepared as described in III.2.2.3 were extracted using Quick-RNA™ Plant Miniprep kit (ZYMO RESEARCH, USA) according to the manufacturer's instructions. Samples were ground into fine powder in lipid nitrogen using mortar and pestle, transferred into a 2 mL Eppendorf tube containing 800 µL RNA lysis buffer, and mixed by vortexing for 20 sec. All following steps of the extraction were performed at room temperature; if not stated differently, all centrifugations were done at 10000xg for 30 sec. Initially, each lysate was transferred to a Zymo-Spin™ IICG Column followed by a centrifugation at 16000 xg for 1 min. An equal volume of ethanol (95-100%) was added to the collected filtrate and well mixed by pipetting. The solution was loaded onto a Zymo-Spin™ IICR Column prior to centrifugation. The flow-through was then discarded. Then, 400 µL RNA Prep Buffer was added to the column and centrifugation was carried out to discard the flow. A Volume of 700 µL RNA Wash Buffer was added and then the column was

centrifuged again. This step was repeated by adding 400 μ L RNA Wash buffer into the column and centrifuging for 1 min to ensure complete removal of the buffer. After that, the column was placed onto a nuclease-free 1.5 ml Eppendorf tube and 50 μ L of RNase-free water was added directly to the column matrix to impregnate for 1-2 min. The column was then centrifuged for 1 min at 16000xg. The eluted RNA can be processed immediately with further steps or stored at -80°C .

To ensure a complete depletion of gDNA, an additional DNase treatment was performed after RNA extraction. For this purpose, 5 μ L of 10X DNaseTURBO buffer and 2 μ L of TURBO DNase I (Cat. AM2238, Invitrogen) were added to the eluted RNA, gently mixed by pipetting, and incubated at 37°C . After 30 minutes of incubation, 2 μ L of TURBO DNase I was added to each sample that were further incubated at 37°C for 30 minutes. Then, RNA was precipitated by adding 28.5 μ L LiCl (7.5 M) (Cat. AM9480, Invitrogen) and stored at -20°C overnight. Following, centrifugation took place at maximum speed (14000 rpm) for 30 minutes at 4°C . After centrifugation, supernatant was removed by pipetting. Then, 500 μ L 70% ethanol was added, and the tube was inverted 5 times, and centrifuged at 4°C for 5 min at 14000 rpm. Then, the remaining ethanol was carefully removed using a pipet tip, and the pellet was allowed to dry at room temperature for another 5 min. Finally, RNA was re-suspended into 30 μ L nuclease-free water. The concentration and purity of the extracted total RNA were determined with a NanoDrop™ One/OneC Microvolume UV-Vis Spectrophotometer (Thermo Scientific). Only the RNA samples with a 260/280 ratio greater than 1.8 were used for the further analyses. RNA samples were kept at -80°C .

III.2.7.2 Determination of RNA quality using PCR and agarose gel electrophoresis

Polymerase chain reaction (PCR) was performed to control the contamination of genomic DNA (gDNA) after the RNA purification. In the PCR, the primers designed for *HvTIP41* gene (qTIP41_fw and qTIP41_rv: Table III.1) were used. *HvTIP41* was reported as one of the most stable reference genes in barley under abiotic stress (Hua et al. 2015), hence its primers for the gene expression analysis were designed for previous barley projects and provided by my supervisor Dr.

Bergougoux. The PCR reaction was consisted of 200ng of RNA sample, 1X Green GoTaq™ Flexi Buffer (Promega) with 0.25µL of 10 mM dNTPs mixture, 0.25 µL of each forward and reverse primers at 10 µM, 0.05 µL of GoTag® DNA polymerase, nuclease-free water up to 20 µL. The PCR conditions include an initial denaturation at 95°C for 5 min, followed by 35 cycles of denaturation at 95°C for 45s, primers annealing at 55°C for 30s, elongation at 72°C for 1 min/kb; the PCR amplification was completed by a final elongation at 72°C for 10 min and 10 min of holding at 22°C. PCR was also performed with barley gDNA as a positive control. A sample containing water instead of RNA was used as a negative control. PCR reaction was run in a Prime thermocycle (TECHNE). The PCR products were confirmed by electrophoresis onto a 1% (w/v) agarose gel in Tris-acetate-ethylenediamine tetra acetic acid (2 M Tris, 50 mM EDTA) buffer (TAE buffer) containing ethidium bromide (EtBr) (10 µl of 0,5% ethidium bromide solution was mixed into 50 ml of 1% agarose). The electrophoresis was performed at 100 V for 45 min. The gel was transferred to a UV transilluminator to visualize the fragments of nucleic acid on gel. The transilluminator outcome was analyzed in Image Lab™ software 5.1 (Bio-Rad).

Finally, an assessment of RNA integrity by inspection of the 18S and 28S ribosomal RNA bands using denaturing gel electrophoresis was applied. A RNA sample (0.4 µg) was mixed with RNA loading dye prior (R0641, ThermoFisher scientific) and incubated at 70°C in 10 mins for RNA denaturation. After that, the integrity of RNA was checked by using electrophoresis in agarose gel 1% prepared in TAE buffer loaded with prior denatured RNA samples during 30 mins at 80V. Then a transilluminator was used to visualize under UV light the fluorescence of ethidium bromide RNA complexes in gels. Good quality RNA samples perform two intact and clear bands corresponding to the 18S and 28S ribosomal RNAs on the gel.

III.2.7.3 Reverse transcription

Reverse transcription was performed from 2 µg of the total RNA using RevertAid H minus reverse transcriptase (Cat. EP0451, Thermo Scientific, USA). Initially, total RNA was mixed with 1 µl of 100 µmol·l⁻¹ oligo (dT)₁₈ primers (S0131, ThermoFisher Scientific) and the reaction volume was adjusted to 13 µl with nuclease-free water (Qiagen). The RNA-primer mixture was heated to 65°C for 5 min and then

immediately incubated on ice. The reaction mixture for reverse transcription was prepared by combining 1X reverse transcriptase buffer, 1 mM of dNTPs (Invitrogen) and 200 U of RevertAid H Minus transcriptase. The reaction mixture was incubated at 42°C for 60 min and then terminated at 70°C for 10 min. The samples were kept at -20°C for near future experiment, and -80°C for long term storage.

III.2.7.4 Real-time quantitative reverse transcription polymerase chain reaction (qRT-PCR)

For real-time PCR, cDNA was diluted 5 times and used in a reaction containing 1X gbSG PCR Master Mix (Cat. 3005, Generi Biotech), 500nM of References dye (Lot. 270009002, ROX (6-Carboxy-X-Rhodamine) dye, Generi Biotech) and 250 nM of each primer. Primers for qRT-PCR are designed as described in III.2.2 and indicated in table III.1 for the five closest barley *LBD* genes presenting putative orthologs of *OsCRL1*, *OsCRL1-like*, *ZmRTCS*, *ZmRTCL*, *AtLBD16*, *AtLBD18*. To determine the best reference gene(s), a set of putative genes selected based on literature (Hruz et al. 2008) and *in silico* prediction using Genevestigator® (Nebion AG; data not shown) were analyzed for their stability across ours with geNorm v3.5 software (Hua et al. 2015; Vandesompele et al. 2002). The expression profile across the different samples was analyzed for 6 potential reference genes (Hv*ACT*: AK248432.1; Hv*EF2α*: AK361008.1; Hv5439: AK360511.1; Hv20934: AY972629.1; Hv*TIP41*: AK373706.1; Hv*EIF5A2*: AK357300.1) (Hua et al. 2015), indicated in table III.1. Finally, the expression of three reference genes (Hv*ACT*: AK248432.1; Hv*EF2α*: AK361008.1; Hv5439: AK360511.1) were selected as the most stable across the samples under the investigation and were consequently used as normalizer for the genes of interest. The specificity of the primers was checked by not only BLAST restricted to barley genome as described in III.2.2, but also sequencing by Sanger method for confirmation of the specificity of the amplified products (Seqme, Czechia). qRT-PCR was carried out on a Step One Plus Real-Time PCR system (Applied Biosystems, USA), in an optical 96-well plate, as following protocol: an initial denaturation for 10 min at 95 °C, followed by 40 cycles of 15 s at 95 °C, 1 min at 60 °C. Melting curve analysis was performed after 40 cycles to verify primer specificity. Each sample was analyzed in six independent biological replicates and in technical

triplicates. Each independent biological replicate represented a pool of 10 explants. The cycle threshold value for the gene of interest was normalized in respect to the three best HK genes and the geometric mean of expression was calculated. The relative expression was determined using the $\Delta\Delta C_t$ mathematical model corrected for the PCR efficiency (Michael W. Pfaffl 2001). The relative quantification was compared to the T0 sample corresponding to stem bases of seedlings harvested before treatment with 1-NAA. Nonparametric Kruskal-Wallis ANOVA supported statistical significance followed by a post-hoc multiple comparison of mean rank using GraphPad Prism version 10.0.0 for Windows (GraphPad Software, Boston, Massachusetts USA, www.graphpad.com).

III.2.8 Bacterial transformation and culture

III.2.8.1 *E. coli* transformation by heat shock and growth conditions:

Initially, Eppendorf tubes containing 50 μ l of chemically competent *E. coli* TOP10 bacterial cells were thawed on ice (about 5 minutes (min)); 2 to 5 μ L of plasmid/ligated products were supplemented. The tube was mixed gently by pipetting and incubated on ice for 20 min. After the incubation, it was heat-shocked at 42°C for 60s without shaking and immediately put back on ice for 2 min. Following, the transfected bacterial cells were recovered by supplementation of 450 μ L of Super Optimal Broth (SOC) (Cat.15544034, ThermoFisher) medium and grown with shaking (~150 rpm) at 37°C for 40 min. After bacterial activation, each transformation culture was spread onto Luria Broth (LB) medium plate containing suitable antibiotic and 15 g.L⁻¹ agar. Afterward, the bacterial culture was grown overnight at 37°C for forming colonies. From the plate containing isolated colonies, a few isolated colonies were taken to initiate the same number of liquid LB cultures for DNA plasmid isolation and validation. Finally, fresh bacterial liquid cultures containing the final construct were mixed with glycerol in ratio 1:1 (v/v) and stored at -80°C.

III.2.8.2 *A. tumefaciens* transformation via electroporation and growth conditions

Fifty μ L of electro-competent cells were mixed with 1 to 2 μ L of plasmid. The mixtures were then mixed gently and transferred carefully to the bottom of a pre-

chilled 1 mm sterile electroporation cuvettes (VWR). Subsequently, the cuvettes were immediately placed in an electroporator (ECM 399 Electroporation System, BTX Harvard apparatus) that was set up to use at 25 μ F, 1800 V, 200 Ω and main switch was on power supply. After electroporation, the shocked bacterial cells in the cuvettes were placed immediately on ice and then gently mixed with 450 μ L of pre-chilled liquid LB medium. The transfected cells were transferred back to a 1.5 mL Eppendorf tubes and incubated at 28°C for 2 hours with gently shaking (~ 150 rpm). Bacteria were then plated onto a selective LB medium containing 15 g.L⁻¹ agar, Rifampycin (50 μ g.mL⁻¹) and the appropriate antibiotic allowing the selection of the plasmid. Plates were incubated for 48 hours at 28°C. Afterward, the isolated colonies were selected for LB liquid culture and finally stored at -80°C with supplied 50% glycerol.

III.2.9 Transactivation assay in rice protoplasts

III.2.9.1 Plant growing conditions

The *O. sativa* cv. Kitaake was used for protoplast isolation. For this purpose, seeds were manually hulled, disinfected in 70% (v/v) ethanol for 2 min, and then rinsed twice with autoclaved distilled water. Seeds were further immersed for 30 min in 4% (v/v) sodium hypochlorite solution containing 0.1% (v/v) tween-20. Finally, the seeds were rinsed six times with autoclaved distilled water and then dried with sterilized tissue papers. After disinfection, hulled seeds were incubated under dark *in vitro* conditions in flasks containing half-strength Murashige and Skoog (MS/2) medium (M0221, Duchefa), half-strength Gamborg B5 vitamin (G0415, Duchefa) and 3.5 g per liter of plant agar (P1001, Duchefa) with pH 5.8. Plants were grown in the dark at 28°C \pm 2°C with relative humidity of approximately 60%.

III.2.9.2 Cloning for transient transformation

The coding DNA sequences (CDS) of *HvCRL1* (*HORVU.MOREX.r3.4HG0408280*) and *HvCRL1-L1* (*HORVU.MOREX.r3.6HG0630410*) genes were amplified from cDNA obtained from 2 μ g of RNA extracted from the stem base of barley cv. Golden Promise seedlings grown in the presence of 1-NAA. Then, the CDSs of the two *HvLBD* genes were cloned into the pRT104 vector (Reinhard Töpfer, Volker Matzeit, Bruno Gronenborn

1987) at the *NcoI* and *BamHI* restriction sites to allow the expression under the control of Cauliflower Mozaic Virus 35S constitutive promoter (CaMV35S-P). The pRT104 vector was illustrated using BioRender (Fig III.4). High-fidelity PCR amplification was performed using a Phusion® High-Fidelity DNA Polymerase (M0530, New England Biolabs [NEB]) and *HvLBD*-specific primers associated with appropriate restriction endonucleases sites (Table III.1). The PCR products and pRT104 vector were first restricted using double digestion reactions with *BamHI*-HF (R3136, NEB) and *NcoI*-HF (R3193, NEB), to create cohesive sites. Then, the digestion products were purified using NucleoSpin Gel and PCR Clean-up kit (cat.740609, Macherey-Nagel), according to manual instructions, before ligation to generate pRT104::35S-HvCRL1 and pRT104::35S-HvCRL-L1 effector constructs. Vectors were transfected into *E.coli* TOP 10 strain, as previously described in III.2.8.1. Bacteria were cultivated in Ampicillin (100 mg.L⁻¹) selective LB medium, and plasmid were isolated by using a NucleoBond Xtra Midi kit for transfection-grade plasmid DNA (cat. 740410, Macherey-Nagel). The purified plasmids were validated by restriction and Sanger sequencing (Seqme, Czechia).

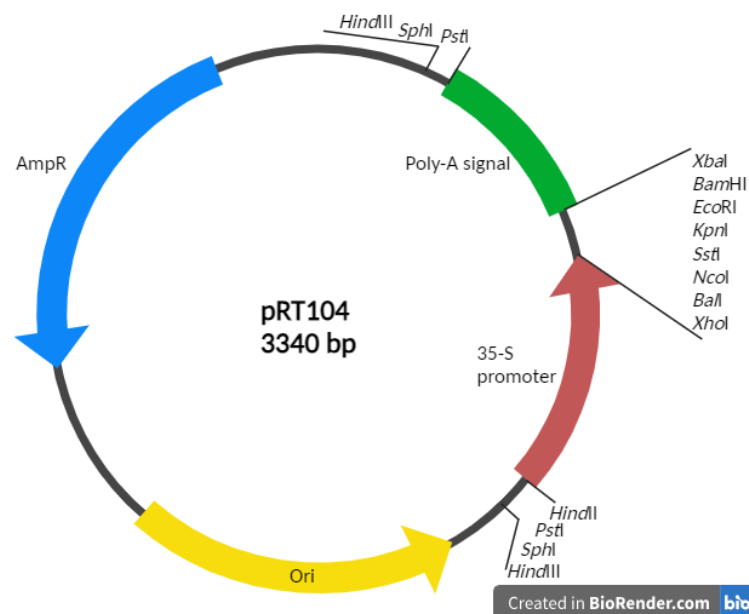


Figure III.4: The plasmid pRT104 map. The vector carries the quantitative 35S promoter and the polyadenylation signal of CaMV strain Cabb B-D and was constructed in modified polylinkers of pUC18/19.

Other vectors required for the assay were kindly provided by IRD, France (Gonin et al., 2022). There was the normalizer vector, p2rL7::35SrLUC plasmid, which was developed from the p2rL7 backbone (De Sutter et al. 2005) fused with *Renilla luciferase (LUC)* genes. The other was an effector, which was developed from a pGusSH-47 plasmid (Pasquali et al., 1994) carrying the GUS-encoding gene under the drive of enrichment native or mutated *LBD* or *CRL1*-boxes tetramers *cis*-regulatory motifs (-138 to -92 upstream position in promoter region) (Fig III.5-A) associated with a minimal *CaMV 35S -47* promoter (Husbands et al. 2007; Gonin et al. 2022).

III.2.9.3 Protoplast isolation and transience

Protoplast isolation and transfection were performed based on the previously described protocol (Cacas et al. 2017) with modification to adapt to rice tissue (Gonin et al., 2022). Primarily, leaves and shoots of 9-day-old rice seedlings were sliced into 0.5-1.0 mm strips with sharp razor blades. The strips were transferred quickly into 30 ml of enzymatic solution consisting of 1.5% [w/v] cellulase R10 (C8001, Duchefa Biochemie B.V., Haarlem, 0.4% [w/v] macerozyme R10 [M8002, Duchefa Biochemie B.V., Haarlem, the Netherlands]), 0.4M mannitol, 20mM KCl, 20mM MES, 10mM CaCl₂, BSA 0.1% [w/v] and pH 5.7. Vacuum was applied for 10 min to infiltrate strips with the enzyme solution. The infiltrated sliced tissues were incubated in dark for 4 h at 28°C. Following filtering and washing steps, rice protoplasts were co-transformed with a tripartite vector system that comprises (1) a reporter plasmid carrying the LBD *cis*-motif elements promoter-driven *β -D-glucuronidase (GUS)-encoding uidA* gene, (2) a reference plasmid carrying the *LUC* gene and (3) an effector plasmid carrying *HvLBD* genes under the control of the CaMV35S promoter. The transfection in rice protoplasts was carried out by polyethylene glycol (PEG) (Yoo, Cho, and Sheen 2007) with the three plasmids in a ratio of 2:2:6 (GUS:LUC:effector). After transformation, the protoplasts were cultured at 28 ± 2°C in dark for 18 h, then collected, frozen in liquid nitrogen, and stored at -80°C for further analysis. GUS and LUC activities were measured as described previously (Zarei et al. 2011), using a Varioscan LUX from ThermoFisher installed with SkanIt™ Software for Microplate Readers to measure the fluorescence and luminescence. GUS activities were related to LUC activities in the same samples to correct the transformation and protein extraction efficiencies. For

Renilla reniformis luciferase (LUC) gene driven by CaMV 35S promoter. The expression of the gene can be followed by enzymatic activity or fluorescence activity is detected. If the protein is not a TF (empty vector), no change in fluorescence or activity is detected. If the cis-regulatory motif was mutated, no significant change in fluorescence activity is detected. *Cis*-RM or *mCis*-RM: *Cis*-regulatory motif or mutated *cis*-regulatory motif; Pro: promoter. CRISPR/Cas⁹-mediated gene knock-out.

III.2.10 Knock-out barley *crl1* mutant generated by CRISPR-Cas⁹

III.2.10.1 Design of gRNA for HvLBDs Knock-Out constructs

Single guide RNAs (sgRNAs) were designed to target *HvCRL1* (*HORVU.MOREX.r3.4HG0408280*) or *HvCRL1-L1* (*HORVU.MOREX.r3.6HG0630410*), using DESKGEN KNOCKIN tool (<https://www.deskgen.com/guidebook/ki.html>) (Hough et al. 2016). The full CDS sequences of both candidate genes were retrieved from the Morex assembly (International Barley Genome Sequencing Consortium (IBSC) et al., 2021), Ensemble Plants database (https://plants.ensembl.org/Hordeum_vulgare/Info/Index). To generate the *lbd* loss-of-function mutants and minimize off-targets in the host-plant genome, the target sequences for sgRNAs were ideally selected in the nucleotide sequence upstream of the conserved LBD domain of the two candidate genes. The sgRNAs with the highest specific efficiency target for Cas⁹ with the best activity and off-target scores in different similar positions in the whole host plant genome were priority to be selected (Table III.3).

Table III.3: Sequences of selected gRNAs

Gene	Position of mutation from ATG	strand	sgRNA sequence (5'...3')	PAM	activity	Off-target
<i>HvCRL1</i>	94	1	ATGACCGCTGGATCGCTCGG	CGG	69	97
	84	-1	GGAGACAACAACGATCAGGT	CGG	71	92
<i>HvCRL1-L1</i>	5	1	GGATTAATACTCGATGGCTG	CGG	60.6	47.1
	15	1	TCGATGGCTGCGGCTCCTGG	CGG	64.7	65.8
	21	1	GCTGCGGCTCCTGGCGGTGG	TGG	52.1	46

III.2.10.2 Cloning CRISPR-Cas⁹ constructs for stable plant transformation in barley:

III.2.10.2.1. Sub-clone oligo duplex into pSH91 plasmid:

After selection of sgRNAs, the whole cassette of forward (F) and reverse (R) oligonucleotides (oligo) were designed with the complement sequence of the sgRNA and additional specific 5'-end overhang corresponding to *BsaI* restriction enzyme (RE) sequence to be compatible with sub-cloning into pSH91 plasmid (Fig.III.6). Therefore, single strand oligos were synthesized (Sigma-Aldrich) in standard de-salted while adding GGCG at the 5'-end of forward oligo, and AAAC at the 5'end of reverse oligo (Table III.1). Following, the double strand (ds) oligonucleotide was annealed in 50 μ L-reaction including 2 μ M of single oligonucleotide (forward and reverse), 1X T4 DNA ligase buffer (Cat.46300018, ThermoFisher) and nuclease-free water (Cat.129117, QIAGEN). The oligo-duplex annealing reaction was carried out in a Biometra T-Personal 48 Thermocycler with the following regime: 95°C in 4 minutes, 70 °C in 10 minutes, from 70 °C, ramp-down to 4 °C at 1 °C/min.

Parallely, pSH91 plasmid, which contains all the required features for CRISPR-Cas9 system as well as *BsaI* RE cleavage sites for cloning and kanamycin resistant gene for bacterial selection (Fig.III.7), was amplified into *E. coli* TOP10 culture grown over-night in 100 mL of liquid LB/kanamycin (50 μ g. mL⁻¹) medium at 37°C with constant shaking. Subsequently, plasmid was purified from *E. coli* culture using NucleoBond® Xtra Midi (Cat.740410, Macherey-Nagel). To generate *BsaI* 5'-protruding-ends linearization vector, cleavage of pSH91 plasmid was performed in a final volume of 50 μ L. The restriction reaction contained 2 μ g of pSH91 plasmid, 1 μ L of *BsaI*-HF (1U) (#R3535, NEB), 1X rCut-smart® buffer (B6004, NEB) and nuclease-free water (Cat.129117, QIAGEN). The mixture was gently mixed by inversion, spun down and incubated for 2 hours at 37°C. Before the ligation reaction, the digested plasmid was always purified following PCR clean-up protocol of the NucleoSpin Gel and PCR clean up kit (#740609, Macherey-Nagel). The concentration of DNA was quantified by NanoDrop Microvolume Spectrophotometer (ThermoFisher). Additionally, the restricted products were confirmed by

electrophoresis onto a 1% (w/v) agarose gel in 1X TAE (Tris-acetate-EDTA) buffer containing ethidium bromide (EtBr).

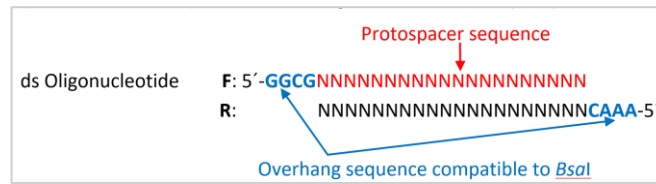


Figure III.6: Whole cassette of oligonucleotide duplex structure for CRISPR-Cas⁹ sub-cloning. Protospacer sequence is presented in red color; specific overhang at 5'-end of single oligonucleotide is presented in blue color. Oligonucleotides containing protospacer and complemented sequence are illustrated as forward (F) and reverse (R), respectively.

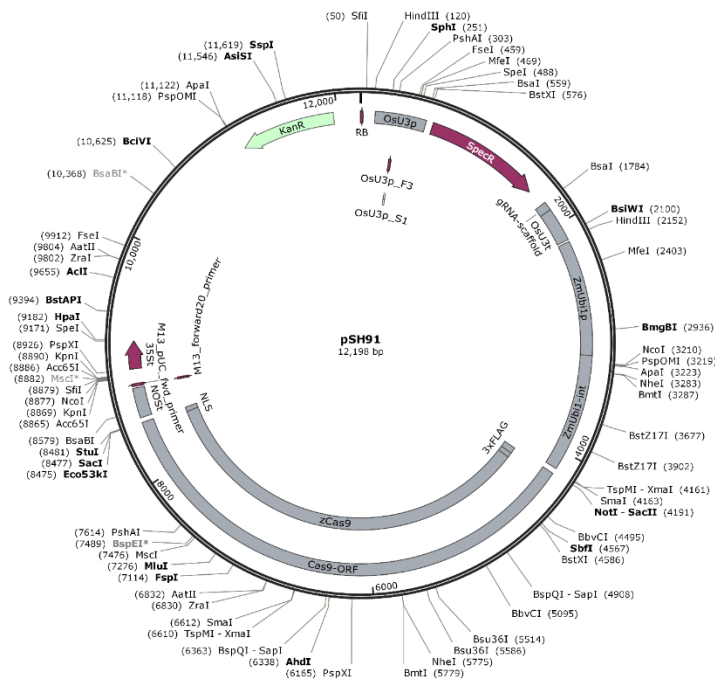


Figure III.7: SnapGene-constructed genetic map of the pSH91 plasmid for CRISPR-Cas⁹ system establishment. The size of DNA circular plasmid is 12198 bp. KanR, Kanamycin resistance gene. SpecR, Spectinomycin/Streptomycin (Strep/Spec) resistance gene for bacterial selection. OsU3p/t: U3 snRNA promoter/terminator from rice. ZmUbi1p/int, Ubiquitin 1 promoter/first intron from maize. zCas⁹, *Zea mays*-codon-optimized Cas9. NOST: Nopaline synthase gene terminator; 35St, 35S terminator. NLS, a nuclear localization signal, which helps Cas⁹ complex can localize to the nucleus immediately upon entering the cell. 3xFLAG, small tags sequence, used for protein affinity purification with less likely to affect protein function (Geny et al. 2021). Cas9-ORF, Open reading frame of Cas9 protein. Restriction enzymes are listed outside of circular plasmid.

The ligation of the oligo-duplex and the pSH91 plasmid was done in a reaction including 5U of T4 DNA ligase enzyme (Cat.EL0011, ThermoFisher), 1X T4 DNA ligase buffer (Cat.46300018, ThermoFisher), 30-100 ng of the purified cohesive-end linearized pSH91, more than 1 µg of oligo duplex and nuclease-free water (Cat.129117, QIAGEN) up to 10 µl. The reaction was incubated overnight at 16°C. Five µL of the ligated product were used to transfect *E. coli* TOP10 competent cells by heat-shock. After transfection, bacterial cells were plated onto LB-agar medium supplied with 50 mg.L⁻¹ of kanamycin. Colonies growing in selection media were screened by PCR, enzymatic restriction, and Sanger sequencing.

The screening of colonies by PCR was always performed in a 25 µL-reaction. The single colony was picked up with a sterilized pipette tip and streaked onto a freshly prepared solid LB-agar medium plate supplemented with kanamycin (50mg.L⁻¹). The cells of the colony remaining on the surface of the pipette tip were immersed and carefully mixed in the prepared PCR reaction. The PCR reaction consisted of 5X Green GoTaq™ Flexi Buffer (Promega) with 0.25 µL of 10 mM dNTPs mixture, 0.25 µL of each forward and reverse primers (OsU3P_F1 and OsU3T_R1, sequence in the table III.1) at 10 µM, 0.05 µL of GoTag® DNA polymerase, nuclease-free water up to 25 µL. The PCR conditions were an initial denaturation at 95°C for 10 min, followed by 35 cycles of denaturation at 95°C for 45s, primers annealing at 53°C for 30s, elongation at 72°C for 1 min/kb; the PCR amplification was completed by a final elongation at 72°C for 10 min and 10 min of holding at 22°C. PCR reaction was run in a Prime thermocycle (TECHNE). Parallely, the LB plate containing streaked colony bacteria were incubated at 37°C overnight and then stored at 4°C for further purpose.

After the colony PCR, the putative colonies were continuously verified by using *Hind*III-HF (R3104, NEB) RE. First and foremost, the plasmid was isolated following the manufacturer's protocol of the QIAprep® Spin Miniprep Kit (QIAGEN). Starting from 10 ml of overnight bacterial culture of single colony picked from LB plate stored at 4°C and grown activated in LB liquid medium containing kanamycin. Plasmid DNA was restricted following the supplier' standard protocols in 20 µL volume of reaction. The mixtures were then incubated at optimal temperature and duration. Afterward, the results were visualized by agarose gel electrophoresis.

The sgRNA-Cas9 expression cassette was sent for Sanger sequencing (SeqMe, Czechia) using pSH91_primer (sequence in table III.1).

III.2.10.2.2. Clone CRISPR-Cas9-gRNA cassette from pSH91 into the final binary expression p2716i-2x35S-TE9 vector:

The complex CRISPR/Cas9 with specific target sequence was transferred into the binary vector 271p6i-2x35s-TE9 (p271-35S) (Fig.III.8) (DNA-Cloning-Service, Hamburg, Germany) by *Sfi*I-restriction enzyme giving rise to the vectors p271-35S::*HvCRL1*-gRNA1, p271-23635S::*HvCRL1*-gRNA2 and p271-35S::*HvCRL1-L1*-gRNA1, p271-35S::*HvCRL1-L1*-gRNA2 and p271-23735S::*HvCRL1-L1*-gRNA3. The sub-cloned pSH91 with gRNA and p271-35S were parallelly and individually digested by the *Sfi*I restriction enzyme (R0123, NEB). The digestion reaction was carried out in a final volume of 50 μ L containing 2 μ g of plasmid, 1X rCutSmart buffer (NEB), 2U of *Sfi*I enzyme and nuclease-free water. The digestion mixtures were incubated for 4 hours at 50°C. Before ligation, the digested products were always purified using NucleoSpin Gel and PCR clean up kit (#740609, Macherey-Nagel), following PCR clean-up protocol in manual.

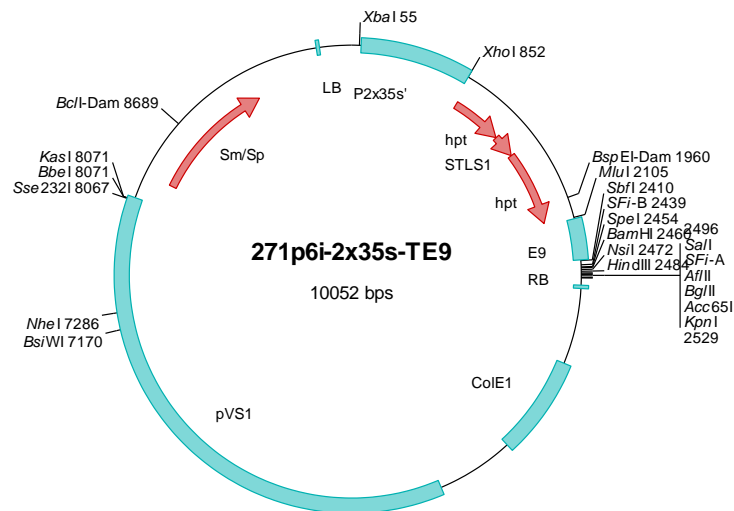


Figure III.8: Molecular feature circle map of binary vector 271p6i-2x35s-TE9 (DNA-Cloning-Service, Hamburg, Germany) (Holubová et al. 2018). The size of DNA circular plasmid is 10052 bp. The vector was established by ligation of P2x35s-Xba-Xho into 269p6i-TE9. Hpt: Hygromycin resistant gene for transgenic plant selection. STLS1: Intron (upstream region) of the nuclear photosynthetic gene ST-LS1 from potato. E9: terminator of the ribulose-1,5-isphosphate carboxylase small subunit (*rbcS*) E9 gene from *Pisum sativum* L. RB: right border. LB: left border. ColE1: ColE1 Origin region for high-copy-number of replications. pVS1: origin of replication for the

Pseudomonas plasmid pVS1. Sm/Sp: Strep/Spec resistance gene for *Agrobacterium* bacteria. 2Px35S: cauliflower mosaic virus (CaMV) 35S promoter with a duplicated enhancer region. Restriction enzymes are listed outside of circular plasmid.

The ligation of purified protruded-end CRISPR-Cas9-gRNA cassette into the linearized p271 expression vector was done using T4 DNA ligase enzyme (Cat.EL0011, ThermoFisher), *Sfi*I-digested at 10:1 molar ratio (insert:vector; calculated by NEBioCalculator [<https://nebiocalculator.neb.com/#!/ligation>]), 1X T4 DNA ligase buffer (Cat.46300018, ThermoFisher) and nuclease-free water (Cat.129117, QIAGEN) up to 10 μ l. The reaction was incubated overnight at 16°C. After ligation, 5 μ L of pre-ice-chilled ligated product was transfected *E. coli* TOP10 competent cells by heatshock. After transformation, bacterial cells were plated onto LB-agar medium supplied with 50 mg.L⁻¹ of Spectinomycin. Colonies growing in selection media were screened by PCR, enzymatic restriction by *Not*I and Sanger sequencing (SeqMe, Czechia) using pSH91_rev (table III.3). Those binary expression constructs (Fig.III.9) were then introduced into the *A. tumefaciens* supervirulent strain AGL1 using electroporation protocol and then stored at -80°C with supplementation of 50% glycerol.

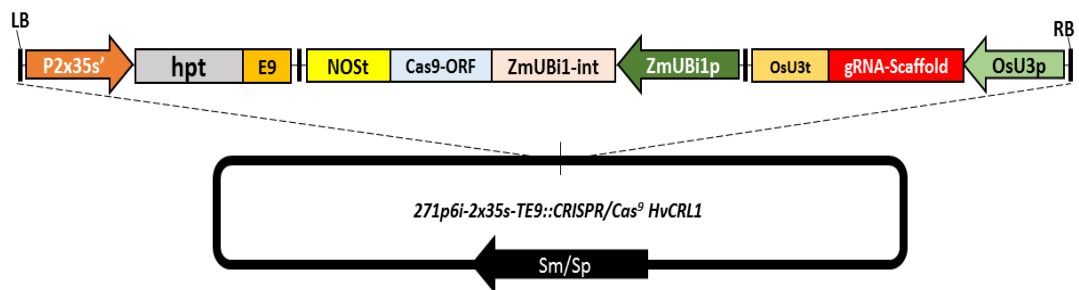


Figure III.9: The map of the final CRISPR-Cas9-sgRNA cassette. A CRISPR-Cas9 cassette was inserted in the 271p6i-2x35s-TE9 vector.

III.2.10.3 Stable *Agrobacterium*-mediated transformation of barley immature embryos

Before performing stable transformation of immature barley embryos, the donor plant material was grown in soil in a controlled phytotron with conditions as follows: Pots filled with a mixture of 94% peat mix substrate (Gramoflor GmbH & Co. KG, Germany) and 6% perlite (Perlit Ltd., Czech Republic). Plants were cultivated in a growth-chamber set to simulate a 12-h photoperiod (136 μ mol.m⁻².s⁻¹ photon flux

density) and a light/dark temperature regime of 14/12°C with a relative humidity (RH) of 60%. The light source was a combination of low-pressure mercury discharge lamps and sodium lamps providing a photosynthetically active radiation (PAR)/ light intensity of ca. 300 $\mu\text{mol photons m}^{-2} \text{s}^{-1}$. At the tiller elongation stage (BBCH code 39), the plants were transferred to summer condition phytotron maintained at 18/16°C with a 16-h photoperiod (170 $\mu\text{mol/m}^2/\text{s}$ photon flux density). Plants were fertilized every week with 6 g of YaraMila Complex (YARA Agri Czech Republic, Czech Republic) containing: 12% N (5% nitrate), 11% P₂O₅, 18% K₂O, 2.7% MgO, 20% SO₃, 0.015% B, 0.2% Fe, 0.02% Mn and 0.02% Zn.

The barley immature embryos were transformed via *Agrobacterium*-mediated transformation protocols (Marthe, Kumlehn, and Hensel 2015), using homozygous di-haploid (D-H) 1.6 barley (*H. vulgare*) cv. 'Golden Promise'. Briefly, barley spikes containing immature embryos with a size of 1.5-2mm were collected; the awns were removed, and the spikes were placed in a bottle standing in an ice bath. The grains were disinfected for 3 min in 70% (v/v) ethanol and then 15 min in 2.4% (w/v) of freshly prepared NaOCl supplied with 0.1% (v/v) Tween 20. Then, the embryos were isolated from each caryopsis and the embryo axis was removed. The embryos were then immersed in freshly prepared liquid cocultivation medium (BCCM). A bacterial culture was grown at 28°C, shaking at 150 rpm in MGL (supplementary note.S2) culture medium containing of rifamycin (50 mg.L⁻¹), carbenicillin (100 mg.L⁻¹) and streptomycin (50 mg.L⁻¹). After collecting, cca. 50 enough embryos were collected, the BCCM was replaced with the *A. tumefaciens* culture; vacuum was applied for 1 min. After 10 min without any agitation under *in vitro* condition, the embryos were washed out from the bacterial culture and grown in BCCM at 21°C in the dark for 48-72h. The generated and transgenic calli from the embryos were selected firstly by using hygromycin. After 4 weeks of growing in the dark condition at 24°C, the calluses were transferred to light conditions (136 $\mu\text{mol/m}^2 / \text{s}$ photon flux density for 16h photoperiod). After the emergence of the first shoots with a 2-3 cm leaf length, the plantlets were transferred to rooting media. The plantlets with developed roots were subsequently transferred to the soil.

III.2.10.4 Genotyping of CRISPR-edited transgenic barley lines and mutation analysis:

At T₀ generation, one selects transgenic plants that integrated the T-DNA into their genome and present a mutation at the target site. Thus, the regenerated plants were first checked by PCR for the integration of the T-DNA using T-DNA specific primers (Three primer couples were designed to recognize gRNA coding sequence, *Cas⁹* and *hpt* genes, table III.1). To determine the type of mutation, a PCR reaction using primers flanking the targeted DNA region was performed; the PCR product was verified type of mutation by the Cleaved Amplified Polymorphic Sequences (CAPS) assays and then Sanger-sequenced by commercial service (Seqme, Czechia), and the mutation was predicted using DECODR (<https://decodr.org>) (Bloh et al. 2021). Barley plants that show a potential mutation were retained for homozygous selection and phenotyping.

Mutated lines were screened from the T₁ generation to obtain homozygous lines without T-DNA insertion. To select mutants that have segregated out the T-DNA, from T₁ to next generations, PCR with specific primers flanking the target sequence were performed and then CAPS assay was developed to check the mutation types. Several PCR were performed to confirm the existence of T-DNA as well as amplify the genomic regions flanking the target site of each interested gene, using specific primers listed in table III.1. The strategy to select stable mutant without T-DNA insertion and purpose of each PCR are illustrated in fig. III.10.

Initially, genomic DNA was extracted from barley young leaves using a modified phenol-chloroform-isoamyl alcohol extraction (Pallotta et al. 2000) and quantified using NanoDrop Spectrophotometer (Thermo Scientific, Wilmington, USA); the gDNA concentration was adjusted to 100 ng/μL for any PCR amplification. PCR amplification reactions were performed in a total volume of 20 μL and contained 50 ng of template DNA, 0.2 mM of dNTPs, 250 nM each of forward and reverse primers, 0.25 units of GoTaq® Flexi DNA Polymerase (M8291, Promega) and 1X Green GoTaq™ Flexi Buffer (Promega). PCR was run using a Bibby Scientific Techne 5 Prime Thermal Cycler 5PRIMEG, with the following parameters: initial denaturation at 95°C for 10 min followed by 30 cycles at [95°C for 30 s, annealing for 30s, extension

1min/kb at 72°C], and followed by a final extension at 72°C for 10 min. Detailed information of the primers used for T-DNA detection and CAPS assays is provided in table III.1.

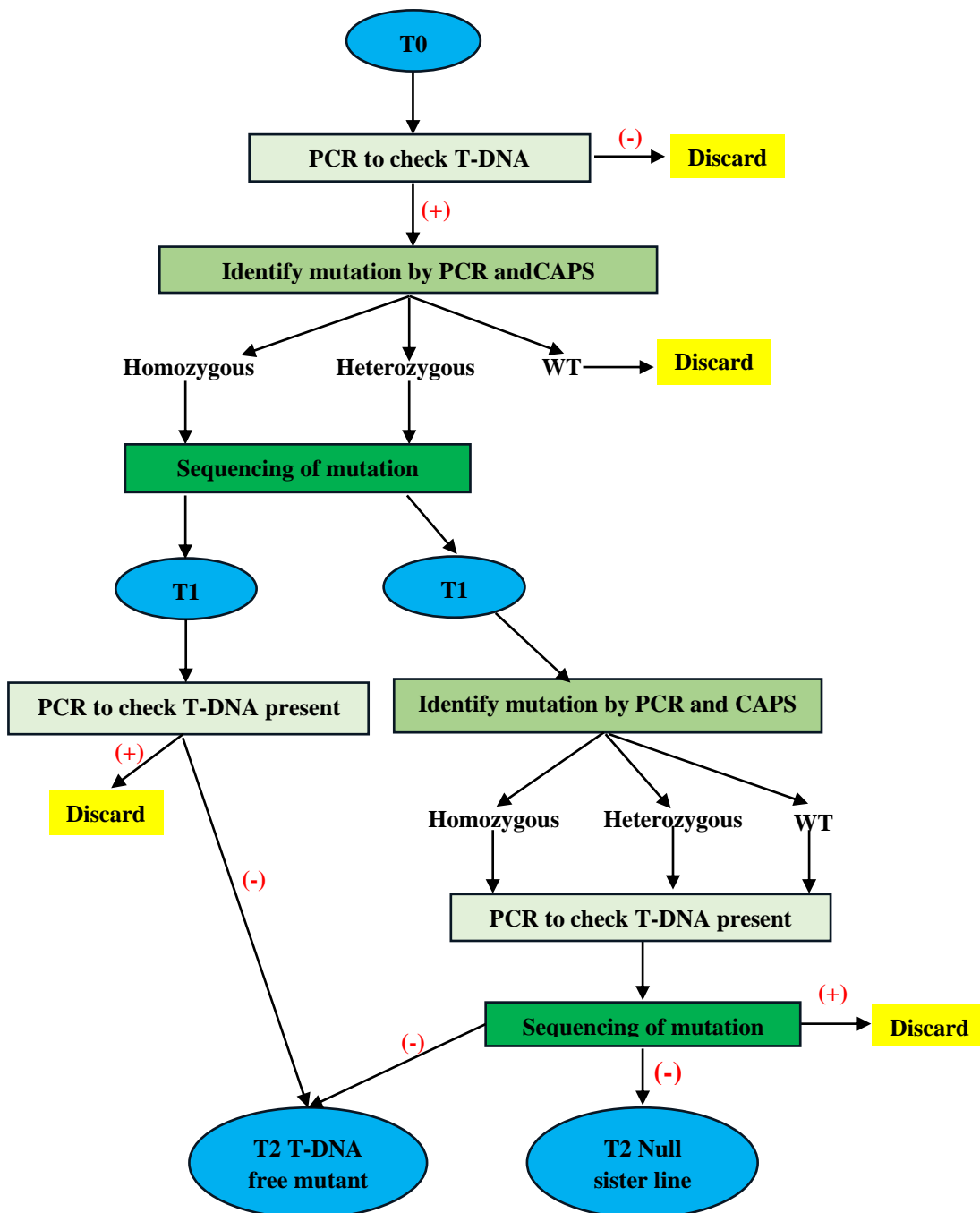


Figure III.10: Strategy to select T-DNA-free stable mutant from CRIPSR/Cas9 method. PCR to check T-DNA present was done using primers on the gRNA, Cas9 and HPT region. To detect mutations, a series of PCR and CAPS assays were done

based on each specific sequence of mutation. The mutation was finally sequenced by the Sanger method.

SNP polymorphisms identified between different mutation lines, non-mutated line and WT were converted into CAPS (Cleaved Amplified Polymorphic Sequences) markers. In brief, genome editing CRISPR/Cas9 technology generally produces small insertions/deletions (indels) which were easily and rapidly detected through altering a restriction enzyme (RE) recognition site. That RE site can be readily distinguished from wild-type alleles based on the CAPS technique whose principle is presented in fig III.11-A (Thiel et al. 2004; Hodgens, Nimchuk, and Kieber 2017). The RE sequences were screened on <https://restrictionmapper.org/> with the condition to cover the cutting site of Cas⁹ nuclease, which is generally located 3-4 nucleotides upstream of the PAM sequence. If a restriction site is created or altered by the mutation such that only one allele contains the restriction site, a polymerase chain reaction (PCR) followed by an enzymatic restriction can be used to distinguish the two alleles. Moreover, depending on the sequences of the candidate genes and position of gRNA, in many cases of CRISPR-induced alleles, no such RE sites are naturally present at the cutting sites of Cas⁹ enzyme in the target sequences. In this case, a species-agnostic web tool, called indCAPS (a derived CAPS which is compatible with indels) and developed based on Python, was altered to purposefully introduce mismatches in the oligonucleotide primers to create a restriction site in one, but not both, of the amplified templates, the principle of dCAPs assay is presented in fig III.11-B. To design PCR primers to identify CRISPR/Cas⁹ alleles, we access indCAPS at (<http://indcaps.kieber.cloudapps.unc.edu/>) (Hodgens, Nimchuk, and Kieber 2017).

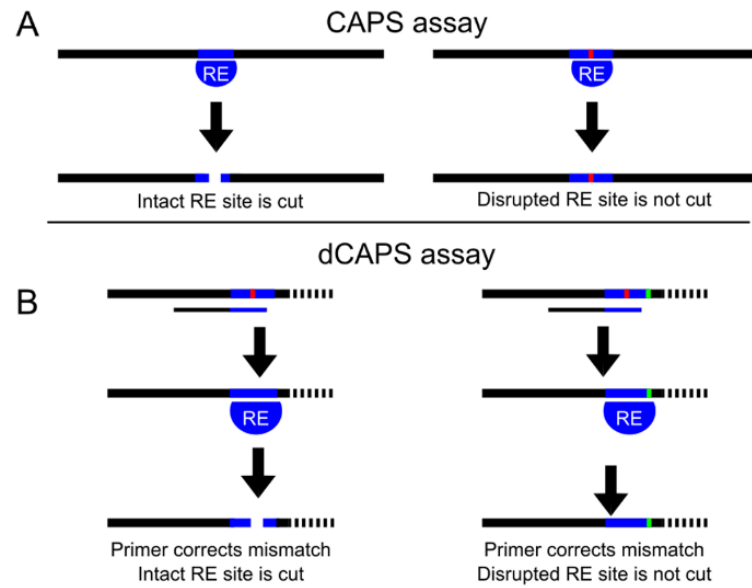


Figure III.11: CAPS/DCAPS markers can distinguish alleles. **(A)** Diagram of CAPS technique. An amplicon centered on a restriction site (blue bar) disrupted by a SNP or indel (red bar) is differentially cleaved by a restriction enzyme (RE) in the wild-type vs mutant. **(B)** Diagram of the dCAPS technique. A restriction site can be introduced into either the wild-type or mutant target sequences using mismatched oligonucleotide primers to discriminate two sequences. The mutation (green bar) disrupts the introduced restriction site such that it is not cleaved by the restriction enzyme (RE). Gel electrophoresis can be used to identify the size difference between the wild-type and mutant fragments in both the CAPS and dCAPS methods (Hodgens, Nimchuk, and Kieber 2017).

III.2.10.5 Nuclear DNA ploidy assessment of transgenic plants:

DNA samples for the ploidy measurement were prepared according to (Doležel, Greilhuber, and Suda 2007). A flow cytometry was used to determine the level of nuclear DNA content in transgenic plants, by evaluating the relative fluorescence intensity of Propidium iodide (PI)-stained nuclei. In brief, approximately 2 cm long fresh samples were cut and chopped in a petri dish containing 500 μL of Otto I buffer (0.1 M citric acid, 0.5% Tween 20). A 42 μm nylon mesh was used to filter the isolated nuclear homogenate. After that, an addition of 1ml Otto II buffer (0.4 M Na_2HPO_4) containing 50 $\mu\text{g mL}^{-1}$ RNase and 50 $\mu\text{g mL}^{-1}$ propidium iodide was provided. The ploidy was analyzed on a Partec PAS I flow cytometer (Partec GmbH, Münster, Germany) equipped with a high-pressure mercury arc lamp, by recording the relative fluorescence intensity of at least 3000 nuclei. Then, a FlowMax software was

used to analyze the data. The *wild-type* barley cv. Golden Promise was used as a diploid standard.

III.2.10.6 Plant phenotyping

To phenotype the root system of mutant, grains of the wild-type Golden Promise DH1-6, null sister, and mutant lines were used. Initially, the barley cv. Golden Promise grains were sterilized by immersing in 70% ethanol for 30 seconds; then rinse once in sterilized deionized water; prior to immersing in 3% hypochlorite for 3 minutes and finally extensively rinsing 6 times in sterilized deionized water. The sterilized grains were then gently dried on sterile tissue paper. After sterilization, the grains were placed in petri dishes with 3 layers of wet filter papers and put at 4°C for 3 days of vernalization to stimulate homogeneous germination. Then, the grains were transferred for germination in phytotron with a photoperiod of 15°C/16 hours light and 12°C/8 hours darkness. Two days after germination (DAG), young seedlings with 1 to 2 cm – long shoot were transferred to the sand-filled pots (Ø:10 cm x h:10 cm) containing cleaned beach sand over a 1 cm layer of soil in the bottom to avoid sand leaching during watering. The plants were grown for 8 weeks in the same conditions and regularly watered once per two days, with a 1X nutritive solution recommended by the commercial product (Kristalon™ 280 start, Agro, Czechia). The pots were kept in the same phytotron for 8 weeks.

Eight-week-old barley plants were removed from the pots. After carefully washing excess sand and soil from the roots, the number of crown roots and embryonic roots were counted, the length of the longest (deepness of the root system) was measured with a ruler to the nearest mm and the total fresh root was determined with a scale, for each plant. Finally, the root architecture of each plant was scanned, using EPSON scan program, with ImageScanner III LabScan 6.0 with a 600-dpi resolution and saved as tiff-formatted photos.

III.2.11 Complementation of two putative genes in rice *crl1* mutant

III.2.11.1 Establishment of genetic constructs for complementation assay

The two barley genes (*HvCRL1* and *HvCRL1-L1*) were amplified from cDNA obtained from RNA extracted from stem bases of cv. GP seedlings grown in the crown root inducible system for 6h after inducing by 1-NAA. They were amplified using a specific couple of primers associated with BP flanking sequences for further cloning (Table III.1). *HvLBDs* were recombined using BP clonase (Invitrogen 11789020, Invitrogen, Carlsbad, CA, USA) into the Gateway binary vector pCAMBIA5300.OE (Khong et al. 2015). This vector was modified from pCAMBIA2300 plasmid (CAMBIA, Australia). By the addition of the maize ubiquitin promoter (pUbi), to drive expression of protein coding sequences of interest in an enhancer effect (Christensen and Quail 1996). This vector has been also supplemented by the Gateway cassette attP1-ccdB-attP2 sequence located between the pUbi and a Tnos (NOS terminator). This cassette contains suitable recombination sites being specific for recombinase BP reaction and maintaining orientation and being in phase with reading frame of cDNA. In the transfer-DNA (T-DNA) region of the pC5300-OE, the intron of the castor bean catalase gene (CAT) 1 has been inserted into the Hygromycin resistant gene (HPT) for plant transformation's selecting (Miki and McHugh 2004). The selective antibiotic for selection in bacteria is Kanamycin, encoding by the *NEOMYCIN PHOSPHOTRANSFERASE* gene (*NPT II*). Subsequently, the constructs were further confirmed by restriction enzyme digestions using *EcoRI* and *BamHI* individually. Finally, successful clones were validated by sequencing for all constructs.

Four constructs were established for complementation assay including (1) pC5300.OE::*HvCRL1*, (2) pC5300.OE::*HvCRL1-L1*, (3) pC5300.OE-empty as a negative control.

III.2.11.2 Stable transformation in rice

Plants were transformed with the binary vector pC5300.OE::*HvLBD*. Plasmids previously were transferred into hypervirulent *Agrobacterium tumefaciens* strain

AGL1, developed in IPK, Germany (Marthe et al., 2015). The *crl1* mutant in the Taichung 65 background was used for gene overexpression. Cultivar was genetically transformed previously described (Sallaud et al. 2003; Toki et al. 2006). Transgenic plants were selected based on hygromycine resistance as well as with PCR, using specific primer for HvLBD cDNA (Table III.1). A non-transgenic line (without T-DNA) was kept as negative control (null sister).

III.2.11.3 Phenotypic characterization of HvCRL1 and HvCRL-L1 complemented *crl1* rice mutant.

To phenotyping the root system of complemented transgenic plant, seeds of WT TC65, *crl1* mutant, OverExpress-HvCRL1, OverExpress-HvCRL-L1, transgenic TC65 with empty pRT104 vector were used. Initially, the rice cv. TC65 seeds were sterilized by immersing in 70% ethanol for 30 seconds; then rinse once in sterilized deionized water; prior to immersing in 3% hypochlorite for 3 minutes and finally extensively rinsing 6 times in sterilized deionized water. The sterilized seeds were then gently dried by sterilized tissue paper. After sterilization, the grains were placed in a square petri dish (24x24 cm) containing 250 ml of ½ MS medium (pH 5.8) in the middle line in the dishes. Plates were sealed with 2 layers of parafilm and covered half by aluminum foil and transferred for germination in phytotrol with a photoperiod of 25°C±2°C /12 hours light and 22°C±2°C /12 hours darkness. The plates were standing vertically for 14 days. Plates with 14 day-after-sowing rice plants were scanned, using EPSON scan program, with ImageScanner III LabScan 6.0 with a 600-dpi resolution and saved as tiff-formatted photo. The number of crown roots per plant was manually counted and scanned again.

III.3 Results and discussions

III.3.1.1 Identification and classification of the barley *LBD* gene family members and their phylogenetic analysis

Initially, only fifteen sequences were identified in the PlantTFDB as putative LBD proteins in barley and considered for the study. With the characterization of the barley LBD protein family (Guo et al. 2016) and the recent barley annotation (Mascher et al. 2021), the number of LBD proteins in barley rose to 31.

To identify the *LBD* gene family members in barley (*HvLBD* genes), BLAST search of the barley reference genome (MorexV3 pseudomolecules assembly; Mascher et al. 2021) was performed using the LOB domain (PF03195) characteristic of this transcription factor family. To be easier to illustrate and track *HvLBD* genes on the phylogenetic tree when using CFVisual_V2.1.5 (Fig.III.12-C), the 31 *HvLBD* genes were consistently numbered from 1 to 31, according to the increasing ordered positions of the genes among chromosomes from 1H to 7H (i.e., *HvLBD1* was named for the gene *HORVU.MOREX.r3.1HG0013280* with the first position in the chromosome 1; continuously *HvLBD2* was named for *HORVU.MOREX.r3.1HG0025890* until finally, *HvLBD31* was named for *HORVU.MOREX.r3.7HG0675910*) (Table III.3). Thirty-one genes were identified as putative LBD proteins in barley (Table III.3) and their amino acid sequences were retrieved from barley reference genome database (MorexV3) and represented in supplementary table S3. They were located among the 7 barley chromosomes (Fig.III.12-A). Chromosomes 3H and 4H contained the most *LBD* genes (9 and 10, respectively). Four genes were located on 1H and 5H. Two *LBD* genes were distributed in 2H, while only one was located on each of chromosomes 6H, and 7H. The identified *HvLBD* proteins had from 101 (*HORVU.MOREX.r3.5HG0493820*) to 380 (*HORVU.MOREX.r3.3HG0322090*) amino acids (Supplementary table S4). The gene IDs corresponding to the former 2012, 2016 annotations (Mascher et al. 2013; 2017) and the last available annotation of the barley Morex reference genome V3 (Mascher et al. 2021), orthologous genes in *Arabidopsis* and rice, chromosome position, length of cDNA, length of amino acid sequence and proteins' clades were also provided in the table III.4. The analysis of the gene structure identified that genes comprised 1 to 4 exons (Fig.III.12-C).

Table III.4: *HvLBD* family genes in barley

Gene name	Gene ID – Morex V1 (2012) ^a	Gene ID – Morex V2 (2016) ^b	Gene ID – MOREX V3 (2021) ^c	Orthologous genes in Arabidopsis	Orthologous genes in rice	Class	Chromosome position	cDNA length (bp)	Amino acid length (aa)
HvLBD1	MLOC_68570	HORVU1Hr1G012720	HORVU.MOREX.r3.1HG0013280	<i>AtLBD1</i>	Os05g0123000	IA	1H:32858742-32859389	648	215
HvLBD2	MLOC_56075	HORVU1Hr1G024490	HORVU.MOREX.r3.1HG0025890	<i>AtLBD13</i>	Os05g0165450	IA	1H:108737412-108738979	711	236
HvLBD3	MLOC_54949	HORVU1Hr1G060290	HORVU.MOREX.r3.1HG0062250	<i>AtLBD4</i>	Os05g0346800	IA	1H:412519516-412520188	570	189
HvLBD4	MLOC_61156	HORVU1Hr1G064640	HORVU.MOREX.r3.1HG0066110	<i>AtLBD10</i>	Os05g0417000	IA	1H:432284186-432287558	1046	261
HvLBD5	MLOC_11838	HORVU2Hr1G035160	HORVU.MOREX.r3.2HG0129400	<i>AtLBD38</i>	Os07g0589000	II	2H:123950142-123951312	1051	237
HvLBD6	MLOC_58304	HORVU2Hr1G066080	HORVU.MOREX.r3.2HG0159010	<i>AtLBD40</i>	n/a	II	2H:403038120-403039423	1304	302
HvLBD7	-	-	HORVU.MOREX.r3.3HG0230650	n/a	n/a	IA	3H:23459332-23460307	822	273
HvLBD8	-	HORVU3Hr1G016320	HORVU.MOREX.r3.3HG0233680	<i>AtLBD41</i>	Os01g0511000	II	3H:32334938-32336111	1174	282
HvLBD9	-	HORVU3Hr1G016690	HORVU.MOREX.r3.3HG0233930	<i>AtLBD25</i>	Os01g0169400	IA	3H:33653864-33655875	1347	257

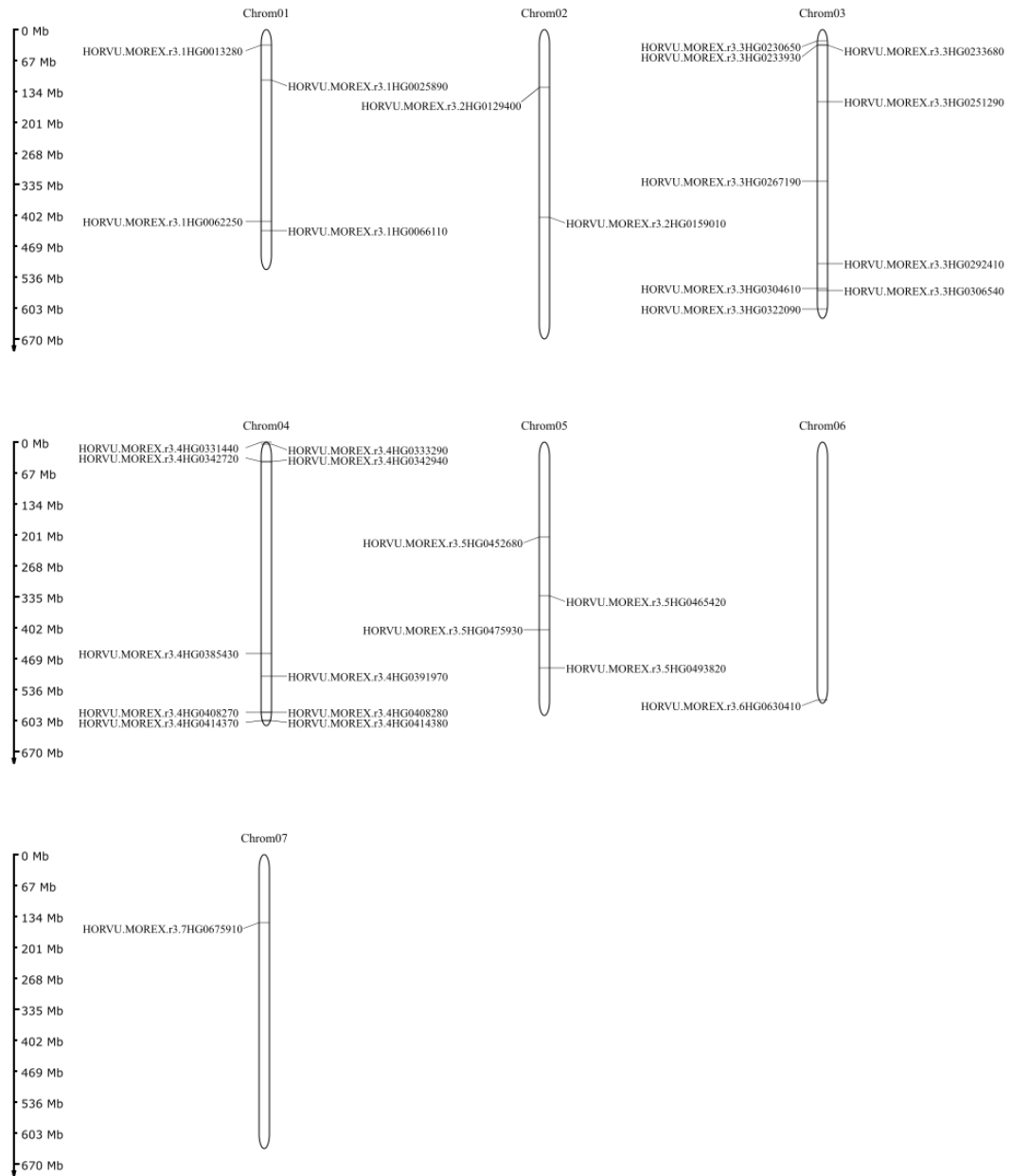
HvLBD10	-	HORVU3Hr 1G033360/ HORVU3Hr 1G033370	HORVU.MOREX.r3.3HG 0251290	<i>AtLBD2</i>	Os01g0242400	IA	3H:154707698-154708482	696	231
HvLBD11	-	-	HORVU.MOREX.r3.3HG 0267190	n/a	Os01g0571800	IA	3H:325189509-325190408	900	299
HvLBD12	-	HORVU3Hr 1G075370	HORVU.MOREX.r3.3HG 0292410	<i>AtLBD20</i>	Os01g0772100	IB	3H:504453001-504453788	702	233
HvLBD13	MLOC_ 16076	HORVU3Hr 1G088440	HORVU.MOREX.r3.3HG 0304610	<i>AtLBD15</i>	Os01g0825000	IA	3H:556521538-556522824	879	292
HvLBD14		HORVU3Hr 1G090250	HORVU.MOREX.r3.3HG 0306540	<i>AtLBD6</i>	Os01g0889400	IA	3H:561725882-561728765	1233	259
HvLBD15	MLOC_ 81908	HORVU3Hr 1G109250	HORVU.MOREX.r3.3HG 0322090	<i>AtLBD22</i>	Os08g0402100	IA	3H:600625873-600627313	1441	380
HvLBD16	MLOC_ 52276	HORVU4Hr 1G000880	HORVU.MOREX.r3.4HG 0331440	<i>AtLBD29</i>	n/a	IB	4H:409243-410060	678	225
HvLBD17	MLOC_ 57082	HORVU4Hr 1G002480	HORVU.MOREX.r3.4HG 0333290	<i>AtLBD4</i>	n/a	IA	4H:5374752-5376521	525	174
HvLBD18	MLOC_ 51325	HORVU4Hr 1G013380	HORVU.MOREX.r3.4HG 0342720	<i>AtLBD37</i>	Os03g0609500	II	4H:41436713-41438172	687	228
HvLBD19	MLOC_ 66372	HORVU4Hr 1G013630	HORVU.MOREX.r3.4HG 0342940	<i>AtLBD10</i>	Os03g0612400	IA	4H:42787943-42791015	1655	301

HvLBD20	MLOC_ 73009	HORVU4Hr 1G056890	HORVU.MOREX.r3.4HG 0385430	<i>AtLBD1</i>	Os03g0287400	IA	4H:455870238-455871003	675	224
HvLBD21	MLOC_ 55239	HORVU4Hr 1G063160	HORVU.MOREX.r3.4HG 0391970	<i>AtLBD30</i>	Os03g0246900	IB	4H:503127551-503129186	771	256
HvLBD22	MLOC_ 10783	HORVU4Hr 1G080150	HORVU.MOREX.r3.4HG 0408270	<i>AtLBD29</i>	Os03g0149000	IB	4H:581752326-581752880	555	184
HvLBD23/ HvCRL1	MLOC_ 10784	HORVU4Hr 1G080160	HORVU.MOREX.r3.4HG 0408280	<i>AtLBD29</i> ,	OsCRL1/ Os03g0149100	IB	4H:581759414-581760406	993	284
HvLBD24	MLOC_ 65651	HORVU4Hr 1G086700	HORVU.MOREX.r3.4HG 0414370	<i>AtLBD41</i>	Os01g0511000	II	4H:599196625-599197491	867	288
HvLBD25	-	HORVU4Hr 1G086690	HORVU.MOREX.r3.4HG 0414380	n/a	Os01g0511000	II	4H:599204157-599204966	810	269
HvLBD26	-	-	HORVU.MOREX.r3.5HG 0452680	n/a	n/a	IA	5H:203642428-203643135	708	235
HvLBD27	MLOC_ 5148	HORVU5Hr 1G047610	HORVU.MOREX.r3.5HG 0465420	<i>AtLBD4</i>	Os11g0106900/ Os12g0106200	IA	5H:330681277-330681810	534	177
HvLBD28	-	HORVU5Hr 1G057690	HORVU.MOREX.r3.5HG 0475930	<i>AtLBD22</i>	n/a	IA	5H:404849815-404850936	1122	373
HvLBD29	-	-	HORVU.MOREX.r3.5HG 0493820	n/a	n/a	IA	5H:486489688-486489993	306	101
HvLBD30/ HvCRL1- L1	MLOC_ 61947	-	HORVU.MOREX.r3.6HG 0630410	<i>AtLBD16</i>	Os02g0820500	IB	6H:555132287-555133359	943	210

HvLBD31	MLOC_ - 20803	HORVU.MOREX.r3.7HG 0675910	<i>AtLBD18</i>	IB	7H:146421739-146423131	687	228
---------	------------------	-------------------------------	----------------	----	------------------------	-----	-----

a, b, c: Identification numbers of barley *LBD* genes (International Barley Genome Sequencing Consortium et al., in 2012, 2016 and 2021, respectively), barley cv. Morex sequence. n/a: no data is available on <http://plants.ensembl.org/index.html>. The orthologous genes in Arabidopsis and rice (*Oryza sativa* cv. Japonica) were retrieved from the orthologous analysis in the barley gene family database (BGFD) and EnsemblePlants barley MorexV3 assembly. Three classes of LBD protein were identified manually (Zhang et al. 2020).

A



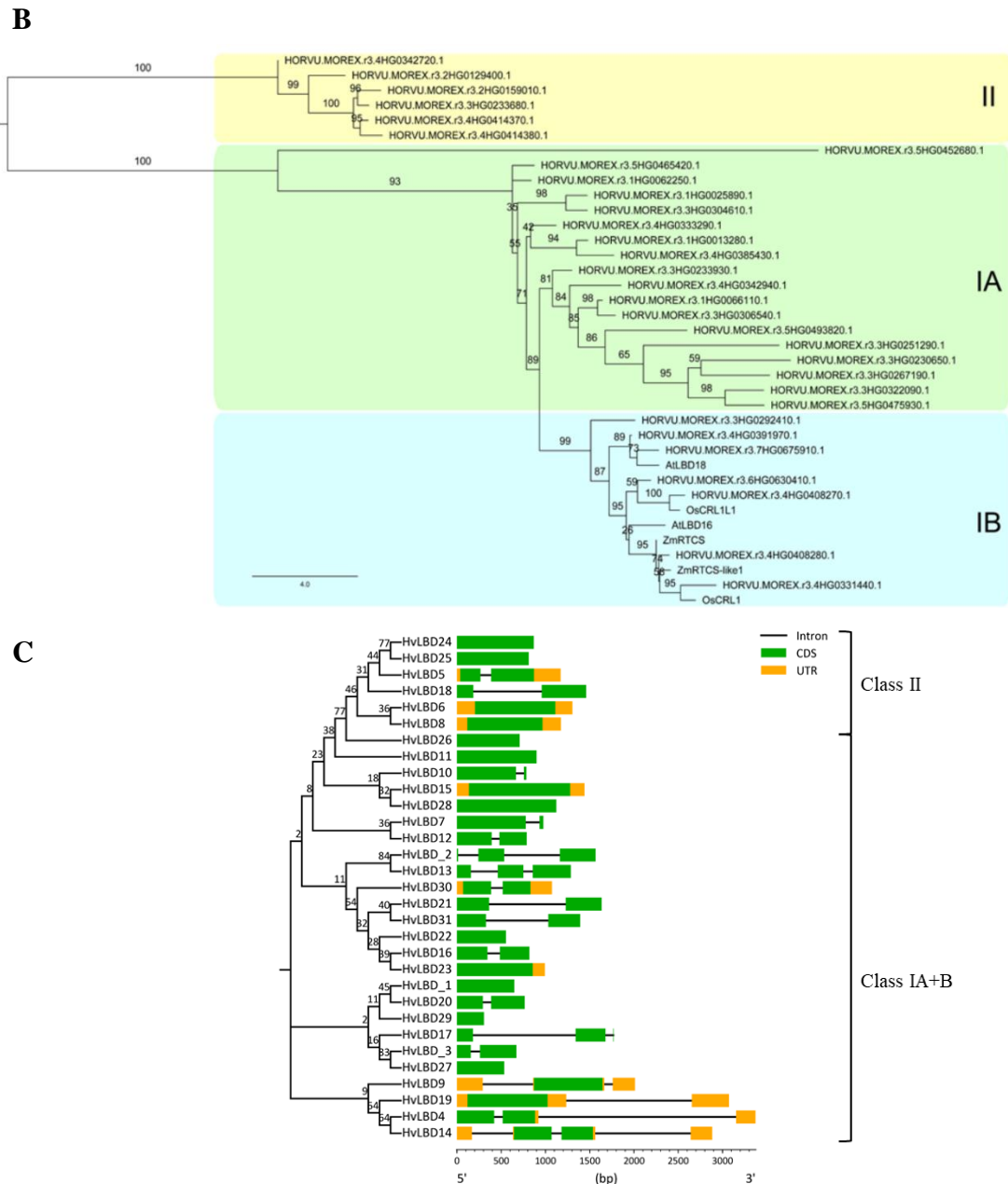


Figure III.12: In silico characterization of barley LBD proteins. (A) Localization of the putative LBD proteins on the 7 chromosomes of barley. The chart has been built with MG2C (Chao et al. 2021). (B) Phylogenetic analysis of the 31 barley LBD proteins. The analysis has been ran with learnMSA (Becker and Stanke 2022) and default parameters. Sequences of rice (*Os*), maize (*Zm*) and Arabidopsis (*At*) genes encoding known key initiators of crown (*Os* and *Zm*) and adventitious (*At*) roots have been included in the analysis. The protein-coding sequences were aligned using learnMSA (Becker and Stanke 2022) under default options. The phylogenetic tree was analysed with IQtree 1.6.2. (Nguyen et al. 2015). The best protein model was identified using -m MFP option, and the branch supports were tested by UFBoot2 (Hoang et al. 2018) with 10000 replicates. (C) Phylogenetic relationship among the thirty-one

HvLBD proteins. The gene structure of the 31 HvLBD genes was drawn with CFVisual tool. The tree was generated in the form of an Inferred ancestral state, using the Maximum Likelihood method and Jones et al. w/freq. model. Evolutionary analyses were conducted in MEGA 11 (Tamura, Stecher, and Kumar 2021). The tree shows a set of possible amino acids (states) at each ancestral node based on their inferred likelihood at site 1. Initial tree(s) for the heuristic search were obtained automatically by applying Neighbor-Join and BioNJ algorithms to a matrix of pairwise distances estimated using the JTT model, and then selecting the topology with superior log likelihood value. The rates among sites were treated as a Gamma distribution using 5 Gamma Categories (Gamma Distribution option). All positions containing gaps and missing data were eliminated (complete deletion option). There were a total of 71 positions in the final dataset. Bootstrap analysis was conducted with 500 iterations

The phylogenetic relationship among barley LBD proteins was determined for the 31 barley LBD proteins using MEGA 11 (Tamura, Stecher, and Kumar 2021). Three classes of LBD proteins were manually distinguished based on the prediction of the presence or absence of the coiled-coil motif (Table III.3 and Fig.III.12-B) (Lupas, Van Dyke, and Stock 1991). Twenty-five proteins belonged to class I, characterized by the conserved N-terminal sequence made of a zinc finger C-block, a gly-ala-ser-block, and a leucine-like coiled-coil zipper module. Class I is subdivided into Class IA and Class IB (Fig.III.12-B) (Coudert et al. 2013; Zhang et al. 2020). The six other LBD proteins determined Class II, characterized by the absence of leucine-like coiled-coil motif in the conserved N-terminal region (Fig.III.12-B and C). The alignment indicated that the HvLBD proteins were identified including 31 LBDs in barley and 5 of them in class IB (HORVU.MOREX.r3.4HG0408280, HORVU.MOREX.r3.4HG0331440, HORVU.MOREX.r3.4HG0391970, HORVU.MOREX.r3.6HG0630410 and HORVU.MOREX.r3.4HG0408270) were phylogenetically related to rice OsCRL1, maize ZmRTCS and ZmRTCS-like1, Arabidopsis AtLBD16 and AtLBD18 that have been characterized as key actors of CR initiation in rice and maize, and lateral root initiation in *Arabidopsis*, respectively (Fig.III.12-B). While combining the function reports and evolutionary relationship between LBD proteins, molecular functions can be attributed to different groups. In this regard, the barley HvLBD proteins clustering in Class II might regulate anthocyanin synthesis and nitrogen responses; HvLBD proteins belonging to Class IA might play primary roles in the lateral root formation, whereas HvLBD of Class IB

may have main functions in leaf adaxial–abaxial polarity, plant reproduction, and adventitious rooting (Y. Zhang et al. 2020). The barley class IB contains 7 HvLBD proteins, one of them (HORVU.Morex.r3.4HG0408280) clustering with the well-characterized rice CRL1 and maize RTCS proteins (Inukai 2005; H. Liu et al. 2005; C. Xu et al. 2015), suggesting that it could be their ortholog and play a role in the crown root initiation in barley. Consequently, we named it HvCRL1.

III.3.1.2 Expression profiles of the *HvLBD* genes

The expression profiles of *HvLBD* genes during the development of barley were determined based on data retrieved from the EoRNA barley expression database (<https://ics.hutton.ac.uk/eorna/index.html>). Because this database was based on an old annotation of the reference cv. Morex genome (Mascher et al. 2017), the expression of only 26 *HvLBD* genes could be obtained. The expression data from epidermis, embryos, anthers, internodes, leaves, root, grains, palea, lemma, rachis, lodicule, etiolated, inflorescences and shoots in different stages of development were visualized as a heat map (Fig.III.13). Expression profile of five putative barley *LBD* genes, which are orthologous to rice, maize and Arabidopsis *LBD* genes involved in CR and lateral root initiation, were marked by red star in the figure III.13 (HvLBD23: HORVU.MOREX.r3.4HG0408280, HvLBD22: HORVU.MOREX.r3.4HG0408270, HvLBD30: HORVU.MOREX.r3.6HG0630410, HvLBD16: HORVU.MOREX.r3.4HG0331440, HvLBD21: HORVU.MOREX.r3.4HG0391970.

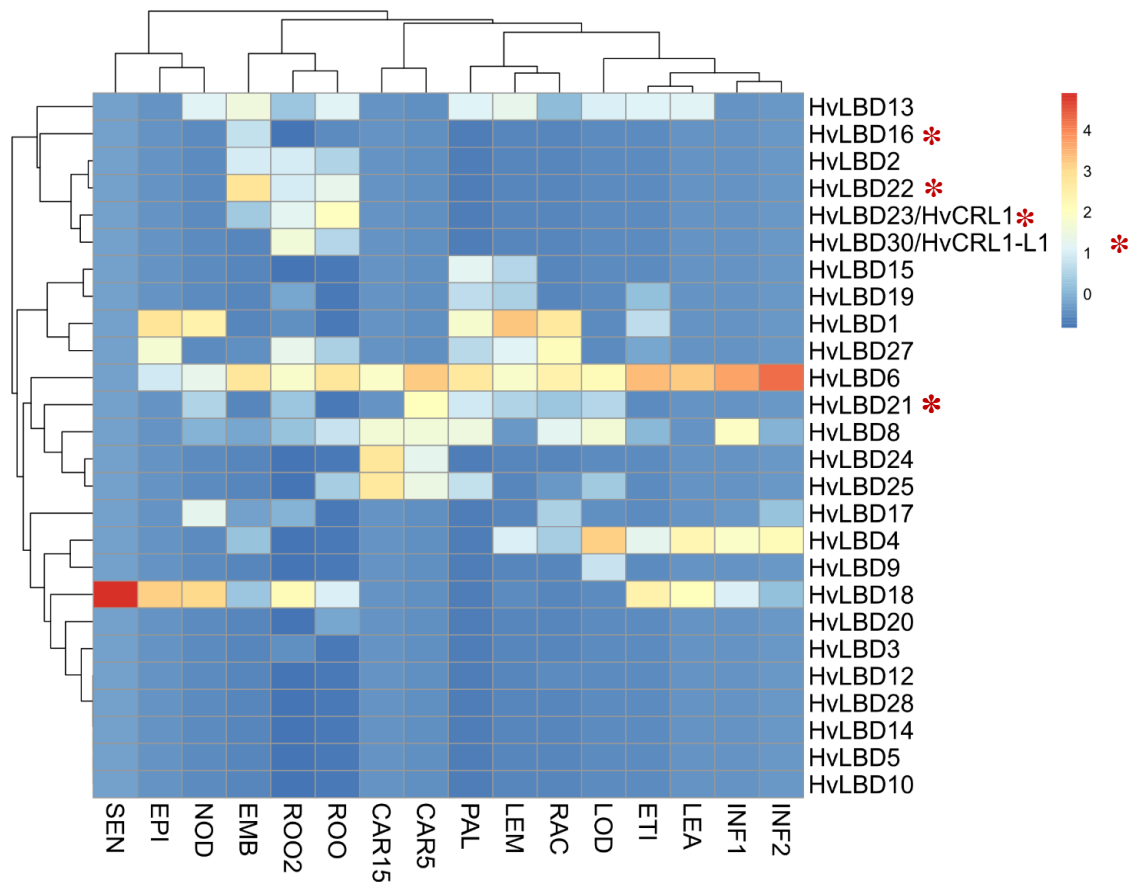


Figure III.13: Heat map of the expression profiling of *HvLBD* genes in different tissues. The heat map was created with ClustVis web tool (<https://biit.cs.ut.ee/clustvis/>) (Metsalu and Vilo 2015), using the barley reference transcript dataset (BART) in EoRNA barley expression database with transcripts per million (TPM) (<https://ics.hutton.ac.uk/eorna/index.html>). Original values are $\ln(x)$ -transformed; Columns are centered; Unit variance scaling was applied to columns; Both rows and columns are clustered using correlation distance and average linkage including 26 rows corresponding to 26 genes with available expression profile and 16 columns corresponding to different tissues. The color scale bar represents the expression values of the genes. Three bio replicates were selected for each sample. Current EoRNA contains both BART transcripts and the predicted transcripts from the Barley Pseudomolecules (HORVU 2017). Senescing leaf (2 months): (SEN). Epidermis (4 weeks): (EPI). Developing tillers at six leaf stage, 3rd internode: (NOD). 4-day embryos dissected from germinating grains: (EMB). Root (4 weeks): (ROO2). Roots from the seedlings (10 cm shoot stage): (ROO). Developing grain, bracts removed (15 days post anthesis (DPA): (CAR15). Developing grain, bracts removed (5DPA): (CAR5). Palea (6 weeks PA): (PAL). Lemma (6 weeks PA): (LEM). Rachis (5 weeks PA): (RAC). Lodicule (6 weeks PA): (LOD). Etiolated (10-day old seedling): (ETI). Shoots from the seedlings (10 cm shoot stage): (LEA). Young developing inflorescences (5mm): (INF1). Developing inflorescences (1-1.5cm): (INF2).

The study of lateral- or crown-root initiation is tedious because it occurs only in a few cells inside the root or the stem base, respectively. Moreover, it occurs unpredictably. To circumvent this problem, a Lateral Root Inducible System (LRIS) has been developed in *Arabidopsis* and maize to study lateral root initiation (Crombez et al. 2016). By treating seedlings consecutively with an auxin transport inhibitor and a synthetic auxin, one can control the synchronous initiation of lateral roots, consequently allowing abundant sampling of a desired developmental stage. Here, we used the same system to synchronously initiate crown roots (Fig.III.14) and named it Crown Root Inducible System (CRIS).

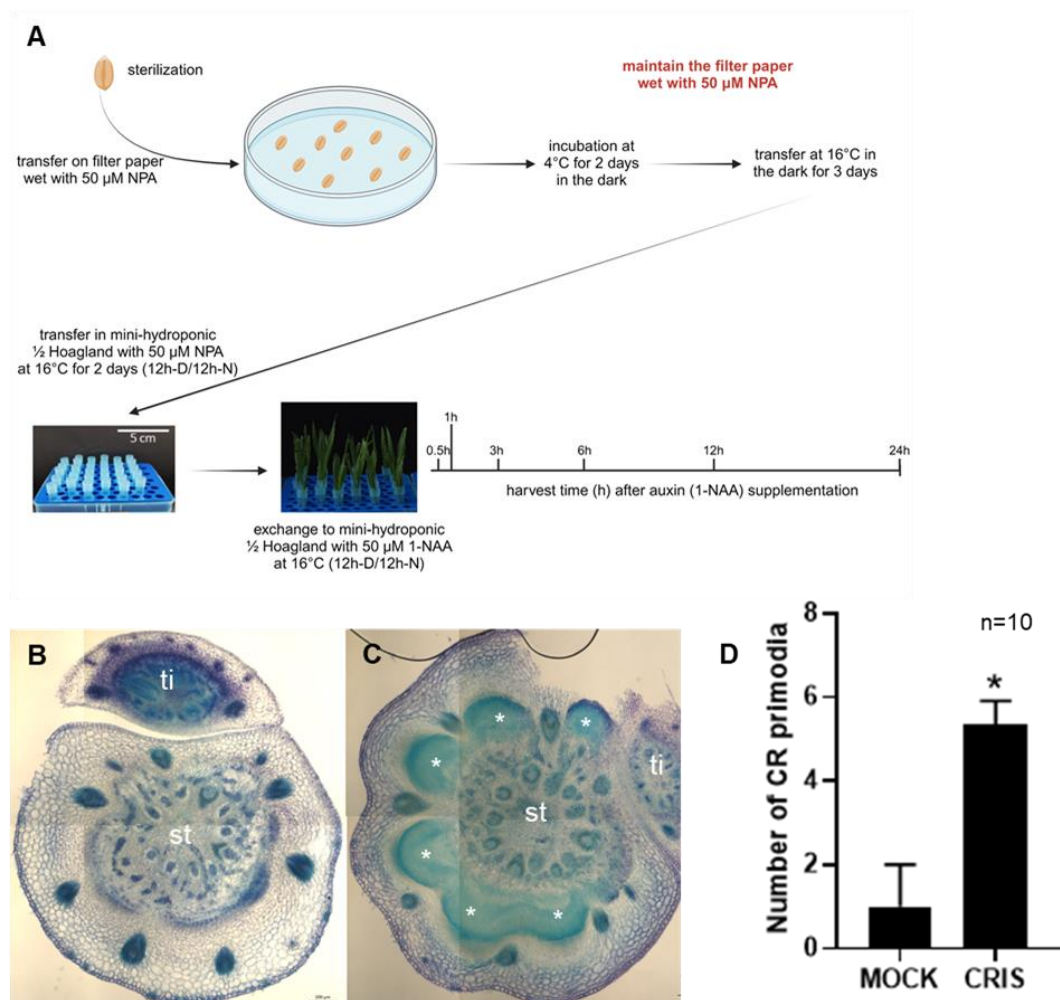


Figure III.14: Crown-root inducible system (CRIS). **A)** Schematic representation of the system and the sample collection. The picture was prepared with Biorender. **B)** and **C)** Hand-made transversal section across the stem base of 5 days-old seedlings grown for 3 days in 50 μM NPA (B) or in 50 μM 1-NAA (C). Sections were stained in 0.1% toluidine blue. Pictures were acquired with a Zeiss microscope with a 5x objective.

The full section was reconstructed using the Free Online Image Combiner (Adobe Express). ti: new tiller; st: stele; *: root apical meristem. **D**) Determination of the number of crown root in barley 10 days after auxin-induction. Student's *t* test was performed to determine the static significance; *n* = 10.

The cross-section of the stem base of barley seedlings treated for 3 days with 1-NAA revealed the presence of a ring of several root primordia at the same stage of development (Fig.III.14-C). This was not the case in the stem base of seedlings that were kept in the presence of the NPA (An auxin accumulation - and transportation – inhibitor) (Fig.III.14-B). Seedlings treated with 1-NAA had a significantly higher number of crown roots 10 days after auxin-induction (Fig.III.14-D). We demonstrated that the CRIS is an effective model to synchronously stimulate the production of crown roots in barley.

Consequently, the CRIS was used to study the expression profile of 5 *HvLBD* genes belonging the Class IB and phylogenetically related to genes encoding proteins that are key regulators of lateral or crown roots initiation was investigated by real-time qRT-PCR. These genes were: MLOC_10784 (HORVU.MOREX.r3.4HG0408280), MLOC_10783 (HORVU.MOREX.r3.4HG0408270), MLOC_61947 (HORVU.MOREX.r3.6HG0630410), MLOC_52276 (HORVU.MOREX.r3.4HG0331440) and MLOC_55239 (HORVU.MOREX.r3.4HG0391970). For this purpose, barley stem bases were collected before (*T*₀) and after 3, 6, 9, 12 and 24 hours treated with 1-NAA.

Six genes were evaluated toward their ability to be used as reference genes, which is a fundamental requirement for the proper quantification of gene expression. Besides the well-known *actine* and *EF2α* genes, 4 other genes were selected with Genevestigator based on the criteria of a specific expression in crown/roots: EIF52A, TIP41, 5439 and 20934. The specificity of the primer pairs was confirmed first by the presence of a single peak in the melting curve and second by the presence of a single band on the agarose gel (Fig.III.15).

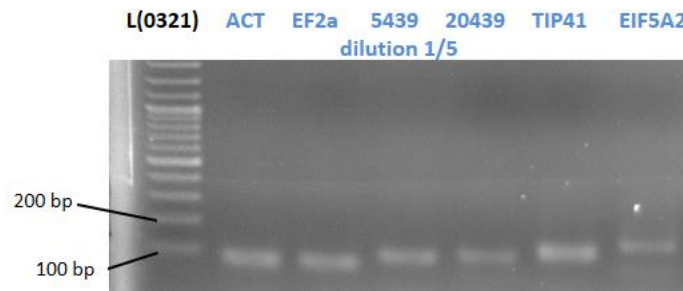


Figure III.15: PCR products of housekeeping genes showed a single band. L (0321): Ladder GeneRuler 100 bp Plus DNA Ladder - Thermo Fisher Scientific

The expression of candidate reference genes was detected by qRT-PCR in 5 samples collected from the stem base of barley seedlings grown in the CRIS and sampled at different time 1-NAA treatment. Their expression was plotted as a function of cycle threshold (Ct) values (Fig.III.16). The average Ct values of the candidate genes ranged from 18 to 31 in all samples, mainly between 22 and 26. Among all these genes, *EF2 α* showed the highest expression with an average Ct value of 22.8, whereas *EIF52A* showed the lowest expression level with an average value of 26.5. The Ct value variation indicated the difference in candidate gene expression stability among the different samples analyzed: smaller Ct variation of the gene across sample, more stable expression.

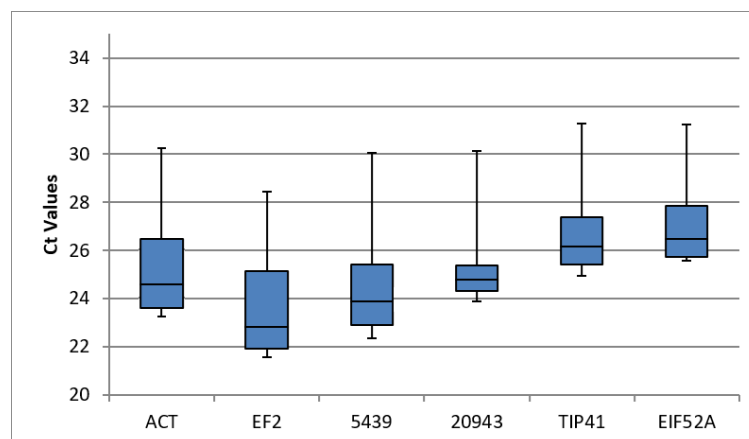


Figure III.16: Expression levels of candidate reference genes across all samples. The line across the box depicts median.

The geNorm v3.5 software was used to analyze the gene expression stability (Vandesompele et al. 2002). The reference genes were ranked according to the average M value expression (the larger the M value, the worse the gene's expression stability

(Fig.III.17). In this study, all potential reference genes presented an M value lower than the cutoff established by Vandesompele et al. 2002 ($M < 0.15$). *Hv5439* and *EF2 α* had the lowest M values with the highest expression stability, while *EIF52A* had the highest M value with the lowest expression stability.

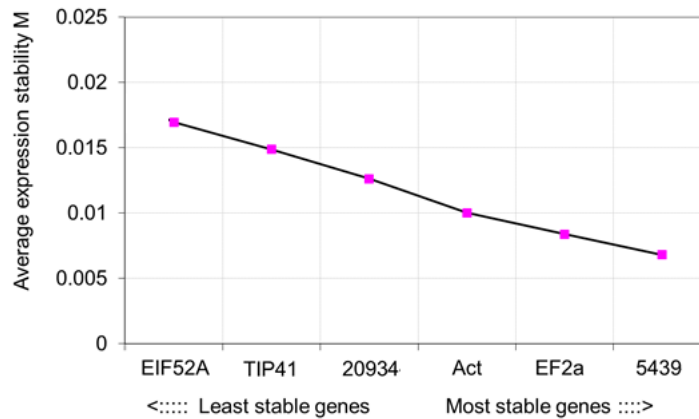


Figure III.17: Gene expression stability and ranking of 6 candidate reference genes as calculated by geNorm (Vandesompele et al., 2002).

Following the MIQE (Minimum information for publication of quantitative real-time PCR Experiments) recommendations (Bustin et al. 2009), we identified three reference genes that were used to normalize qRT-PCR data: *actin*, *EF2 α* and *Hv5439* genes.

qRT-PCR was used to analyze the expression of the five ClassIB *HvLBD* genes during crown-root initiation. Two barley *LBD* genes (*HORVU.Morex.r3.4HG0331440* and *HORVU.Morex.v3.4HG040880*) were not detected in our conditions, suggesting that they are not expressed in the stem base of barley. Whereas *HORVU.Morex.r3.4HG0408270* was detected in our conditions; its expression was very low and not affected by auxin treatment, indicating that it most probably has no function during crown root initiation. The transcripts of the *HvCRL1* (*HORVU.Morex.r3.4HG0408280*) gene highly accumulated within the first 3h of auxin treatment in the stem base of young seedlings (Fig.III.18). In a transcriptomic analysis based on CRIS (GEO: GSE171320, unpublished), *HvCRL1* is significantly up-regulated 1h following auxin-induced initiation of crown roots. Altogether, this indicated that *HvCRL1* is a prime target of the auxin signaling pathway. Finally, *HORVU.Morex.r3.6HG0630410* gene was found to accumulate significantly in the stem base of young seedlings treated for 6h by auxin, suggesting that it could be part of the mechanisms regulating crown root initiation in barley. Because *HORVU.Morex.r3.6HG0630410* is not the closest ortholog of rice *CRL1* but seems to

be involved in crown root initiation; this gene was referred to as *HvCRL1-Like1* (*HvCRL1-L1*).

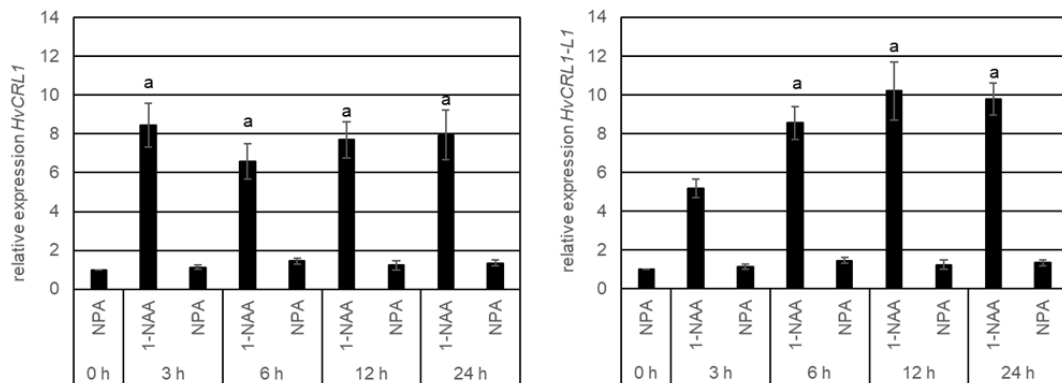


Figure III.18: Gene expression analysis by qRT-PCR of two *LBD* genes (*HvCRL1* and *HvCRL1-L1*) of Class IB expressed in the stem base of young barley seedlings grown in the Crown Root Inducible System (CRIS) based on auxin-induced root initiation (Crombez et al. 2016). Normalization was done using 3 reference genes: *Actin*, *Hv5439* and *EIF152*. The graph shows means \pm SEM (n=6). The statistical significance was assessed by a non-parametric Kruskal-Wallis followed by a multiple comparisons test (GraphPad Prism 10). a: statistically significantly different from the control “0h-NPA” (p -value < 0.001).

This delay compared to *HvCRL1* suggested that *HvCRL1-L1* is not a direct target of the auxin signaling pathway. For both genes, the expression did not change when the seedlings were kept in the inhibitor of polar auxin transport (NPA), confirming that changes in their respective expression were related to auxin induction only.

We analyzed the 5,000 bp promoter region of both *HvCRL1* and *HvCRL1-L1* genes (Fig.III.19). Using the consensus Auxin Response Factor (ARF) binding sequence, Auxin Response Element (AuxRE: TGTCNN), we highlighted only AuxRE that form tandems with a maximum of 24 bp spacing (Cancé et al. 2022). In the promoter of *HvCRL1*, we found 10 AuxRE tandems. Except for two tandems that form everted repeats (ER: two AuxREs orientated back-to-back in different strands of DNA), all others form direct repeats (DR: two AuxREs following each other in the same DNA strand) (Freire-Rios et al. 2020). In the promoter of *HvCRL1-L1*, out of the 5 identified AuxRE tandems, 4 presented a DR conformation, whereas the fifth one was made of inverted repeats (IRs; double sites in which two AuxREs are oriented towards each other in different strands of DNA). Further analysis is required to

determine which AuxRE cis-regulating elements are responsible for the auxin-mediated regulation of both genes.

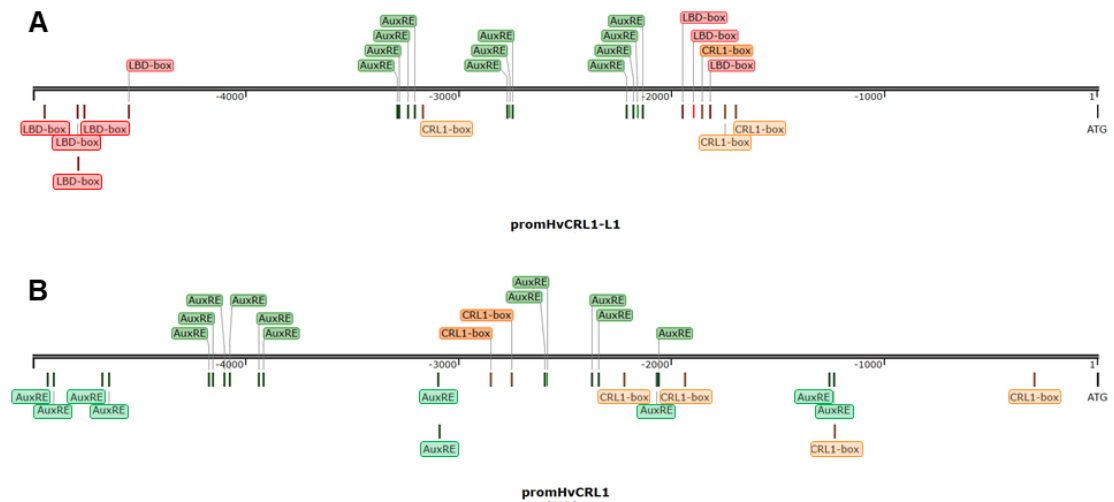


Figure III.19: Identification of AuxRE (TGTCNN) and LBD-box (GCGGCG)/CRL1-box (CAC[A/C]C) in the 5000 bp-promoter sequence of **A)** *HvCRL1-L1* and **B)** *HvCRL1* genes.

With the assertion that *HvCRL1-L1* is not a direct target of the auxin signaling pathway but rather a down-stream target of *HvCRL1*, we analyzed the promoter sequence of *HvCRL1-L1* for the presence of 1) the LBD-box (GCGGCG) that is the consensus sequence recognized by LBD transcription factors (Husbands et al. 2007), and 2) the CRL1-box (CAC[A/C]C) that has been characterized to be also recognized with high affinity by the rice *CRL1* (Gonin et al. 2022). Interestingly, we observed that the promoter of *HvCRL1-L1* contains both LBD- and CRL1-boxes (Fig.III.18-A), forming notably a cluster of 6 boxes in the region –1953 to –1695 bp. This reinforces our idea that if *HvCRL1-L1* is not a direct downstream target of *HvCRL1*, *HvCRL1-L1* expression might be at least regulated by different LBD proteins. In contrast, no LBD-box was found in the promoter region of *HvCRL1*. Interestingly, several CRL1-boxes were present in the promoter region of *HvCRL1*. It is, however, most unlikely that a feedback loop or other LBD transcription factors could regulate the expression of *HvCRL1*. Indeed, the dimerization of LBD transcription factors is necessary for their DNA-binding activity (Lee et al. 2017). A structure-function analysis showed that homodimeric LOB domain of *Ramosa2* from wheat (TtRa2LD) harbors optimal binding affinity toward *cis*-regulating elements when they are in very close vicinity

(W. F. Chen et al. 2019). Because in the promoter of *HvCRL1*, the CRL1-boxes are far apart from each other, it is unlikely that an LBD dimer could bind the DNA and regulate the expression of this gene.

HvCRL1-L1 is phylogenetically the closest ortholog of the rice *DEGENERATED HULL1 (DH1)* gene (Fig.III.20; 73.50% of identity as determined by ClustalOmega) which has been demonstrated to play a role in glume formation (Li et al. 2008). In barley, the glume primordia are already well developed in 18-day-old seedlings (Waddington et al. 1983; Thiel et al. 2021; Alonso-Peral et al. 2011), suggesting that the regulatory machinery has been activated earlier during the development. In our study, we collected the stem bases of approx. 12 days-old young barley seedlings. Because we did not proceed with the dissection of the different tissues, the shoot apical meristem is present in the sample and could have transitioned from vegetative to reproductive development. However, further investigation is required to determine whether *HvCRL1-L1* could affect glume development.

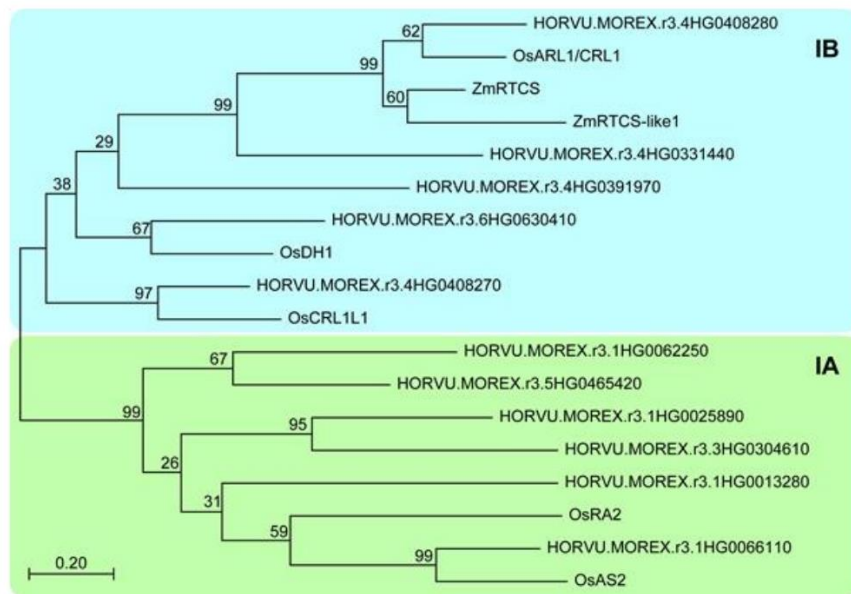


Figure III.20: The another phylogenetic tree of the LBD proteins including known rice sequences (Os) was built by MEGA11 (Tamura, Stecher, and Kumar 2021).

III.3.1.3 *HvCRL1* binds the LBD-box *in vivo*

To validate that *HvCRL1* and *HvCRL1-L1* are transcription factors recognizing and binding to the LBD-box, initially identified as the consensual DNA binding site of the ASYMMETRIC LEAVES2 (AS2) (Husbands et al. 2007) LBD

protein, we performed a *trans*-activation assay in rice protoplasts. For this purpose, rice protoplasts were co-transformed with a tripartite vector system that comprises (1) a reporter plasmid triggering the expression of the β -D-glucuronidase (GUS)-encoding *uidA* gene under the control of a minimal promoter and a tetramer of either the LBD-box or its mutated version, (2) an effector plasmid allowing the expression of either HvLBD genes under the control a minimal CaMV35S promoter and (3) a reference plasmid carrying the Renilla luciferase gene. The relative enzymatic activity of the reporter protein was monitored *in vitro* and normalized to the constitutive luciferase activity. While the empty vector had minimal or no effect on GUS activity, HvCRL1 significantly trans-activated the LBD-box promoter in rice protoplasts (Fig.III.21). This activation was strongly reduced when the LBD-box was mutated. In contrast, the increase in the GUS reporter activity of the LBD-box by HvCRL1-L1 was not found to be significant.

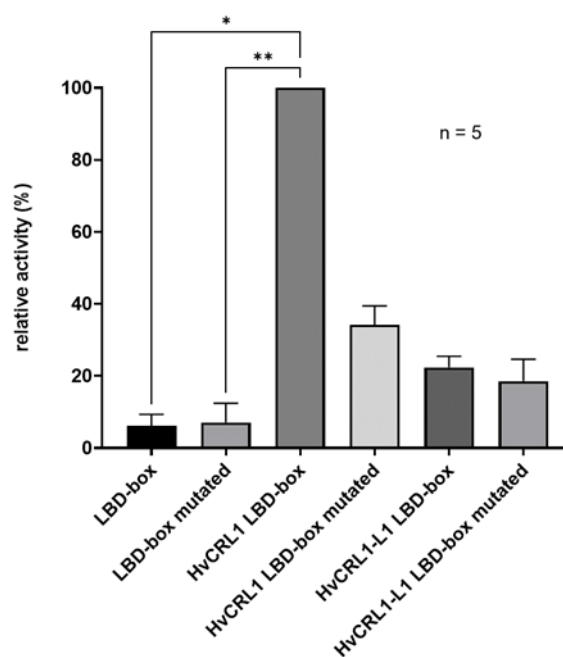


Figure III.21: Transactivation assay in rice protoplast with HvCRL1 and HvCRL1-L1. Rice protoplasts were co-transformed with an effector plasmid carrying either HvCRL1 or HvCRL1-L1 gene under the control of the 35S promoter and reporter plasmids carrying LBD box motif (LBD-box) or its mutated version (LBD-box mutated) fused to GUS. A reference plasmid carrying the Renilla luciferase gene under the control of the 35S promoter was co-transformed to correct for transformation and protein extraction efficiencies. The control represents protoplasts that were transfected with an empty effector plasmid. The data were expressed as a percentage of the highest

activity observed for HvCRL1. The graph represents the average \pm SEM of 5 independent experiments. The statistics were assessed with GraphPad Prism 10 (One-way ANOVA non-parametric Kruskal-Wallis followed by a Dunn's multiple comparisons test).

It has been demonstrated that the LBD-box can be bound by different LBD transcription factors such as RTCS in maize, HvRAMOSA2 in barley or AS2, and AtLBD18 in Arabidopsis. LBD transcription factors form dimers to bind to the DNA, recognizing pairs of LBD-boxes with different affinities depending on the number of bases between two consecutive LBD-boxes (Chen et al. 2019). Recent studies have highlighted that LBD transcription factors have a relaxed DNA binding specificity, explaining how they could regulate a plethora of developmental programs (Gonin et al. 2022). Thus, the fact that HvCRL1-L1 did not significantly induce changes in GUS reporter activity might reflect that this specific LBD transcription factor might recognize a different DNA binding site. In addition, LBD transcription factors can form heterodimers or interact with other regulatory proteins. For example, in maize, RTCS and RTCL can form heterodimers (Majer et al. 2012). AS2 LOB can interact with bHLH048, decreasing the affinity of AS2 for the LBD-box, and consequently suggesting that such a heterodimerization process could be a post-translational mechanism that regulates LBD transcription factor activity (Husbands et al. 2007). More recently, CRL1 was shown to interact with WUSCHEL-related Homeobox11 (WOX11), a homeodomain transcription factor also involved in crown root differentiation in rice (Geng et al. 2023). The interaction of WOX11 with CRL1 promotes the binding of WOX11 on the promoter of CYTOKININ OXYDASE/DEHYDROGENASE4 (OsCKX4), and the expression of this latter, which encodes a cytokinin oxidase that favors crown root initiation by reducing locally cytokinin levels. In addition, WOX11 can interact with another rice LBD transcription factor, LBD16, that facilitates the initiation and elongation of rice crown roots by modulating cell division (Geng et al. 2024). WOX11 binds the LBD16 promoter, interacting with a demethylase JMJ706 that epigenetically unlocks LBD16 expression. In turn, when LBD16 is expressed enough, it can compete with JMJ706 to bind with WOX11 on the LBD16 promoter, which results in re-methylating the locus, leading to the repression of LBD16 expression. This stresses that LBD transcription factors can

interact with a wide range of proteins and are also involved in post-translational regulatory mechanisms, particularly for regulating crown root formation. Such interactions between HvCRL1-L1 and other proteins should be explored. This could better explain its biological activity than a direct binding on target gene promoters.

III.3.1.4 Both HvCRL1 and HvCRL1-L1 are involved in crown root formation

To assess the role of the *HvCRL1* and *HvCRL1-L1* genes in the initiation of the crown root, using the CRISPR-Cas9 methodology and *Agrobacterium*-mediated transformation of the immature embryo of barley, we obtained different independent lines of barley knocked-out either in *HvCRL1* or *HvCRL1-L1* genes. For the *HvCRL1* gene, all independent mutants contained a 1-base deletion. For the *HvCRL1-L1* gene, different types of deletion-based mutations (-1, -10, -13 and -19 bp) and insertion-based mutation (+1 bp) were obtained (Fig.III.22).

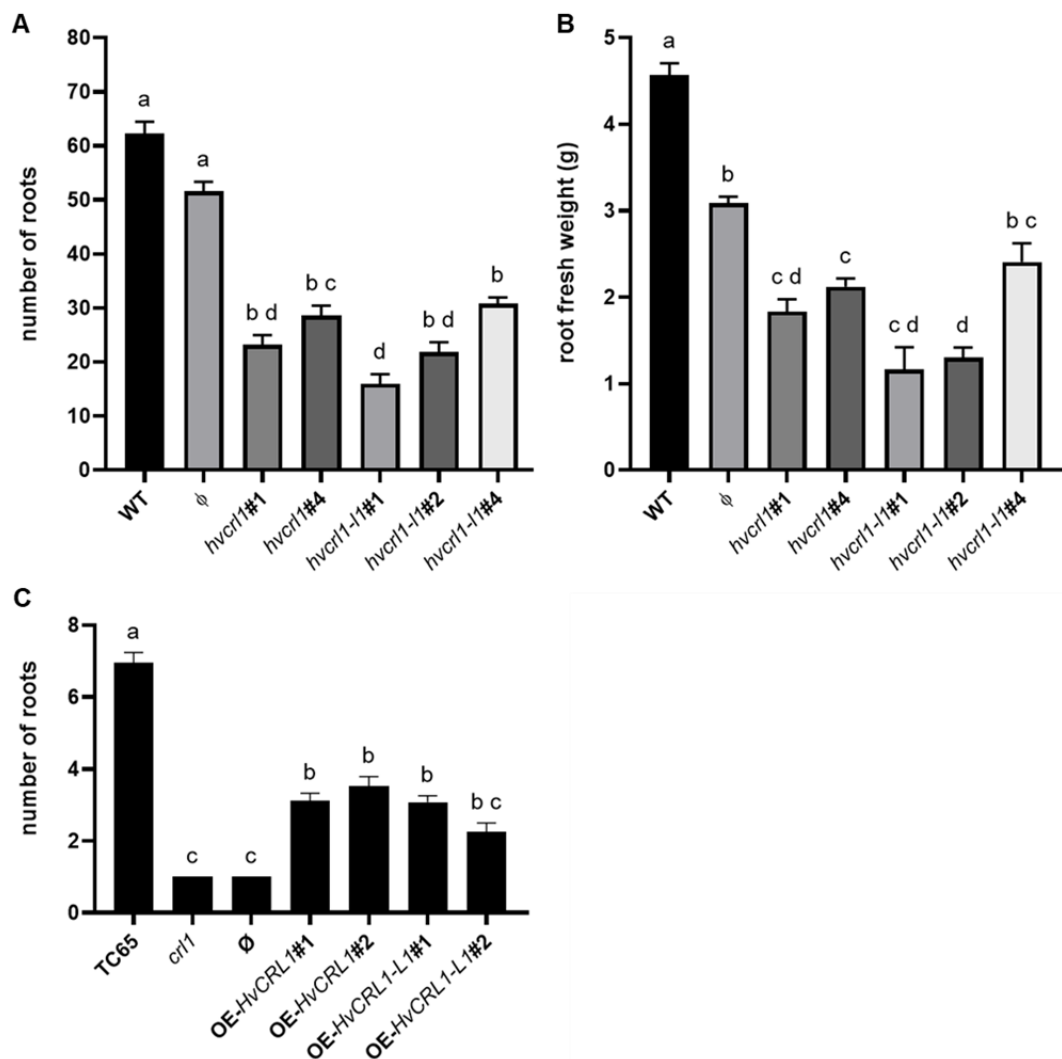


Figure III.23: Role of HvCRL1 and HvCRL1-L1 in the formation of crown roots. **(A)** Number of crown roots of different *hvcr1* and *hvcr1-l1* knocked-out lines of barley obtained by CRISPR-Cas⁹. **(B)** Fresh weight of the total root system of different *hvcr1* and *hvcr1-l1* knocked-out lines of barley obtained by CRISPR-Cas⁹. **(C)** Complementation of the crown-root less phenotype of the rice *cr1* mutant by overexpression of *HvCRL1* or *HvCRL1-L1* genes. *HvCRL1* or *HvCRL1-L1* were overexpressed in the rice *cr1* mutant in the cv. TC65 genetic background. An empty vector was used as a control (ϕ). The graphs represent average \pm SEM; Statistical significance was assessed by a Brown-Forsythe and Welch ANOVA test followed by Dunn's multiple comparisons (GraphPad Prism 10.2.2). Bars with identical letters are not significantly different ($p < 0.05$).

In parallel, we overexpressed the two barley genes in the rice *cr1* mutant (Inukai et al. 2005), which has a crown root-less phenotype due to a defect in crown root initiation (Fig.III.23-C). The overexpression of both *HvCRL1* and *HvCRL1-L1*

gene resulted in a significantly higher number of roots in the rice seedlings, indicating that both genes can partially complement the *crll* rice mutant by restoring crown root initiation. However, we could not observe a root phenotype similar to the wild-type rice cv. TC65. This could be due i) either to the fact that barley *HvCRL1* and *HvCRL1-L1* genes are too different from the endogenous rice *CRL1* or ii) the 2 barley genes are absolutely required to fully reverse the crown root-less phenotype of the rice *crll* mutant. The co-overexpression of the 2 barley genes could partially answer that question.

Altogether, our data confirmed that both *HvCRL1* and *HvCRL1-L1* play a role barley's crown root formation and development.

III.4 Conclusions

The barley genome contains 31 genes encoding LATERAL ORGAN BOUNDARIES (LBD) proteins that can be classified into class I and class II based on their structure. The class I is itself divided into two subclasses: class IA and class IB. While combining the function reports and evolutionary relationship between LBD proteins, molecular functions can be attributed to different groups. In this regard, the barley HvLBD proteins clustering in Class II might regulate anthocyanin synthesis and nitrogen responses. HvLBD proteins belonging to Class IA might play primary roles in the lateral root formation, whereas HvLBD of Class IB may have main functions in leaf adaxial–abaxial polarity, plant reproduction, and adventitious rooting (Zhang et al. 2020). The barley class IB contains proteins clustering with the well-characterized rice *CRL1* and maize *RTCS* proteins (Liu et al. 2005; Xu et al. 2015), suggesting that they could play a role in the crown root initiation in barley.

The current study identified and characterized two LBD transcription factors from barley, *HvCRL1* and *HvCRL1-L1* that are closely phylogenetically related to the rice *CRL1* transcription factor. Both partially complement the root-less phenotype of the rice *crll* mutant, and barley *Hvcrll* and *Hvcrll-l1* loss-of-function mutants show a reduction in crown root number, showing that they are both involved in the regulation of this developmental process. We showed that the expression profile of these two genes during crown root formation presents a thigh time delay and that *HvCRL1-L1*

can bind the LBD box whereas HvCRL1 cannot. This suggests that both proteins likely cooperate through different molecular pathways in regulating crown root formation in barley. This is reminiscent of what was described in maize for RTCS and RTCL (Xu et al. 2015) or, more recently, in rice for CRL1 and LBD16 (Geng et al. 2023; Geng et al. 2024). To better understand the mechanisms of action of these two barley LBD transcription factors it will be interesting to test their capacity to interact with each other and other proteins. The capacity of the LBD transcription factor to interact with other proteins is often a critical step in regulating their biochemical and biological function (Beckman et al. 2011; Husbands et al. 2007; Geng et al. 2024).

ANNEXES – Supplementary data

Supplementary Note S1: Hoagland's solution:

Stock solution of macronutrients: 1 mol·l⁻¹ KNO₃; 1 mol·l⁻¹ Ca(NO₃)₂·4 H₂O; 0,2 mol·l⁻¹ NH₄NO₃; the volume was adjusted to 500 ml with Milli-Q H₂O. Stock solution of 1 mol·l⁻¹ MgSO₄·7 H₂O, the volume was adjusted to 500 ml with Milli-Q H₂O. Stock solution of 1 mol·l⁻¹ KH₂PO₄, pH 6.0, the volume was adjusted to 250 ml with Milli-Q H₂O. Stock solution of Fe-EDTA: 30 mmol·l⁻¹ EDTA-2Na·2 H₂O and 28 mmol·l⁻¹ FeSO₄·7 H₂O in 1 mol·l⁻¹ KOH, the volume was adjusted to 1 l with Milli-Q H₂O. Stock solution of micronutrients: 46 mmol·l⁻¹ H₃BO₃; 2,28 mmol·l⁻¹ MnCl₂·4 H₂O; 0,77 mmol·l⁻¹ ZnSO₄·7 H₂O; 0,20 mmol·l⁻¹ CuSO₄; 0,50 mmol·l⁻¹ Na₂MoO₄·2 H₂O, the volume was adjusted to 1 l with Milli-Q H₂O.

For ½ Hoagland's solution: 2,5 ml stock solution of macronutrients; 1 ml stock solution of MgSO₄·7 H₂O; 0,25 ml stock solution of KH₂PO₄; 0,5 ml stock solution of Fe-EDTA; 0,25 ml stock solution of micronutrients were mixed and the volume was adjusted to 1 l with Milli-Q H₂O.

Supplementary Note S2: MG/L medium:

One liter was prepared with 250 mg KH₂PO₄; 100 mg NaCl; 100 mg MgSO₄·7 H₂O; 1 g L-glutamic acid; 5 g mannitol; 5 g tryptone; 2,5 g yeast extract. The pH was adjusted to 7.0. After autoclaving of the medium, 0,1 g biotin was added. For solid medium: 12 g agar was added.

Table S3: Amino acid sequence of the LBD genes in barley

HvLBD1	HORVU.MOREX.r3.1HG0013280.1 MESSGDTAPLHSSPTPTSPAMATGTAVVMSPCAACKILRRRCVDRCVLAPYFPPTDPHKFATAHRVFGASNIKLLQD LPEEQRADAVSSMVYEAAARARDPVYGSAGAICQLQRQVDGLKAQLARAQAEAAARAHHAHLVALLCVEVATAA ATPPQDAYCSGGGGSQSQLAAPPVGSAPADALYVVDGSAAGGGGIMQAGHVGWVADEPLWT
HvLBD2	HORVU.MOREX.r3.1HG0025890.1 MSTASDWQQDHEVGGKIKSESTAEADRMMAAARRSSSLPAAGAGPASTPSFNTMTPCAACKLLRRRCAQECPFSPFFS PLEPHKFASVHKVFGASNVSKMLLEVHESQRGDAANSLVYEANLRLRDPVYGCMGAILTLQQQVHALEAELAAVRAE ILKHRYRPAAAAAAAAAVPNVPPSSHASQLLAAGGHRPAGAMGLPAPAVGPVASASSSTTVYAAASSSTDYSSITHENAP YFG
HvLBD3	HORVU.MOREX.r3.1HG0062250.1 MAGGSPCASCKLLRRRCKDCIFAPFFPADDPHKFAIVHKVFGASNVSKMLLELPVQQRGDAVSSLVYEANARVRDPV YGCVGAISFLQNQVSQLQMQLAVAQAEILCIQMQRDGCQSQDDAGRNDGHSLAAMQQMVVDDTAAAEAFMQNG GGGFPPQLMSSYGGAPASNVHHYGGQDHLKRESLWT
HvLBD4	HORVU.MOREX.r3.1HG0066110.1 MASSASSFPGSVITMASSAAAAGAASSGAAGTGSPCAACKFLRRKCQPDCVFAPYFPPDNPQKFVHVHRVFGASNVT KLLNELNPYQREDAVNSLAYEADMRLRDPVYGCVGVISVLQHQLRQLQDLARARYELSKYQAAAAVAVSASVGCN GTPAMADFIGNTVPNCTQNFISHSTAIGAGLGFQHDQFAAVQMLARSYEGEGAVARLGVNNGSGGGYDFGYTSGM GPVSGLGPLGGGPFLKHGTAGGDERHTAAQ
HvLBD5	HORVU.MOREX.r3.2HG0129400.1 MRGSEAAVSTSTSGMSCNGCRVLRKGCNDACMLRPCLLWIEGADAQGHATIFAAKFFGRAGLMSFLTAVPESQRPA VFQSLLYEAAGRTINPVGGAVGLLWAGSWHLCEAAVQTVLRGGAIRPLPELAGGVPEGGVGGSDLFASSRRAVVG STYSMAKRVTPRKTWAPEAAASHHQEPSCDLGLFLTPGSAAAEGERRARRAGTPSMSSDGSVTTTLAGAGADGDKEPE LLNLFV

HvLBD6	HORVU.MOREX.r3.2HG0159010.1 MRLSCNGCRVLRKGCSEDCSIRPCLQWIKSPEAQANATVFLAKFYGRAGLMNINAGTDDSLRPGIFRSLLYEACGRIV NPIYGSVGLLWSNNWQMCQAAVEAVLSGKPIVQVSSEDAADRTPLKAYDIRHVSTSPAADGRLHKVAKPGRTRFK RASSASSHHNPSSDSNNKPKPQPRPTAEEELDRQHRKEMEEGAFQRAPSHESSDSRHEDPVEPHSQQEASADTEAEAG SHVSQAEQEQEQSTEPAADHAEVEKDDEELGLELTLGFAPVAARPAGCHLSVRTAAEPAFVGLRFL
HvLBD7	HORVU.MOREX.r3.3HG0230650.1 MPLPAATQQEQQQPACAACKHQRRRCTAECPLARYFPHDRPGLFRSAHRLFGVSNILKTLRRAGPDRAHRDDAMRG IAYEAAAWDAYPSGGCLPVIAALESQLRHDHGVLRLCLHAQIRHCRRRQHQSPTPLSVQPPTAGVPPAPTSSNTHGFDQ HNHAPASSRLHGDDNGDDGVADAAPPWAMQPLYYKGASAMAGMGGAQAQEEEDHQYQLLFDHAAAAVGHRQHEY DDISPFLELEDIIDGGDDRHHDRTPPYGSNRYQLTNDRTIIDVC
HvLBD8	HORVU.MOREX.r3.3HG0233680.1 MRMSCNGCRVLRKGCGEGETIRPCLEWIRSPDAQANATVFLAKFYGRAGLLNLLAAVPDAGLRPPLFRSLLYEACGR MVNPVYGSVGLLWSAQWEACQAAVEAVLKGRPIVRVSSDAPLAPCDIRHVAKPDRPAAAGTLPGVSRAGRTRFKRAS SSTAKTKSSFSDANKHDDGLDQAPSHEESAGSHVEDGGMAVEQAREEESSEGTEVDAGSHVSQAEHSPAPPVAKDEE AHGDEIGLELTLGIQTVAPRLVVRSPACFGASSSNAQSSHIGLLELPVS
HvLBD9	HORVU.MOREX.r3.3HG0233930.1 MASPSTGNSIVSVVVAATTPGAGAPCAACKFLRRKCLPGCVFAPYFPPEEPQKFANVHKVFGASNVTKLLNELPPH QREDAVSSLA YEAEARVKDPVYGCVGAISVLQRQVHRLQKELDAAHTELLRYACGELGSIPTALPVVVTAGVPSGRLSS AVMPCPGQLAGGMYSGGGGGFRRLGLVDAIVQPPLSAGCYYNMRSNNNAGGSVAADVAPVQIPYASMANWAVN AISTITTTSGSESIGMDHKEGGDSSM
HvLBD10	HORVU.MOREX.r3.3HG0251290.1 MTGGVNGVGGGGGGACA VCKHQRRKCEPNCELAA YFPANRMNDFRALHLVFGVANLTKLIKANATEAARRRAAET LTWEARWRERDPSEGCYREVSLRRENAVLRAENAALRRRADQCACCATTLQQHQQQILLVSAYNNGARPPGGVLH

	GASAGVVPGGYYNGNAGAVRTANGNARPHVSAQAPQTTMAGYAQGDRHHAASNGARPGAAGQAEAREKSNARCE AQRTAS
HvLBD11	HORVU.MOREX.r3.3HG0267190.1 MRRSTGPRVRARAHTCRLLSFLLPPPSTWPFKPKISCAGAGPAPGMSATPRHPPETAESSSGLSSSSSYPPVAAA VVPAQ HPACSACKHQRRKCAPGCPLAPYFPADKPGSFRNSHRLFGIKNILRILTTAGPENRDDCMKSILYEADARASDPVHGSC GICRSHERELASATAELALVKKRLQLHGHA VQNR SAPDAPGFISPDQPWMTQPPLMYPIQEGQQQAIYGTSVPAAAVKI DEDATIGVKLDEDDVMSMQHDDHAQGRTVVG AHYGRIEPPSSSSCRSSDTS PRGLLNRRAF
HvLBD12	HORVU.MOREX.r3.3HG0292410.1 MQEPLPPRKRGGAVHGSAAREQQQQQQADETSSSSSAGPGAPCGACKFLRRRCVPGCVFAPHFSGSGRERGAAQFAA VHRVFGASNVAKLLSRVPVALRRDARTVCYEAQARVADPVYGCVTILALQHQVALLQGQLSVLQTQLFNCRLALA SMHPDTAEQLAVLQPAYSAASAPSQMVNYDDLPAVDFMDVEPQMRGLESLSLQSQPPHRDEDESQGVSPFSGNAGQR QL
HvLBD13	HORVU.MOREX.r3.3HG0304610.1 MPCLLSTLSFLAIPNFTLLYHVPVRLSSPRSQLFLCHSPSPKRGEHASMSTERERLDEIGKKIKREPDPAAIAGVVVAVSP TEHHVHRRLGPGIGGAVNIATPCAACKLLRRRCAHECPFAPYFSPHEPHKFAAVHKVFGASNVSKMLLEVPEAERADA ASSLVYEANLRLRDPVYGCMGAISMLQQQVNALEAELEAVRAEIFKHRYRQAGVGVGVGAANLIVDDGAAAAGGFM PPSTTLVHTADVVSVAEAGQEVATLPATPTATAYAAGQPSSADYSSLNTSEHDAYFG
HvLBD14	HORVU.MOREX.r3.3HG0306540.1 MASSASSLPAPGGSVITLAASSAGGNGAGGVC GTGSPCAACKFLRRKCQPD CVFAPYFPPDNPQK FVHVHRVFGASN VTKLLNELHPYQREDAVN SLAYEADMRLRDPVYGCVA VISILQRNLRQLQQDLARAKYELSKYQSAAGPNGSQAMA EFIGSAVPNGVASFINVGHS AALG SVGGVTGFGQDQQFAAVQMLSR SYEAAEPIARLGLNGSY EFGYSASAMTGAGSV PGLGMLGGSPFLKPGIAGSDERGGAGQ
HvLBD15	HORVU.MOREX.r3.3HG0322090.1

HvLBD21	<p>MDYSNEATNTAAAQPYGRSMSPPSRVSSCSPPPVFPLMGNAPSSPPTIVLSPCAACKVLRRCADGCMLAPYFPPTEPA KFTTAHRVFGASNIIKLLQDLPESSRADAVSSMVYEAEARLRDPVYGCAGAVCRLQKEANELKVDLARAQADLLSIQT QHANLLALVCVEFAANHRGDQQHQHQPPLADQLNSIGGSGGGALYQQLYDSDLDSASWEEARQLWT</p> <p>HORVU.MOREX.r3.4HG0391970.1</p> <p>MSSGVGSSTLGGCGGPSGSGSGGGGGGLGGGGGGPCGACKFLRRKCVSECIFAPYFDSEQGAAHFAAVHKVFGASNV SKLLLQIPAHKRLDAVVTICYEAQARLRDPVYGCVAHIFALQQQVNLQAELTYLQTHLATLELPSPLPAAPQLPMA MPAQFSISDLPSTTNIPTTIDLSALFEPPAQPWALQQHHQHQLRQPSYGAMAHRGGSSMAEGSAGSGSGDLQTLAREL LDRHGRSGVKPELQPPPPHPR</p>
HvLBD22	<p>HORVU.MOREX.r3.4HG0408270.1</p> <p>MAGAGVTTTGSPCGACKFLRRRCAAECVFAPYFCAEDGASQFAAIHKVFGASNAKLLQQVAPGDRSEAAATVTYEA QARLRDPVYGCVAHIFALQQQVAALQAQVAHARTQAQLGAAATAMHPLLQQQAWQQAAAAEHDHHSITSTQSSSGC YSGAHQRSDGSSLHGAEMYACGYGEQEEGSY</p>
HvLBD23	<p>HORVU.MOREX.r3.4HG0408280.1</p> <p>MALGRPLHPNHPQQQQQRSPQHRQRQSGRPPSDPAVITDRLMSMTGLGSPCGACKFLRRKCARGCVFAPYFCHEQG AAHFAAIHKVFGASNVSKLLAHLPISDRAEAAVTVSYEQAARLRDPVYGCVAHIFALQQQVMTLQAQLASLKAHAPP APQGMQQHQDDVKGYVGGGAADQYGHGAYQWYNGNGAAAQQQCAYGNGGAVAGHDSITALLSGSAASDYMM YHALEQSASDDDRHAAAAFEAADQSSFGTEESGWRSSSGYQDCEDLQSVAYAYLNRS</p>
HvLBD24	<p>HORVU.MOREX.r3.4HG0414370.1</p> <p>MRASCNGCRVLRKGTDDCTIRPCLAWIRGADAQANATVFLAKFYGRAGLLNLLAAGTDAALRPALFRSLLYEACGR VANPVYGATGLFCMGRWEACQDAVQAVFEGRRIAVQSEAVRHPGLVAAFDVRHVPKPMVVPAPPGLGVSRAGRT MFKRASSSTAKPTISSGAKHGDLDRAPSHEEPAGSHDHVVEDGGMAVAVAVAAKQVRGESSADTGAEAHSHVSQAE QNLPMPLAQGGDDDEVGLELTLGFGPATRLLRSPPARPDAARRSSAECGHIGLLELPLV</p>
HvLBD25	<p>HORVU.MOREX.r3.4HG0414380.1</p>

MRASCNGCRVLRKGCADDCTIRPCLAWMRSPDAQANATVFLAKFYGRAGLINLLAAAPDDAQRPALFRSLLYEACGR
 ATNPVYGASGLFSTGNWEACQAAVQAVLEGRRIPQVGADQAAPHPGLTAA YGVRRIPKDTIDRAPAALRVS RAGRTS
 FKRAS PSSSAAGRNGSDCSHDHVVEDDGKAPEDMHKRGESSSSEAEAGSHVSQAAQSASATVPQVAQDDGEIGLELTL
 GFGPATRVLRSPPPPPPPPAARAMSGHIGLLLGLTV

HvLBD26 HORVU.MOREX.r3.5HG0452680.1

MATFIPVKFTEFCQPDATMPFGKELVQITKDLRIALPTITGKPASSYPEDSR YRIEVHIPGRTFQPRTEPMDFKFI PPNWIL
 GRDMAIHCALGRIKEEYKGGPISPD LFTVSR RNEDGEI ISSKTKDALLSYAQTLEKYS GTLEHHVIKDARKIKQLSLRELE
 LEEAAWEAHEHELEVKDFLERIEK LKTRVAYLEEELDMGENLHPEGDVAPLISNDE DYQESSTEGPV TMLF

HvLBD27 HORVU.MOREX.r3.5HG0465420.1

MAGAQTGSSATPCASC KLLRRRCARDCVFAPYFPPE DPHRFATVHRVFGASN VSKMLQELPAAQRADAVSSLVYEAT
 ARM RDPVYGCAG AISYLQQQVSQLQVQLAV AQAEI IQRINHPSPSAAFHLQELQQRQAQQQQM QMDDDDKAYSSL
 VMQN DLMSTLLLQEACLK KESLWT

HvLBD28 HORVU.MOREX.r3.5HG0475930.1

MPTTTDGADAPDLA GRAMTRSSSPSPPPAACHLQITTVATTAANNSDNPSSPV AHAQSSSSRVAGAAAGSGQNQACAA
 CKYQRRKCNPDCLAPYFPADQQR RFLNAHRLFGVGH IQATLRET PPD LHTDAMRALIFQAEARACDPVGGCCR IILD
 YENHLLAAQAELAALLSHLDLCRHQAAAAAIAQDAYVDDPGMQLLAPGPNPADVHDVLYAGHEINNAQANHH DHD
 HYL VGAADQVQPQKHQPPYDYFYDGPAAAGDESSSHAWGNAGNVHVHQQYGNGVKAESPVALGVQIETQFVN AFD
 VKPEIAAAGAVVMEHDAGSGASFEDHHLEQKVAATVVKNELIDHHA AAHMAAESSSRCQLELGFSSF

HvLBD29 HORVU.MOREX.r3.5HG0493820.1

MAMEAQWRVGD PVYGCAGVINRLQEEILATQCELARTRAQLAIVLAHGAQQAPPSAPLLPPPHSPQSAGGDRVAGVH
 LQRQGPQLDAPSVDPDEF LLDLDEF

HvLBD30 HORVU.MOREX.r3.6HG0630410.1

MAAAPGGGGGGVAGVAGSPCGACKFLRRRCVAECVFAPYFSSEQGAARFAAIHKVFGASNAAKLLAHLPLADRCE
AVVTITYEAQSRLRDPVYGCVAQIFALQQQVAILQAQLMQARAQIACGVQSTTSPVSHHQQQPWSQDTSIAALLRQQE
NVSSFAAGGALLPELMSGDVSMLQQHCGGKVEGGGGGAGDLQYLAQAMMQSSNYSL

HvLBD31 HORVU.MOREX.r3.7HG0675910.1

MSGSSTSVGVGVGAMLSGSSGGPCGACKFLRRKCTDDCIFAPYFSDSQGVEHFTAVHKVFGASNVSKLLNQTPPKRL
DAAITICYEAKARLRDPAYGCVADIFALQQQVENLQAEVGFHARLRTLQQTSPPPFPSPPYMPMTTEFSISEMASLSNV
PNTIDISSLFDPSMQWAFQQQQEHHQQRHQPCGQTEEGSGGIGNTNSNSGDLQALARELLDRRSTRSTP

REFERENCES

- Aldughpassi, T.M.S. Wolever, E.S.M. Abdel-Aal, 2015. "Barley." *Encyclopedia of Food and Health*: 328-331, <https://doi.org/10.1016/B978-0-12-384947-2.00055-6>.
- Abbe, E. C., and O. L. Stein. 1954. "The Growth of the Shoot Apex in Maize: Embryogeny." *American Journal of Botany* 41 (4): 285. <https://doi.org/10.2307/2438600>.
- Ahmad M. Alqudah. 2015. Developmental and genetic analysis of pre-anthesis phases in barley (*Hordeum vulgare* L.). PhD dissertation. <http://dx.doi.org/10.25673/1519>
- Abbe, E. C., and O. L. Stein. 1954. "The Growth of the Shoot Apex in Maize: Embryogeny." *American Journal of Botany* 41 (4): 285. <https://doi.org/10.2307/2438600>.
- Ahmad Naz, Ali, Alexandra Ehl, Klaus Pillen, and Jens Léon. 2012. "Validation for Root-Related Quantitative Trait Locus Effects of Wild Origin in the Cultivated Background of Barley (*Hordeum Vulgare* L.)." *Plant Breeding* 131 (3): 392–98. <https://doi.org/10.1111/j.1439-0523.2012.01972.x>.
- Akman, Hayati, and Ali Topal. 2014. "Developments of Root Length and Secondary Root of Wheat and Barley in Different Growth Stages." *Turkish Journal of Agricultural and Natural Sciences Special Issue*, no. 1: 830. www.turkjans.com.
- Ali, M. Liakat, Jon Luetchens, Josiel Nascimento, Timothy M. Shaver, Greg R. Kruger, and Aaron J. Lorenz. 2015. "Genetic Variation in Seminal and Nodal Root Angle and Their Association with Grain Yield of Maize under Water-Stressed Field Conditions." *Plant and Soil* 397 (1–2): 213–25. <https://doi.org/10.1007/s11104-015-2554-x>.
- Alqudah, Ahmad M., Ravi Koppolu, Gizaw M. Wolde, Andreas Graner, and Thorsten Schnurbusch. 2016. "The Genetic Architecture of Barley Plant Stature." *Frontiers in Genetics* 7 (JUN): 1–15. <https://doi.org/10.3389/fgene.2016.00117>.
- Anders, Simon, Paul Theodor Pyl, and Wolfgang Huber. 2015. "HTSeq-A Python Framework to Work with High-Throughput Sequencing Data." *Bioinformatics* 31 (2): 166–69. <https://doi.org/10.1093/bioinformatics/btu638>.
- Arifuzzaman, Md, Mohammed A. Sayed, Shumaila Muzammil, Klaus Pillen, Henrik Schumann, Ali Ahmad Naz, and Jens Léon. 2014. "Detection and Validation of Novel QTL for Shoot and Root Traits in Barley (*Hordeum Vulgare* L.)." *Molecular Breeding* 34 (3): 1373–87. <https://doi.org/10.1007/s11032-014-0122-3>.
- Atkinson, Jonathan A., Amanda Rasmussen, Richard Traini, Ute Voß, Craig

- Sturrock, Sacha J. Mooney, Darren M. Wells, and Malcolm J. Bennett. 2014. "Branching out in Roots: Uncovering Form, Function, and Regulation." *Plant Physiology* 166 (2): 538–50. <https://doi.org/10.1104/pp.114.245423>.
- Bai, Tuanhui, Zhidan Dong, Xianbo Zheng, Shangwei Song, Jian Jiao, Miaomiao Wang, and Chunhui Song. 2020. "Auxin and Its Interaction With Ethylene Control Adventitious Root Formation and Development in Apple Rootstock." *Frontiers in Plant Science* 11 (October): 1–14. <https://doi.org/10.3389/fpls.2020.574881>.
- Baik, Byung Kee, and Steven E. Ullrich. 2008. "Barley for Food: Characteristics, Improvement, and Renewed Interest." *Journal of Cereal Science* 48 (2): 233–42. <https://doi.org/10.1016/j.jcs.2008.02.002>.
- Becker, Felix, and Mario Stanke. 2022. "LearnMSA: Learning and Aligning Large Protein Families." *GigaScience* 11: 1–14. <https://doi.org/10.1093/gigascience/giac104>.
- Bellini, Catherine, Daniel I. Pacurar, and Irene Perrone. 2014. "Adventitious Roots and Lateral Roots: Similarities and Differences." *Annual Review of Plant Biology* 65: 639–66. <https://doi.org/10.1146/annurev-arplant-050213-035645>.
- Berckmans, Barbara, Valya Vassileva, Stephan P.C. Schmid, Sara Maes, Boris Parizot, Satoshi Naramoto, Zoltan Magyar, et al. 2011. "Auxin-Dependent Cell Cycle Reactivation through Transcriptional Regulation of Arabidopsis E2Fa by Lateral Organ Boundary Proteins." *Plant Cell* 23 (10): 3671–83. <https://doi.org/10.1105/tpc.111.088377>.
- Blattner, Frank R. 2018. *Taxonomy of the Genus Hordeum and Barley (Hordeum Vulgare)*. Springer International Publishing. https://doi.org/10.1007/978-3-319-92528-8_2.
- Bloh, Kevin, Rohan Kanchana, Pawel Bialk, Kelly Banas, Zugui Zhang, Byung Chun Yoo, and Eric B. Kmiec. 2021. "Deconvolution of Complex DNA Repair (DECODR): Establishing a Novel Deconvolution Algorithm for Comprehensive Analysis of CRISPR-Edited Sanger Sequencing Data." *CRISPR Journal* 4 (1): 120–31. <https://doi.org/10.1089/crispr.2020.0022>.
- Borisjuk, Ljudmilla, Hardy Rolletschek, and Volodymyr Radchuk. 2020. "Advances in the Understanding of Barley Plant Physiology: Factors Determining Grain Development, Composition, and Chemistry," no. February: 53–96. <https://doi.org/10.19103/as.2019.0060.03>.
- Bothmer, Roland von, Kazuhiro Sato, Helmut Knüpfper, and Theo van Hintum. 2003. "Chapter 1 Barley Diversity—an Introduction." *Developments in Plant Genetics and Breeding* 7 (C): 3–8. [https://doi.org/10.1016/S0168-7972\(03\)80003-8](https://doi.org/10.1016/S0168-7972(03)80003-8).
- Bothmer, Roland von, Kazuhiro Sato, Takao Komatsuda, Shozo Yasuda, and

- Gerhard Fischbeck. 2003. *Chapter 2 The Domestication of Cultivated Barley. Developments in Plant Genetics and Breeding*. Vol. 7. Elsevier B.V. [https://doi.org/10.1016/S0168-7972\(03\)80004-X](https://doi.org/10.1016/S0168-7972(03)80004-X).
- Brodersen, Craig R., and Adam B. Roddy. 2016. “New Frontiers in the Three-Dimensional Visualization of Plant Structure and Function.” *American Journal of Botany* 103 (2): 184–88. <https://doi.org/10.3732/ajb.1500532>.
- Bustin, Stephen A., Vladimir Benes, Jeremy A. Garson, Jan Hellemans, Jim Huggett, Mikael Kubista, Reinhold Mueller, et al. 2009. “The MIQE Guidelines: Minimum Information for Publication of Quantitative Real-Time PCR Experiments.” *Clinical Chemistry* 55 (4): 611–22. <https://doi.org/10.1373/clinchem.2008.112797>.
- Cacas, Jean Luc, Martial Pré, Maxime Pizot, Maimouna Cissoko, Issa Diedhiou, Aida Jalloul, Patrick Doumas, Michel Nicole, and Antony Champion. 2017. “GhERF-IIb3 Regulates the Accumulation of Jasmonate and Leads to Enhanced Cotton Resistance to Blight Disease.” *Molecular Plant Pathology* 18 (6): 825–36. <https://doi.org/10.1111/mpp.12445>.
- Cai, Gaochao, and Mutez Ali Ahmed. 2022. “The Role of Root Hairs in Water Uptake: Recent Advances and Future Perspectives.” *Journal of Experimental Botany* 73 (11): 3330–38. <https://doi.org/10.1093/jxb/erac114>.
- Campaign, Smap- Field. 2011. “Crop Identification and BBCH Staging Manual :”
- Cancé, Coralie, Raquel Martin-Arevalillo, Kenza Boubekeur, and Renaud Dumas. 2022. “Auxin Response Factors Are Keys to the Many Auxin Doors.” *New Phytologist* 235 (2): 402–19. <https://doi.org/10.1111/nph.18159>.
- Caroline Marcon , Anja Paschold, and Frank Hochholdinger, and Abstract. 2013. “Genetic Control of Root Organogenesis in Cereals.” *Methods in Molecular Biology* 959 (January): 1–19. <https://doi.org/10.1007/978-1-62703-221-6>.
- Chao, Jiangtao, Zhiyuan Li, Yuhe Sun, Oluwaseun Olayemi Aluko, Xinru Wu, Qian Wang, and Guanshan Liu. 2021. “MG2C: A User-Friendly Online Tool for Drawing Genetic Maps.” *Molecular Horticulture* 1 (1): 1–4. <https://doi.org/10.1186/s43897-021-00020-x>.
- Charlton, WA. 1996. “Lateral Root Initiation.” In *Plant Roots, the Hidden Half, 2nd Ed.*, edited by Y Waisel, A Eshel, and U Kfkaki, 149–73. Marcel Dekker, New York.
- Chen, Huilong, Xiaoming Song, Qian Shang, Shuyan Feng, and Weina Ge. 2022. “CFVisual: An Interactive Desktop Platform for Drawing Gene Structure and Protein Architecture.” *BMC Bioinformatics* 23 (1): 1–9. <https://doi.org/10.1186/s12859-022-04707-w>.
- Chen, Lin, and Yunpeng Liu. 2024. “The Function of Root Exudates in the Root

- Colonization by Beneficial Soil Rhizobacteria.” *Biology* 13 (2): 95. <https://doi.org/10.3390/biology13020095>.
- Chen, Wei Fei, Xiao Bin Wei, Stephane Rety, Ling Yun Huang, Na Nv Liu, Shuo Xing Dou, and Xu Guang Xi. 2019. “Structural Analysis Reveals a ‘Molecular Calipers’ Mechanism for a LATERAL ORGAN BOUNDARIES DOMAIN Transcription Factor Protein from Wheat.” *Journal of Biological Chemistry* 294 (1): 142–56. <https://doi.org/10.1074/jbc.RA118.003956>.
- Chloupek, Oldrich, Brian P. Forster, and William T.B. Thomas. 2006. “The Effect of Semi-Dwarf Genes on Root System Size in Field-Grown Barley.” *Theoretical and Applied Genetics* 112 (5): 779–86. <https://doi.org/10.1007/s00122-005-0147-4>.
- Chow, Chi Nga, Tzong Yi Lee, Yu Cheng Hung, Guan Zhen Li, Kuan Chieh Tseng, Ya Hsin Liu, Po Li Kuo, Han Qin Zheng, and Wen Chi Chang. 2019. “Plantpan3.0: A New and Updated Resource for Reconstructing Transcriptional Regulatory Networks from Chip-Seq Experiments in Plants.” *Nucleic Acids Research* 47 (D1): D1155–63. <https://doi.org/10.1093/nar/gky1081>.
- Christensen, a H, and P H Quail. 1996. “Ubiquitin Promoter-Based Vectors for High-Level Expression of Selectable and/or Screenable Marker Genes in Monocotyledonous Plants.” *Transgenic Research* 5 (3): 213–18. <http://www.ncbi.nlm.nih.gov/pubmed/8673150>.
- Ciais, Ph, M. Reichstein, N. Viovy, A. Granier, J. Ogée, V. Allard, M. Aubinet, et al. 2005. “Europe-Wide Reduction in Primary Productivity Caused by the Heat and Drought in 2003.” *Nature* 437 (7058): 529–33. <https://doi.org/10.1038/nature03972>.
- Collins, Helen M., Rachel A. Burton, David L. Topping, Ming Long Liao, Antony Bacic, and Geoffrey B. Fincher. 2010. “Variability in Fine Structures of Noncellulosic Cell Wall Polysaccharides from Cereal Grains: Potential Importance in Human Health and Nutrition.” *Cereal Chemistry* 87 (4): 272–82. <https://doi.org/10.1094/CCHEM-87-4-0272>.
- Cong, Wen Feng, Ellis Hoffland, Long Li, Johan Six, Jian Hao Sun, Xing Guo Bao, Fu Suo Zhang, and Wopke Van Der Werf. 2015. “Intercropping Enhances Soil Carbon and Nitrogen.” *Global Change Biology* 21 (4): 1715–26. <https://doi.org/10.1111/gcb.12738>.
- Cornelia Marthe , Jochen Kumlehn, and Goetz Hensel. 2015. “Barley (*Hordeum Vulgare* L.) Transformation Using Immature Embryos.” *Methods in Molecular Biology* 1–1223 (Methods in Molecular Biology, vol. 1223): 71–83. <https://doi.org/10.1007/978-1-4939-1695-5>.
- Correa, José, Johannes A. Postma, Michelle Watt, and Tobias Wojciechowski. 2019. “Soil Compaction and the Architectural Plasticity of Root Systems.” *Journal of Experimental Botany* 70 (21): 6019–34. <https://doi.org/10.1093/jxb/erz383>.

- Coudert, Yoan, Martine Bès, Thi Van Anh Le, Martial Pré, Emmanuel Guiderdoni, and Pascal Gantet. 2011. "Transcript Profiling of Crown Rootless1 Mutant Stem Base Reveals New Elements Associated with Crown Root Development in Rice." *BMC Genomics* 4: 1–12.
- Coudert, Yoan, Anne Dievart, Gaetan Droc, and Pascal Gantet. 2013. "ASL/LBD Phylogeny Suggests That Genetic Mechanisms of Root Initiation Downstream of Auxin Are Distinct in Lycophytes and Euphyllophytes." *Molecular Biology and Evolution* 30 (3): 569–72. <https://doi.org/10.1093/molbev/mss250>.
- Coudert, Yoan, Van Anh Thi Le, Hélène Adam, Martine Bès, Florence Vignols, Stefan Jouannic, Emmanuel Guiderdoni, and Pascal Gantet. 2015. "Identification of CROWN ROOTLESS1-Regulated Genes in Rice Reveals Specific and Conserved Elements of Postembryonic Root Formation." *New Phytologist* 206 (1): 243–54. <https://doi.org/10.1111/nph.13196>.
- Coudert, Yoan, Christophe Périn, Brigitte Courtois, Ngan Giang Khong, and Pascal Gantet. 2010. "Genetic Control of Root Development in Rice, the Model Cereal." *Trends in Plant Science* 15 (4): 219–26. <https://doi.org/10.1016/j.tplants.2010.01.008>.
- Coudert, Yoan, Anh Le Thi, and Pascal Gantet. 2013. "Rice: A Model Plant to Decipher the Hidden Origin of Adventitious Roots." *Plant Roots: The Hidden Half, Fourth Edition*, no. July: 145–54. <https://doi.org/10.1201/b14550-15>.
- Dahleen, Lynn S., and Muthusamy Manoharan. 2007. "Recent Advances in Barley Transformation." *In Vitro Cellular and Developmental Biology - Plant* 43 (6): 493–506. <https://doi.org/10.1007/s11627-007-9068-z>.
- Dawson, Ian K., Joanne Russell, Wayne Powell, Brian Steffenson, William T.B. Thomas, and Robbie Waugh. 2015. "Barley: A Translational Model for Adaptation to Climate Change." *New Phytologist* 206 (3): 913–31. <https://doi.org/10.1111/nph.13266>.
- Dharmasiri, Nihal, Sunethra Dharmasiri, and Mark Estelle. 2005. "The F-Box Protein TIR1 Is an Auxin Receptor." *Nature* 435 (7041): 441–45. <https://doi.org/10.1038/nature03543>.
- Dharmasiri, Nihal, and Mark Estelle. 2004. "Auxin Signaling and Regulated Protein Degradation." *Trends in Plant Science* 9 (6): 302–8. <https://doi.org/10.1016/j.tplants.2004.04.003>.
- Doležel, Jaroslav, Johann Greilhuber, and Jan Suda. 2007. "Estimation of Nuclear DNA Content in Plants Using Flow Cytometry." *Nature Protocols* 2 (9): 2233–44. <https://doi.org/10.1038/nprot.2007.310>.
- Dorlodot, Sophie de, Brian Forster, Loïc Pagès, Adam Price, Roberto Tuberosa, and Xavier Draye. 2007. "Root System Architecture: Opportunities and Constraints for Genetic Improvement of Crops." *Trends in Plant Science* 12 (10): 474–81.

<https://doi.org/10.1016/j.tplants.2007.08.012>.

- Evans, Matthew M.S. 2007. “The Indeterminate Gametophyte1 Gene of Maize Encodes a LOB Domain Protein Required for Embryo Sac and Leaf Development.” *Plant Cell* 19 (1): 46–62. <https://doi.org/10.1105/tpc.106.047506>.
- FAO. 2022. *Statistical Year Book : World Food and Agriculture, 2022. World Food and Agriculture – Statistical Yearbook 2022*. Vol. 2022.
- Faye, Awa, Bassirou Sine, Jean Louis Chopart, Alexandre Grondin, Mikael Lucas, Abdala Gamby Diedhiou, Pascal Gantet, et al. 2019. “Development of a Model Estimating Root Length Density from Root Impacts on a Soil Profile in Pearl Millet (*Pennisetum Glaucum* (L.) R. Br). Application to Measure Root System Response to Water Stress in Field Conditions.” *PLoS ONE* 14 (7): 1–18. <https://doi.org/10.1371/journal.pone.0214182>.
- Freire-Rios, Alejandra, Keita Tanaka, Isidro Crespo, Elmar Van der Wijk, Yana Sizontsova, Victor Levitsky, Simon Lindhoud, et al. 2020. “Architecture of DNA Elements Mediating ARF Transcription Factor Binding and Auxin-Responsive Gene Expression in Arabidopsis.” *Proceedings of the National Academy of Sciences of the United States of America* 117 (39): 24557–66. <https://doi.org/10.1073/pnas.2009554117>.
- Fukaki, Hidehiro, Yoko Okushima, and Masao Tasaka. 2007. “Auxin - Mediated Lateral Root Formation in Higher Plants” 256 (07): 111–37. [https://doi.org/10.1016/S0074-7696\(07\)56004-3](https://doi.org/10.1016/S0074-7696(07)56004-3).
- Gao, Yingzhi, and Jonathan P Lynch. 2016. “Reduced Crown Root Number Improves Water Acquisition under Water Deficit Stress in Maize (*Zea Mays* L .)” 67 (15): 4545–57. <https://doi.org/10.1093/jxb/erw243>.
- Geng, Leping, Qi Li, Lele Jiao, Yimeng Xiang, Qiyu Deng, Dao Xiu Zhou, and Yu Zhao. 2023. “WOX11 and CRL1 Act Synergistically to Promote Crown Root Development by Maintaining Cytokinin Homeostasis in Rice.” *New Phytologist* 237 (1): 204–16. <https://doi.org/10.1111/nph.18522>.
- Geng L, Tan M, Deng Q, Wang Y, Zhang T, Hu X, Ye M, Lian X, Zhou DX, Zhao Y (2024). Transcription factors WOX11 and LBD16 function with histone demethylase JMJ706 to control crown root development in rice. *Plant Cell*. <https://doi.org/10.1093/plcell/koad318>.
- Geny, Sylvain, Simon Pichard, Arnaud Poterszman, and Jean Paul Concordet. 2021. “Gene Tagging with the CRISPR-Cas9 System to Facilitate Macromolecular Complex Purification.” *Methods in Molecular Biology* 2305: 153–74. https://doi.org/10.1007/978-1-0716-1406-8_8.
- Giehl, Ricardo F.H., and Nicolaus von Wirén. 2014. “Root Nutrient Foraging.” *Plant Physiology* 166 (2): 509–17. <https://doi.org/10.1104/pp.114.245225>.

- Gonin, Mathieu, Véronique Bergougnoux, Thu D. Nguyen, Pascal Gantet, and Antony Champion. 2019. “What Makes Adventitious Roots?” *Plants* 8 (7): 1–24. <https://doi.org/10.3390/plants8070240>.
- Gonin, Mathieu, Kwanho Jeong, Yoan Coudert, Jeremy Lavarenne, Giang Thi Hoang, Martine Bes, Huong Thi Mai To, et al. 2022. “CROWN ROOTLESS1 Binds DNA with a Relaxed Specificity and Activates OsROP and OsbHLH044 Genes Involved in Crown Root Formation in Rice.” *Plant Journal* 111 (2): 546–66. <https://doi.org/10.1111/tpj.15838>.
- Gou, Jiqing, Steven H. Strauss, Chung Jui Tsai, Kai Fang, Yiru Chen, Xiangning Jiang, and Victor B. Busov. 2010. “Gibberellins Regulate Lateral Root Formation in Populus through Interactions with Auxin and Other Hormones.” *Plant Cell* 22 (3): 623–39. <https://doi.org/10.1105/tpc.109.073239>.
- Gozukirmizi, Nermin, and Elif Karlik. 2017. “Barley (*Hordeum Vulgare* L.) Improvement Past, Present and Future.” *Book: Brewing Technology*. <https://doi.org/10.5772/intechopen.68359>.
- Gregory, Peter J. 2007. *Plant Roots: Growth, Activity and Interaction with Soils*. <https://doi.org/10.1002/9780470995563>.
- Guo, Bao-jian, Jun Wang, Shen Lin, Zheng Tian, Kai Zhou, Hai-ye Luan, Chao Lyu, Xin-zhong Zhang, and Ru-gen Xu. 2016. “A Genome-Wide Analysis of the ASYMMETRIC LEAVES2 / LATERAL ORGAN BOUNDARIES (AS2 / LOB) Gene Family in Barley (*Hordeum Vulgare* L .) *#” 17 (10): 763–74. <https://doi.org/10.1631/jzus.B1500277>.
- Gurr, Geoff M., Zhongxian Lu, Xusong Zheng, Hongxing Xu, Pingyang Zhu, Guihua Chen, Xiaoming Yao, et al. 2016. “Multi-Country Evidence That Crop Diversification Promotes Ecological Intensification of Agriculture.” *Nature Plants* 2 (3): 22–25. <https://doi.org/10.1038/NPLANTS.2016.14>.
- Hall, Benjamin, and Asheesh Lanba. 2019. “Three-Dimensional Analysis of Biological Systems via a Novel Laser Ablation Technique.” *Journal of Laser Applications* 31 (2). <https://doi.org/10.2351/1.5096089>.
- Harris, Jeanne M. 2015. “Abscisic Acid: Hidden Architect of Root System Structure.” *Plants*. MDPI AG. <https://doi.org/10.3390/plants4030548>.
- He, Tianhua, Tefera Tolera Angessa, and Chengdao Li. 2023. “Pleiotropy Structures Plant Height and Seed Weight Scaling in Barley despite Long History of Domestication and Breeding Selection.” *Plant Phenomics* 5: 1–9. <https://doi.org/10.34133/plantphenomics.0015>.
- Hensel, Goetz, Christine Kastner, Sylwia Oleszczuk, Jan Riechen, and Jochen Kumlehn. 2009. “Agrobacterium-Mediated Gene Transfer to Cereal Crop Plants: Current Protocols for Barley, Wheat, Triticale, and Maize.”

- International Journal of Plant Genomics* 2009.
<https://doi.org/10.1155/2009/835608>.
- Herder, Griet Den, Gert Van Isterdael, Tom Beeckman, and Ive De Smet. 2010. “The Roots of a New Green Revolution.” *Trends in Plant Science* 15 (11): 600–607.
<https://doi.org/10.1016/j.tplants.2010.08.009>.
- Himanen, Kristiina, Elodie Boucheron, Steffen Vanneste, Janice De Almeida Engler, Dirk Inzé, and Tom Beeckman. 2002. “Auxin-Mediated Cell Cycle Activation during Early Lateral Root Initiation.” *The Plan* 14 (October): 2339–51.
<https://doi.org/10.1105/tpc.004960.1>.
- Hisano, Hiroshi, Mai Tsujimura, Hideya Yoshida, Toru Terachi, and Kazuhiro Sato. 2016. “Mitochondrial Genome Sequences from Wild and Cultivated Barley (*Hordeum Vulgare*).” *BMC Genomics* 17 (1): 1–12.
<https://doi.org/10.1186/s12864-016-3159-3>.
- Hoang, Diep Thi, Olga Chernomor, Arndt Von Haeseler, Bui Quang Minh, and Le Sy Vinh. 2018. “UFBoot2: Improving the Ultrafast Bootstrap Approximation.” *Molecular Biology and Evolution* 35 (2): 518–22.
<https://doi.org/10.1093/molbev/msx281>.
- Hochholdinger, Frank, Woong June Park, Michaela Sauer, and Katrin Woll. 2004. “From Weeds to Crops: Genetic Analysis of Root Development in Cereals.” *Trends in Plant Science* 9 (1): 42–48.
<https://doi.org/10.1016/j.tplants.2003.11.003>.
- Hochholdinger, Frank, Katrin Woll, Michaela Sauer, and Diana Dembinsky. 2004. “Genetic Dissection of Root Formation in Maize (*Zea Mays*) Reveals Root-Type Specific Developmental Programmes.” *Annals of Botany* 93 (4): 359–68.
<https://doi.org/10.1093/aob/mch056>.
- Hochholdinger, Frank, Peng Yu, and Caroline Marcon. 2018. “Genetic Control of Root System Development in Maize.” *Trends in Plant Science* 23 (1): 79–88.
<https://doi.org/10.1016/j.tplants.2017.10.004>.
- Hodgens, Charles, Zachary L. Nimchuk, and Joseph J. Kieber. 2017. “IndCAPS: A Tool for Designing Screening Primers for CRISPR/Cas9 Mutagenesis Events.” *PLoS ONE* 12 (11): 1–11. <https://doi.org/10.1371/journal.pone.0188406>.
- Holme, Inger Bæksted, Henrik Brinch-Pedersen, Mette Lange, and Preben Bach Holm. 2006. “Transformation of Barley (*Hordeum Vulgare* L.) by *Agrobacterium Tumefaciens* Infection of *in Vitro* Cultured Ovules.” *Plant Cell Reports* 25 (12): 1325–35. <https://doi.org/10.1007/s00299-006-0188-4>.
- Holubová, Katarína, Goetz Hensel, Petr Vojta, Petr Tarkowski, Véronique Bergougnoux, and Petr Galuszka. 2018. “Modification of Barley Plant Productivity through Regulation of Cytokinin Content by Reverse-Genetics Approaches.” *Frontiers in Plant Science* 871 (November): 1–18.

<https://doi.org/10.3389/fpls.2018.01676>.

- Hostetler, Ashley N., Rajdeep S. Khangura, Brian P. Dilkes, and Erin E. Sparks. 2021. "Bracing for Sustainable Agriculture: The Development and Function of Brace Roots in Members of Poaceae." *Current Opinion in Plant Biology* 59: 101985. <https://doi.org/10.1016/j.pbi.2020.101985>.
- Hough, Soren H., Ayokunmi Ajetunmobi, Leigh Brody, Neil Humphryes-Kirilov, and Edward Perello. 2016. "Desktop Genetics." *Personalized Medicine* 13 (6): 517–21. <https://doi.org/10.2217/pme-2016-0068>.
- Hruz, Tomas, Oliver Laule, Gabor Szabo, Frans Wessendorp, Stefan Bleuler, Lukas Oertle, Peter Widmayer, Wilhelm Gruissem, and Philip Zimmermann. 2008. "Genevestigator V3: A Reference Expression Database for the Meta-Analysis of Transcriptomes." *Advances in Bioinformatics* 2008: 1–5. <https://doi.org/10.1155/2008/420747>.
- Hua, Wei, Jinghuan Zhu, Yi Shang, Junmei Wang, Qiaojun Jia, and Jianming Yang. 2015. "Identification of Suitable Reference Genes for Barley Gene Expression Under Abiotic Stresses and Hormonal Treatments." *Plant Molecular Biology Reporter* 33 (4): 1002–12. <https://doi.org/10.1007/s11105-014-0807-0>.
- Humplík, Jan F., Véronique Bergougnoux, and Elizabeth Van Volkenburgh. 2017. "To Stimulate or Inhibit? That Is the Question for the Function of Abscisic Acid." *Trends in Plant Science*. Elsevier Ltd. <https://doi.org/10.1016/j.tplants.2017.07.009>.
- Husbands, Aman, Elizabeth M. Bell, Bin Shuai, Harley M S Smith, and Patricia S. Springer. 2007. "Lateral Organ Boundaries Defines a New Family of DNA-Binding Transcription Factors and Can Interact with Specific BHLH Proteins." *Nucleic Acids Research* 35 (19): 6663–71. <https://doi.org/10.1093/nar/gkm775>.
- Ikeda, A., M. Ueguchi-Tanaka, Y. Sonoda, H. Kitano, M. Koshioka, Y. Futsuhara, M. Matsuoka, and J. Yamaguchi. 2001. "Slender Rice, a Constitutive Gibberellin Response Mutant, Is Caused by a Null Mutation of the SLR1 Gene, an Ortholog of the Height-Regulating Gene GAI/RGA/RHT/D8." *Plant Cell* 13 (5): 999–1010. <https://doi.org/10.1105/tpc.13.5.999>.
- International, The, Barley Genome, and Sequencing Consortium. 2012. "A Physical , Genetic and Functional Sequence Assembly of the Barley Genome." *Nature* 491 (7426): 711–16. <https://doi.org/10.1038/nature11543>.
- Inukai, Y. 2005. "Crown Rootless1, Which Is Essential for Crown Root Formation in Rice, Is a Target of an AUXIN RESPONSE FACTOR in Auxin Signaling." *The Plant Cell Online* 17 (5): 1387–96. <https://doi.org/10.1105/tpc.105.030981>.
- Itoh, Jun-Ichi, Ken-Ichi Nonomura, Kyoko Ikeda, Shinichiro Yamaki, Yoshiaki Inukai, Hiroshi Yamagishi, Hidemi Kitano, and Yasuo Nagato. 2005. "Rice Plant Development: From Zygote to Spikelet." *Plant & Cell Physiology* 46 (1):

23–47. <https://doi.org/10.1093/pcp/pci501>.

- Jaganathan, Deepa, Karthikeyan Ramasamy, Gothandapani Sellamuthu, Shilpha Jayabalan, and Gayatri Venkataraman. 2018. “CRISPR for Crop Improvement: An Update Review.” *Frontiers in Plant Science* 9 (July): 1–17. <https://doi.org/10.3389/fpls.2018.00985>.
- Jansen, Leentje, Ianto Roberts, Riet De Rycke, and Tom Beeckman. 2012. “Phloem-Associated Auxin Response Maxima Determine Radial Positioning of Lateral Roots in Maize.” *Philosophical Transactions of the Royal Society of London. Series B, Biological Sciences* 367 (1595): 1525–33. <https://doi.org/10.1098/rstb.2011.0239>.
- Jia, Zhongtao, Ying Liu, Benjamin D. Gruber, Kerstin Neumann, Benjamin Kilian, Andreas Graner, and Nicolaus von Wirén. 2019. “Genetic Dissection of Root System Architectural Traits in Spring Barley.” *Frontiers in Plant Science* 10 (April): 1–14. <https://doi.org/10.3389/fpls.2019.00400>.
- Jin, Jinpu, Feng Tian, De Chang Yang, Yu Qi Meng, Lei Kong, Jingchu Luo, and Ge Gao. 2017. “PlantTFDB 4.0: Toward a Central Hub for Transcription Factors and Regulatory Interactions in Plants.” *Nucleic Acids Research* 45 (D1): D1040–45. <https://doi.org/10.1093/nar/gkw982>.
- Jinek, Martin, Krzysztof Chylinski, Ines Fonfara, Michael Hauer, Jennifer A Doudna, and Emmanuelle Charpentier. 2012. “A Programmable Dual-RNA – Guided” 337 (August): 816–22.
- Kang, Na Young, Han Woo Lee, and Jungmook Kim. 2013. “The AP2/EREBP Gene PUCHI Co-Acts with LBD16/ASL18 and LBD18/ASL20 Downstream of ARF7 and ARF19 to Regulate Lateral Root Development in Arabidopsis.” *Plant and Cell Physiology* 54 (8): 1326–34. <https://doi.org/10.1093/pcp/pct081>.
- Khong, Giang Ngan, Pratap Kumar Pati, Frédérique Richaud, Boris Parizot, Przemyslaw Bidzinski, Chung Duc Mai, Martine Bès, et al. 2015. “OsMADS26 Negatively Regulates Resistance to Pathogens and Drought Tolerance in Rice.” *Plant Physiology*, no. September 2016: pp.01192.2015. <https://doi.org/10.1104/pp.15.01192>.
- Kidwai, Maria, Priyanka Mishra, and Catherine Bellini. 2023. “Species-Specific Transcriptional Reprogramming during Adventitious Root Initiation.” *Trends in Plant Science* 28 (2): 128–30. <https://doi.org/10.1016/j.tplants.2022.11.003>.
- Kim, Dae Sung, Nak Hyun Kim, and Byung Kook Hwang. 2015. “The Capsicum Annuum Class IV Chitinase ChitIV Interacts with Receptor-like Cytoplasmic Protein Kinase PIK1 to Accelerate PIK1-Triggered Cell Death and Defence Responses.” *Journal of Experimental Botany* 66 (7): 1987–99. <https://doi.org/10.1093/jxb/erv001>.
- Kim, Daehwan, Geo Perteua, Cole Trapnell, Harold Pimentel, Ryan Kelley, and

- Steven L. Salzberg. 2013. “TopHat2: Accurate Alignment of Transcriptomes in the Presence of Insertions, Deletions and Gene Fusions.” *Genome Biology* 14 (4). <https://doi.org/10.1186/gb-2013-14-4-r36>.
- Kitomi, Yuka, Eiko Hanzawa, Noriyuki Kuya, Haruhiko Inoue, Naho Hara, Sawako Kawai, Noriko Kanno, et al. 2020. “Root Angle Modifications by the DRO1 Homolog Improve Rice Yields in Saline Paddy Fields.” *Proceedings of the National Academy of Sciences of the United States of America* 117 (35): 21242–50. <https://doi.org/10.1073/pnas.2005911117>.
- Kitomi, Yuka, Hiroki Inahashi, Hinako Takehisa, Yutaka Sato, and Yoshiaki Inukai. 2012. “OsIAA13-Mediated Auxin Signaling Is Involved in Lateral Root Initiation in Rice.” *Plant Science* 190: 116–22. <https://doi.org/10.1016/j.plantsci.2012.04.005>.
- Kitomi, Yuka, Hiroko Ito, Tokunori Hobo, Koichiro Aya, Hidemi Kitano, and Yoshiaki Inukai. 2011. “The Auxin Responsive AP2/ERF Transcription Factor CROWN ROOTLESS5 Is Involved in Crown Root Initiation in Rice through the Induction of OsRR1, a Type-A Response Regulator of Cytokinin Signaling.” *Plant Journal* 67 (3): 472–84. <https://doi.org/10.1111/j.1365-313X.2011.04610.x>.
- Kitomi, Yuka, Atsushi Ogawa, Hidemi Kitano, and Yoshiaki Inukai. 2008. “CRL4 Regulates Crown Root Formation through Auxin Transport in Rice.” *Plant Root* 2: 19–28. <https://doi.org/10.3117/plantrout.2.19>.
- Klie, Sebastian, and Zoran Nikoloski. 2012. “The Choice between MapMan and Gene Ontology for Automated Gene Function Prediction in Plant Science.” *Frontiers in Genetics* 3 (JUN): 1–14. <https://doi.org/10.3389/fgene.2012.00115>.
- Komatsuda, Takao, Mohammad Pourkheirandish, Congfen He, Perumal Azhaguvel, Kiroyuki Kanamori, Dragan Perovic, Nils Stein, et al. 2007. “Six-Rowed Barley Originated from a Mutation in a Homeodomain-Leucine Zipper I-Class Homeobox Gene.” *Proceedings of the National Academy of Sciences of the United States of America* 104 (4): 1424–29. <https://doi.org/10.1073/pnas.0608580104>.
- Kořínková, Nikola, Irene M. Fontana, Thu D. Nguyen, Pouneh Pouramini, Véronique Bergougnoux, and Goetz Hensel. 2022. “Enhancing Cereal Productivity by Genetic Modification of Root Architecture.” *Biotechnology Journal* 17 (7): 1–13. <https://doi.org/10.1002/biot.202100505>.
- Kücke, M., H. Schmid, and A. Spiess. 1995. “A Comparison of Four Methods for Measuring Roots of Field Crops in Three Contrasting Soils.” *Plant and Soil* 172 (1): 63–71. <https://doi.org/10.1007/BF00020860>.
- Kumlehn, Jochen, Liliya Serazetdinova, Goetz Hensel, Dirk Becker, and Horst Loerz. 2006. “Genetic Transformation of Barley (*Hordeum Vulgare* L.) via Infection of Androgenetic Pollen Cultures with *Agrobacterium Tumefaciens*.”

- Plant Biotechnology Journal* 4 (2): 251–61. <https://doi.org/10.1111/j.1467-7652.2005.00178.x>.
- LANDES, A., and J. R. PORTER. 1989. “Comparison of Scales Used for Categorising the Development of Wheat, Barley, Rye and Oats.” *Annals of Applied Biology* 115 (2): 343–60. <https://doi.org/10.1111/j.1744-7348.1989.tb03393.x>.
- Large, E. C. 1954. “Growth Stages in Cereals Illustration of the Feekes Scale.” *Plant Pathology* 3 (4): 128–29. <https://doi.org/10.1111/j.1365-3059.1954.tb00716.x>.
- Lavarenne, Jérémy, Mathieu Gonin, Soazig Guyomarc’h, Jacques Rouster, Antony Champion, Christophe Sallaud, Laurent Laplaze, Pascal Gantet, and Mikaël Lucas. 2019. “Inference of the Gene Regulatory Network Acting Downstream of CROWN ROOTLESS 1 in Rice Reveals a Regulatory Cascade Linking Genes Involved in Auxin Signaling, Crown Root Initiation, and Root Meristem Specification and Maintenance.” *Plant Journal*, 954–68. <https://doi.org/10.1111/tpj.14487>.
- Lazzeri, P. A. 1995. “Stable Transformation of Barley via Direct DNA Uptake. Electroporation- and PEG-Mediated Protoplast Transformation.” *Methods in Molecular Biology (Clifton, N.J.)* 49: 95–106. <https://doi.org/10.1385/0-89603-321-x:95>.
- LeClere, Sherry, Rosie Tellez, Rebekah A. Rampey, Seiichi P T Matsuda, and Bonnie Bartel. 2002. “Characterization of a Family of IAA-Amino Acid Conjugate Hydrolases from Arabidopsis.” *Journal of Biological Chemistry* 277 (23): 20446–52. <https://doi.org/10.1074/jbc.M111955200>.
- Lee, Han Woo, Chuloh Cho, Shashank K. Pandey, Yoona Park, Min Jung Kim, and Jungmook Kim. 2019. “LBD16 and LBD18 Acting Downstream of ARF7 and ARF19 Are Involved in Adventitious Root Formation in Arabidopsis.” *BMC Plant Biology* 19 (1): 1–11. <https://doi.org/10.1186/s12870-019-1659-4>.
- Lee, Han Woo, Na Young Kang, Shashank K. Pandey, Chuloh Cho, Sung Haeng Lee, and Jungmook Kim. 2017. “Dimerization in LBD16 and LBD18 Transcription Factors Is Critical for Lateral Root Formation.” *Plant Physiology* 174 (1): 301–11. <https://doi.org/10.1104/pp.17.00013>.
- Lee, Han Woo, and Jungmook Kim. 2013. “EXPANSINA17 Up-Regulated by LBD18/ASL20 Promotes Lateral Root Formation during the Auxin Response.” *Plant and Cell Physiology* 54 (10): 1600–1611. <https://doi.org/10.1093/pcp/pct105>.
- Lee, Han Woo, Min-jung Kim, Nan Young Kim, Sung Haeng Lee, and Jungmook Kim. 2013. “LBD18 Acts as a Transcriptional Activator That Directly Binds to the EXPANSIN14 Promoter in Promoting Lateral Root Emergence of Arabidopsis” 16: 212–24. <https://doi.org/10.1111/tpj.12013>.

- Li, Anchang, Lingxiao Zhu, Wenjun Xu, Liantao Liu, and Guifa Teng. 2022. "Recent Advances in Methods for in Situ Root Phenotyping." *PeerJ* 10: 1–29. <https://doi.org/10.7717/peerj.13638>.
- Li, Chaonan, Jingyi Wang, Long Li, Jialu Li, Mengjia Zhuang, Bo Li, Qiaoru Li, et al. 2022. "TaMOR Is Essential for Root Initiation and Improvement of Root System Architecture in Wheat." *Plant Biotechnology Journal* 20 (5): 862–75. <https://doi.org/10.1111/pbi.13765>.
- Li, Juan, Yunyuan Xu, and Kang Chong. 2012. "The Novel Functions of Kinesin Motor Proteins in Plants." *Protoplasma* 249 (SUPPL.2): 95–100. <https://doi.org/10.1007/s00709-011-0357-3>.
- Li, Tingting, Jianxin Bian, Minqiang Tang, Hongbin Shanguan, Yan Zeng, Ruihan Luo, Huifan Sun, et al. 2022. "BGFD: An Integrated Multi-Omics Database of Barley Gene Families." *BMC Plant Biology* 22 (1): 1–11. <https://doi.org/10.1186/s12870-022-03846-9>.
- Li, Xiaogang, Alexandre Jousset, Wietse de Boer, Víctor J. Carrión, Taolin Zhang, Xingxiang Wang, and Eiko E. Kuramae. 2019. "Legacy of Land Use History Determines Reprogramming of Plant Physiology by Soil Microbiome." *ISME Journal* 13 (3): 738–51. <https://doi.org/10.1038/s41396-018-0300-0>.
- Li, Xinxin, Rensen Zeng, and Hong Liao. 2016. "Improving Crop Nutrient Efficiency through Root Architecture Modifications." *Journal of Integrative Plant Biology* 58 (3): 193–202. <https://doi.org/10.1111/jipb.12434>.
- Liu, Hongjia, Shoufeng Wang, Xiaobo Yu, Jie Yu, Xiaowei He, Shelong Zhang, Huixia Shou, and Ping Wu. 2005. "ARL1, a LOB-Domain Protein Required for Adventitious Root Formation in Rice." *Plant Journal* 43 (1): 47–56. <https://doi.org/10.1111/j.1365-313X.2005.02434.x>.
- Liu, Shiping, Jirong Wang, Lu Wang, Xiaofei Wang, Yanhong Xue, Ping Wu, and Huixia Shou. 2009. "Adventitious Root Formation in Rice Requires OsGNOM1 and Is Mediated by the OsPINs Family." *Cell Research* 19 (9): 1110–19. <https://doi.org/10.1038/cr.2009.70>.
- Liu, Yehe, Andrew M. Rollins, Richard M. Levenson, Farzad Fereidouni, and Michael W. Jenkins. 2021. "Pocket MUSE: An Affordable, Versatile and High-Performance Fluorescence Microscope Using a Smartphone." *Communications Biology* 4 (1): 1–14. <https://doi.org/10.1038/s42003-021-01860-5>.
- Liu, Zhaojun, Ricardo Fabiano Hettwer Giehl, Anja Hartmann, Mohammad Reza Hajirezaei, Sebastien Carpentier, and Nicolaus von Wirén. 2021. "Seminal and Nodal Roots of Barley Differ in Anatomy, Proteome and Nitrate Uptake Capacity." *Plant and Cell Physiology* 61 (7): 1297–1308. <https://doi.org/10.1093/PCP/PCAA059>.
- Lo, Shuen Fang, Show Ya Yang, Ku Ting Chen, Yue Ie Hsing, Jan A.D. Zeevaart,

- Liang Jwu Chen, and Su May Yu. 2008. “A Novel Class of Gibberellin 2-Oxidases Control Semidwarfism, Tillering, and Root Development in Rice.” *Plant Cell* 20 (10): 2603–18. <https://doi.org/10.1105/tpc.108.060913>.
- Lobet, Guillaume, Michael P. Pound, Julien Diener, Christophe Pradal, Xavier Draye, Christophe Godin, Mathieu Javaux, et al. 2015. “Root System Markup Language: Toward a Unified Root Architecture Description Language.” *Plant Physiology* 167 (3): 617–27. <https://doi.org/10.1104/pp.114.253625>.
- Lohse, Marc, Axel Nagel, Thomas Herter, Patrick May, Michael Schroda, Rita Zrenner, Takayuki Tohge, Alisdair R. Fernie, Mark Stitt, and Björn Usadel. 2014. “Mercator: A Fast and Simple Web Server for Genome Scale Functional Annotation of Plant Sequence Data.” *Plant, Cell and Environment* 37 (5): 1250–58. <https://doi.org/10.1111/pce.12231>.
- Lone, Ajaz A., Mudasir H. Khan, Zahoor A. Dar, and Shabir H. Wani. 2016. “Breeding Strategies for Improving Growth and Yield under Waterlogging Conditions in Maize: A Review.” *Maydica* 61 (1): 1–11.
- López-Bucio, José, Alfredo Cruz-Ramírez, and Luis Herrera-Estrella. 2003. “The Role of Nutrient Availability in Regulating Root Architecture.” *Current Opinion in Plant Biology* 6 (3): 280–87. [https://doi.org/10.1016/S1369-5266\(03\)00035-9](https://doi.org/10.1016/S1369-5266(03)00035-9).
- Love, Michael I., Wolfgang Huber, and Simon Anders. 2014. “Moderated Estimation of Fold Change and Dispersion for RNA-Seq Data with DESeq2.” *Genome Biology*. <https://doi.org/10.1186/s13059-014-0550-8>.
- Lucob-Agustin, Nonawin, Tsubasa Kawai, Mana Kano-Nakata, Roel R. Suralta, Jonathan M. Niones, Tomomi Hasegawa, Mayuko Inari-Ikeda, Akira Yamauchi, and Yoshiaki Inukai. 2021. “Morpho-Physiological and Molecular Mechanisms of Phenotypic Root Plasticity for Rice Adaptation to Water Stress Conditions.” *Breeding Science* 71 (1): 20–29. <https://doi.org/10.1270/jsbbs.20106>.
- Lupas, Andrei, Marc Van Dyke, and Jeff Stock. 1991. “Predicting Coiled Coils from Protein Sequences.” *Science* 252 (5009): 1162–64. <https://doi.org/10.1126/science.252.5009.1162>.
- Luxovx, Maria. 1986. “The Seminal Root Primordia in Barley and the Participation of Their Non-Meristematic Cells in Root Construction.” *Biologia Plantarum (Praha)* 28 (3): 161–67.
- Lynch JP (2007) Roots of the second green revolution. *Aust J Bot* 55: 493–512. <https://doi.org/10.1071/BT06118>
- Lynch, Jonathan P. 2013. “Steep, Cheap and Deep: An Ideotype to Optimize Water and N Acquisition by Maize Root Systems.” *Annals of Botany* 112 (2): 347–57. <https://doi.org/10.1093/aob/mcs293>.

- Lynch, Jonathan P., Christopher F. Strock, Hannah M. Schneider, Jagdeep Singh Sidhu, Ishan Ajmera, Tania Galindo-Castañeda, Stephanie P. Klein, and Meredith T. Hanlon. 2021a. *Root Anatomy and Soil Resource Capture*. *Plant and Soil*. Vol. 466. Springer International Publishing. <https://doi.org/10.1007/s11104-021-05010-y>.
- Mai, C D, N T P Phung, H T M To, M Gonin, G T Hoang, K L Nguyen, V N Do, B Courtois, and P Gantet. 2014. “Genes Controlling Root Development in Rice.” *Rice* 7 (30): 1–11. <https://doi.org/10.1186/s12284-014-0030-5>.
- Majer, Christine, and Frank Hochholdinger. 2011. “Defining the Boundaries: Structure and Function of LOB Domain Proteins.” *Trends in Plant Science* 16 (1): 47–52. <https://doi.org/10.1016/j.tplants.2010.09.009>.
- Majer, Christine, Changzheng Xu, Kenneth W. Berendzen, and Frank Hochholdinger. 2012. “Molecular Interactions of Rootless Concerning Crown and Seminal Roots, a LOB Domain Protein Regulating Shoot-Borne Root Initiation in Maize (*Zea Mays* L.)” *Philosophical Transactions of the Royal Society B: Biological Sciences* 367 (1595): 1542–51. <https://doi.org/10.1098/rstb.2011.0238>.
- Makowska, B., B. Bakera, and M. Rakoczy-Trojanowska. 2015. “The Genetic Background of Benzoxazinoid Biosynthesis in Cereals.” *Acta Physiologiae Plantarum*. Polish Academy of Sciences, Institute of Slavic Studies. <https://doi.org/10.1007/s11738-015-1927-3>.
- Maqbool, Saman, Muhammad Adeel Hassan, Xianchun Xia, Larry M. York, Awais Rasheed, and Zhonghu He. 2022. “Root System Architecture in Cereals: Progress, Challenges and Perspective.” *Plant Journal* 110 (1): 23–42. <https://doi.org/10.1111/tpj.15669>.
- Mascher, Martin, Heidrun Gundlach, Axel Himmelbach, Sebastian Beier, Sven O. Twardziok, Thomas Wicker, Volodymyr Radchuk, et al. 2017. “A Chromosome Conformation Capture Ordered Sequence of the Barley Genome.” *Nature* 544 (7651): 427–33. <https://doi.org/10.1038/nature22043>.
- Mascher, Martin, Gary J. Muehlbauer, Daniel S. Rokhsar, Jarrod Chapman, Jeremy Schmutz, Kerrie Barry, María Muñoz-Amatriaín, et al. 2013. “Anchoring and Ordering NGS Contig Assemblies by Population Sequencing (POPSEQ).” *Plant Journal* 76 (4): 718–27. <https://doi.org/10.1111/tpj.12319>.
- Mascher, Martin, Thomas Wicker, Jerry Jenkins, Christopher Plott, Thomas Lux, Chu Shin Koh, Jennifer Ens, et al. 2021. “Long-Read Sequence Assembly: A Technical Evaluation in Barley.” *Plant Cell* 33 (6): 1888–1906. <https://doi.org/10.1093/plcell/koab077>.
- Mayer, Klaus F.X., Mihaela Martis, Pete E. Hedley, Hana Šimková, Hui Liu, Jenny A. Morris, Burkhard Steuernagel, et al. 2011. “Unlocking the Barley Genome by Chromosomal and Comparative Genomics.” *Plant Cell* 23 (4): 1249–63.

- <https://doi.org/10.1105/tpc.110.082537>.
- Meng, Funing, Dan Xiang, Jianshu Zhu, Yong Li, and Chuanzao Mao. 2019. “Molecular Mechanisms of Root Development in Rice.” *Rice* 12 (1): 1–10. <https://doi.org/10.1186/s12284-018-0262-x>.
- Mergemann, H., and M. Sauter. 2000. “Ethylene Induces Epidermal Cell Death at the Site of Adventitious Root Emergence in Rice.” *Plant Physiology* 124 (2): 609–14. <https://doi.org/10.1104/pp.124.2.609>.
- Metsalu, Tauno, and Jaak Vilo. 2015. “ClustVis: A Web Tool for Visualizing Clustering of Multivariate Data Using Principal Component Analysis and Heatmap.” *Nucleic Acids Research* 43 (W1): W566–70. <https://doi.org/10.1093/nar/gkv468>.
- Michael W. Pfaffl. 2001. “A New Mathematical Model for Relative Quantification in Real-Time RT–PCR.” *Nucleic Acids Res* 29 (9): e45. <https://doi.org/10.1111/j.1365-2966.2012.21196.x>.
- Middleton, Christopher P., Nils Stein, Beat Keller, Benjamin Kilian, and Thomas Wicker. 2013. “Comparative Analysis of Genome Composition in Triticeae Reveals Strong Variation in Transposable Element Dynamics and Nucleotide Diversity.” *Plant Journal* 73 (2): 347–56. <https://doi.org/10.1111/tpj.12048>.
- Miki, Brian, and Sylvia McHugh. 2004. “Selectable Marker Genes in Transgenic Plants: Applications, Alternatives and Biosafety.” *Journal of Biotechnology* 107 (3): 193–232. <https://doi.org/10.1016/j.jbiotec.2003.10.011>.
- Milne, Linda, Micha Bayer, Paulo Rapazote-Flores, Claus Dieter Mayer, Robbie Waugh, and Craig G. Simpson. 2021. “EORNA, a Barley Gene and Transcript Abundance Database.” *Scientific Data* 8 (1): 1–10. <https://doi.org/10.1038/s41597-021-00872-4>.
- Milner, Sara G., Matthias Jost, Shin Taketa, Elena Rey Mazón, Axel Himmelbach, Markus Oppermann, Stephan Weise, et al. 2019. “Genebank Genomics Highlights the Diversity of a Global Barley Collection.” *Nature Genetics* 51 (2): 319–26. <https://doi.org/10.1038/s41588-018-0266-x>.
- Monat, Cécile, Sudharsan Padmarasu, Thomas Lux, Thomas Wicker, Heidrun Gundlach, Axel Himmelbach, Jennifer Ens, et al. 2019. “TRITEX: Chromosome-Scale Sequence Assembly of Triticeae Genomes with Open-Source Tools.” *Genome Biology* 20 (1): 1–18. <https://doi.org/10.1186/s13059-019-1899-5>.
- Moreno-Risueno MA, Van Norman JM, Moreno A, Zhang J, Ahnert SE, Benfey PN. 2010. “Oscillating Gene Expression Determines Competence for Periodic Arabidopsis Root Branching.” *Science* 329 (1306–11): 1–12. <https://doi.org/10.1126/science.1191937.Oscillating>.

- Morita, Miyo T., Chieko Saito, Akihiko Nakano, and Masao Tasaka. 2007. "Endodermal-Amyloplast Less 1 Is a Novel Allele of SHORT-ROOT." *Advances in Space Research* 39 (7): 1127–33. <https://doi.org/10.1016/j.asr.2006.12.020>.
- Muthreich, Nils, Christine Majer, Mary Beatty, Anja Paschold, André Schützenmeister, Yan Fu, Waqas Ahmed Malik, et al. 2013. "Comparative Transcriptome Profiling of Maize Coleoptilar Nodes during Shoot-Borne Root Initiation." *Plant Physiology* 163 (1): 419–30. <https://doi.org/10.1104/pp.113.221481>.
- Nadolska-Orczyk, Anna, Izabela K. Rajchel, Waław Orczyk, and Sebastian Gasparis. 2017. "Major Genes Determining Yield-Related Traits in Wheat and Barley." *Theoretical and Applied Genetics* 130 (6): 1081–98. <https://doi.org/10.1007/s00122-017-2880-x>.
- Naz, Ali Ahmad, Md Arifuzzaman, Shumaila Muzammil, Klaus Pillen, and Jens Léon. 2014. "Wild Barley Introgression Lines Revealed Novel QTL Alleles for Root and Related Shoot Traits in the Cultivated Barley (*Hordeum Vulgare* L.)." *BMC Genetics* 15 (1): 1–12. <https://doi.org/10.1186/s12863-014-0107-6>.
- Nevo, E., A. Ordentlich, A. Beiles, and I. Ràskin. 1992. "Genetic Divergence of Heat Production within and between the Wild Progenitors of Wheat and Barley: Evolutionary and Agronomical Implications." *Theoretical and Applied Genetics* 84 (7–8): 958–62. <https://doi.org/10.1007/BF00227410>.
- Newton, Adrian Clive, Andrew J. Flavell, Timothy S. George, Philip Leat, Barry Mullholland, Luke Ramsay, Cesar Revoredo-Giha, et al. 2011. "Crops That Feed the World 4. Barley: A Resilient Crop? Strengths and Weaknesses in the Context of Food Security." *Food Security* 3 (2): 141–78. <https://doi.org/10.1007/s12571-011-0126-3>.
- Nguyen, Lam Tung, Heiko A. Schmidt, Arndt Von Haeseler, and Bui Quang Minh. 2015. "IQ-TREE: A Fast and Effective Stochastic Algorithm for Estimating Maximum-Likelihood Phylogenies." *Molecular Biology and Evolution* 32 (1): 268–74. <https://doi.org/10.1093/molbev/msu300>.
- Ni, Jun, Gaohang Wang, Zhenxing Zhu, Huanhuan Zhang, Yunrong Wu, and Ping Wu. 2011. "OsIAA23-Mediated Auxin Signaling Defines Postembryonic Maintenance of QC in Rice." *Plant Journal* 68 (3): 433–42. <https://doi.org/10.1111/j.1365-313X.2011.04698.x>.
- Ohashi-Ito, Kyoko, Kuninori Iwamoto, and Hiroo Fukuda. 2018. "LOB DOMAIN-CONTAINING PROTEIN 15 Positively Regulates Expression of VND7, a Master Regulator of Tracheary Elements." *Plant and Cell Physiology* 59 (5): 989–96. <https://doi.org/10.1093/pcp/pcy036>.
- Okushima, Yoko, Hidehiro Fukaki, Makoto Onoda, Athanasios Theologis, and Masao Tasaka. 2007. "ARF7 and ARF19 Regulate Lateral Root Formation via

- Direct Activation of LBD/ASL Genes in Arabidopsis.” *Plant Cell* 19 (1): 118–30. <https://doi.org/10.1105/tpc.106.047761>.
- Omary, Moutasem, Naama Gil-Yarom, Chen Yahav, Evyatar Steiner, Anat Hendelman, and Idan Efroni. 2022. “A Conserved Superlocus Regulates Above- and Belowground Root Initiation.” *Science* 375 (6584). <https://doi.org/10.1126/science.abf4368>.
- Orman-Ligeza, Beata, Boris Parizot, Pascal P Gantet, Tom Beeckman, Malcolm J Bennett, and Xavier Draye. 2013. “Post-Embryonic Root Organogenesis in Cereals: Branching out from Model Plants.” *Trends in Plant Science* 18 (8): 459–67. <https://doi.org/10.1016/j.tplants.2013.04.010>.
- Paez-Garcia, Ana, Christy M. Motes, Wolf Rüdiger Scheible, Rujin Chen, Elison B. Blancaflor, and Maria J. Monteros. 2015. “Root Traits and Phenotyping Strategies for Plant Improvement.” *Plants* 4 (2): 334–55. <https://doi.org/10.3390/plants4020334>.
- Pallotta, M. A., R. D. Graham, P. Langridge, D. H.B. Sparrow, and S. J. Barker. 2000. “RFLP Mapping of Manganese Efficiency in Barley.” *Theoretical and Applied Genetics* 101 (7): 1100–1108. <https://doi.org/10.1007/s001220051585>.
- Park, Woong June, Frank Hochholdinger, and Alfons Gierl. 2004. “Release of the Benzoxazinoids Defense Molecules during Lateral- and Crown Root Emergence in Zea Mays.” *Journal of Plant Physiology* 161 (8): 981–85. <https://doi.org/10.1016/j.jplph.2004.01.005>.
- Pasam, Raj K., Rajiv Sharma, Alexander Walther, Hakan Özkan, Andreas Graner, and Benjamin Kilian. 2014. “Genetic Diversity and Population Structure in a Legacy Collection of Spring Barley Landraces Adapted to a Wide Range of Climates.” *PLoS ONE* 9 (12): 1–29. <https://doi.org/10.1371/journal.pone.0116164>.
- Passarinho, Paul A., and Sacco C. de Vries. 2002. “Arabidopsis Chitinases : A Genomic Survey .” *The Arabidopsis Book* 1 (January): e0023. <https://doi.org/10.1199/tab.0023>.
- Passot, Sixtine, Fatoumata Gnacko, Daniel Moukouanga, Mikaël Lucas, Soazig Guyomarc’h, Beatriz Moreno Ortega, Jonathan A. Atkinson, et al. 2016. “Characterization of Pearl Millet Root Architecture and Anatomy Reveals Three Types of Lateral Roots.” *Frontiers in Plant Science* 7 (June2016): 1–11. <https://doi.org/10.3389/fpls.2016.00829>.
- Péret, Benjamin, Bert De Rybel, Ilda Casimiro, Eva Benková, Ranjan Swarup, Laurent Laplaze, Tom Beeckman, and Malcolm J. Bennett. 2009. “Arabidopsis Lateral Root Development: An Emerging Story.” *Trends in Plant Science* 14 (7): 399–408. <https://doi.org/10.1016/j.tplants.2009.05.002>.
- Perrot-Rechenmann, Catherine. 2010. “Cellular Responses to Auxin: Division versus

- Expansion.” *Cold Spring Harbor Perspectives in Biology* 2 (5): 1–15. <https://doi.org/10.1101/cshperspect.a001446>.
- Porco, Silvana, Antoine Larrieu, Yajuan Du, Allison Gaudinier, Tatsuaki Goh, Kamal Swarup, Ranjan Swarup, et al. 2016. “Lateral Root Emergence in Arabidopsis Is Dependent on Transcription Factor LBD29 Regulation of Auxin Influx Carrier LAX3.” *Development (Cambridge)* 143 (18): 3340–49. <https://doi.org/10.1242/dev.136283>.
- Ramireddy, Eswarayya, Seyed A. Hosseini, Kai Eggert, Sabine Gillandt, Heike Gnad, Nicolaus von Wirén, and Thomas Schmülling. 2018. “Root Engineering in Barley: Increasing Cytokinin Degradation Produces a Larger Root System, Mineral Enrichment in the Shoot and Improved Drought Tolerance.” *Plant Physiology* 177 (3): 1078–95. <https://doi.org/10.1104/pp.18.00199>.
- Rampey, R. A., Rosie Tellez, R. A. Rampey, Seiichi P T Matsuda, and Bartel. 2004. “A Family of Auxin-Conjugate Hydrolases That Contributes to Free Indole-3-Acetic Acid Levels during Arabidopsis Germination.” *Plant Physiology* 135 (2): 978–88. <https://doi.org/10.1104/pp.104.039677>.
- Reinhard Töpfer, Volker Matzeit, Bruno Gronenborn, Jozef Schell and Hans-Henning Steinbiss. 1987. “A Set of Plant Expression Vectors for Transcriptional and Translational Fusions.” *Nucleic Acids Research* 15 (14): 5890.
- RIAZ, Asad, Ahmad M. ALQUDAH, Farah KANWAL, Klaus PILLEN, Ling zhen YE, Fei DAI, and Guo ping ZHANG. 2023. “Advances in Studies on the Physiological and Molecular Regulation of Barley Tillering.” *Journal of Integrative Agriculture* 22 (1): 1–13. <https://doi.org/10.1016/j.jia.2022.08.011>.
- Rich, Sarah M., and Michelle Watt. 2013. “Soil Conditions and Cereal Root System Architecture: Review and Considerations for Linking Darwin and Weaver.” *Journal of Experimental Botany* 64 (5): 1193–1208. <https://doi.org/10.1093/jxb/ert043>.
- Robinson, Hannah, Lee Hickey, Cecile Richard, Emma Mace, Alison Kelly, Andrew Borrell, Jerome Franckowiak, and Glen Fox. 2016. “Genomic Regions Influencing Seminal Root Traits in Barley.” *The Plant Genome* 9 (1): 1–13. <https://doi.org/10.3835/plantgenome2015.03.0012>.
- Robinson, Hannah, Alison Kelly, Glen Fox, Jerome Franckowiak, Andrew Borrell, and Lee Hickey. 2018. “Root Architectural Traits and Yield: Exploring the Relationship in Barley Breeding Trials.” *Euphytica* 214 (9): 1–16. <https://doi.org/10.1007/s10681-018-2219-y>.
- Rostamza, M., R. A. Richards, and M. Watt. 2013. “Response of Millet and Sorghum to a Varying Water Supply around the Primary and Nodal Roots.” *Annals of Botany* 112 (2): 439–46. <https://doi.org/10.1093/aob/mct099>.
- Roycewicz, Peter S., and Jocelyn E. Malamy. 2014. “Cell Wall Properties Play an

- Important Role in the Emergence of Lateral Root Primordia from the Parent Root.” *Journal of Experimental Botany* 65 (8): 2057–69.
<https://doi.org/10.1093/jxb/eru056>.
- Saengwilai, Patompong, Xiaoli Tian, and Jonathan Paul Lynch. 2014. “Low Crown Root Number Enhances Nitrogen Acquisition from Low-Nitrogen Soils in Maize.” *Plant Physiology* 166 (2): 581–89.
<https://doi.org/10.1104/pp.113.232603>.
- Sallaud, C., D. Meynard, J. Van Boxtel, C. Gay, M. Bès, J. P. Brizard, P. Larmande, et al. 2003. “Highly Efficient Production and Characterization of T-DNA Plants for Rice (*Oryza Sativa* L.) Functional Genomics.” *Theoretical and Applied Genetics* 106 (8): 1396–1408. <https://doi.org/10.1007/s00122-002-1184-x>.
- Samarah, N. H., A. M. Alqudah, J. A. Amayreh, and G. M. McAndrews. 2009. “The Effect of Late-Terminal Drought Stress on Yield Components of Four Barley Cultivars.” *Journal of Agronomy and Crop Science* 195 (6): 427–41.
<https://doi.org/10.1111/j.1439-037X.2009.00387.x>.
- Sato, Kazuhiro. 2020. “History and Future Perspectives of Barley Genomics.” *DNA Research* 27 (4): 1–8. <https://doi.org/10.1093/dnares/dsaa023>.
- Schindelin, Johannes, Ignacio Arganda-Carreras, Erwin Frise, Verena Kaynig, Mark Longair, Tobias Pietzsch, Stephan Preibisch, et al. 2012. “Fiji: An Open-Source Platform for Biological-Image Analysis.” *Nature Methods* 9 (7): 676–82.
<https://doi.org/10.1038/nmeth.2019>.
- Schmid, Karl, Benjamin Kilian, and Joanne Russell. 2018. *Barley Domestication, Adaptation and Population Genomics*. Springer International Publishing.
https://doi.org/10.1007/978-3-319-92528-8_17.
- Schreiber, Miriam, Martin Mascher, Jonathan Wright, Sudharasan Padmarasu, Axel Himmelbach, Darren Heavens, Linda Milne, Bernardo J. Clavijo, Nils Stein, and Robbie Waugh. 2020. “A Genome Assembly of the Barley ‘Transformation Reference’ Cultivar Golden Promise.” *G3: Genes, Genomes, Genetics* 10 (6): 1823–27. <https://doi.org/10.1534/g3.119.401010>.
- Schulte, Daniela, Timothy J. Close, Andreas Graner, Peter Langridge, Takashi Matsumoto, Gary Muehlbauer, Kazuhiro Sato, et al. 2009. “The International Barley Sequencing Consortium - At the Threshold of Efficient Access to the Barley Genome.” *Plant Physiology* 149 (1): 142–47.
<https://doi.org/10.1104/pp.108.128967>.
- Schwacke, Rainer, Gabriel Y. Ponce-Soto, Kirsten Krause, Anthony M. Bolger, Borjana Arsova, Asis Hallab, Kristina Gruden, Mark Stitt, Marie E. Bolger, and Björn Usadel. 2019. “MapMan4: A Refined Protein Classification and Annotation Framework Applicable to Multi-Omics Data Analysis.” *Molecular Plant* 12 (6): 879–92. <https://doi.org/10.1016/j.molp.2019.01.003>.

- Sebastian, Jose, Muh Ching Yee, Willian Goudinho Viana, Rubén Rellán-Álvarez, Max Feldman, Henry D. Priest, Charlotte Trontin, et al. 2016. “Grasses Suppress Shoot-Borne Roots to Conserve Water during Drought.” *Proceedings of the National Academy of Sciences of the United States of America* 113 (31): 8861–66. <https://doi.org/10.1073/pnas.1604021113>.
- Sekiya, Nobuhito, Fumitaka Shiotsu, Jun Abe, and Shigenori Morita. 2013. “Distribution and Quantity of Root Systems of Field-Grown Erianthus and Napier Grass.” *American Journal of Plant Sciences* 04 (12): 16–22. <https://doi.org/10.4236/ajps.2013.412a1003>.
- SHA, Xiao qian, Hong hui GUAN, Yu qian ZHOU, Er hu SU, Jian GUO, Yong xiang LI, Deng feng ZHANG, et al. 2023. “Genetic Dissection of Crown Root Traits and Their Relationships with Aboveground Agronomic Traits in Maize.” *Journal of Integrative Agriculture* 22 (11): 3394–3407. <https://doi.org/10.1016/j.jia.2023.04.022>.
- Shaaf, Salar, Gianluca Bretani, Abhisek Biswas, Irene Maria Fontana, and Laura Rossini. 2019. “Genetics of Barley Tiller and Leaf Development.” *Journal of Integrative Plant Biology* 61 (3): 226–56. <https://doi.org/10.1111/jipb.12757>.
- Shashidhar, He. 2012. *Methodologies for Root Drought Studies in Rice*. <http://books.google.com/books?hl=en&lr=&id=1kkAHUiBJGsC&oi=fnd&pg=PR5&dq=Methodologies+for+root+drought+studies+in+rice&ots=GCLLLhWPnP&sig=l4pdzF9gMUNdrDfIY8br3dKXh3w>.
- Shekhar V., Stöckle D., Thellmann M., Vermeer J.E.M. 2019. “The role of plant root systems in evolutionary adaptation Curr. Top. Dev. Biol., 131, pp. 55-80. <https://doi.org/10.1016/bs.ctdb.2018.11.011>
- Shelden, Megan C., and Rana Munns. 2023. “Crop Root System Plasticity for Improved Yields in Saline Soils.” *Frontiers in Plant Science* 14 (February): 1–14. <https://doi.org/10.3389/fpls.2023.1120583>.
- Shuai, Bin, Cristina G Reynaga-pen, and Patricia S Springer. 2002. “The LATERAL ORGAN BOUNDARIES Gene Defines a Novel, Plant-Specific Gene Family.” *Society* 129 (June): 747–61. <https://doi.org/10.1104/pp.010926.1>.
- Smith, S., and I. De Smet. 2012. “Root System Architecture: Insights from Arabidopsis and Cereal Crops.” *Philosophical Transactions of the Royal Society B: Biological Sciences* 367 (1595): 1441–52. <https://doi.org/10.1098/rstb.2011.0234>.
- Sparks, Erin E. 2023. “Maize Plants and the Brace Roots That Support Them.” *New Phytologist* 237 (1): 48–52. <https://doi.org/10.1111/nph.18489>.
- Steffens, Bianka, Alexander Kovalev, Stanislav N. Gorb, and Margret Sauter. 2012. “Emerging Roots Alter Epidermal Cell Fate through Mechanical and Reactive Oxygen Species Signaling.” *Plant Cell* 24 (8): 3296–3306.

<https://doi.org/10.1105/tpc.112.101790>.

- Steffens, Bianka, and Margret Sauter. 2009. "Epidermal Cell Death in Rice Is Confined to Cells with a Distinct Molecular Identity and Is Mediated by Ethylene and H₂O₂ through an Autoamplified Signal Pathway." *Plant Cell* 21 (1): 184–96. <https://doi.org/10.1105/tpc.108.061887>.
- Steingrobe, B., H. Schmid, and N. Claassen. 2001. "Root Production and Root Mortality of Winter Barley and Its Implication with Regard to Phosphate Acquisition." *Plant and Soil* 237 (2): 239–48. <https://doi.org/10.1023/A:1013345718414>.
- Strock, Christopher F., Hannah M. Schneider, Tania Galindo-Castañeda, Benjamin T. Hall, Bart Van Gansbeke, Diane E. Mather, Mitchell G. Roth, et al. 2019. "Laser Ablation Tomography for Visualization of Root Colonization by Edaphic Organisms." *Journal of Experimental Botany* 70 (19): 5327–42. <https://doi.org/10.1093/jxb/erz271>.
- Strock, Christopher F., Hannah M. Schneider, and Jonathan P. Lynch. 2022. "Anatomics: High-Throughput Phenotyping of Plant Anatomy." *Trends in Plant Science* 27 (6): 520–23. <https://doi.org/10.1016/j.tplants.2022.02.009>.
- Sullivan, Paul, Elke Arendt, and Eimear Gallagher. 2013. "The Increasing Use of Barley and Barley By-Products in the Production of Healthier Baked Goods." *Trends in Food Science and Technology* 29 (2): 124–34. <https://doi.org/10.1016/j.tifs.2012.10.005>.
- Sutter, Valerie De, Rudy Vanderhaeghen, Sofie Tilleman, Freya Lammertyn, Isabelle Vanhoutte, Mansour Karimi, Dirk Inzé, Alain Goossens, and Pierre Hilsen. 2005. "Exploration of Jasmonate Signalling via Automated and Standardized Transient Expression Assays in Tobacco Cells." *Plant Journal* 44 (6): 1065–76. <https://doi.org/10.1111/j.1365-313X.2005.02586.x>.
- Swarup, Kamal, Eva Benková, Ranjan Swarup, Ilda Casimiro, Benjamin Péret, Yaodong Yang, Geraint Parry, et al. 2008. "The Auxin Influx Carrier LAX3 Promotes Lateral Root Emergence" 10 (8). <https://doi.org/10.1038/ncb1754>.
- Takahashi, Hideyuki, and Tom K. Scott. 1991. "Hydrotropism and Its Interaction with Gravitropism in Maize Roots." *Plant Physiology* 96 (2): 558–64. <https://doi.org/10.1104/pp.96.2.558>.
- Takahashi, Hirokazu, and Christophe Pradal. 2021. "Root Phenotyping: Important and Minimum Information Required for Root Modeling in Crop Plants." *Breeding Science* 71 (1): 109–16. <https://doi.org/10.1270/jsbbs.20126>.
- Tamura, Koichiro, Glen Stecher, and Sudhir Kumar. 2021. "MEGA11: Molecular Evolutionary Genetics Analysis Version 11." *Molecular Biology and Evolution* 38 (7): 3022–27. <https://doi.org/10.1093/molbev/msab120>.

- Tan, Xu, Luz Irina A. Calderon-Villalobos, Michal Sharon, Changxue Zheng, Carol V. Robinson, Mark Estelle, and Ning Zheng. 2007. "Mechanism of Auxin Perception by the TIR1 Ubiquitin Ligase." *Nature* 446 (7136): 640–45. <https://doi.org/10.1038/nature05731>.
- Taner, Akar, Avci Muzaffer, and Dusunceli Fazil. 2004. "Barley: Post-Harvest Operations." *Food and Agriculture Organization of the United Nations*, 1–64. <http://www.fao.org/3/a-au997e.pdf>.
- Taramino, Graziana, Michaela Sauer, Jay L. Stauffer, Dilbag Multani, Xiaomu Niu, Hajime Sakai, and Frank Hochholdinger. 2007. "The Maize (*Zea Mays* L.) RTCS Gene Encodes a LOB Domain Protein That Is a Key Regulator of Embryonic Seminal and Post-Embryonic Shoot-Borne Root Initiation." *Plant Journal* 50 (4): 649–59. <https://doi.org/10.1111/j.1365-313X.2007.03075.x>.
- Thiel, Thomas, Raja Kota, Ivo Grosse, Nils Stein, and Andreas Graner. 2004. "SNP2CAPS: A SNP and INDEL Analysis Tool for CAPS Marker Development." *Nucleic Acids Research* 32 (1): 1–5. <https://doi.org/10.1093/nar/gnh006>.
- Thimm, Oliver, Oliver Bläsing, Yves Gibon, Axel Nagel, Svenja Meyer, Peter Krüger, Joachim Selbig, Lukas A. Müller, Seung Y. Rhee, and Mark Stitt. 2004. "MAPMAN: A User-Driven Tool to Display Genomics Data Sets onto Diagrams of Metabolic Pathways and Other Biological Processes." *Plant Journal* 37 (6): 914–39. <https://doi.org/10.1111/j.1365-313X.2004.02016.x>.
- Toki, Seiichi, Naho Hara, Kazuko Ono, Haruko Onodera, Akemi Tagiri, Seibi Oka, and Hiroshi Tanaka. 2006. "Early Infection of Scutellum Tissue with *Agrobacterium* Allows High-Speed Transformation of Rice." *The Plant Journal: For Cell and Molecular Biology* 47 (6): 969–76. <https://doi.org/10.1111/j.1365-313X.2006.02836.x>.
- Tong, Cen, Camilla Beate Hill, Gaofeng Zhou, Xiao Qi Zhang, Yong Jia, and Chengdao Li. 2021. "Opportunities for Improving Waterlogging Tolerance in Cereal Crops—Physiological Traits and Genetic Mechanisms." *Plants* 10 (8): 1–22. <https://doi.org/10.3390/plants10081560>.
- Uga, Yusaku, Yuka Kitomi, Satoru Ishikawa, and Masahiro Yano. 2015. "Genetic Improvement for Root Growth Angle to Enhance Crop Production." *Breeding Science* 65 (2): 111–19. <https://doi.org/10.1270/jsbbs.65.111>.
- Uga, Yusaku, Kazuhiko Sugimoto, Satoshi Ogawa, Jagadish Rane, Manabu Ishitani, Naho Hara, Yuka Kitomi, et al. 2013. "Control of Root System Architecture by DEEPER ROOTING 1 Increases Rice Yield under Drought Conditions." *Nature Genetics* 45 (9): 1097–1102. <https://doi.org/10.1038/ng.2725>.
- Valenzuela, Hector, Jody Smith, Tropical Plant, and Natural Resources. 2002. "Barley." *The College of Tropical Agriculture and Human Resources (CTAHR)*, 2–4. www.turkjans.com.

- Vandesompele, Jo, Katleen De Preter, Filip Pattyn, Bruce Poppe, Nadine Van Roy, Anne De Paepe, and Frank Speleman. 2002. "Accurate Normalization of Real-Time Quantitative RT-PCR Data by Geometric Averaging of Multiple Internal Control Genes." *Genome Biology* 3 (7). <https://doi.org/10.1007/s00603-018-1496-z>.
- Vlamiš, J., and D. E. Williams. 1962. "Ion Competition in Manganese Uptake by Barley Plants." *Plant Physiology* 37 (5): 650–55. <https://doi.org/10.1104/pp.37.5.650>.
- Voss-Fels, Kai P., Hannah Robinson, Stephen R. Mudge, Cecile Richard, Saul Newman, Benjamin Wittkop, Andreas Stahl, et al. 2018. "VERNALIZATION1 Modulates Root System Architecture in Wheat and Barley." *Molecular Plant* 11 (1): 226–29. <https://doi.org/10.1016/j.molp.2017.10.005>.
- Voss-Fels, Kai P., Rod J. Snowdon, and Lee T. Hickey. 2018. "Designer Roots for Future Crops." *Trends in Plant Science* 23 (11): 957–60. <https://doi.org/10.1016/j.tplants.2018.08.004>.
- Vyroubalová, Š, M. Šmehilová, P. Galuszka, and L. Ohnoutková. 2011. "Genetic Transformation of Barley: Limiting Factors." *Biologia Plantarum* 55 (2): 213–24. <https://doi.org/10.1007/s10535-011-0032-8>.
- Walia, Harkamal, Clyde Wilson, Pascal Condamine, Abdelbagi M. Ismail, Jin Xu, Xinping Cui, and Timothy J. Close. 2007. "Array-Based Genotyping and Expression Analysis of Barley Cv. Maythorpe and Golden Promise." *BMC Genomics* 8: 1–14. <https://doi.org/10.1186/1471-2164-8-87>.
- Wallsten, Johanna, and Kjell Martinsson. 2009. "Effects of Maturity Stage and Feeding Strategy of Whole Crop Barley Silage on Intake, Digestibility and Milk Production in Dairy Cows." *Livestock Science* 121 (2–3): 155–61. <https://doi.org/10.1016/j.livsci.2008.06.004>.
- Wang, Lingling, Mengxue Guo, Yong Li, Wenyuan Ruan, Xiaorong Mo, Zhongchang Wu, Craig J. Sturrock, et al. 2018. "LARGE ROOT ANGLE1, Encoding OsPIN2, Is Involved in Root System Architecture in Rice." *Journal of Experimental Botany* 69 (3): 385–97. <https://doi.org/10.1093/jxb/erx427>.
- Weaver, J.E., F.C. Jean and J.W. Crist. 1922. "Development and Activities of Roots of Crop Plants; a Study in Crop Ecology,." *Agronomy and Horticulture -- Faculty Publications*, 511. <https://doi.org/10.5962/bhl.title.79313>.
- Xie, Fuliang, Peng Xiao, Dongliang Chen, Lei Xu, and Baohong Zhang. 2012. "MiRDeepFinder: A MiRNA Analysis Tool for Deep Sequencing of Plant Small RNAs." *Plant Molecular Biology* 80 (1): 75–84. <https://doi.org/10.1007/s11103-012-9885-2>.
- Xu, Changzheng, Feng Luo, and Frank Hochholdinger. 2016. "LOB Domain Proteins: Beyond Lateral Organ Boundaries." *Trends in Plant Science* 21 (2):

- 159–67. <https://doi.org/10.1016/j.tplants.2015.10.010>.
- Xu, Changzheng, Huanhuan Tai, Muhammad Saleem, Yvonne Ludwig, Christine Majer, Kenneth W. Berendzen, Kerstin A. Nagel, et al. 2015. “Cooperative Action of the Paralogous Maize Lateral Organ Boundaries (LOB) Domain Proteins RTCS and RTCL in Shoot-Borne Root Formation.” *New Phytologist* 207 (4): 1123–33. <https://doi.org/10.1111/nph.13420>.
- Xu, Jian, and Jing Han Hong. 2013. “Root Development: Genetics and Genomics of Rice.” *Plant Genetics and Genomics: Crops and Models* 5, 297–316. <https://doi.org/10.1007/978-1-4614-7903-1>.
- Xu, Lin, Yi Xu, Aiwu Dong, Yue Sun, Limin Pi, Yuquan Xu, and Hai Huang. 2003. “Novel As1 and As2 Defects in Leaf Adaxial-Abaxial Polarity Reveal the Requirement for ASYMMETRIC LEAVES1 and 2 and ERECTA Functions in Specifying Leaf Adaxial Identity.” *Development* 130 (17): 4097–4107. <https://doi.org/10.1242/dev.00622>.
- Yang, Tony, Kadambot H.M. Siddique, and Kui Liu. 2020. “Cropping Systems in Agriculture and Their Impact on Soil Health-A Review.” *Global Ecology and Conservation* 23: e01118. <https://doi.org/10.1016/j.gecco.2020.e01118>.
- Yoo, Sang Dong, Young Hee Cho, and Jen Sheen. 2007. “Arabidopsis Mesophyll Protoplasts: A Versatile Cell System for Transient Gene Expression Analysis.” *Nature Protocols* 2 (7): 1565–72. <https://doi.org/10.1038/nprot.2007.199>.
- Zarei, Adel, Ana Paula Körbes, Parisa Younessi, Gregory Montiel, Antony Champion, and Johan Memelink. 2011. “Two GCC Boxes and AP2/ERF-Domain Transcription Factor ORA59 in Jasmonate/Ethylene-Mediated Activation of the PDF1.2 Promoter in Arabidopsis.” *Plant Molecular Biology* 75 (4–5): 321–31. <https://doi.org/10.1007/s11103-010-9728-y>.
- Zhan, Ai, and Jonathan P. Lynch. 2015. “Reduced Frequency of Lateral Root Branching Improves N Capture from Low-N Soils in Maize.” *Journal of Experimental Botany* 66 (7): 2055–65. <https://doi.org/10.1093/jxb/erv007>.
- Zhang, Qifa, and Rod A. Wing. 2013. “Genetics and Genomics of Rice.” *Genetics and Genomics of Rice*, no. July 2013: 1–402. <https://doi.org/10.1007/978-1-4614-7903-1>.
- Zhang, Yuwen, Ziwen Li, Biao Ma, Quancan Hou, and Xiangyuan Wan. 2020. “Phylogeny and Functions of LOB Domain Proteins in Plants.” *International Journal of Molecular Sciences* 21 (7). <https://doi.org/10.3390/ijms21072278>.
- Zheng, Yi, Chen Jiao, Honghe Sun, Hernan G. Rosli, Marina A. Pombo, Peifen Zhang, Michael Banf, et al. 2016. “ITAK: A Program for Genome-Wide Prediction and Classification of Plant Transcription Factors, Transcriptional Regulators, and Protein Kinases.” *Molecular Plant* 9 (12): 1667–70. <https://doi.org/10.1016/j.molp.2016.09.014>.

- Zhou, Yaping, Mauritz Leonard Sommer, and Frank Hochholdinger. 2021. “Cold Response and Tolerance in Cereal Roots.” *Journal of Experimental Botany* 72 (21): 7474–81. <https://doi.org/10.1093/jxb/erab334>.
- Zhu, Zhen Xing, Yu Liu, Shao Jun Liu, Chuan Zao Mao, Yun Rong Wu, and Ping Wu. 2012. “A Gain-of-Function Mutation in OsIAA11 Affects Lateral Root Development in Rice.” *Molecular Plant* 5 (1): 154–61. <https://doi.org/10.1093/mp/ssr074>.

CURRICULUM VITAE

PERSONAL DATA

Surname and first name: Nguyen, Dieu Thu

Title: M.sc

Place and date of birth: Hanoi – Vietnam, the 10th November, 1989

Nationality: Vietnamese

Email: thu.nguyen01@upol.cz

EDUCATION

01.2017 – PRESENT

Full-time PhD student in Department of Biochemistry, Faculty of Science, Palacký University Olomouc, Czech Republic.

Research topic: Initiation and development of crown roots in barley (*Hordeum vulgare* L.): genetic investigation and comparison with rice, the plant model for cereals.

Supervisor: Dr. Véronique Bergougnoux; Consultant: Prof. Pascal Gantet.

09.2012 – 09.2014

Master of Science student in Biotechnology – Pharmacology Department, University of Science and Technology of Hanoi (USTH) – Vietnam France University, Hanoi, Vietnam. (USTH relates to authorization of the Université de Montpellier, Aix-Marseille University, Université Claude-Bernard-Lyon-I, which issued the master diplomas with levels within the framework of the European Higher Education Area).

Research topic: Establishment of binary plasmid constructs for functional analysis of a *LRR-RLK* gene from *Oryza sativa*.

Supervisor: Dr. JOUANNIC Stéphane - UMR DIADE – IRD, Montpellier, France

06.2007 – 06.2011

Engineer in Biotechnology, Biotechnology Department, Hanoi Open University, Hanoi, Vietnam.

EMPLOYMENT

01.2017 - 06.2024

Researcher at Plant Genetics and Engineering research group, Czech Advanced Technology and Research Institute, Palacký University Olomouc, Czech Republic

SCHOLARSHIP

J. L. Fischer Scholarship to foreign doctoral students (2017-2020), Faculty of Science, Palacký University, Olomouc, Czech Republic.

CONFERENCE PRESENTATIONS

Kim Nhung Ta, Thi Loan Ha, **Thu Nguyen Dieu**, Thi Hoang Giang, Duc chung Mai, Thu Phuong Nhung Phung, Thu Hoai Tran, Brigitte Courtois, Pascal Gantet, Michel Lebrun, Nang Vinh Do, Stephane Jouannic 2016. Genome-wide association mapping for yield-related traits in a Vietnamese landrace rice collection. P2.12 - 14th International Symposium on Rice Functional Genomics (ISRFG), 26 – 29 September 2016, Le Corum, Montpellier, France.

Nguyen DT, Pantet P, Bergougnoux V. 2017. LATERAL ORGAN BOUNDARIES-DOMAIN protein of barley (*Hordeum vulgare* L.): role during crown-root initiation and regulation by auxin. Green For Good IV, 19-22 June 2017, Olomouc, Czech Republic.

Nguyen Dieu Thu, Mathieu Gonin, Lavarenne Jeremy, Myriam Collin, Gantet Pascal, Bergougnoux Veronique 2018. Anatomical and molecular dissection of crown-root initiation in barley (*Hordeum vulgare* L.). Green For Good V, 10 - 13 June 2019, Olomouc, Czech Republic.

Nguyen D.T., Kořínková N., Gonin M., Champion A., Gantet P., Bergougnoux V. 2019. A dissection of genetic and molecular mechanism regulating the initiation of crown root in barley (*Hordeum vulgare* L.). XXIII Meeting of the Spanish Society of Plant Physiology/XVI Spanish Portuguese Congress of Plant Physiology Pamplona, 26 - 28 June 2019.

Nguyen D.T., Gonin M, Hensel G., Gantet P., Bergougnoux V. 2021. Role of LBD transcription factors in initiation of crown-roots in barley (*Hordeum vulgare* L.).

International plant systems biology (iPSB), the second EMBO workshop, 26-27 April 2021, Virtual.

Nguyen D.T., Kokáš F., Techer A., Hensel G., Gantet P., Bergounoux V. 2021. Understanding crown-roots development in barley (*Hordeum vulgare* L.), the first step towards the production of crops with enhanced root architectural traits. European Federation of biotechnology (EFB) 2021 – Virtual conference, 10 – 14 May 2021.

Nguyen D.T., Gonin M, Hensel G., Gantet P., Bergounoux V. 2021. Role of LOB-domain proteins in crown-root initiation and development in barley (*Hordeum vulgare* L.). The 8th International Symposium about root structure and function. June 12-16, 2022, High Tatras, Horný Smokovec, Slovakia.

Nguyen D.T., Kovačik M., Pečinka A., Gantet P., Bergounoux V. 2022. Crown Root Inducible System as a method to study transcript profiling of crown root initiation in barley (*Hordeum vulgare* L.). Green For Good VI, 12 – 15 September 2022, Olomouc, Czech Republic.

PUBLICATIONS

TA Kim Nhung, KHONG Ngan Giang, HA Thi Loan, **NGUYEN Dieu Thu**, MAI Duc Chung, HOANG Thi Giang, PHUNG Thi Phuong Nhung, BOURRIE Isabelle, COURTOIS Brigitte, TRAN Thu Hoai, DINH Bach Yen, LA Tuan Nghia, DO Nang Vinh, LEBRUN Michel, GANTET Pascal, JOUANNIC Stefan. “A genome-wide association study using a Vietnamese landrace panel of rice (*Oryza sativa*) reveals new QTLs controlling panicle morphological traits”. BMC Plant Biology (2018) 18:282.

Mathieu Gonin, Véronique Bergounoux, **Thu D. Nguyen**, Pascal Gantet and Antony Champion. “What Makes Adventitious Roots? A review”. Plants 2019, 8, 240; doi:10.3390/plants8070240

Kořínková N*, Fontana IM*, **Nguyen TD***, Pouramini P, Bergounoux V, Hensel G. “Enhancing cereal productivity by genetic modification of root architecture – a review” Biotechnol. J. 2022;2100505. <https://doi.org/10.1002/biot.202100505>.

* all 3 authors participate equally as first author to the manuscript preparation.

Mortaza Khodaeiaminjan, Dominic Knoch, Marie Rose Ndella Thiaw, Cintia F. Marchetti, Nikola Kořínková, Alexie Techer, **Thu D. Nguyen**, Jianting Chu, Valentin Bertholomey, Ingrid Doridant, Pascal Gantet, Andreas Graner, Kerstin Neumann, Veronique Bergougnoux. “Genome-wide association study in two-row spring barley landraces identifies QTLs associated with plantlets root system architecture traits in well-watered and osmotic stress conditions”. *Front. Plant Sci.*, 03 April 2023. Sec. Plant Development and EvoDevo Volume 14 – 2023. <https://doi.org/10.3389/fpls.2023.1125672>

MANUSCRIPTS UNDER THE REVIEW

Thu Dieu Nguyen, Filip Zavadil Kokáš, Mathieu Gonin, Jérémy Lavarenne, Myriam Colin, Pascal Gantet, and Véronique Bergougnoux. Transcriptional changes during crown-root development and emergence in barley (*Hordeum vulgare* L.). *BMC Plant biology*.

The article manuscript was submitted to *BMC Plant Biology* on 16 June 2023 UTC and resubmitted the revision on 9 April 2024 UTC. Ref: Submission ID 1ffd5ce6-d5b2-4f97-ba8d-622c47e46026. It is currently under the second reviewing.

Thu Dieu Nguyen, Mathieu Gonin, Michal Motyka, Antony Champion, Goetz Hensel, Pascal Gantet, Véronique Bergougnoux. Two lateral organ boundary domain transcription factors HvCRL1 and HvCRL1-1L regulate shoot-borne root formation in barley (*Hordeum vulgare* L.).

The article manuscript was submitted to *BMC Plant Biology* on 17 April 2024 UTC *Journal of Plant Growth Regulation*. It is currently under peer review.

COURSE ATTENTION

Attending a workshop on Real-Time PCR, including qbase+ hand-on data analysis. This workshop had been organized by SEQme, Dobris in Brno, Czech Republic on November 8 – 9, 2018.

SUPPLEMENT 1

Review article.

Mathieu Gonin, Véronique Bergounoux, **Thu D. Nguyen**, Pascal Gantet and Antony Champion. “What Makes Adventitious Roots? A review”. *Plants* 2019, 8, 240; doi:10.3390/plants8070240

SUPPLEMENT 2

Review article.

Kořínková N*, Fontana IM*, Nguyen TD*, Pouramini P, Bergougnoux V, Hensel G.
“Enhancing cereal productivity by genetic modification of root architecture – a
review” *Biotechnol. J.* 2022;2100505. <https://doi.org/10.1002/biot.202100505>.

* all 3 authors participate equally as first author to the manuscript preparation.

SUPPLEMENT 3

Research article.

Mortaza Khodaeiaminjan, Dominic Knoch, Marie Rose Ndella Thiaw, Cintia F. Marchetti, Nikola Kořínková, Alexie Techer, **Thu D. Nguyen**, Jianting Chu, Valentin Bertholomey, Ingrid Doridant, Pascal Gantet, Andreas Graner, Kerstin Neumann, Veronique Bergougnoux. “Genome-wide association study in two-row spring barley landraces identifies QTLs associated with plantlets root system architecture traits in well-watered and osmotic stress conditions”. *Front. Plant Sci.*, 03 April 2023. *Sec. Plant Development and EvoDevo* Volume 14 – 2023. <https://doi.org/10.3389/fpls.2023.1125672>

SUPPLEMENT 4

Research article (under reviewing)

Thu Dieu Nguyen, Filip Zavadil Kokáš, Mathieu Gonin, Jérémy Lavarenne, Myriam Colin, Pascal Gantet, and Véronique Bergounoux. Transcriptional changes during crown-root development and emergence in barley (*Hordeum vulgare* L.). *BMC Plant biology*.

The article manuscript was submitted to *BMC Plant Biology* on 16 June 2023 UTC and resubmitted the revision on 9 April 2024 UTC. Ref: Submission ID 1ffd5ce6-d5b2-4f97-ba8d-622c47e46026. It is currently under the second reviewing.

SUPPLEMENT 5

Research article (under reviewing)

Thu Dieu Nguyen, Mathieu Gonin, Michal Motyka, Antony Champion, Goetz Hensel, Pascal Gantet, Véronique Bergounoux. Two lateral organ boundary domain transcription factors HvCRL1 and HvCRL1-1L regulate shoot-borne root formation in barley (*Hordeum vulgare* L.).

The article manuscript was submitted to BMC Plant Biology on 17 April 2024 UTC Journal of Plant Growth Regulation. It is currently under peer review.

PALACKÝ UNIVERSITY IN OLOMOUC

Faculty of Science

Department of Biochemistry



Initiation and development of crown roots in barley

(Hordeum vulgare L.)

Summary of Ph.D Thesis

Author:	Dieu Thu Nguyen, M.Sc.
Study Program:	P1416 Biochemistry
Form of Studies:	Full-time
Supervisor:	Véronique H�elene Bergougnoux-Fojt�ık, Ph.D.
Consultant:	prof. Pascal Gantet

Olomouc 2024

This Ph.D. thesis has been completed within the framework of the Ph.D. study program P1416 Biochemistry and done at the Czech Advanced Technology and Research Institute-Centre of the Region Haná (CATRIN-CRH), Palacký University in Olomouc, under the supervision of Dr. Véronique H elene Bergougnoux-Fojt ık in the period 2017-2024.

Ph.D. candidate **Dieu Thu Nguyen, M.Sc.**

¹Department of Biochemistry,
Faculty of Science, Palacký University Olomouc
Šlechtitelů 27, 78371 Olomouc, Czech Republic

²Czech Advanced Technology and Research Institute
Centre of the Haná Region for Biotechnological and
Agricultural Research, Palacký University Olomouc,
Šlechtitelů 241/27, 77900 Olomouc, Czech Republic.

Supervisor **V eronique H elene Bergougnoux-Fojt ık, Ph.D.**

Czech Advanced Technology and Research Institute,
Centre of the Haná Region for Biotechnological and
Agricultural Research, Palacký University Olomouc,
Šlechtitelů 241/27, 77900 Olomouc, Czech Republic.

Reviewers

This summary of the Ph.D. thesis has been sent out on

The oral defense will take place at the Faculty of Science, Šlechtitelů 27, Olomouc on.....

The Ph.D. thesis is available at the biology branch in the Library in Holic, Šlechtitelů 27, Olomouc.

Prof. Mgr. Marek Petřivalský, Dr.
Chairman of the Committee for Ph.D. thesis
Faculty of Science, Palacký University
Olomouc

Acknowledgments

I would like to express my greatest gratitude to my doctoral supervisor, Dr. Véronique Héline Bergougnoux-Fojtík for accepting my doctoral work, her expert guidance, and important constructive suggestions as well as kind support and great correction during my PhD studies. I would like to express my sincere gratitude to my doctoral consultant, Prof. Dr. Pascal Gantet for his kindness, encouragement, and great patience in dedicating his valuable time to discussing and supporting me in my scientific career.

I would like to give my gratitude to Prof. Mgr. Marek Petřivalský, Dr. for his willingness to support me to finish my long Ph.D study.

I would like to thank all my colleagues at the Palacký University Olomouc, especially at the barley research group, who supported and encouraged me in my research. I would particularly thank to Cintia and Yuliya. They are not only my excellent senior colleagues in science, but also great friends for the life in Czech Republic. I would like to especially thank: Nikola, Betka, David K., Alexi, Carlos for accompanying me through the journey with a lot of discussions and help, both in the lab and outside the lab. My special thanks go to Věra Chytilová for her kind help in plant growing in greenhouse, to all kind technicians in the group for the barley transformation work and their nice company. I am also really appreciated to Asst. Prof. Petr Galuszka for his open mind and help in the beginning of my PhD study in the Department of Molecular Biology. I would like to thank Prof. Ivo Frébort for giving me the opportunity to work at the CATRIN-CRH.

I would like to thank to Dr. Götz Hensel and his transformation group in IPK, Germany for the significant help in preparation of barley transgenic CRISPR/Cas⁹ lines.

I would like to thank Dr. Mathieu Gonin and Myriam Colin for their kind collaboration in transactivation assay and histology in IRD, Montpellier, France and their open mind and friendship. I would like to express my gratitude to my master supervisor, Dr. Stéphane Jouannic, my senior colleagues in Agricultural Genetic Institute, Hanoi for their kindness, encouragement, open mind, and availabilities for all my questions and emails during my scientific career. I want to thank all the colleagues in IRD, Montpellier for helping me during the time I made the internship there.

I would like to express my gratitude to all the friends who support me last seven years of my life in Czech Republic. They are my second family in Czech Republic. Please let me give my heartfelt thanks to: Kristina and her family, Katka J. and her family, Claudia, Alba, Honza and Venca, Auguste and Justinas, Denisa and whole family, Domcha.

Finally, my special appreciation and gratitude would like to go to my great family, dear parents, brother and his little family in Vietnam, my love and his family in Czech, my best friend – Hanh. This PhD would not be possible without their love, endless support, and encouragement.

Souhrn

Kořenový systém hraje klíčovou roli v růstu a vývoji rostlin, zajišťuje příjem vody a živin a reaguje na měnící se podmínky prostředí. Obiloviny se vyznačují svazčítým kořenovým systémem, který se skládá z primárního kořene a ze seminálních kořenů vyvíjejících se již během embryogeneze, a dále z post-embryonálních laterálních a nodálních kořenů (NK), které se vyvíjí z kořene nebo ze stonku. Porozumění mechanismům regulace zakládání a vývoje kořenů představuje první krok k selekci plodin s vylepšenými vlastnostmi kořenové architektury, a to prostřednictvím buď markerem asistované selekce nebo přímé genetické modifikace. Ječmen (*Hordeum vulgare* L.) je významnou plodinou, která se umísťuje na čtvrtém místě na světě jak z hlediska množství, tak pěstební plochy a stal se modelovou rostlinou pro malozrnné obiloviny z rodiny *Triticaceae* pěstované v mírném pásu. V první části výzkumu jsme provedli kompletní transkriptomickou studii báze stonku semenáčků ječmene 1 den po vyklíčení a 10 dní po vyklíčení, kdy se tvoří NK, abychom pochopili molekulární mechanismus řídící tvorbu NK. RNA-seq analýza ukázala, že vývoj NK zahrnuje geny kódující proteiny s úlohami v určení identity buněk, aktivaci buněčného cyklu, kontrole hormonálního stavu, buněčné smrti a modifikaci buněčné stěny. Tyto geny jsou pravděpodobně zapojeny do různých kroků tvorby NK, od založení a diferenciacie primordia až po jeho průnik skrze epidermis, a odhalily aktivaci různých hormonálních drah během tohoto procesu. Ve druhé části studie jsme se podrobně zaměřili na identifikaci a funkční charakterizaci genů kódujících rostlinné LATERAL ORGAN BOUNDARIES (LOB) DOMAIN (LBD) transkripční faktory (LBD TF), které mají úlohu během zakládání NK v ječmeni. U rýže je CROWNROOTLESS1 (CRL1) LBD TF hlavním regulátorem zakládání NK, ten je pod přímou kontrolou auxinem řízené signální dráhy zprostředkované přes auxin response factor (ARF) TF. Ve studii byly v ječmeni identifikovány dva fylogeneticky úzce příbuzné geny CRL1 (nazvané HvCRL1 a Hv-CRL1-L1). V indukovatelném systému NK jsou oba kandidátní geny exprimovány v reakci na auxin během raných stádií tvorby NK v bázi stonku, přičemž HvCRL1-L1 vykazuje časové zpoždění ve srovnání s HvCRL1. Transientní aktivační eseje v protoplastech rýže ukázaly, že HvCRL1 může vázat známou DNA sekvenci rozpoznávanou LBD TF, zatímco HvCRL1-L1 ne. Oba geny mohou částečně komplementovat mutanta *crl1* u rýže. Mutace vedoucí ke ztrátě funkce v každém genu dramaticky narušuje tvorbu NK v ječmeni. Výsledky dokazují, že oba TF jsou zapojeny do regulace tvorby NK v ječmeni, ale pravděpodobně v tomto vývojovém procesu působí prostřednictvím odlišných a vzájemně se doplňujících drah.

Abstract

Root systems have critical roles in plant growth, development, ensuring water and nutrient uptake, and response to changing environmental conditions. In cereals, the fibrous root system comprises primary and seminal roots that develop during embryogenesis, and lateral- and crown roots (CRs) that develop post-embryonically from root or stem, respectively. Understanding the mechanisms regulating root initiation and development represents the first step towards the selection of crops with enhanced root architectural traits via either marker-assisted-selection or direct genetic modification. Barley (*Hordeum vulgare* L.) is an important crop, ranking at the fourth place worldwide both in terms of quantity and cultivation area, and has become a plant model for the small-grain temperate cereals of the Triticaceae family. In the first part of the research, we investigated a whole transcriptomic study in the barley stem base of 1 day-after-germination (DAG) and 10DAG seedlings, when CRs are formed to understand the molecular mechanism controlling CR formation. The RNA-seq analysis indicated that CR development involved genes encoding proteins with roles in cell identity priming, cell cycle activation, hormonal status control, cell death and cell wall modification. These genes are likely involved in the different steps of CR formation from initiation to primordia differentiation and emergence and revealed the activation of different hormonal pathways during this process. In the second part of the study, we deeply focus on identification and functional characterization of genes encoding the plant-specific LATERAL ORGAN BOUNDARIES (LOB) DOMAIN (LBD) Transcription factors (LBD TFs) with roles during CR initiation in barley. In rice, the CROWNROOTLESS1 (CRL1) LBD TF is the core regulator of CR initiation and a direct target of the auxin response factor (ARF)-mediated auxin signaling pathway. In our study, two CRL1 phylogenetically closely related genes (named HvCRL1 and Hv-CRL1-L1) were identified in barley. In a CR inducible system, both candidate genes are expressed in response to auxin during the early stages of CR formation in stem base, with a time delay for HvCRL1-L1 in comparison with HvCRL1. Transient activation assays in rice protoplast showed that HvCRL1 could bind a known consensus DNA sequence recognized by LBD transcription factors, whereas HvCRL1-L1 did not. Both genes can partially complement the *crl1* rice mutant. Loss-of-function mutation in each gene dramatically impairs CR formation in barley. The results prove that two TFs are both involved in the regulation of CR formation in barley but likely act through distinct and complementary pathways in this developmental process.

CONTENTS

OBJECTIVES OF THE DOCTORAL STUDIES	8
INTRODUCTION	9
MATERIALS AND METHODS	11
A. TRANSCRIPTOMIC OF BARLEY CROWN-ROOT DEVELOPMENT	11
I. Plant materials and grown conditions	11
II. Imaging of Crown-root primordia by light and confocal microscope.	11
III. Evan blue staining	12
IV. Library preparation and transcriptomic analysis.	12
V. Analysis of gene expression by quantitative real-time transcription polymerase chain reaction (qRT-PCR).	13
VI. Prediction of putative cis-regulating elements related to ethylene and cell death. .	13
VII. Statistical analysis.....	14
B. BARLEY LBD TF IN CROWN ROOT	14
VIII. Plant materials and grown conditions.	14
IX. Identification of LBD protein in barley and phylogenetic analysis.....	14
X. Crown root inducible system.	15
XI. Gene expression analysis by qRT-PCR.	15
XII. Trans-activation essays in rice protoplast.	16
XIII. Knock-out barley <i>cr11</i> mutant generated by CRISPR-Cas ⁹	17
XIV. Complementation of the rice <i>cr11</i> mutant.	18
RESULTS AND DISCUSSION	20
A. TRANSCRIPTOMIC OF BARLEY CROWN-ROOT DEVELOPMENT	20
I. Crown-root primordia development in stem base of the spring barley cv. GP	20
II. Transcriptomic changes in the stem base of 1DAG and 10DAG seedlings of spring barley cv. Golden Promise and functional annotation of differential expressed genes (DEGs).....	21
III. Genes encoding proteins with roles in cell identity priming and cell cycle activation.....	23
IV. Hormonal status during crown root development in barley.	24
V. Genes encoding proteins involved in cell death and cell wall modification.	25
B. BARLEY LBD IN CROWN-ROOT INITIATION	27
VI. LBD gene family analysis in barley and identification of the putative orthologous of rice and maize genes involved in crown root initiation.....	27
VII. Expression profile of the HbLBD genes during crown root initiation.	28
VIII. HvCRL1 binds the LBD-box <i>in vivo</i>	30
IX. Both HvCRL1 and HvCRL1-L1 are involved in crown root formation.....	31
CONCLUSIONS.....	33
REFERENCES.....	34
CONFERENCE PRESENTATIONS	39

PUBLICATIONS	40
MANUSCRIPTS UNDER THE REVIEW	40

Objectives of the doctoral studies

The aim of the PhD study is to investigate the molecular mechanism and the anatomic origin of the crown-root (CR) initiation and development in barley (*Hordeum vulgare* L.). To achieve this goal, the study has been divided into two following specific objectives:

- **Objective (1):** Identification and characterization of molecular events during CR development barley.

For these strategies, a whole transcriptomic study of stem base of barley seedling at the development stages of 1 day after germination (DAG) and 10 DAG, as well as an anatomical overview of crown root initiation in young barley seedlings were revealed.

- **Objective (2):** Identification and functional characterization of genes encoding LATERAL ORGAN BOUNDARIES (LOB) DOMAIN (LBD) transcription factors with a putative role during CR initiation in barley.

For this purpose, methods such as phylogenetic tree analysis, transcriptomic analysis, histology, gene expression analysis by real-time quantitative reverse transcription polymerase chain reaction (qRT-PCR), transactivation assay in rice mesophyll protoplast, CRISPR-Cas⁹ genome editing, and complementation in the rice knock-out mutation were performed.

Introduction

Roots play fundamental roles in the growth and development of plants, ensuring not only anchorage in the soil, but also water and nutrient up-take, and interaction with soil microorganisms which contribute to the regulation of crop productivity (Gonin et al. 2019). Plants can dramatically modify their root system in response to environmental and nutrient conditions (López-Bucio, Cruz-Ramírez, and Herrera-Estrella 2003; Gao and Lynch 2016; X. Li, Zeng, and Liao 2016). Climatic changes are characterized by increasing number and severity of episodes of drought and heat that are responsible for drops in yield. As roots are the first interface between plant and environment, sensing changes in soil moisture and nutrient availability, they represent a good target for new breeding programs.

The typical root system of cereals is composed of the embryonically formed primary and seminal roots, and of the post-embryonically formed adventitious roots that are shoot-borne roots, called crown roots (CR) appearing quickly after germination at the junction between the stem and the root. Primary and seminal roots, and CR can form lateral roots of different orders. All together, they form the characteristic fibrous root system of monocots (Bellini, Pacurar, and Perrone 2014). In some monocots, embryonic primary and seminal roots are not persisting, and the mature root system is constituted exclusively from the CR (Atkinson et al. 2014). In cereals, the CR system dominates and ensures resource acquisition during vegetative growth as well as during reproductive and grain-filling phases. CR number predominantly influences root biomass and the soil portion that the plant will explore and exploit (Orman-Ligeza et al. 2013).

Barley is the fourth most cultivated cereal worldwide (<http://faostat.fao.org/>). The development of high-throughput sequencing in the last decade resulted in the availability of barley genome sequence and annotation (Mayer et al. 2012; Mascher et al. 2021). Finally, the genetic modification of barley for bioengineering is possible since *Agrobacterium*-mediated transformation can be successfully achieved both from immature embryo (Cornelia Marthe, Jochen Kumlehn 2015) or embryogenic pollen culture (Kumlehn et al. 2006). All these criteria, together with its diploid genome, make barley (temperate origin) serve as a complementary model in addition to rice (tropical origin) to study the root system development in Triticaceae.

In the first part of the thesis, using barley as a plant model for Triticaceae, we studied the whole transcriptomic of the stem base of barley seedling at the development stage of 1 day-after-germination (DAG) and 10 DAG when CRs are formed. The analyzed data indicated the possible mechanism underlying CR development and emergence in barley and revealed the activation of different hormonal pathways during this process. This whole transcriptomic study is the first study aiming at understanding the molecular mechanisms controlling CR development in barley.

The second part, also the focus of the PhD study, aims to understand the role of LBD transcription factors during initiation and development of CR in barley. Based on the new annotation, the barley reference genome contains 31 *LBD* genes. The phylogenetic analysis of barley LBD proteins identified two closest orthologous namely *HvCRL1* and *HcCRL1-L1* to the rice *CRL1* gene and the maize *RTCS* and *RTCL* genes, which were characterized as

being involved in CR initiation and development (Liu et al. 2005; Y. Inukai 2005; Majer et al. 2012; C. Xu et al. 2015). Through real-time PCR analysis, the expression of both genes is accumulated in the stem base of barley seedlings in response to auxin induction, with *HvCRL1* transcripts being accumulated earlier than *HvCRL1-L1* transcripts. The *in-silico* analysis of the *HvCRL1-L1* promoter indicated that this gene could be a downstream target of HvCRL1. In addition, using the knock-out barley lines in each of the two genes, as well as the complementation of the *crown rootless1* (*crl1*) rice mutant, we investigated the involvement of these two genes during CR initiation and development in barley.

Materials and Methods

A. Transcriptomic of barley crown-root development

I. Plant materials and grown conditions

The spring barley cultivar Golden Promise (cv. GP) was used in this study. For the purpose of the experiment, grains were immersed for 30 sec in 70% ethanol, washed 3 times in water, then surface sterilized in 3% sodium hypochlorite for 5 min and extensively rinsed in water. Finally, grains were placed on wet paper in Petri dishes and placed in the dark for 2 days at 4°C. Germination was induced by transferring Petri dishes to a culture chamber with a long-photoperiod (16h-day/8h-night) and a temperature regime of 21°C-day/18°C-night. The day of appearance of the primary roots and coleoptile through the seed husk was considered as the germination day. One DAG, half of the germinations were sampled, separating roots, stem bases (1 mm fragment from the root – shoot junction/crown part) and shoots. The rest of the seedlings were kept for 3 more days on wet filter paper in petri dishes, then the transferred into a mini-hydropony system in a modified half-strength Hoagland solution (Vlamis and Williams 1962). At 10 DAG, the rest of the seedlings were harvested, separating roots, stem bases (1.5-2 mm fragment from the root – shoot junction/crown) and shoots as in 1 DAG. Each kind of sample (roots, stem bases and shoots) was a pool of 5 seedlings; samples were immediately frozen in liquid nitrogen and stored at -80°C freezer until use. The experiment was conducted on three independent biological replicates.

II. Imaging of Crown-root primordia by light and confocal microscope.

A 2 mm-long section from the stem base was excised with a scalpel and immediately immersed in fixative solution (4% paraformaldehyde in 1X of phosphate-buffered saline (PBS), pH 7.4). Vacuum was applied twice for 1 min 30 sec. Fixative was changed, and samples were placed overnight at 4°C in the dark. The next day, samples were washed 4 times in 1X PBS for 15 min. Samples were dehydrated in an ethanol series from 50 to 100 % into a sonication condition. Samples were embedded in resin (Technovit® 7100; Electron Microscopy Sciences) according to the instructions. Sections of 4.5 µm were obtained with a HYRAX M40 microtome (Zeiss), stained with either periodic acid Schiff-naphtol blue black (PAS-NBB) or lugol, and mounted in Clearium® Mounting Media (Electron Microscopy Sciences). Sections were observed with an Imager M2 microscope equipped with an Axio Cam MrC5 camera (Zeiss). Pictures were acquired and analyzed with the ZEN software (Zeiss).

The imaging of the stem base by confocal microscopy was performed as previously (Lavarenne et al. 2019). Briefly, the 1 mm-long and 2 mm-long crown of barley seedlings were harvested at 1DAG and 10DAG, respectively, and immediately immersed in ½ Hoagland medium at 4°C overnight. The harvested stem bases were embedded in 5% agarose in sterile distilled water (w/v). Agarose blocks were mounted into an Automate 880 (Phiv platform, MRI imaging facility, Montpellier, France, <https://www.mri.cnrs.fr/>), a custom machine combining an LSM NLO 880 multiphoton microscope (Zeiss, <https://www.zeiss.com>) equipped with a Chameleon Ultra II tunable pulsed laser (690-1080

nm range excitation; Coherent, <https://www.coherent.com>) and an HM 650V vibratome (Microm Microtech, <http://www.mm-france.fr>) for automation of sample cutting (60 μ m) and instant imaging. The images were obtained with an A20x/1.0NA (2.4 mm WD) objective. ZEN and a custom package ZEN EXTENSION NECE (Zeiss) was used for the instrument. Images were acquired and proceed along the whole stem base. An application of ImageJ – Fiji was applied to align the imaged sections (Schindelin et al. 2012). All aligned sections in one stem base were reconstructed in 3 spatial dimensional (3D) structure by using in IMARIS 9.1 (Imaris, <https://imaris.oxinst.com>).

III. Evan blue staining.

Evans blue staining was applied to detect the cell death at the site of root emergence (Mergemann and Sauter 2000). 10 DAG seedlings of cv. GP were immersed in 2% (w/v) Evans blue, prepared in water, for 3 min and subsequently washed in water. Evans blue penetrates only dead cells. Samples were observed with a Zeiss Axio Zoom. V16 Stereo Microscope equipped with a camera. Serial pictures were taken and analyzed with ZEN software (Zeiss).

IV. Library preparation and transcriptomic analysis.

Stem bases (1 to 2 mm-long), corresponding to the zone of crown root emergence of 1DAG and 10DAG seedlings, grown and harvested as previously described in II.1.1, were used for RNA extraction and transcriptomic analyses.

Total RNA was extracted according to the instructions of the ZymoResearch Plant RNA extraction kit and treated by TURBOTM DNase. Libraries were prepared from 2.5 μ g of total RNA according to instructions of the Illumina TruSeq1 Stranded mRNA Sample Preparation Kit (Illumina). Library concentration was assessed with the Kapa Library Quantification Kit (Kapa Biosystem) and all libraries were pooled to the final 8 pM concentration for cluster generation and sequencing. The clusters were generated using an Illumina TruSeq1 PE Cluster Kit v3cBot HS and sequenced on HiSeq PE Flow Cell v3 with a HiSeq 2500 Sequencing System. Three independent biological replicates were sequenced for each sample.

The paired-end reads (50bp-long) generated by sequencing were quality checked and trimmed prior mapping to the reference genome of barley cv. Morex IBSC_v1 (International, Genome, and Consortium 2012) using the Tophat2 splice-read mapper with default parameters (D. Kim et al. 2013). The mapped reads were quantified using HTSeq with respect to the stranded library (Anders, Pyl, and Huber 2015). The differentially expressed gene expression was calculated with the DESeq2 package (Love, Huber, and Anders 2014). Only genes harboring a significant induction or inhibition were considered for further analyses (p -adjusted value ≤ 0.05 , $|\log_2\text{foldchange}| \geq 1$). The functional annotation and enrichment was performed using the automated MapMan BIN ontology in Mercator4 (Lohse et al. 2014; Schwacke et al. 2019). In parallel, the GO enrichment analysis limited to “Biological process” was performed with Shiny GO: the 40 most enriched GO terms were sorted based on their fold enrichment. All data are available at the NCBI archive database under the GEO

(<https://www.ncbi.nlm.nih.gov/geo/query/acc.cgi?acc=GSE87737>).

V. Analysis of gene expression by quantitative real-time transcription polymerase chain reaction (qRT-PCR).

To confirm the differential expression of several interesting genes, qRT-PCR analysis was performed with i) samples used for RNA-seq focused on the 2mm of stem base region of seedlings at 1DAG or 10DAG, and ii) with samples obtained from various tissues (roots, stem bases and shoots) of cv. GP seedlings at 1DAG and 10DAG. Each sample was prepared in 3 independent biological replicates, with each replicate being composed of tissues of 5 seedlings.

Total RNA was extracted with the Quick-RNA Plant Kit (Zymo Research) following manufacturer's instructions. Genomic DNA was removed with an additional treatment with 2U of TURBOTM DNase, and subsequent precipitation with lithium chloride. Total RNA was finally dissolved in RNase-free water. The quantity was determined with a NanoDropTM One/OneC Microvolume UV-Vis Spectrophotometer.

The oligo(dT)₁₈-based cDNA synthesis was performed from 2 µg of the total RNA according to the instructions of the RevertAid First Strand cDNA synthesis kit (Thermo Fisher Scientific). For real-time PCR, cDNA samples were diluted 10 times and used in a reaction containing 1X gbSG PCR master mix (Generi biotech), 200 nM of each primer and 500 nM of ROX as a passive reference. Three technical replicates were run for each sample on a StepONE Plus thermocycler (Applied Biosystems) in a two-step amplification program. The initial denaturation at 94 °C for 2 min was followed by 45 cycles of 94 °C for 5 s and 60 °C for 20 s. HvACT (AK248432), Hv5439 (AK360511, HORVU5Hr1G073510) and EIF5A2 (AK357300) genes were found to be the most stable across the samples under investigation and were consequently used as normalizer. Cycle threshold values for the gene of interest were normalized in respect to the three reference genes and the geometric mean of expression was calculated. The relative expression was determined using the $\Delta\Delta C_t$ mathematical model corrected for the PCR efficiency (E) (Michael W. Pfaffl 2001). The relative quantification was estimated in comparison with either "crown-1DAGRNAseq" or "roots-1DAG" sample. Primers were designed using Primer3Plus (<https://primer3plus.com/cgi-bin/dev/primer3plus.cgi>). Their specificity was firstly checked by blast restricted to barley genome and validated by the dissociation curve and sequencing of the amplified product.

VI. Prediction of putative cis-regulating elements related to ethylene and cell death.

The presence of putative *cis*-regulating elements related to ethylene was predicted with PlantPAN3.0 (Chow et al. 2019) for 3 genes with a potential involvement in cell death during crown-root emergence. The 1kb-long sequence upstream of the ATG was retrieved from barley genome. The sequences were scanned with the "Promoter analysis" tools using the transcription factor binding motifs database from rice.

VII. Statistical analysis.

GraphPad Prism version 9.2.0. was used to prepare all figures and evaluate the statistical analysis. In all cases, the statistical significance was assessed by a two-way ANOVA followed by a Bonferroni multiple comparisons test.

B. Barley LBD TF in crown root

VIII. Plant materials and grown conditions.

The two-rowed spring homozygous diploid 1-6 (DH 1-6) barley (*Hordeum vulgare* L.) cultivar Golden Promise was used for all barley experiments in this study. Plants were sown, and plants were grown in 2 L pots containing a 3:1:2 mixture of garden soil/sand/white and black peat (Klasmann Substrate 2). At the tillering stage (BBCH code 29/30), plants were fertilized with 15g of Osmocote (N, P, K: 19%, 6%, 12%; Scotts, The Netherlands). Cultivation was carried out in a greenhouse in Olomouc (Czech Republic) maintained at 18°C day/16°C night, under varying natural light. When necessary, a 14 h photoperiod was maintained with artificial lighting provided by sodium vapor lamps combined with mercury vapor lamps (500 mmol.m⁻².s⁻¹ at the top of the plant).

Seeds of the *O. sativa* L. cv. Taichung 65 (TC65), *crll* mutant in the genetic background Taichung 65 and cv. Kitaake were originally provided by UMR DIADE-Montpellier (France). TC65 and *crll* seeds were previously obtained from Professor Y. Inukai, Japan (Inukai et al. 2005). For the purpose of seed multiplication and selection of transgenic rice, plants are grown in greenhouses. Seeds were sown in 2 L pots containing ProfiSubstrate (Gramoflor) and placed in pot plates filled with water to maintain wet-soil growing conditions. Plants were fertilized twice a month with 0.3g of AGRO NPK 11/7/7 during vegetative growth and with Kristalon Plod a květ fertilizer (NPK: 5/15/30; AGRO CS a.s., Czechia) from flowering until the seed maturity. The temperature was maintained at 25°C. During winter, a 14 h photoperiod was ensured by a sodium vapor lamp combined with a mercury vapor lamp (500 mmol.m⁻².s⁻¹ at the top of the plant); In Summer, no additional lighting was provided.

IX. Identification of LBD protein in barley and phylogenetic analysis.

Thirty one barley LBD protein sequences were retrieved from the Plant Transcription Factor Database (PlantTFDB) (Jin et al. 2017) and the annotation of the barley Morex reference genome V3 (Mascher et al. 2021). The phylogenetic tree of HvLBD protein was constructed based on the alignment using MUSCLE algorithm and the maximum likelihood (ML) tree construct in the Molecular Evolutionary Genetics Analysis cross computing Platforms (MEGA-11) (Tamura, Stecher, and Kumar 2021) with the following parameters: Bootstrap method with 500 replicates, a non-uniformity of evolutionary rates among sites modeled by using a discrete Gamma distribution (+G), General Time Reversible (JTT) with frequency (+F) model, complete deletion. The zinc finger-like motif, the GAS block, and the leucine-zipper-like coiled-coil motif were determined manually (Zhang et al. 2020). The visualization of gene structures was performed using CFVisual tool (<https://github.com/ChenHuilong1223/CFVisual>) (Chen et al. 2022).

To predict the barley close orthologs of LBD proteins, which were identified in rice and maize with functions in crown root initiation, and in *Arabidopsis* with functions in lateral root initiation, 31 barley LBD protein sequences were aligned to the sequences from rice OsCRL1/Os03t0149100-01 and OsCRL1-like (OsCRL1-L1)/Os03t0149000-01, maize RTCS/GRMZM2G092542_P01 and RTCL/AC149818.2FG009 and Arabidopsis AtLBD16/AT2G42430, AtLBD18/AT2G45420. The analysis involved 37 amino acid sequences and was performed with the same parameters described above.

X. Crown root inducible system.

This system is based on the role of the phytohormone auxin and has been adapted from the lateral root inducible system (LRIS), which was developed in the dicot plant model *Arabidopsis* and maize (Kristiina Himanen et al. 2002; Jansen et al. 2012; Crombez H. et al. 2016). Initially, the barley cv. Golden Promise grains were sterilized as described in II.1.1. After sterilization, the grains were placed in petri dishes on 3 layers of sterilized wet filter papers containing 50 μM N-1-naphthylphthalamic acid (NPA; Sigma Aldrich), an inhibitor of auxin polar transport and put at 4°C for 3 days to mimic vernalization and ensure a homogeneous germination. Then, the grains were transferred for germination in phytotron with a photoperiod of 16°C/12 hours light and 13°C/12 hours darkness, light intensity at 170 $\mu\text{mol photons.m}^{-2}.\text{s}^{-1}$ and 60% relative humidity. Three days DAG, young seedlings with approximately 3 cm of shoot length were transferred to hydroponical culture in ½ strength Hoagland solution containing 50 μM NPA and grown for three more days. Then, the hydroponic solution was replaced by ½ fresh strength Hoagland solution containing 50 μM 1-Naphthaleneacetic acid (1-NAA; Sigma Aldrich) as a source of active auxin. Seedlings were grown in this condition for 24 hours. After that, the NAA-containing solution was replaced by ½ Hoagland solution. Parallely, seedlings grown in only NPA solution were used as negative control. One mm stem bases (junction between root -shoot/crown) were harvested at different time-points just before applying NAA (0 hour (h)), and after NAA induction at 3h, 6h, 12h and 24h for gene expression analysis and anatomical observation experiments. For each time point, each pool sample was collected from 10 stem bases and flash frozen in liquid nitrogen, or immediately used for histological experiment. Each sample was prepared in 6 independent biological replicates for further gene expression analysis.

XI. Gene expression analysis by qRT-PCR.

Samples prepared as described in II.2.3, were ground to a fine powder in liquid nitrogen using mortar and pestle. Total RNA was extracted, and cDNA was synthesized similarly to the previous experiment, described in II.1.5. For qRT-PCR, cDNA, cDNA was diluted 5 times and used in a reaction containing 1X gbSG PCR Master Mix (Generi Biotech), 500nM of References dye (Lot. 270009002, ROX (6-Carboxy-X-Rhodamine), Generi Biotech) and 250 nM of each primer. Primers for qRT-PCR are designed with Primer3Plus for the five closest barley *LBD* genes presenting putative orthologs of *OsCRL1*, *OsCRL1-like*, *ZmRTCS*, *ZmRTCL*, *AtLBD16*, *AtLBD18*. To determine the best reference gene(s), a set of putative genes selected based on literature (Hruz et al. 2008) and *in silico* prediction using Genevestigator® (Nebion AG) were analyzed for their stability across ours with geNorm

v3.5 software (Hua et al. 2015; Vandesompele et al. 2002). Finally, the expression of three reference genes (*HvACT*: AK248432.1; *HvEF2 α* : AK361008.1; *Hv5439*: AK360511.1) were selected. The specificity of the primers was checked by not only BLAST restricted to barley genome, but also sequencing by Sanger method to confirm the specificity of the amplified products (Seqme, Czechia). qRT-PCR was carried out on a Step One Plus Real-Time PCR system (Applied Biosystems, USA), in an optical 96-well plate, as following protocol: an initial denaturation for 10 min at 95 °C, followed by 40 cycles of 15 s at 95 °C, 1 min at 60 °C. Melting curve analysis was performed after 40 cycles to verify primer specificity. Each sample was analyzed in six independent biological replicates and in technical triplicates. Each independent biological replicate represented a pool of 10 explants. The cycle threshold value for the gene of interest was normalized in respect to the three best HK genes and the geometric mean of expression was calculated. The relative expression was determined using the $\Delta\Delta C_t$ mathematical model corrected for the PCR efficiency (Michael W. Pfaffl 2001). The relative quantification was compared to the T0 sample corresponding to stem bases of seedlings harvested before treatment with 1-NAA. Nonparametric Kruskal-Wallis ANOVA supported statistical significance followed by a post-hoc multiple comparison of mean rank using GraphPad Prism version 10.0.0 for Windows (GraphPad Software, Boston, Massachusetts USA, www.graphpad.com).

XII. Trans-activation essays in rice protoplast.

The coding sequences of *HvCRL1* (*HORVU.MOREX.r3.4HG0408280*) and *HvCRL1-L1* (*HORVU.MOREX.r3.6HG0630410*) genes were amplified from cDNA obtained from 2 μ g of RNA extracted from the stem base of barley cv. GP seedlings grown in the presence of 1-NAA. High-fidelity PCR amplification was performed using a Phusion® High-Fidelity DNA Polymerase (New England Biolabs) using primers designed to introduce the *Bam*HI and *Nco*I restriction sites for the coding sequences. The amplified PCR products were cloned inside the *Bam*HI/*Nco*I of the pRT104 vector (Reinhard Töpfer, Volker Matzeit, Bruno Gronenborn 1987) to generate pRT104::35S-HvCRL1 and pRT104::35S-HvCRL-L1 effector constructs. The normalizer vector, p2rL7::35SrLUC, containing the Renilla luciferase (LUC) gene, and the pGusSH-47 reporter plasmids carrying the GUS reporter gene placed under the control of a minimal *CaMV 35S -47* promoter and an LBD-box or CRL1-box tetramers are described in (Gonin et al. 2022).

Protoplast isolation and transfection were performed based on the previously described protocol (Cacas et al. 2017) with modification to adapt to rice tissue (Gonin et al., 2022). Briefly sterilized hulled seeds of the rice cv. Kitaake were sown in cultivation boxes containing 1/2 strength Murashige & Skoog medium supplemented with Gamborg B5 vitamin (Duchefa Biochemie). Seedlings were grown for 9 days in the dark at 19°C. Leaves and shoots of 9-day-old rice seedlings were sliced with sharp razor blades into small pieces that were quickly transferred into 30 ml of enzymatic solution consisting of 30 ml of enzymatic solution. Vacuum was applied for 10 min to infiltrate strips with the enzyme solution. The infiltrated sliced tissues were incubated in dark for 4 h at 28°C. Following filtering and washing steps, rice protoplasts were co-transformed with a tripartite vector system that comprises (1) a reporter plasmid carrying the LBD *cis*-motif elements promoter-driven β -D-

glucuronidase (GUS)-encoding uidA gene, (2) a reference plasmid carrying the *LUC* gene and (3) an effector plasmid carrying *HvLBD* genes under the control of the CaMV35S promoter. The transfection in rice protoplasts was carried out by polyethylene glycol (PEG) (Yoo, Cho, and Sheen 2007) with the three plasmids in a ratio of 2:2:6 (GUS:LUC:effector). After transformation, the protoplasts were cultured at $28 \pm 2^\circ\text{C}$ in dark for 18 h, then collected, frozen in liquid nitrogen, and stored at -80°C for further analysis. GUS and LUC activities were measured as described previously (Zarei et al. 2011), using a Varioscan LUX from ThermoFisher installed with SkanIt™ Software for Microplate Readers to measure the fluorescence and luminescence. GUS activities were related to LUC activities in the same samples to correct the transformation and protein extraction efficiencies. For both genes, 4 to 6 independent biological replicates were analyzed. Values were expressed as relative to the highest value observed with *HvCRL1*. Statistical analysis was performed with GraphPad Prism version 10.0.0 for Windows (GraphPad Software, Boston, Massachusetts USA, www.graphpad.com).

XIII. Knock-out barley *crl1* mutant generated by CRISPR-Cas⁹

Single guide RNAs (sgRNAs) were designed to target *HvCRL1* (*HORVU.MOREX.r3.4HG0408280*) or *HvCRL1-L1* (*HORVU.MOREX.r3.6HG0630410*), using DESKGEN KNOCKIN tool (<https://www.deskgen.com/guidebook/ki.html>) (Hough et al. 2016). The sgRNA were ideally selected upstream of the conserved LBD domain coding sequence. The preparation of the CRISPR-Cas9 vectors was performed as previously described (Holubová et al. 2018). Briefly, the gene-specific oligo-duplex containing a *BsaI* restriction site was integrated into the *BsaI*-digested pSH91 vector. Then, the sgRNA-Cas9 expression cassette was cloned into the binary p ϕ i-d35S-TE9 plasmid through *SfiI* restriction site, to generate vectors p271-35S::*HvCRL1*-gRNA1, p271- 236 35S::*HvCRL1*-gRNA2 and p271-35S::*HvCRL1-L1*-gRNA1, p271-35S::*HvCRL1-L1*-gRNA2 and p271- 237 35S::*HvCRL1-L1*-gRNA3. The binary expression constructs were then introduced into the *A. tumefaciens* supervirulent strain AGL1 using electroporation protocol and then stored at -80°C with supplementation of 50% glycerol.

Before performing stable transformation of immature barley embryos as previously described (Marthe, Kumlehn, and Hensel 2015), the donor plant material barley cv. GP was grown in soil in a phytotron under control conditions ($15^\circ\text{C}/16$ h/light and $12^\circ\text{C}/8$ h/dark, $500 \mu\text{mol.m}^{-2} \text{ s}^{-1}$ light density and suitable fertilizers were frequently applied). All T0 transformants were selected on 50 mg L^{-1} hygromycin and by PCR genotyping using T-DNA-specific primers. To determine the type of mutation, a PCR reaction using primers flanking the targeted DNA region was performed; the PCR product was verified types of mutation by the Cleaved Amplified Polymorphic Sequences (CAPS) assays and then Sanger-sequenced by commercial service (Seqme, Czechia), and the mutation was predicted using DECODR (<https://decodr.org>) (Bloh et al. 2021). Barley plants that show a potential mutation were retained for homozygous selection and phenotyping. The selection of homozygous lines was done according to the CAPS assays, which are based on the fact that SNP polymorphisms identified between different mutant and non-mutant lines, as well as wild type, are converted

into CAPS markers. The webtool indCAPS (<http://indcaps.kieber.cloudapps.unc.edu/>) was used to design the PCR primers and the conditions for CAPS assay.

A flow cytometry inferred DNA ploidy levels was used to determine the level of nuclear DNA content in transgenic plants, by evaluating the relative fluorescence intensity of PI-stained nuclei (Doležel, Greilhuber, and Suda 2007). The ploidy transgenic plants were kept for further analyses.

To phenotype the root system of mutant, grains of the wild-type Golden Promise DH1-6, null sister, and mutant lines were used. Initially, the barley cv. Golden Promise grains were sterilized by immersing in 70% ethanol for 30 seconds; then rinse once in sterilized deionized water; prior to immersing in 3% hypochlorite for 3 minutes and finally extensively rinsing 6 times in sterilized deionized water. The sterilized grains were then gently dried on sterile tissue paper. After sterilization, the grains were placed in petri dishes with 3 layers of wet filter papers and put at 4°C for 3 days of vernalization to stimulate homogeneous germination. Then, the grains were transferred for germination in phytotron with a photoperiod of 15°C/16 hours light and 12°C/8 hours darkness. Two days after germination (DAG), young seedlings with 1 to 2 cm –long shoot were transferred to the sand-filled pots (Ø:10 cm x h:10 cm) containing cleaned beach sand over a 1cm layer of soil in the bottom to avoid sand leaching during watering. The plants were grown for 8 weeks in the same conditions and regularly watered once per two days, with a 1X nutritive solution recommended by the commercial product (Kristalon™ 280 start, Agro, Czechia). The pots were kept in the same phytotron for 8 weeks. Eight-week-old barley plants were removed from the pots. After carefully washing excess sand and soil from the roots, the number of crown roots and embryonic roots were counted, the length of the longest (depth of the root system) was measured with a ruler to the nearest mm and the total fresh root was determined with a scale, for each plant. Finally, the root architecture of each plant was scanned, using EPSON scan program, with ImageScanner III LabScan 6.0 with a 600-dpi resolution and saved as tiff-formatted photos.

XIV. Complementation of the rice *crl1* mutant.

The two barley genes (*HvCRL1* and *HvCRL1-L1*) were amplified from cDNA obtained from RNA extracted from stem bases of cv. GP seedlings grown in the crown root inducible system for 6h after inducing by 1-NAA. They were amplified using a specific couple of primers associated with BP flanking sequences for Gateway™ cloning (Invitrogen) into the binary vector pCAMBIA5300.OE (Khong et al. 2015). This vector was modified from pCAMBIA2300 plasmid (CAMBIA, Australia). By the addition of the maize ubiquitin promoter (pUbi), to drive expression of protein coding sequences of interest in an enhancer effect (Christensen and Quail 1996). The resulting plasmids were validated by Sanger sequencing for all constructs (Seqme, Czechia). Four constructs were established for complementation assay including (1) pC5300.OE::*HvCRL1*, (2) pC5300.OE::*HvCRL1-L1*, (3) pC5300.OE-empty as a negative control. The Agrobacterium-mediated transformation of the rice *crl1* mutant in the cv. TC65 background was performed as previously described (Toki et al. 2006; Sallaud et al. 2003). The presence of the T-DNA in obtained plants was confirmed

by PCR amplification of either one of the *HvLBDs* (Sallaud et al. 2003; Toki et al. 2006). A non-transgenic line (without T-DNA) was kept as negative control (null sister).

To phenotyping the root system of complemented transgenic plant, seeds of WT TC65, *crll* mutant, OE-HvCRL1, OE-HvCRL-L1, transgenic TC65 with empty pRT104 vector were used. Initially, the rice cv. TC65 seeds were sterilized by immersing in 70% ethanol for 30 seconds; then rinse once in sterilized deionized water; prior to immersing in 3% hypochlorite for 3 minutes and finally extensively rinsing 6 times in sterilized deionized water. The sterilized seeds were then gently dried by sterilized tissue paper. After sterilization, the grains were placed in a square petri dish (24x24 cm) containing 250 ml of ½ MS medium (pH 5.8) in the middle line in the dishes. Plates were sealed with 2 layers of parafilm and covered half by aluminum foil and transferred for germination in phytotrol with a photoperiod of 25°C±2°C /12 hours light and 22°C±2°C /12 hours darkness. The plates were standing vertically for 14 days. Plates with 14 day-after-sowing rice plants were scanned, using EPSON scan program, with ImageScanner III LabScan 6.0 with a 600-dpi resolution and saved as tiff-formatted photo. The number of crown roots per plant was manually counted and scanned again.

Results and discussions

A. Transcriptomic of barley crown-root development

I. Crown-root primordia development in stem base of the spring barley cv. GP

Using classical histology and biphoton confocal microscopy, we evidenced that in barley the first CR primodium is already formed at 3DAG (Fig.1-A and B) at the outermost side of the pericycle, that is characterized by cells rich in starch. We designed this region as a ground meristem in comparison to rice. The earliness of CR primordia during seedling establishment has already been described in other monocots. In rice, CRs emerge from the coleoptilar node already 2 to 3DAG (J. Xu and Hong 2013), and in maize, CR already emerge 10 DAG (Hochholdinger et al., 2004). The study of 10 DAG-old seedlings by biphoton confocal microscopy suggested that CR primordia are formed sequentially, i.e., one after each other, with a seemingly averaged distance of 76 μm and 140° angle between two CR primordia (Fig.1-C and D). This disagrees with the observation done in rice or maize, where several CR are produced in whorls (Lavarenne et al., 2019).

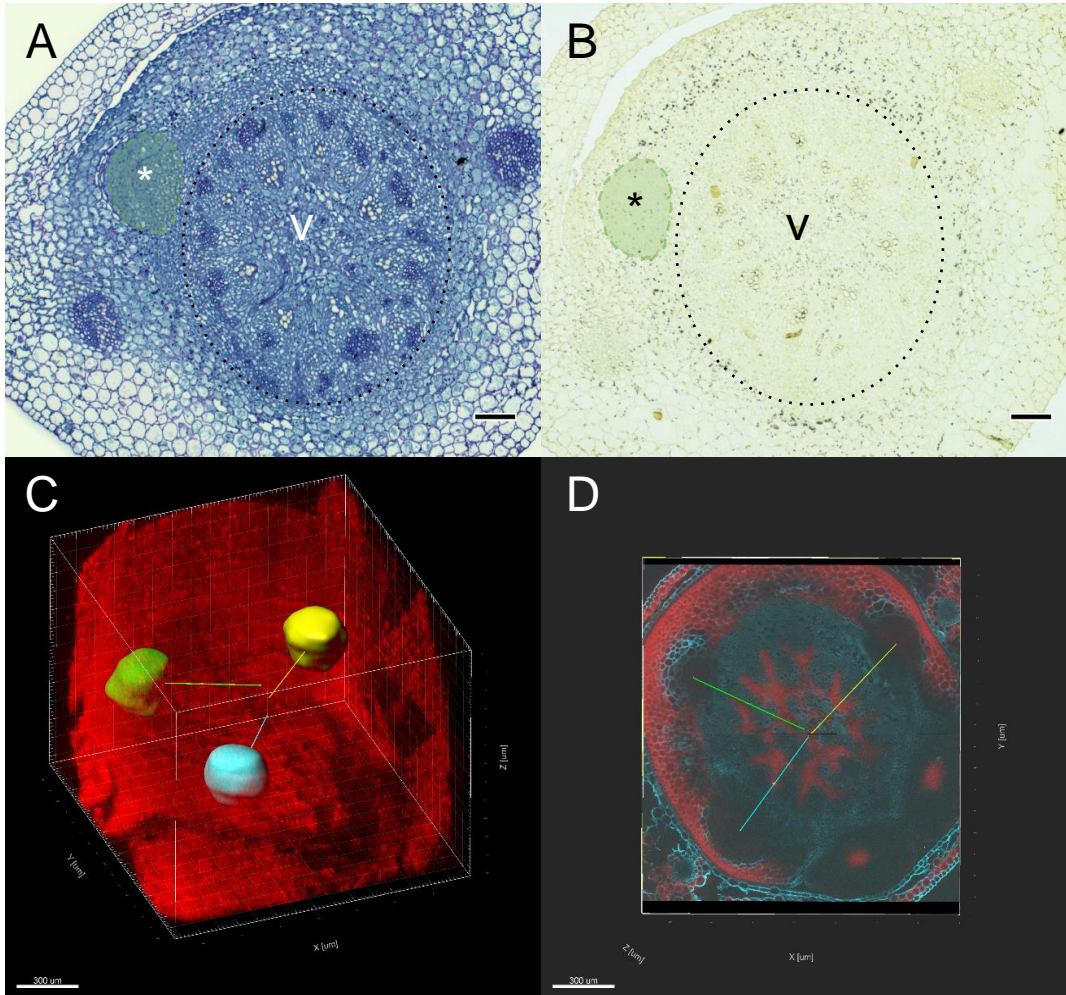


Figure 1: Crown-root primordia development in young barley seedlings. In 3DAG-old seedling, one primodium is formed at the outermost side of the pericycle (A); PAS-NBB staining). The pericycle is surrounded by cells rich in starch as shown by the presence of purple-black dots after staining with lugol solution (B). (C) Result of a block reconstruction in the 3D transparency mode of the whole stem base of a 10 DAG-old barley seedling. CR primordia are identified by different colors: blue,

green and yellow (D) z-axis cross section; the colored traits indicate the angle between each CR primordia. Bars in A and B represent 100 μ m.

For the study, we compared the transcriptome of the crown of 1DAG-old seedlings when no CR primordia could be seen to that of 10 DAG-old seedlings when 1 to 2 CRs already emerged.

II. Transcriptomic changes in the stem base of 1DAG and 10DAG seedlings of spring barley cv. Golden Promise and functional annotation of differential expressed genes (DEGs)

Gene profiling of the CR development in barley was investigated by RNA-seq whole transcriptome analysis, comparing the transcriptome of crown of 10 DAG-old seedlings to that of 1 DAG-old seedlings of the spring barley cv. GP. Differentially expressed genes were determined with DESeq2. Taking the limits of p-adjusted value < 0.05 and a log2foldchange excluding values from -1 to 1, there were 5264 DEGS between GP-10DAG and GP-1DAG, of which 2931 were up-regulated and 2333 were down-regulated in the crown of 10DAG-seedlings compared to the crown of 1DAG-seedlings.

Table 1: Functional annotation enrichment of genes differentially regulated in the crown of 10 DAG-old seedling of barley cv. Golden Promise. The automated annotation was performed using the Mercator resource (Lohse et al. 2014). Only the most enriched category ($\geq 10\%$) are represented. Values represent the percentage of genes in the specific category which were down- or up-regulated in DO10DAG and UP10DAG, respectively.

DO10DAG		UP10DAG	
Photosynthesis	50%	Solute transport	23%
Cell cycle organization	35%	Phytohormone action	22%
DNA damage response	21%	Redox homeostasis	20%
Protein biosynthesis	21%	Protein modification	17%
Chromatin organization	19%	Secondary metabolism	16%
Carbohydrate metabolism	18%	Lipid metabolism	16%
Cytoskeleton organization	16%	Amino acid metabolism	15%
Nucleotide metabolism	15%	Polyamine metabolism	14%
Protein translocation	15%	External stimuli response	14%
Coenzyme metabolism	15%	RNA biosynthesis	14%
RNA processing	13%	Protein homeostasis	13%
Secondary metabolism	10%	Nutrient uptake	12%
Polyamine metabolism	10%	Nucleotide metabolism	10%
		Cell wall organization	10%
		Carbohydrate metabolism	10%

The gene functional annotation was done using the MapMan BIN ontology in Mercator resource (Lohse et al., 2014; Schwacke et al., 2019). Over-represented functional categories are summarized in table 1. Sequences with unknown functions represented up to 50% of the total sequences. Among genes down-regulated in the crown of 10DAG-old seedlings, “DNA”, “cell”, “nucleotide metabolism” and “RNA” represented 19% of the DEGs. This suggested that profound molecular modifications occurred in the crown of seedlings that will enter the program of CR initiation and development. In opposite, genes up-regulated in the crown of 10 DAG-old seedlings belonged to categories “hormone

Even though our study did not focus on the lateral root development, these genes could be also involved in the initiation and development of lateral roots. Indeed, it has been demonstrated that development of lateral roots and CR shared common molecular regulators (Bellini, Pacurar, and Perrone 2014; Meng et al. 2019).

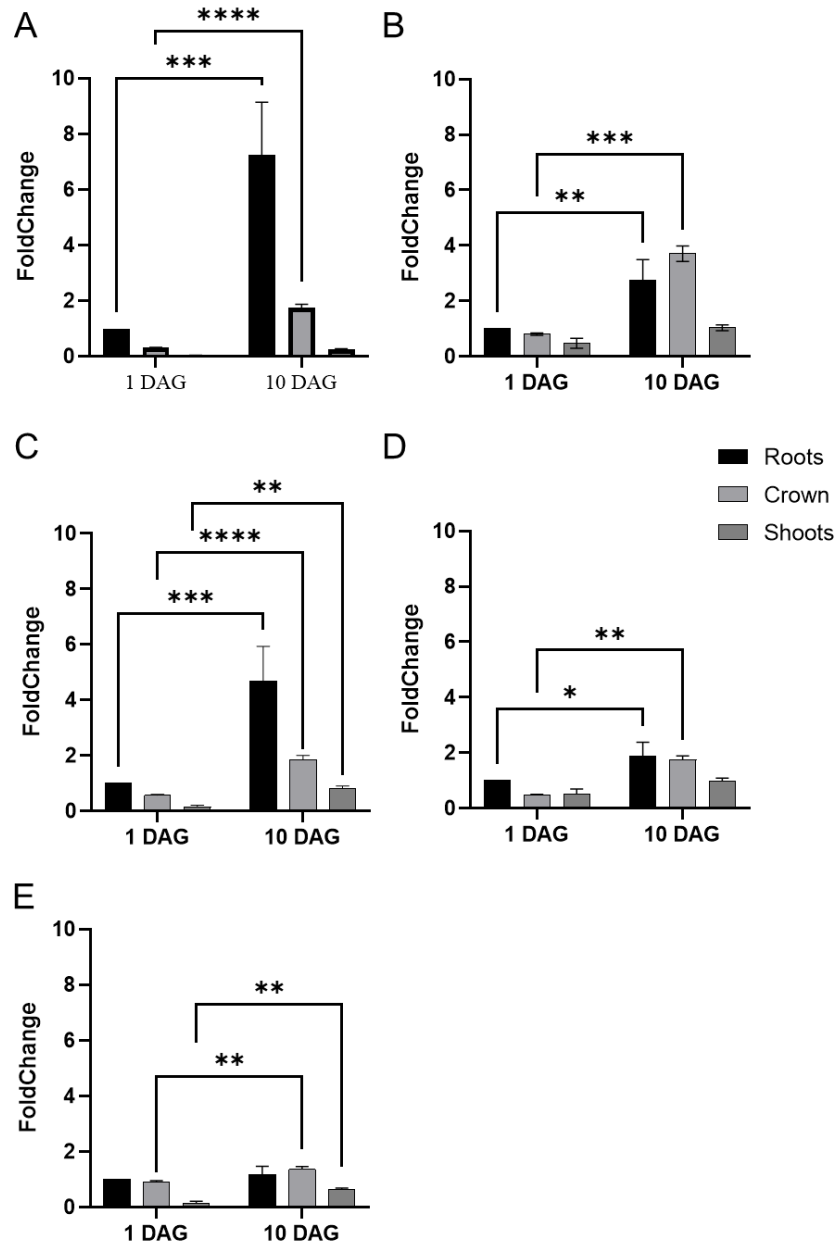


Figure 3: Gene expression analysis by qRT-PCR of PIN (A), SCR-like1 (B), ARGO (C), AuxIAA20 (D) and RRB9 (E) in the roots, crowns and shoots of cv. Golden Promise seedlings grown for 10 days in hydroponic conditions. Normalization was done using 3 reference genes: Actin, Hv5439 and EIF152. The graph shows means \pm SEM (n=3). The statistical significance was assessed by a two-way ANOVA followed by a Bonferroni multiple comparisons test (GraphPad Prism 9.2.0). ****: adjusted P-value < 0.0001; ***: adjusted P-value < 0.001; **: adjusted P-value < 0.01; *: adjusted P-value < 0.05.

III. Genes encoding proteins with roles in cell identity priming and cell cycle activation.

In the crown of 1DAG-seedlings, 12 genes encoding cyclin, cyclin-dependent kinases were up-regulated, suggesting an important activation of the cell cycle. In addition, cdc proteins and anaphase promoting proteins suggested that active cell division occurs. We also

found that 32 kinesin and kinesin-related proteins were up-regulated in the crown of 1DAG seedling initiating CRs. Kinesins form a superfamily of microtubule motor proteins and trigger the unidirectional transport of vesicles and organelles, affect microtubule organization and cellulose microfibril order. They were also described to be involved in cell division and growth (J. Li, Xu, and Chong 2012).

In Arabidopsis, LR initiation is characterized by founder cell identity priming, cell cycle activation and asymmetric division of the founder cells. Auxin maxima are responsible for the up-regulation of cyclins and cyclin-dependent kinases (CDKs) and the concomitant repression of CDK repressors such as KRP1 and KRP2 which inhibits the G1/S transition (Perrot-Rechenmann 2010; Himanen et al. 2002; Fukaki, Okushima, and Tasaka 2007).

IV. Hormonal status during crown root development in barley.

Genes belonging to the category “hormone metabolism” account for a large proportion of sequences over-represented in the crown of 10 DAG-old seedlings (enrichment: 22%).

Auxin is probably the most important hormone that regulates initiation of CRs. Among the genes abundant in the crown of 10DAG-old seedlings, we found 27 genes related to auxin (IAA) metabolism, signal transduction or induced by auxin. IAA maxima are fundamental for root primordia formation and emergence (Kitomi et al. 2008; Jansen et al. 2012; Péret et al. 2009). In our data, two auxin transporter-like proteins and one auxin efflux carrier were identified as up-regulated in the crown of 10DAG-seedlings. These 3 auxin transporters might participate in establishing auxin gradient required for CR development in barley. The release of free auxin from conjugates is often neglected. In the present study, we identified a gene annotated as IAA-amino acid hydrolase (ILR1). IAA-amino acid conjugates function in both the permanent inactivation and temporary storage of auxin, participating thus in auxin homeostasis regulation. ILRs allow releasing free IAA from the amino acid conjugates (LeClere et al. 2002). The Arabidopsis triple hydrolase mutant, *ilr1 iar3 ill2*, had fewer lateral roots than the wild-type, demonstrating the importance of IAA release from conjugate in the initiation of lateral roots (Rampey et al. 2004). Whether IAA is released from IAA-conjugates via ILR1 to support CR primordia formation and development in barley represents an interesting challenge to solve.

Our study revealed that at least 18 genes related to ethylene metabolism and signaling pathway were up-regulated in the crown of 10DAG-seedling, when CRs are already initiated and are emerging from the stem. In rice, ethylene induces the death of epidermal cells at the site of CRs emergence. Thus, through the crack of the epidermis the newly formed root can emerge without damages (Mergemann and Sauter 2000). Our data suggest that in barley, the emergence of CRs is possibly correlated with death of cortex and epidermal cell in an ethylene-mediated response. This is supported by the fact that a gene associated with development and cell death was also up-regulated in the crown of 10DAG-seedling.

Abscisic acid (ABA) is another important hormone. Its role as inhibitor or stimulator of plant growth and development is a constant question of debate (Humplík, Bergougnoux, and Van Volkenburgh 2017). ABA has a dual role in root development: whereas it stimulates the initiation and primordia formation in different species, it often inhibits the emergence from the stem and the subsequent elongation of the root (Harris 2015). Fifteen genes related

to ABA synthesis and signaling pathway were found to be up-regulated in 10DAG-seedlings developing CRs. Among these genes belong two transcripts, annotated as 9-cis-epoxycarotenoid dioxygenase/ NCED, which catalyzes the first committed step of ABA synthesis. This suggested that ABA synthesis takes place in the crown of seedlings developing CRs and that ABA is also important for the development of CRs in barley. Nevertheless, deeper studies would be necessary to precisely determine the role of ABA in the different steps of CR development, i.e., primordium initiation, emergence, and root elongation.

We also found that a gene encoding a gibberellin 2-oxidase, highly abundant in the crown of barley seedling, was up-regulated in 10DAG-seedlings. GAox2 are responsible for the degradation of active gibberellins (GAs). In poplar, GAs negatively regulates lateral root, specifically inhibiting root primordium initiation. The role of GA2ox in regulating GAs homeostasis was also proved in the same study (Gou et al. 2010). In rice, overexpressing GA2ox led to the decrease of endogenous GAs and enhanced CRs root growth (Lo et al. 2008). Similarly, the silencing of SLR1, a negative regulator of the GA signaling pathway, resulted in lower number of CRs in rice (Ikeda et al. 2001). It is thus tempting to postulate that GAs are inhibitors of CR initiation and development in barley and a precise regulation of its homeostasis via GA2ox is required.

V. Genes encoding proteins involved in cell death and cell wall modification.

In rice, the emergence of CRs happens concomitantly to death of nodal epidermal cells above CR primordia (Mergemann and Sauter 2000). In maize, Park and coworker reported the formation of a cavity in the cortex of primary root around the LR primordia, resulting probably from the death of the cells (Park, Hochholdinger, and Gierl 2004). Apoptosis of epidermal cells is controlled by ethylene and is mediated by reactive oxygen species (ROS), which are also involved in CR primordia growth (Steffens et al. 2012), allowing coordinating CR growth with local weakening of the epidermal cell barrier (Steffens and Sauter 2009). In the present study, we demonstrated that genes involved in the ethylene pathway were up-regulated in the crown of 10 DAG-old seedlings (Fig.4-A). The use of the Blue Evan's staining showed that cell death occurred at the site of emergence of CRs (Fig.4-B). It was shown that epidermal cells covering CR primordia might be targeted to die, as they contain lower amount of the METALLOTHIONEIN2b (MT2b), a scavenger of ROS (Steffens and Sauter 2009). Interestingly, a gene encoding a metallothionein was strongly down-regulated in the crown of 10 DAG-old seedlings, suggesting a reduction in ROS scavenging. Our transcriptomic data suggest that emergence of CRs in barley is correlated with cell death, mediated by ethylene and ROS. Thirteen genes annotated as (endo)-chitinases were up-regulated in the crown of 10 DAG-old seedlings. Chitinases are glycosyl hydrolases that catalyze the degradation of chitin, a major constituent of fungi cell wall and exoskeleton of insects. Commonly induced upon pathogen attack, they were for long associated with plant defense. The role of class IV chitinase in cell death was recently reported in pepper (D. S. Kim, Kim, and Hwang 2015). Genes of the functional category "Cell wall" were overrepresented among genes up-regulated in the crown of 10 DAG-old seedling (13%), indicating that profound modifications occur when CR primordia form and develop. These

genes are mainly related to pectin lyases, expansins and xyloglucan endotransglucosylases/hydrolases (XEGs). In Arabidopsis, the newly formed LR has to pass through 3 cell layers: endodermis, cortex and epidermis (Péret et al. 2009). Cells are particularly well attached to each other, especially epidermal cells. Genes encoding proteins affecting cell wall-property integrity (expansins, pectin lyases or XEGs) are expressed in tissues covering the emerging LR primordia. The activity of these enzymes most probably promotes cell separation in advance of developing lateral root primordia to avoid damages of the root meristem (Swarup et al. 2008). Moreover, the cell-wall properties could contribute to the number of LR produced (Roycewicz and Malamy 2014). Indeed, the high-affinity auxin importer Like Aux1 (LAX3) is an important regulator of LR emergence. Its expression in cells situated over the LR primordia regulates the activity of cell wall remodeling enzymes, which are likely to promote cell separation in advance of developing lateral root primordia (Roycewicz and Malamy 2014). In the present study, a gene encoding LAX3, was up-regulated in the crown of 10 DAG-old seedlings where CR are formed and emerging.

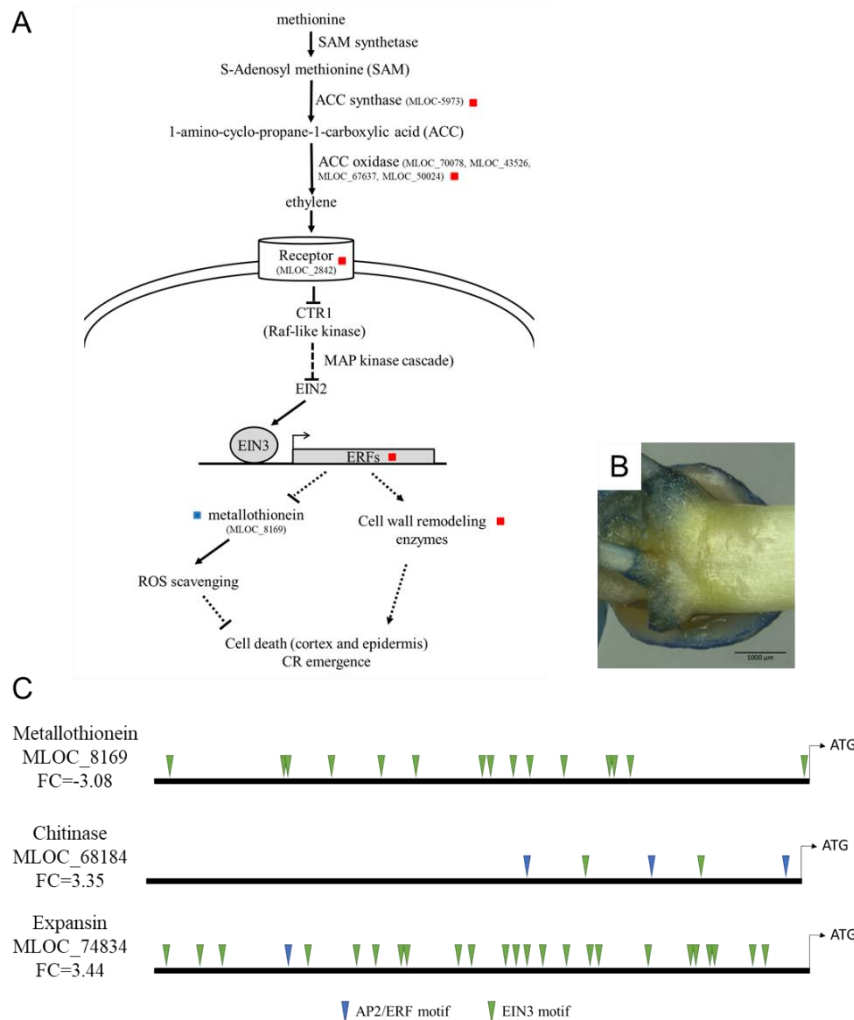


Figure 4: Involvement of ethylene in cell death during crown-root emergence in barley cv. Golden Promise. **(A)** Ethylene biosynthetic and signaling pathway in the context of cell death. Genes identified in the RNAseq data as differentially expressed are indicated (MLOC); colored scares indicate whether they were up-regulated (red) or down-regulated (blue) in the stem base of 10 days-old seedlings. **(B)** Evans blue staining indicates the cell death of the epidermal cell at the site of crown-root emergence. **(C)** Prediction of the presence of ethylene-related cis-regulating elements (AP2/ERF and EIN3 motifs). Prediction was done with PlantPAN3.0, using rice database.

The analysis of the 1.5 kb promoter sequence of three genes encoding a metallothionein, a chitinase and an expansin revealed the presence of numerous AP2/ERF and EIN3 motifs, reinforcing the hypothesis that those gene could be regulated by ethylene during CRs emergence (Fig.4-C).

B. Barley LBD in crown-root initiation

VI. LBD gene family analysis in barley and identification of the putative orthologous of rice and maize genes involved in crown root initiation.

The phylogenetic relationship among barley LBD proteins was determined for the 31 barley LBD proteins using MEGA 11 (Tamura, Stecher, and Kumar 2021). Three classes of LBD proteins were manually distinguished based on the prediction of the presence or absence of the coiled-coil motif (Fig.5)(Lupas, Van Dyke, and Stock 1991). The alignment indicated that the HvLBD proteins were identified including 31 LBDs in barley and 5 of them in class IB (HORVU.MOREX.r3.4HG0408280, HORVU.MOREX.r3.4HG0331440 HORVU.MOREX.r3.4HG0391970, HORVU.MOREX.r3.6HG0630410 and HORVU.MOREX.r3.4HG0408270) were phylogenetically related to rice OsCRL1, maize ZmRTCS and ZmRTCS-like1, Arabidopsis AtLBD16 and AtLBD18 that have been characterized as key actors of CR initiation in rice and maize, and lateral root initiation in *Arabidopsis*, respectively (Fig.5). HvLBD of Class IB may have main functions in leaf adaxial–abaxial polarity, plant reproduction, and adventitious rooting (Zhang et al. 2020b). The barley class IB contains 7 HvLBD proteins, one of them (HORVU.Morex.r3.4HG0408280) clustering with the well-characterized rice CRL1 and maize RTCS proteins (Y. Inukai 2005; Liu et al. 2005; C. Xu et al. 2015), suggesting that it could be their ortholog and play a role in the crown root initiation in barley. Consequently, we named it HvCRL1.

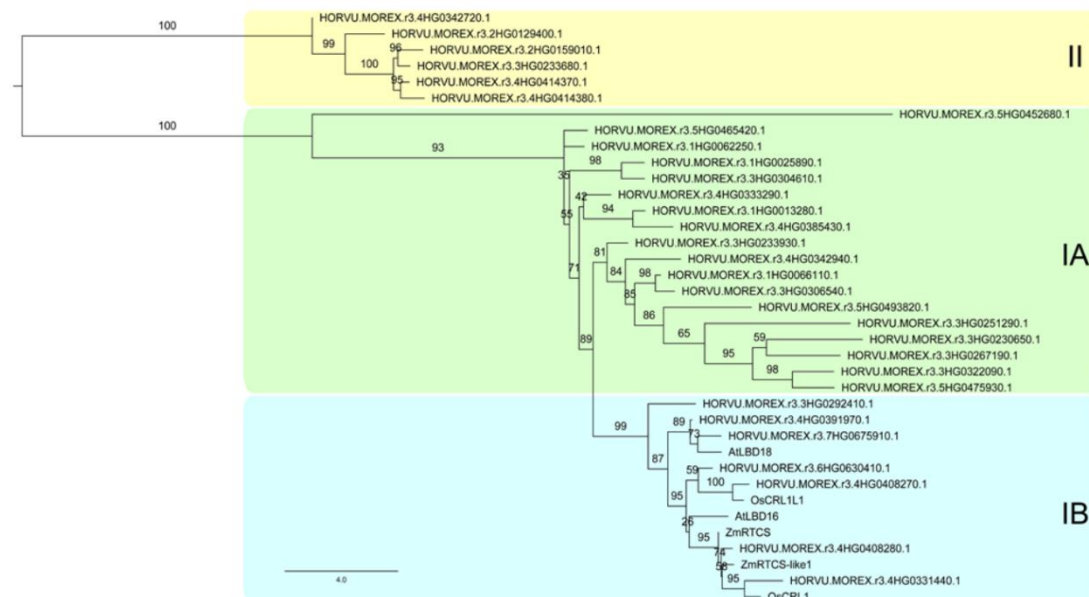


Figure 5: Phylogenetic analysis of the 31 barley LBD proteins. The analysis has been run with learnMSA (Becker and Stanke 2022) and default parameters. Sequences of rice (Os), maize (Zm) and Arabidopsis (At) genes encoding known key initiators of crown (Os and Zm) and adventitious (At) roots have been included in the analysis.

VII. Expression profile of the HbLBD genes during crown root initiation.

By treating seedlings consecutively with an auxin transport inhibitor and a synthetic auxin, one can control the synchronous initiation of lateral roots, consequently allowing abundant sampling of a desired developmental stage. Here, we used a system to synchronously initiate crown roots (Fig.6) and named it Crown Root Inducible System (CRIS). The cross-section of the stem base of barley seedlings treated for 3 days with 1-NAA revealed the presence of a ring of several root primordia at the same stage of development (Fig.6-C). This was not the case in the stem base of seedlings that were kept in the presence of the NPA (auxin-inhibition) (Fig.6-B). Seedlings treated with 1-NAA had a significantly higher number of crown roots 10 days after auxin-induction (Fig.6-D). We demonstrated that the CRIS is an effective model to synchronously stimulate the production of crown roots in barley.

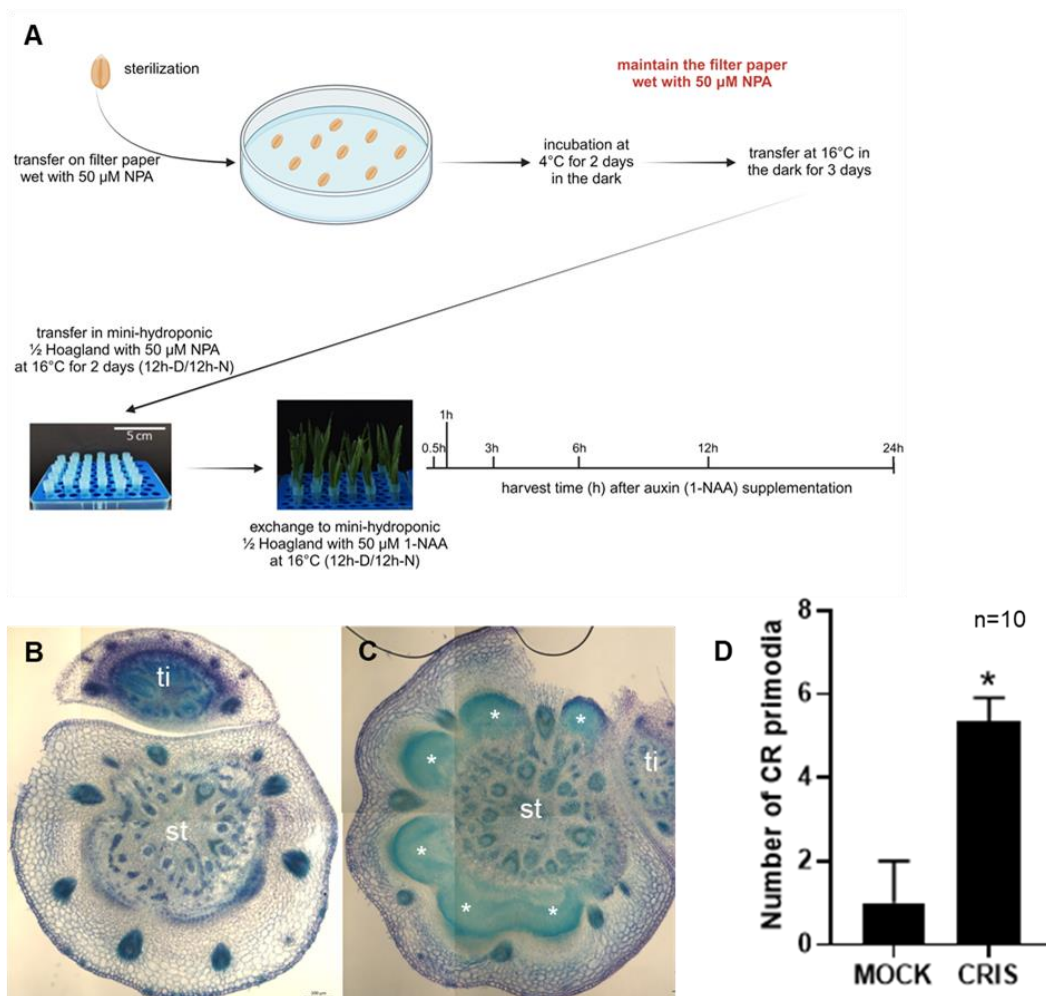


Figure 6: Crown-root inducible system (CRIS). **A**) Schematic representation of the system and the sample collection. The picture was prepared with Biorender. **B**) and **C**) Hand-made transversal section across the stem base of 5 days-old seedlings grown for 3 days in 50 μM NPA (**B**) or in 50 μM 1-NAA (**C**). Sections were stained in 0.1% toluidine blue. Pictures were acquired with a Zeiss microscope with a 5x objective. The full section was reconstructed using the Free Online Image Combiner (Adobe Express). ti: new tiller; st: stele; *: root apical meristem. **D**) Determination of the number of crown root in barley 10 days after auxin-induction. Student's *t* test was performed to determined the statically significance; n = 10.

qRT-PCR was used to analyze the expression of the five ClassIB *HvLBD* genes during crown-root initiation. Two barley *LBD* genes (*HORVU.Morex.r3.4HG0331440* and *HORVU.Morex.v3.4HG040880*) were not detected in our conditions, suggesting that they are not expressed in the stem base of barley. Whereas *HORVU.Morex.r3.4HG0408270* was detected in our conditions; its expression was very low and not affected by auxin treatment, indicating that it most probably has no function during crown root initiation. The transcripts of the *HvCRL1* (*HORVU.Morex.r3.4HG0408280*) gene highly accumulated within the first 3h of auxin treatment in the stem base of young seedlings (Fig.7). In a transcriptomic analysis based on CRIS (GEO: GSE171320, unpublished), *HvCRL1* is significantly up-regulated 1h following auxin-induced initiation of crown roots. Altogether, this indicated that *HvCRL1* is a prime target of the auxin signaling pathway. Finally, *HORVU.Morex.r3.6HG0630410* gene was found to accumulate significantly in the stem base of young seedlings treated for 6h by auxin, suggesting that it could be part of the mechanisms regulating crown root initiation in barley. Because *HORVU.Morex.r3.6HG0630410* is not the closest ortholog of rice *CRL1* but seems to be involved in crown root initiation; this gene was referred to as *HvCRL1-Like1* (*HvCRL1-L1*). This delay compared to *HvCRL1* suggested that *HvCRL1-L1* is not a direct target of the auxin signaling pathway. For both genes, the expression did not change when the seedlings were kept in the inhibitor of polar auxin transport (NPA), confirming that changes in their respective expression were related to auxin induction only.

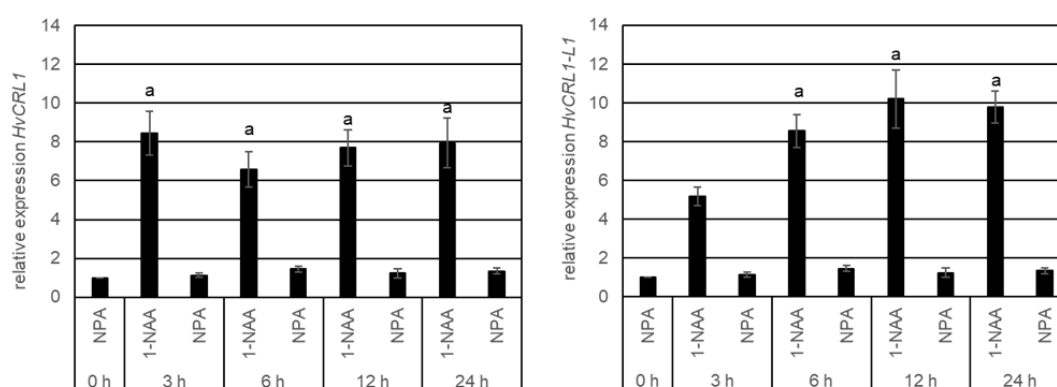


Figure 7: Gene expression analysis by qRT-PCR of two *LBD* genes (*HvCRL1* and *HvCRL1-L1*) of Class IB expressed in the stem base of young barley seedlings grown in the Crown Root Inducible System (CRIS) based on auxin-induced root initiation (Crombez et al. 2016). Normalization was done using 3 reference genes: *Actin*, *Hv5439* and *EIF152*. The graph shows means \pm SEM (n=6). The statistical significance was assessed by a non-parametric Kruskal-Wallis followed by a multiple comparisons test (GraphPad Prism 10). a: statistically significantly different from the control “0h-NPA” (p -value < 0.001).

We analyzed the 5,000 bp promoter region of both *HvCRL1* and *HvCRL1-L1* genes (Fig.8). Using the consensus Auxin Response Factor (ARF) binding sequence, Auxin Response Element (AuxRE: TGTCNN), we highlighted only AuxRE that form tandems with a maximum of 24 bp spacing (Cancé et al. 2022). In the promoter of *HvCRL1*, we found 10 AuxRE tandems. In the promoter of *HvCRL1-L1*, out of the 5 identified AuxRE tandems, 4 presented a DR conformation, whereas the fifth one was made of inverted repeats (IRs);

double sites in which two AuxREs are oriented towards each other in different strands of DNA).

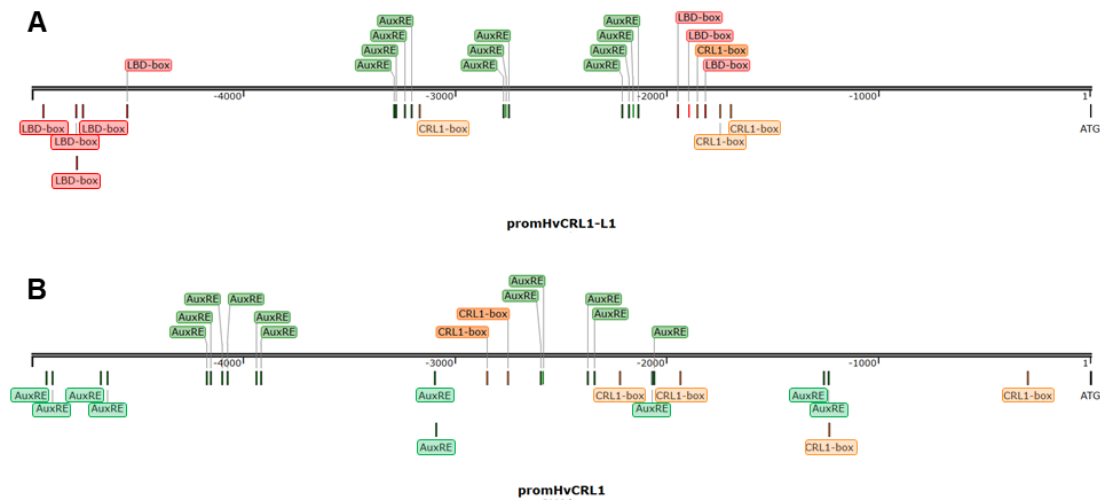


Figure 8: Identification of AuxRE (TGTCNN) and LBD-box (GCGGCG)/CRL1- box (CAC[A/C]C) in the 5000 bp-promoter sequence of **A**) HvCRL1-L1 and **B**) HvCRL1 genes.

VIII. HvCRL1 binds the LBD-box *in vivo*

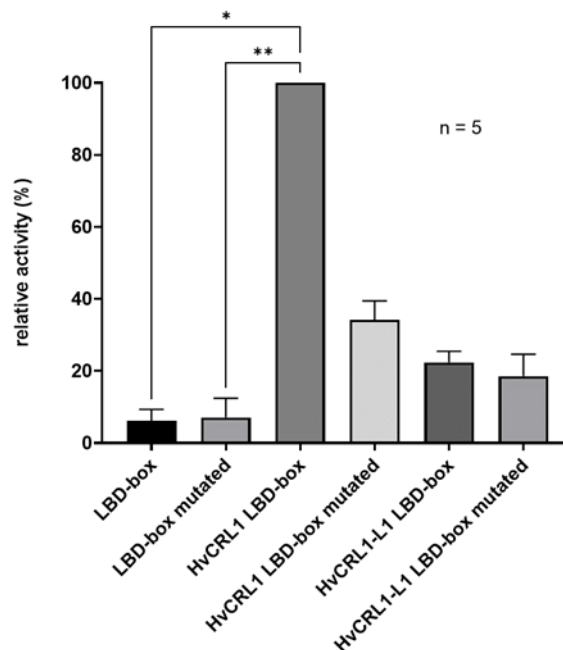


Figure 9: Transactivation assay in rice protoplast with HvCRL1 and HvCRL1-L1. Rice protoplasts were co-transformed with an effector plasmid carrying either HvCRL1 or HvCRL1-L1 gene under the control of the 35S promoter and reporter plasmids carrying LBD box motif (LBD-box) or its mutated version (LBD-box mutated) fused to GUS. A reference plasmid carrying the Renilla luciferase gene under the control of the 35S promoter was co-transformed to correct for transformation and protein extraction efficiencies. The control represents protoplasts that were transfected with an empty effector plasmid. The data were expressed as a percentage of the highest activity observed for HvCRL1. The graph represents the average \pm SEM of 5 independent experiments. The statistics were assessed with GraphPad Prism 10 (One-way ANOVA non-parametric Kruskal-Wallis followed by a Dunn's multiple comparisons test).

of crown roots was observed (Fig.11-A), correlated with a reduction in the fresh weight of the total root system (Fig.11-B).

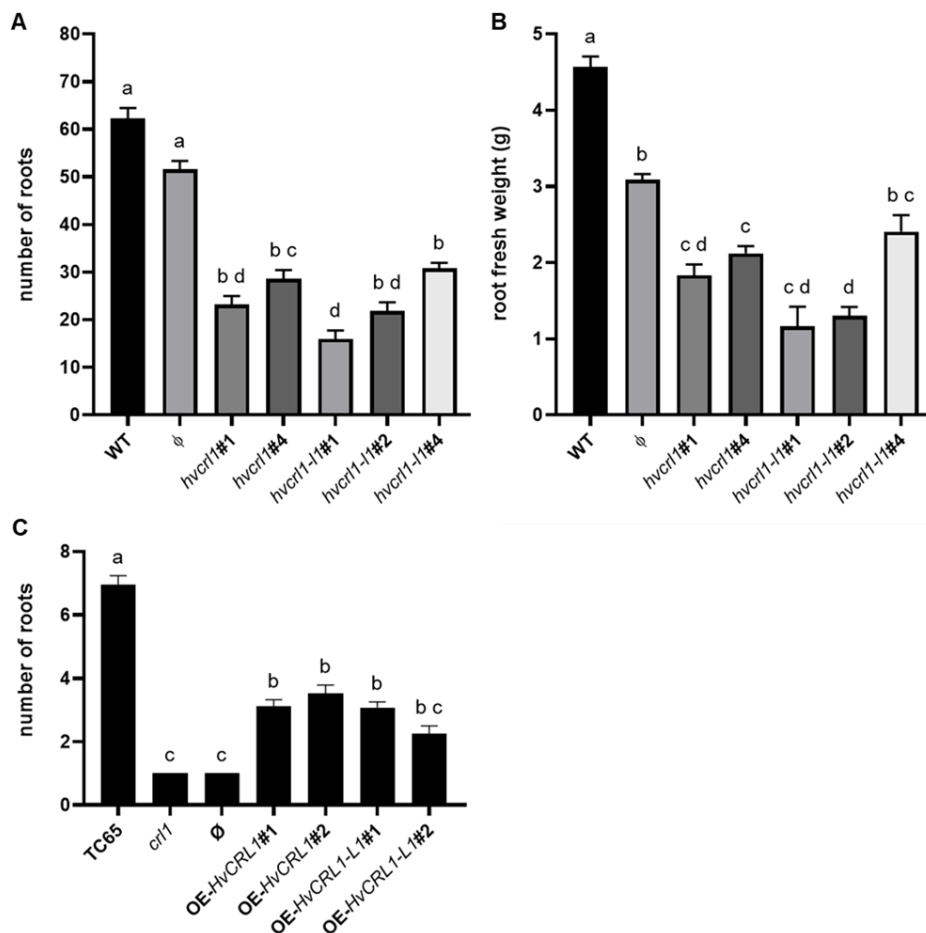


Figure 11: Role of HvCRL1 and HvCRL1-L1 in the formation of crown roots. **(A)** Number of crown roots of different *hvcrl1* and *hvcrl1-l1* knocked-out lines of barley obtained by CRISPR-Cas⁹. **(B)** Fresh weight of the total root system of different *hvcrl1* and *hvcrl1-l1* knocked-out lines of barley obtained by CRISPR-Cas⁹. **(C)** Complementation of the crown-root less phenotype of the rice *cr11* mutant by overexpression of *HvCRL1* or *HvCRL1-L1* genes. *HvCRL1* or *HvCRL1-L1* were overexpressed in the rice *cr11* mutant in the cv. TC65 genetic background. An empty vector was used as a control (∅). The graphs represent average +/- SEM; Statistical significance was assessed by a Brown-Forsythe and Welch ANOVA test followed by Dunn's multiple comparisons (GraphPad Prism 10.2.2). Bars with identical letters are not significantly different ($p < 0.05$).

In parallel, we overexpressed the two barley genes in the rice *cr11* mutant (Yoshiaki Inukai et al. 2005), which has a crown root-less phenotype due to a defect in crown root initiation (Fig.11-C). The overexpression of both *HvCRL1* and *HvCRL1-L1* gene resulted in a significantly higher number of roots in the rice seedlings, indicating that both genes can partially complement the *cr11* rice mutant by restoring crown root initiation.

Conclusions

In the first part of study, we analyzed the transcript profiles of barley young seedlings to increase our understanding of the mechanisms underlying the mechanisms regulating crown-root development and emergence. In addition, we provided an general and first anatomical overview of CR initiation and development in stem base of the young barley seedling. Our study constitutes the first step toward understanding the molecular and physiological mechanisms involved in development and emergence of CR in barley. The data from RNA-seq analysis indicated that CR development involved genes encoding proteins with a role in 1) cell identity priming and cell cycle activation, 2) hormonal status control and 3) cell death and cell wall modification. Further functional studies of identified key genes will be necessary to precise their involvement in CR formation.

The second and main part of my PhD study identified and characterized two LBD transcription factors from barley, HvCRL1 and HvCRL1-L1 that are closely phylogenetically related to the rice CRL1 transcription factor. Both partially complement the root-less phenotype of the rice *crl1* mutant, and barley *Hvcrl1* and *Hvcrl1-11* loss-of-function mutants show a reduction in crown root number, showing that they are both involved in the regulation of this developmental process. We showed that the expression profile of these two genes during crown root formation presents a thigh time delay and that HvCRL1-L1 can bind the LBD box whereas HvCRL1 cannot. This suggests that both proteins likely cooperate through different molecular pathways in regulating crow root formation in barley. This is reminiscent of what was described in maize for RTCS and RTCL (Xu et al. 2015) or, more recently, in rice for CRL1 and LBD16 (Geng et al. 2024; Geng et al. 2023). To better understand the mechanisms of action of these two barley LBD transcription factors it will be interesting to test their capacity to interact with each other and other proteins. The capacity of the LBD transcription factor to interact with other proteins is often a critical step in regulating their biochemical and biological function (Husbands et al. 2007; Geng et al. 2024).

In summary, this thesis presents: i) a transcriptomic study of CR initiation and development and an anatomical overview of CR initiation in barley, and iii) the functional characterization of two key HvLBD genes in CR initiation. The results contribute to the understanding of root establishment and development in cereals. Such knowledge is of importance to develop crops with higher ability of resource usage.

References

- Anders, Simon, Paul Theodor Pyl, and Wolfgang Huber. 2015. "HTSeq-A Python Framework to Work with High-Throughput Sequencing Data." *Bioinformatics* 31 (2): 166–69. <https://doi.org/10.1093/bioinformatics/btu638>.
- Atkinson, Jonathan A., Amanda Rasmussen, Richard Traini, Ute Voß, Craig Sturrock, Sacha J. Mooney, Darren M. Wells, and Malcolm J. Bennett. 2014. "Branching out in Roots: Uncovering Form, Function, and Regulation." *Plant Physiology* 166 (2): 538–50. <https://doi.org/10.1104/pp.114.245423>.
- Becker, Felix, and Mario Stanke. 2022. "LearnMSA: Learning and Aligning Large Protein Families." *GigaScience* 11: 1–14. <https://doi.org/10.1093/gigascience/giac104>.
- Bellini, Catherine, Daniel I. Pacurar, and Irene Perrone. 2014. "Adventitious Roots and Lateral Roots: Similarities and Differences." *Annual Review of Plant Biology* 65: 639–66. <https://doi.org/10.1146/annurev-arplant-050213-035645>.
- Bloh, Kevin, Rohan Kanchana, Pawel Bialk, Kelly Banas, Zugui Zhang, Byung Chun Yoo, and Eric B. Kmiec. 2021. "Deconvolution of Complex DNA Repair (DECODR): Establishing a Novel Deconvolution Algorithm for Comprehensive Analysis of CRISPR-Edited Sanger Sequencing Data." *CRISPR Journal* 4 (1): 120–31. <https://doi.org/10.1089/crispr.2020.0022>.
- Cacas, Jean Luc, Martial Pré, Maxime Pizot, Maimouna Cissoko, Issa Diedhiou, Aida Jalloul, Patrick Doumas, Michel Nicole, and Antony Champion. 2017. "GhERF-IIb3 Regulates the Accumulation of Jasmonate and Leads to Enhanced Cotton Resistance to Blight Disease." *Molecular Plant Pathology* 18 (6): 825–36. <https://doi.org/10.1111/mpp.12445>.
- Cancé, Coralie, Raquel Martin-Arevalillo, Kenza Boubekeur, and Renaud Dumas. 2022. "Auxin Response Factors Are Keys to the Many Auxin Doors." *New Phytologist* 235 (2): 402–19. <https://doi.org/10.1111/nph.18159>.
- Chen, Huilong, Xiaoming Song, Qian Shang, Shuyan Feng, and Weina Ge. 2022. "CFVisual: An Interactive Desktop Platform for Drawing Gene Structure and Protein Architecture." *BMC Bioinformatics* 23 (1): 1–9. <https://doi.org/10.1186/s12859-022-04707-w>.
- Chow, Chi Nga, Tzong Yi Lee, Yu Cheng Hung, Guan Zhen Li, Kuan Chieh Tseng, Ya Hsin Liu, Po Li Kuo, Han Qin Zheng, and Wen Chi Chang. 2019. "Plantpan3.0: A New and Updated Resource for Reconstructing Transcriptional Regulatory Networks from Chip-Seq Experiments in Plants." *Nucleic Acids Research* 47 (D1): D1155–63. <https://doi.org/10.1093/nar/gky1081>.
- Christensen, a H, and P H Quail. 1996. "Ubiquitin Promoter-Based Vectors for High-Level Expression of Selectable and/or Screenable Marker Genes in Monocotyledonous Plants." *Transgenic Research* 5 (3): 213–18. <http://www.ncbi.nlm.nih.gov/pubmed/8673150>.
- Cornelia Marthe , Jochen Kumlehn, and Goetz Hensel. 2015. "Barley (*Hordeum Vulgare* L.) Transformation Using Immature Embryos." *Methods in Molecular Biology* 1–1223 (Methods in Molecular Biology, vol. 1223): 71–83. <https://doi.org/10.1007/978-1-4939-1695-5>.
- Doležel, Jaroslav, Johann Greilhuber, and Jan Suda. 2007. "Estimation of Nuclear DNA Content in Plants Using Flow Cytometry." *Nature Protocols* 2 (9): 2233–44. <https://doi.org/10.1038/nprot.2007.310>.
- Fukaki, Hidehiro, Yoko Okushima, and Masao Tasaka. 2007. "Auxin - Mediated Lateral Root Formation in Higher Plants" 256 (07): 111–37. [https://doi.org/10.1016/S0074-7696\(07\)56004-3](https://doi.org/10.1016/S0074-7696(07)56004-3).
- Gao, Yingzhi, and Jonathan P Lynch. 2016. "Reduced Crown Root Number Improves Water Acquisition under Water Deficit Stress in Maize (*Zea Mays* L .)" 67 (15): 4545–57. <https://doi.org/10.1093/jxb/erw243>.
- Gonin, Mathieu, Véronique Bergougnoux, Thu D. Nguyen, Pascal Gantet, and Antony Champion. 2019. "What Makes Adventitious Roots?" *Plants* 8 (7): 1–24. <https://doi.org/10.3390/plants8070240>.

- Gou, Jiqing, Steven H. Strauss, Chung Jui Tsai, Kai Fang, Yiru Chen, Xiangning Jiang, and Victor B. Busov. 2010. "Gibberellins Regulate Lateral Root Formation in Populus through Interactions with Auxin and Other Hormones." *Plant Cell* 22 (3): 623–39. <https://doi.org/10.1105/tpc.109.073239>.
- Harris, Jeanne M. 2015. "Abscisic Acid: Hidden Architect of Root System Structure." *Plants*. MDPI AG. <https://doi.org/10.3390/plants4030548>.
- Himanen, Kristiina, Elodie Boucheron, Steffen Vanneste, Janice De Almeida Engler, Dirk Inzé, and Tom Beeckman. 2002. "Auxin-Mediated Cell Cycle Activation during Early Lateral Root Initiation." *The Plan* 14 (October): 2339–51. <https://doi.org/10.1105/tpc.004960.1>.
- Holubová, Katarína, Goetz Hensel, Petr Vojta, Petr Tarkowski, Véronique Bergougnoux, and Petr Galuszka. 2018. "Modification of Barley Plant Productivity through Regulation of Cytokinin Content by Reverse-Genetics Approaches." *Frontiers in Plant Science* 871 (November): 1–18. <https://doi.org/10.3389/fpls.2018.01676>.
- Hough, Soren H., Ayokunmi Ajetunmobi, Leigh Brody, Neil Humphries-Kirilov, and Edward Perello. 2016. "Desktop Genetics." *Personalized Medicine* 13 (6): 517–21. <https://doi.org/10.2217/pme-2016-0068>.
- Hruz, Tomas, Oliver Laule, Gabor Szabo, Frans Wessendorp, Stefan Bleuler, Lukas Oertle, Peter Widmayer, Wilhelm Gruissem, and Philip Zimmermann. 2008. "Genevestigator V3: A Reference Expression Database for the Meta-Analysis of Transcriptomes." *Advances in Bioinformatics* 2008: 1–5. <https://doi.org/10.1155/2008/420747>.
- Hua, Wei, Jinghuan Zhu, Yi Shang, Junmei Wang, Qiaojun Jia, and Jianming Yang. 2015. "Identification of Suitable Reference Genes for Barley Gene Expression Under Abiotic Stresses and Hormonal Treatments." *Plant Molecular Biology Reporter* 33 (4): 1002–12. <https://doi.org/10.1007/s11105-014-0807-0>.
- Humplík, Jan F., Véronique Bergougnoux, and Elizabeth Van Volkenburgh. 2017. "To Stimulate or Inhibit? That Is the Question for the Function of Abscisic Acid." *Trends in Plant Science*. Elsevier Ltd. <https://doi.org/10.1016/j.tplants.2017.07.009>.
- Husbands, Aman, Elizabeth M. Bell, Bin Shuai, Harley M S Smith, and Patricia S. Springer. 2007. "Lateral Organ Boundaries Defines a New Family of DNA-Binding Transcription Factors and Can Interact with Specific BHLH Proteins." *Nucleic Acids Research* 35 (19): 6663–71. <https://doi.org/10.1093/nar/gkm775>.
- Ikeda, A., M. Ueguchi-Tanaka, Y. Sonoda, H. Kitano, M. Koshioka, Y. Futsuhara, M. Matsuoka, and J. Yamaguchi. 2001. "Slender Rice, a Constitutive Gibberellin Response Mutant, Is Caused by a Null Mutation of the SLR1 Gene, an Ortholog of the Height-Regulating Gene GAI/RGA/RHT/D8." *Plant Cell* 13 (5): 999–1010. <https://doi.org/10.1105/tpc.13.5.999>.
- International, The, Barley Genome, and Sequencing Consortium. 2012. "A Physical, Genetic and Functional Sequence Assembly of the Barley Genome." *Nature* 491 (7426): 711–16. <https://doi.org/10.1038/nature11543>.
- Inukai, Y. 2005. "Crown Rootless1, Which Is Essential for Crown Root Formation in Rice, Is a Target of an AUXIN RESPONSE FACTOR in Auxin Signaling." *The Plant Cell Online* 17 (5): 1387–96. <https://doi.org/10.1105/tpc.105.030981>.
- Inukai, Yoshiaki, Tomoaki Sakamoto, Miyako Ueguchi-tanaka, Yohko Shibata, Kenji Gomi, Iichiro Umemura, Yasuko Hasegawa, Motoyuki Ashikari, Hidemi Kitano, and Makoto Matsuoka. 2005. "The Crown Rootless1 Gene in Rice Is Essential for Crown Root Formation and Is a Target of an AUXIN RESPONSE FACTOR in Auxin Signaling" 17 (May): 1–10. <https://doi.org/10.1105/tpc.105.030981.1>.
- Jansen, Leentje, Ianto Roberts, Riet De Rycke, and Tom Beeckman. 2012. "Phloem-Associated Auxin Response Maxima Determine Radial Positioning of Lateral Roots in Maize." *Philosophical Transactions of the Royal Society of London. Series B, Biological Sciences* 367 (1595): 1525–33. <https://doi.org/10.1098/rstb.2011.0239>.
- Jin, Jinpu, Feng Tian, De Chang Yang, Yu Qi Meng, Lei Kong, Jingchu Luo, and Ge Gao. 2017. "PlantTFDB 4.0: Toward a Central Hub for Transcription Factors and Regulatory Interactions

- in Plants.” *Nucleic Acids Research* 45 (D1): D1040–45. <https://doi.org/10.1093/nar/gkw982>.
- Khong, Giang Ngan, Pratap Kumar Pati, Frédérique Richaud, Boris Parizot, Przemyslaw Bidzinski, Chung Duc Mai, Martine Bès, et al. 2015. “OsMADS26 Negatively Regulates Resistance to Pathogens and Drought Tolerance in Rice.” *Plant Physiology*, no. September 2016: pp.01192.2015. <https://doi.org/10.1104/pp.15.01192>.
- Kim, Dae Sung, Nak Hyun Kim, and Byung Kook Hwang. 2015. “The Capsicum Annuum Class IV Chitinase ChitIV Interacts with Receptor-like Cytoplasmic Protein Kinase PIK1 to Accelerate PIK1-Triggered Cell Death and Defence Responses.” *Journal of Experimental Botany* 66 (7): 1987–99. <https://doi.org/10.1093/jxb/erv001>.
- Kim, Daehwan, Geo Pertea, Cole Trapnell, Harold Pimentel, Ryan Kelley, and Steven L. Salzberg. 2013. “TopHat2: Accurate Alignment of Transcriptomes in the Presence of Insertions, Deletions and Gene Fusions.” *Genome Biology* 14 (4). <https://doi.org/10.1186/gb-2013-14-4-r36>.
- Kitomi, Yuka, Atsushi Ogawa, Hidemi Kitano, and Yoshiaki Inukai. 2008. “CRL4 Regulates Crown Root Formation through Auxin Transport in Rice.” *Plant Root* 2: 19–28. <https://doi.org/10.3117/plantroot.2.19>.
- Kumlehn, Jochen, Liliya Serazetdinova, Goetz Hensel, Dirk Becker, and Horst Loerz. 2006. “Genetic Transformation of Barley (*Hordeum Vulgare* L.) via Infection of Androgenetic Pollen Cultures with *Agrobacterium Tumefaciens*.” *Plant Biotechnology Journal* 4 (2): 251–61. <https://doi.org/10.1111/j.1467-7652.2005.00178.x>.
- Lavarenne, Jérémy, Mathieu Gonin, Soazig Guyomarc’h, Jacques Rouster, Antony Champion, Christophe Sallaud, Laurent Laplaze, Pascal Gantet, and Mikael Lucas. 2019. “Inference of the Gene Regulatory Network Acting Downstream of CROWN ROOTLESS 1 in Rice Reveals a Regulatory Cascade Linking Genes Involved in Auxin Signaling, Crown Root Initiation, and Root Meristem Specification and Maintenance.” *Plant Journal*, 954–68. <https://doi.org/10.1111/tbj.14487>.
- LeClere, Sherry, Rosie Tellez, Rebekah A. Rampey, Seiichi P T Matsuda, and Bonnie Bartel. 2002. “Characterization of a Family of IAA-Amino Acid Conjugate Hydrolases from Arabidopsis.” *Journal of Biological Chemistry* 277 (23): 20446–52. <https://doi.org/10.1074/jbc.M111955200>.
- Li, Juan, Yunyuan Xu, and Kang Chong. 2012. “The Novel Functions of Kinesin Motor Proteins in Plants.” *Protoplasma* 249 (SUPPL.2): 95–100. <https://doi.org/10.1007/s00709-011-0357-3>.
- Li, Xinxin, Rensen Zeng, and Hong Liao. 2016. “Improving Crop Nutrient Efficiency through Root Architecture Modifications.” *Journal of Integrative Plant Biology* 58 (3): 193–202. <https://doi.org/10.1111/jipb.12434>.
- Liu, Hongjia, Shoufeng Wang, Xiaobo Yu, Jie Yu, Xiaowei He, Shelong Zhang, Huixia Shou, and Ping Wu. 2005. “ARL1, a LOB-Domain Protein Required for Adventitious Root Formation in Rice.” *Plant Journal* 43 (1): 47–56. <https://doi.org/10.1111/j.1365-313X.2005.02434.x>.
- Lo, Shuen Fang, Show Ya Yang, Ku Ting Chen, Yue Ie Hsing, Jan A.D. Zeevaart, Liang Jwu Chen, and Su May Yu. 2008. “A Novel Class of Gibberellin 2-Oxidases Control Semidwarfism, Tillering, and Root Development in Rice.” *Plant Cell* 20 (10): 2603–18. <https://doi.org/10.1105/tpc.108.060913>.
- Lohse, Marc, Axel Nagel, Thomas Herter, Patrick May, Michael Schroda, Rita Zrenner, Takayuki Tohge, Alisdair R. Fernie, Mark Stitt, and Björn Usadel. 2014. “Mercator: A Fast and Simple Web Server for Genome Scale Functional Annotation of Plant Sequence Data.” *Plant, Cell and Environment* 37 (5): 1250–58. <https://doi.org/10.1111/pce.12231>.
- López-Bucio, José, Alfredo Cruz-Ramírez, and Luis Herrera-Estrella. 2003. “The Role of Nutrient Availability in Regulating Root Architecture.” *Current Opinion in Plant Biology* 6 (3): 280–87. [https://doi.org/10.1016/S1369-5266\(03\)00035-9](https://doi.org/10.1016/S1369-5266(03)00035-9).
- Love, Michael I., Wolfgang Huber, and Simon Anders. 2014. “Moderated Estimation of Fold Change and Dispersion for RNA-Seq Data with DESeq2.” *Genome Biology*. <https://doi.org/10.1186/s13059-014-0550-8>.

- Lupas, Andrei, Marc Van Dyke, and Jeff Stock. 1991. "Predicting Coiled Coils from Protein Sequences." *Science* 252 (5009): 1162–64. <https://doi.org/10.1126/science.252.5009.1162>.
- Majer, Christine, Changzheng Xu, Kenneth W. Berendzen, and Frank Hochholdinger. 2012. "Molecular Interactions of Rootless Concerning Crown and Seminal Roots, a LOB Domain Protein Regulating Shoot-Borne Root Initiation in Maize (*Zea Mays* L.)." *Philosophical Transactions of the Royal Society B: Biological Sciences* 367 (1595): 1542–51. <https://doi.org/10.1098/rstb.2011.0238>.
- Marthe, Cornelia, Jochen Kumlehn, and Goetz Hensel. 2015. "Barley (*Hordeum Vulgare* L.) Transformation Using Immature Embryos." *Methods in Molecular Biology* 1223: 71–83. https://doi.org/10.1007/978-1-4939-1695-5_6.
- Mascher, Martin, Thomas Wicker, Jerry Jenkins, Christopher Plott, Thomas Lux, Chu Shin Koh, Jennifer Ens, et al. 2021. "Long-Read Sequence Assembly: A Technical Evaluation in Barley." *Plant Cell* 33 (6): 1888–1906. <https://doi.org/10.1093/plcell/koab077>.
- Mayer, Klaus F X, Robbie Waugh, Peter Langridge, Timothy J Close, Roger P Wise, Andreas Graner, Takashi Matsumoto, et al. 2012. "A Physical, Genetic and Functional Sequence Assembly of the Barley Genome." *Nature* 491 (7426): 1–83. <https://doi.org/10.1038/nature11543>.
- Meng, Funing, Dan Xiang, Jianshu Zhu, Yong Li, and Chuanzao Mao. 2019. "Molecular Mechanisms of Root Development in Rice." *Rice* 12 (1): 1–10. <https://doi.org/10.1186/s12284-018-0262-x>.
- Mergemann, H., and M. Sauter. 2000. "Ethylene Induces Epidermal Cell Death at the Site of Adventitious Root Emergence in Rice." *Plant Physiology* 124 (2): 609–14. <https://doi.org/10.1104/pp.124.2.609>.
- Michael W. Pfaffl. 2001. "A New Mathematical Model for Relative Quantification in Real-Time RT-PCR." *Nucleic Acids Res* 29 (9): e45. <https://doi.org/10.1111/j.1365-2966.2012.21196.x>.
- Orman-Ligeza, Beata, Boris Parizot, Pascal P Gantet, Tom Beeckman, Malcolm J Bennett, and Xavier Draye. 2013. "Post-Embryonic Root Organogenesis in Cereals: Branching out from Model Plants." *Trends in Plant Science* 18 (8): 459–67. <https://doi.org/10.1016/j.tplants.2013.04.010>.
- Park, Woong June, Frank Hochholdinger, and Alfons Gierl. 2004. "Release of the Benzoxazinoids Defense Molecules during Lateral- and Crown Root Emergence in *Zea Mays*." *Journal of Plant Physiology* 161 (8): 981–85. <https://doi.org/10.1016/j.jplph.2004.01.005>.
- Péret, Benjamin, Bert De Rybel, Ilda Casimiro, Eva Benková, Ranjan Swarup, Laurent Laplaze, Tom Beeckman, and Malcolm J. Bennett. 2009. "Arabidopsis Lateral Root Development: An Emerging Story." *Trends in Plant Science* 14 (7): 399–408. <https://doi.org/10.1016/j.tplants.2009.05.002>.
- Perrot-Rechenmann, Catherine. 2010. "Cellular Responses to Auxin: Division versus Expansion." *Cold Spring Harbor Perspectives in Biology* 2 (5): 1–15. <https://doi.org/10.1101/cshperspect.a001446>.
- Rampey, R. A., Rosie Tellez, R. A. Rampey, Seiichi P T Matsuda, and Bartel. 2004. "A Family of Auxin-Conjugate Hydrolases That Contributes to Free Indole-3-Acetic Acid Levels during Arabidopsis Germination." *Plant Physiology* 135 (2): 978–88. <https://doi.org/10.1104/pp.104.039677>.
- Reinhard Töpfer, Volker Matzeit, Bruno Gronenborn, Jozef Schell and Hans-Henning Steinbiss. 1987. "A Set of Plant Expression Vectors for Transcriptional and Translational Fusions." *Nucleic Acids Research* 15 (14): 5890.
- Roycewicz, Peter S., and Jocelyn E. Malamy. 2014. "Cell Wall Properties Play an Important Role in the Emergence of Lateral Root Primordia from the Parent Root." *Journal of Experimental Botany* 65 (8): 2057–69. <https://doi.org/10.1093/jxb/eru056>.
- Sallaud, C., D. Meynard, J. Van Boxtel, C. Gay, M. Bès, J. P. Brizard, P. Larmande, et al. 2003. "Highly Efficient Production and Characterization of T-DNA Plants for Rice (*Oryza Sativa* L.)

- Functional Genomics.” *Theoretical and Applied Genetics* 106 (8): 1396–1408.
<https://doi.org/10.1007/s00122-002-1184-x>.
- Schindelin, Johannes, Ignacio Arganda-Carreras, Erwin Frise, Verena Kaynig, Mark Longair, Tobias Pietzsch, Stephan Preibisch, et al. 2012. “Fiji: An Open-Source Platform for Biological-Image Analysis.” *Nature Methods* 9 (7): 676–82.
<https://doi.org/10.1038/nmeth.2019>.
- Schwacke, Rainer, Gabriel Y. Ponce-Soto, Kirsten Krause, Anthony M. Bolger, Borjana Arsova, Asis Hallab, Kristina Gruden, Mark Stitt, Marie E. Bolger, and Björn Usadel. 2019. “MapMan4: A Refined Protein Classification and Annotation Framework Applicable to Multi-Omics Data Analysis.” *Molecular Plant* 12 (6): 879–92.
<https://doi.org/10.1016/j.molp.2019.01.003>.
- Steffens, Bianka, Alexander Kovalev, Stanislav N. Gorb, and Margret Sauter. 2012. “Emerging Roots Alter Epidermal Cell Fate through Mechanical and Reactive Oxygen Species Signaling.” *Plant Cell* 24 (8): 3296–3306. <https://doi.org/10.1105/tpc.112.101790>.
- Steffens, Bianka, and Margret Sauter. 2009. “Epidermal Cell Death in Rice Is Confined to Cells with a Distinct Molecular Identity and Is Mediated by Ethylene and H₂O₂ through an Autoamplified Signal Pathway.” *Plant Cell* 21 (1): 184–96.
<https://doi.org/10.1105/tpc.108.061887>.
- Swarup, Kamal, Eva Benková, Ranjan Swarup, Ilda Casimiro, Benjamin Péret, Yaodong Yang, Geraint Parry, et al. 2008. “The Auxin Influx Carrier LAX3 Promotes Lateral Root Emergence” 10 (8). <https://doi.org/10.1038/ncb1754>.
- Tamura, Koichiro, Glen Stecher, and Sudhir Kumar. 2021. “MEGA11: Molecular Evolutionary Genetics Analysis Version 11.” *Molecular Biology and Evolution* 38 (7): 3022–27.
<https://doi.org/10.1093/molbev/msab120>.
- Toki, Seiichi, Naho Hara, Kazuko Ono, Haruko Onodera, Akemi Tagiri, Seibi Oka, and Hiroshi Tanaka. 2006. “Early Infection of Scutellum Tissue with Agrobacterium Allows High-Speed Transformation of Rice.” *The Plant Journal : For Cell and Molecular Biology* 47 (6): 969–76.
<https://doi.org/10.1111/j.1365-313X.2006.02836.x>.
- Vandesompele, Jo, Katleen De Preter, Filip Pattyn, Bruce Poppe, Nadine Van Roy, Anne De Paepe, and Frank Speleman. 2002. “Accurate Normalization of Real-Time Quantitative RT-PCR Data by Geometric Averaging of Multiple Internal Control Genes.” *Genome Biology* 3 (7).
<https://doi.org/10.1007/s00603-018-1496-z>.
- Vlamiš, J., and D. E. Williams. 1962. “Ion Competition in Manganese Uptake by Barley Plants.” *Plant Physiology* 37 (5): 650–55. <https://doi.org/10.1104/pp.37.5.650>.
- Xu, Changzheng, Huanhuan Tai, Muhammad Saleem, Yvonne Ludwig, Christine Majer, Kenneth W. Berendzen, Kerstin A. Nagel, et al. 2015. “Cooperative Action of the Paralogous Maize Lateral Organ Boundaries (LOB) Domain Proteins RTCS and RTCL in Shoot-Borne Root Formation.” *New Phytologist* 207 (4): 1123–33. <https://doi.org/10.1111/nph.13420>.
- Xu, Jian, and Jing Han Hong. 2013. “Root Development: Genetics and Genomics of Rice.” *Plant Genetics and Genomics: Crops and Models* 5, 297–316. <https://doi.org/10.1007/978-1-4614-7903-1>.
- Yoo, Sang Dong, Young Hee Cho, and Jen Sheen. 2007. “Arabidopsis Mesophyll Protoplasts: A Versatile Cell System for Transient Gene Expression Analysis.” *Nature Protocols* 2 (7): 1565–72. <https://doi.org/10.1038/nprot.2007.199>.
- Zarei, Adel, Ana Paula Körbes, Parisa Younessi, Gregory Montiel, Antony Champion, and Johan Memelink. 2011. “Two GCC Boxes and AP2/ERF-Domain Transcription Factor ORA59 in Jasmonate/Ethylene-Mediated Activation of the PDF1.2 Promoter in Arabidopsis.” *Plant Molecular Biology* 75 (4–5): 321–31. <https://doi.org/10.1007/s11103-010-9728-y>.
- Zhang, Yuwen, Ziwen Li, Biao Ma, Quancan Hou, and Xiangyuan Wan. 2020. “Phylogeny and Functions of LOB Domain Proteins in Plants.” *International Journal of Molecular Sciences*.
<https://doi.org/10.3390/ijms21072278>.

CONFERENCE PRESENTATIONS

Nguyen DT, Pantet P, Bergounoux V. 2017. LATERAL ORGAN BOUNDARIES-DOMAIN protein of barley (*Hordeum vulgare* L.): role during crown-root initiation and regulation by auxin. Green For Good IV, 19-22 June 2017, Olomouc, Czech Republic.

Nguyen Dieu Thu, Mathieu Gonin, Lavarenne Jeremy, Myriam Collin, Gantet Pascal, Bergounoux Veronique 2018. Anatomical and molecular dissection of crown-root initiation in barley (*Hordeum vulgare* L.). Green For Good V, 10 - 13 June 2019, Olomouc, Czech Republic.

Nguyen D.T., Kořínková N., Gonin M., Champion A., Gantet P., Bergounoux V. 2019. A dissection of genetic and molecular mechanism regulating the initiation of crown root in barley (*Hordeum vulgare* L.). XXIII Meeting of the Spanish Society of Plant Physiology/XVI Spanish Portuguese Congress of Plant Physiology Pamplona, 26 - 28 June 2019.

Nguyen D.T., Gonin M, Hensel G., Gantet P., Bergounoux V. 2021. Role of LBD transcription factors in initiation of crown-roots in barley (*Hordeum vulgare* L.). International plant systems biology (iPSB), the second EMBO workshop, 26-27 April 2021, Virtual.

Nguyen D.T., Kokáš F., Techer A., Hensel G., Gantet P., Bergounoux V. 2021. Understanding crown-roots development in barley (*Hordeum vulgare* L.), the first step towards the production of crops with enhanced root architectural traits. European Federation of biotechnology (EFB) 2021 – Virtual conference, 10 – 14 May 2021.

Nguyen D.T., Gonin M, Hensel G., Gantet P., Bergounoux V. 2021. Role of LOB-domain proteins in crown-root initiation and development in barley (*Hordeum vulgare* L.). The 8th International Symposium about root structure and function. June 12-16, 2022, High Tatras, Horný Smokovec, Slovakia.

Nguyen D.T., Kovačik M., Pečinka A., Gantet P., Bergounoux V. 2022. Crown Root Inducible System as a method to study transcript profiling of crown root initiation in barley (*Hordeum vulgare* L.). Green For Good VI, 12 – 15 September 2022, Olomouc, Czech Republic.

PUBLICATIONS

Mathieu Gonin, Véronique Bergounoux, **Thu D. Nguyen**, Pascal Gantet and Antony Champion. “What Makes Adventitious Roots? A review”. *Plants* 2019, 8, 240; doi:10.3390/plants8070240

Kořínková N*, Fontana IM*, **Nguyen TD***, Pouramini P, Bergounoux V, Hensel G. “Enhancing cereal productivity by genetic modification of root architecture – a review” *Biotechnol. J.* 2022;2100505. <https://doi.org/10.1002/biot.202100505>.

* all 3 authors participate equally as first author to the manuscript preparation.

Mortaza Khodaeiaminjan, Dominic Knoch, Marie Rose Ndella Thiaw, Cintia F. Marchetti, Nikola Kořínková, Alexie Techer, **Thu D. Nguyen**, Jianting Chu, Valentin Bertholomey, Ingrid Doridant, Pascal Gantet, Andreas Graner, Kerstin Neumann, Veronique Bergounoux. “Genome-wide association study in two-row spring barley landraces identifies QTLs associated with plantlets root system architecture traits in well-watered and osmotic stress conditions”. *Front. Plant Sci.*, 03 April 2023. *Sec. Plant Development and EvoDevo* Volume 14 – 2023. <https://doi.org/10.3389/fpls.2023.1125672>

MANUSCRIPTS UNDER THE REVIEW

Thu Dieu Nguyen, Filip Zavadil Kokáš, Mathieu Gonin, Jérémy Lavarenne, Myriam Colin, Pascal Gantet, and Véronique Bergounoux. Transcriptional changes during crown-root development and emergence in barley (*Hordeum vulgare* L.). *BMC Plant biology*.

The article manuscript was submitted to *BMC Plant Biology* on 16 June 2023 UTC and resubmitted the revision on 9 April 2024 UTC. Ref: Submission ID 1ffd5ce6-d5b2-4f97-ba8d-622c47e46026. It is currently under the second reviewing.

Thu Dieu Nguyen, Mathieu Gonin, Michal Motyka, Antony Champion, Goetz Hensel, Pascal Gantet, Véronique Bergounoux. Two lateral organ boundary domain transcription factors HvCRL1 and HvCRL1-1L regulate shoot-borne root formation in barley (*Hordeum vulgare* L.).

The article manuscript was submitted to *BMC Plant Biology* on 17 April 2024 UTC *Journal of Plant Growth Regulation*. It is currently under peer review.